"Development of a Test Method for Testing Stress Corrosion Cracking of

7000 Series Aluminium Alloys for Automotive Applications"

Von der Fakultät für Georessourcen und Materialtechnik der
Rheinisch-Westfälischen Technischen Hochschule Aachen

zur Erlangung des akademischen Grades einer

Doktorin der Ingenieurwissenschaften

genehmigte Dissertation

vorgelegt von

Neeta Magaji-Mehta, M.Sc. RWTH

Berichter: Univ.-Prof. Dr.-Ing. habil. Brita Daniela Zander

Univ.-Prof. Dr. rer. nat. Robert Spatschek

Tag der mündlichen Prüfung: 12.10.2023

Diese Dissertation ist auf den Internetseiten der Universitätsbibliothek online verfügbar

ACKNOWLEDGEMENT

ABSTRACT

In recent years, the Al-Zn-Mg-(Cu) aluminium alloys, also known as the aluminium 7xxx series, have drawn considerable attention in the automotive industry owing to its high strength-to-weight ratio, making it a favored candidate for light-weight automobile construction. Nonetheless, a prominent challenge associated with these alloys is their high risk of susceptibility to stress corrosion cracking (SCC), which poses a significant risk of spontaneous failures in the service life of an automobile. Stress corrosion cracking is a complex phenomenon, involving the simultaneous effect of a susceptible material, minimum threshold stress, and a corrosive medium. Understanding the effects of SCC with respect to automobile poses a serious challenge due to the difficulty in predicting the influence of critical factors, such as stress conditions and environmental variations in the complex automotive lifecycle. This work aims to scientifically analyse the critical influencing factors, with a primary focus on their synergistic interactions occurring in the complex automotive lifecycle. This knowledge is then incorporated into designing a novel accelerated SCC test, called the MBSC test, which can test the SCC susceptibility of the 7xxx alloys specifically for the automotive application.

In this thesis, a novel design approach, called Design for Six Sigma (DFSS), was the primary design methodology. The DFSS is a customer-centric product development methodology that enables the designing of complex products or processes systematically. The potential use of this methodology for the development of future corrosion test methods was assessed in this thesis. Four alloys, each with varying contents of Zn, Mg and Cu, and varying temper treatments were studied in this work, hence providing a range of SCC susceptibility for testing. The effects of various factors that are critical to SCC were clustered into environmental and mechanical parameters and individually analysed. The significant environmental parameters were investigated through Design of Experiment. The significant mechanical parameters were experimentally investigated on the three chosen mechanical specimens and compared to the specimen stresses occurring in critical in-service load conditions. Finally, an outdoor exposure test was carried out, the results of which were used to validate the Mercedes Benz Stress Corrosion Test (MBSC).

The results showed that using the DFSS was advantageous in structuring the complex analysis of the automotive lifecycle and efficiently implementing it in the designing of the

Abstract

MBSC Test. A key benefit of using this approach was the ability to study the influencing parameters as an integrated whole rather than studying them individually under carefully controlled parameters, which is typically observed in most scientific studies. A significant outcome of this thesis was highlighting the potential of DFSS method as a standardized framework for the development of future corrosion test methods, particularly in the context of SCC tests.

The results of the individual and synergistic effects from the above investigations served as the basis for the development of a new test method, the Mercedes Benz Stress Corrosion Test (MBSC). Studying the influence of environmental parameters revealed critical parameters such as test temperature and range of temperature variation in the MBSC corrosion test cycle had a significant influence on the SCC susceptibility. Moreover, anions and cations, NH_4^+ and NO_3^- in the salt solution, had a significant influence on the intergranular corrosion of the tested alloys. This in turn acted as accelerator for initiation points for SCC, thus increasing SCC susceptibility. Similarly, qualitative analysis of the various mechanical specimens showed the significant influence of mechanical parameters such as load propagation mode, stress distribution and stress magnitude on the SCC susceptibility of the tested alloys. Optimal environmental and mechanical parameters for the MBSC test were derived through this analysis. The results obtained from the MBSC test were consequently validated by showing a high correlation to the outdoor exposure test results.

With the help of the DFSS method, a novel test was created to the needs of the automotive industry which can represent the SCC corrosion susceptibility of 7xxx Al alloys during the service life of a vehicle. The MBSC allows an exact differentiation between SCC susceptible and non-susceptible 7xxx Al alloys. It should be emphasized that the MBSC test can also identify only slightly susceptible alloys, which is not possible with ASTM G47-98, a widely used standard test for SCC susceptibility. The MBSC has a high significance for the automotive industry, as it allows a differentiated selection of 7xxx aluminium alloys for future automotive designing.

DEUTSCHE ZUSAMMENFASSUNG

Die Al-Zn-Mg-(Cu)-Aluminiumlegierungen, auch bekannt als 7xxxer-Serie der Aluminiumlegierungen, haben in den letzten Jahren aufgrund ihres sehr guten Festigkeits-Gewichts-Verhältnisses in der Automobilindustrie große Aufmerksamkeit erregt und sind damit ein beliebter Kandidat für den Leichtbau. Eines der Hauptprobleme im Zusammenhang mit dieser hochfesten Legierungsserie ist jedoch die hohe Anfälligkeit für Spannungsrisskorrosion (SpRK), die zu spontanen Ausfällen während der Nutzungsdauer eines Fahrzeugs führen kann. Spannungsrisskorrosion ist ein komplexes Phänomen, das auftritt, wenn ein anfälliges Material, eine Überschreitung der Grenzspannung und ein korrosives Medium zusammenkommen. Da es schwierig und komplex ist die kritischen Einflussfaktoren wie Spannungsbelastungen und Umwelteinflüsse vorherzusagen, stellt das Verständnis der Auswirkungen von Spannungsrisskorrosion während der Betriebsdauer eines Fahrzeuges eine ernsthafte Herausforderung dar. Ziel dieser Arbeit ist es, die kritischen Einflussfaktoren und ihre synergistischen Wechselwirkungen während der Betriebszeit eines Fahrzeuges wissenschaftlich zu analysieren. Diese Analyse fließen dann in einen neuen SpRK-Test, dem MBSC ein, mit dem die Spannungsrissempfindlichkeit der 7xxx Aluminiumlegierungen gezielt für die Anwendung in der Automobilindustrie getestet werden sollen.

Bei der Konzeption der Prüfmethode wird in dieser Arbeit ein neuer Ansatz namens Design for Six Sigma (DFSS) verwendet. Dabei handelt es sich um eine systematische Produktentwicklungs-Methode, die es ermöglicht, komplexe Produkte oder Prozesse systematisch zu gestalten. Der Einsatz dieser Methodik für die Entwicklung künftiger Korrosionsprüfverfahren wurde in dieser Arbeit bewertet. Für die Testentwicklung werden vier Legierungen mit unterschiedlichen Zn-, Mg- und Cu-Gehalten und die Wärmebehandlungsstufen T4, T6 und T7 verwendet, sodass eine Reihe verschiedener SpRK-Anfälligkeiten gegeben ist. Die verschiedenen Faktoren, die für SpRK im Fahrzeugbetrieb entscheidend sind, werden in Umwelt- und mechanische Parameter geclustert und jeweils für sich analysiert. Die signifikanten Umweltparameter werden mit Hilfe der statistischen Versuchsplanung DoE (Design of Experiment) untersucht. Die mechanischen Parameter werden anhand der drei ausgewählten Proben experimentell untersucht und mit den Probenspannungen verglichen, die bei kritischen Betriebslasten

im Fahrzeug auftreten. Parallel wurden die Legierungen unter Spannung in der Freibewitterung getestet. Die Ergebnisse aus der Freibewitterung werden zur Validierung des Mercedes Benz Stress Corrosion Test verwendet.

Die Ergebnisse haben gezeigt, dass der Einsatz des DFSS vorteilhaft war, um die komplexe Analyse des Lebenszyklus eines Automobils zu strukturieren und dieses Wissen effizient für die Entwicklung der neuartigen Testmethode einzusetzen. Ein Hauptvorteil bei der Anwendung der DFSS war die Möglichkeit, die komplexen Einflussparameter ganzheitlich zu untersuchen und nicht nur einzelne, definierten Laborbedingungen, wie es in den meisten wissenschaftlichen Studien der Fall ist. Eine wichtige Aussage dieser Arbeit war das Potenzial der DFSS-Methode als standardisierter Ansatz für die Entwicklung zukünftiger Korrosionsprüfverfahren.

Die Ergebnisse der Einzel- und Synergieeffekte aus den genannten Untersuchungen dienen als Grundlage für die Entwicklung einer neuen Prüfmethode, dem Mercedes Benz Stress Corrosion Test (MBSC). Der signifikante Einfluss Umgebungsparameter wie Testtemperatur und Temperatursprünge auf die Spannungsrisskorrosion im MBSC-Testzyklus nachgewiesen. Bei der Untersuchung des Einflusses von Umweltparametern war festgestellt, dass Anionen und Kationen, insbesondere NH_4^+ und NO_3^-, einen signifikanten Einfluss auf interkristalline Korrosion haben und somit als Initiator für SpRK werden und den SpRK-anfälligkeit erhöhen. Ferner wurde in der Arbeit optimale Parametern für den beschleunigten Korrosionstest mit Blick auf die unterschiedliche SpRK-Anfälligkeit der getesteten Legierungen analysiert und diskutiert. Zuletzt werden die Ergebnisse des MBSC-Tests durch den Nachweis einer hohen Korrelation zu den Ergebnissen der Freibewitterung validiert.

Mit Hilfe der DFSS-Methode wurde ein auf die Belange der Fahrzeugindustrie neuer Test kreiert, mit dem die SpRK-Korrosionsanfälligkeit von 7xxx Al-Legierungen während der Laufzeit eines Fahrzeuges dargestellt wird. Der MBSC ermöglicht eine exakte Unterscheidung von SpRK anfälligen und nicht anfälligen 7xxx Al-Legierungen. Hervorzuheben ist, dass mit dem MBSC-Test auch nur leicht anfällige Legierungen identifiziert, werden können, was mit dem ASTM G47-98, einem verbreiteten Standard-Test auf SpRK-Anfälligkeit, nicht möglich ist. Deswegen hat der MBSC-Test eine hohe Bedeutung für den Fahrzeugindustrie.

CONTENT

NOMENCLATURE

Abbreviations

SCC	Stress Corrosion Cracking
DFSS	Design for Six Sigma
DCOV	Definition, Conceptualisation, Optimisation and Validation
MBSC	Mercedes Benz Stress Corrosion Test
DMAIC	Define, Measure, Analyse, Improve and Control
PGP	Product Generation Process
DoE	Design of Experiment
MSA	Measurement System Analysis
OVAT	One Variable at a Time
EN	European Norm
AW	Aluminium Wrought Alloy
AIDE	Adsorption Induced Dislocation Emission
ADAC	Anodic Dissolution Assisted Cracking
CELP	Corrosion Enhanced Localised Plasticity
DIN	Deutsches Institut für Normung
EIC	Environmentally Assisted Cracking
EPFM	Elastic Plastic Fracture Mechanics
GPZ	Guinier-Preston Zone
HELP	Hydrogen Enhanced Localised Plasticity

Nomenclature

HIC   Hydrogen Induced Cracking

IGC   Inter-Granular Corrosion

IGSCC   Inter-Granular Stress Corrosion Cracking

ISO   International Organisation for Standardization

KI   Stress Intensity Factor (Mode I)

KIC   Critical Stress Intensity Factor

KISCC   Threshold Stress Intensity Factor For SCC

LEFM   Linear Elastic Fracture Mechanics

AES   Atomic Emission Spectroscopy

RRA   Retrogression And Re-Aging

SSRT   Slow Strain Rate Test

PFZ   Precipitate Free Zone

ASTM   American Society for Testing and Materials

Rp0.2   Yield strength

Rm   Ultimate Tensile Strength

A30   Elongation

Greek Symbols

α supersaturated solid solution

η' semi-coherent intermediate $MgZn_2$ phase or Mg (Zn, Cu) phase

η incoherent equilibrium $MgZn_2$ or Mg (Zn, Cu)$_2$ phase

Chapter 1 INTRODUCTION AND KEY OBJECTIVES

The automotive industry has undergone a period of immense transformation in recent years. Increased customer demands and stricter regulatory requirements have forced the industry to focus its research and development on sustainability and resource efficiency.[1] One of the strategies in-line with this research is the lightweight construction and use of lightweight materials in automobiles.[2-4] Use of lightweight materials leads to increased engine efficiency and reduced carbon emissions, which is currently the need of the hour. [5] Moreover, in order to achieve the ambitious CO_2 targets currently set by various governments, automobile companies must also powerfully move towards battery technologies and other sustainable fuel consumption methods, which again underscores the need for lightweight construction in order to be energy efficient [6] A larger share of this change will go toward implementing high strength steels, however, aluminium has also gained increased attention to substitute steel. Due to its good strength-to-weight ratio and relatively low costs compared to other lightweight alloys such as titanium and magnesium, aluminium is emerging as a promising alternative. [7, 8]

The aluminium alloys currently used in the automotive industry are Al-Mg (5xxx series) alloys and precipitation hardenable Al-Mg-Si (6xxx series) alloys.[7] The limitation of the maximum strength attainable in these alloys led to the development of high-strength Al-Zn-Mg-(Cu) alloys, also known as the 7xxx series aluminium alloys, in the early 1940s and has since then drawn considerable attention for various applications.[9] Its tensile strengths can extend up to 600MPa, thus having comparable specific strength to steels and is considerably higher than the attainable strengths of the present standard 6xxx series automotive alloys. However, the corrosion properties and underlying mechanisms of the 7xxx alloy are yet to be fully understood in order to determine its potential to be used in the automotive industry. One of the concerns regarding the usage of 7xxx alloy is its high risk of susceptibility to stress corrosion cracking (SCC). This phenomenon could lead to spontaneous failures in the service life of an automobile, thus causing safety issues which need to be understood and controlled before the successful adoption of the 7xxx alloy in the automobile industry.[9]

Stress corrosion cracking is a complex phenomenon, involving the simultaneous effect of a susceptible material, minimum threshold stress, and a corrosive medium.[9] Several years of research have led to considerable progress in understanding the nature and causes of SCC and develop ways of preventing SCC through microstructural modifications. [10, 11] However, due to the safety considerations of an automobile, it is imperative to understand the phenomenon fundamentally and design the components so as to avoid any embrittlement or cracking, which could potentially cause failures in the automobile. One of the key requirements to do so is to develop a reliable test method that can accurately evaluate the sensitivity of the alloy to SCC in the automotive applications. This has been a challenge until now due to the complex interactions of various environmental and mechanical parameters. On successful development of a reliable test method, the potential to use the 7xxx alloys in the automobile structure as well as the risks involved can be assessed scientifically. Moreover, the development of a reliable test method will facilitate the understanding the impact of the exhaustive list of influencing parameters on the SCC susceptibility and gain a deeper understanding of the SCC behaviour of the 7xxx alloys.

1.1. Key Objectives and Key Questions

This thesis aims to achieve two key objectives. The first objective is to scientifically understand the influence of key parameters on the SCC susceptibility of the 7xxx alloys and represent this knowledge by designing an accelerated corrosion test. This test method is aimed to provides a reliable baseline for the development and potential applications of the 7xxx alloys in the automobile sector by accurately assessing the SCC susceptibility of these alloys in automotive lifecycle conditions. The second objective is the development and assessment of a methodology which can be used to develop SCC corrosion tests. Each of these objectives is discussed in detail below:

1) ***Analysis of key parameters influencing SCC susceptibility of 7xxx alloys in an automotive lifecycle and representation of these parameters in an accelerated SCC test***

In an automotive lifecycle, a material is exposed to a complex array of environmental and mechanical parameters that could impact the SCC susceptibility of the 7xxx alloy. These parameters have not only individual effects, but also synergistic effects on the

SCC susceptibility of the 7xxx alloys. Thus, testing of SCC, specifically with respect to automobile, poses a serious challenge due to the difficulty in representing and reproducing the automotive lifecycle in an accelerated corrosion test. Although there are already several standardized as well as non-standardized tests that are available to test SCC [12] there is large variations in data received from these tests and the parameters of testing play a very important role in test results, making it easy to misinterpret them.[13-15]. Moreover, extensive research done on the 7xxx alloys for the last few decades have also involved several experimentations in which, experiments are specifically designed to iteratively study and understand individual effects of chosen individual parameters under carefully monitored laboratory conditions. In these laboratory conditions, simulating a wide range of parameters with interactive effects would not only be difficult to implement but could also cause misinterpretation in data and limit the mechanistic understanding of the SCC process. As a result, the behaviour of the 7xxx alloys in these laboratory conditions could vary considerably compared to the actual behaviour of the material in real-world applications, which are generally far more complex and uncontrolled. This difference could potentially lead to variations in the SCC behaviour of the studied alloys, thus leading to misinterpretation or focus on the wrong influencing parameters.

This thesis aims to scientifically analyse the automotive lifecycle by identifying all crucial parameters that can influence SCC and then studying its influence on the 7xxx alloys individually as well as synergistically. With the help of this knowledge, the thesis aims to design a test method which would represent the complexities of an automotive lifecycle in an accelerated form. This knowledge would also in turn help in identifying the key factors and provide relevant direction to focus on for future mechanistic studies of the 7xxx alloys. Keeping these key objectives in mind, the following research questions have been identified which are addressed in the scope of this thesis:

1.1. *What are the key environmental factors that occur in an automotive lifecycle and how do they influence SCC behaviour of the 7xxx alloys?* This question focuses on scientifically understanding the nature and magnitude of the critical environmental factors influencing the SCC behaviour of the 7xxx alloys. With a special focus on the synergistic effects of the various environmental factors present in real-life applications, this question aims to analyse the SCC behaviour of the 7xxx alloys in the complex interactions of the real-world environment rather than individual

environmental parameters. Furthermore, this question aims to utilize this analysis to successfully represent the critical environmental conditions in an accelerated corrosion test which would then aid in qualification of the 7xxx alloys for the automotive application.

1.2. ***What are the critical mechanical parameters that an alloy is exposed to in an automotive lifecycle and how do they influence SCC behaviour of the 7xxx alloys?*** This question aims to gather a deeper understanding of the nature and magnitude of critical stresses that occur in an automobile lifecycle, with a focus on critical stress applications. This knowledge would then be utilized to represent the appropriate stresses in a mechanical specimen in the accelerated SCC test. This analysis would also give potential guidelines for future efficient designing of automotive parts of 7xxx alloys with respect to boundary stresses.

1.3. ***How does the susceptibility of alloys in the developed test method correlate to their behaviour in outdoor exposures?*** This question focuses on the behaviour of the alloys in the real world through long-term outdoor exposure test. To validate the applicability of the developed test method, the output of the test is compared to that of the outdoor exposure test to aim towards a high correlation between the two. This correlation, between the developed test and the outdoor exposure test, would then aid in understanding the SCC behaviour of 7xxx alloys in the real-world application.

1.4. ***What is the influence of alloy content and temper states on the SCC susceptibility of the 7xxx alloys?*** The metallurgical state of the alloy plays an important role in determining its mechanical properties, which in turn is important in determining its utility in the automobile. It also plays an important role in the SCC susceptibility of the alloy. Through the analysis of a wide range of alloys with varied alloy content and temper states, this thesis aims to understand the influence of these metallurgical factors on the SCC susceptibility of the 7xxx alloys. The learning could potentially provide a direction in the future for the alloys and temper states which can be used in the automobile considering their mechanical properties and SCC susceptibility.

2)   Development of a methodology to systematically design and develop stress corrosion tests.

The second key focus in this thesis is the novel methodology itself, which is used to develop the SCC corrosion test method. The complex SCC process is influenced simultaneously by environmental, mechanical as well as metallurgical factors. In order to structure the study and systematically design the test method, the framework of a strategic product development methodology called Design for Six Sigma (DFSS) has been used in this thesis. DFSS is a development methodology that is used to design or re-design products or processes in a systematic and cross-functional manner. [16] Although DFSS is a popular methodology used in the automotive industry for physical product development, this is the first time that this method is used to design a complex stress corrosion test method. The main advantage of the DFSS methodology is its ability to methodically analyse each requirement of the new product and convert them into tangible technical requirements, which are then used as the base to conceptualise and optimise the product being developed. In this thesis, the DFSS framework is used to systematically evaluate the SCC properties of the 7xxx alloys with respect to its various interactive parameters. The DFSS process is not a rigid standardized process, but rather a flexible framework with several models available to choose from.[17] This thesis assesses the DFSS framework and its available tools and design a proof of concept for the methodology which could potentially be used as a template to develop industry-relevant corrosion tests in the future. The developed methodology is compared to conventional corrosion test developments, to understand its potential to replace the conventional methodologies. With this objective in mind, the following questions are focused on, in the thesis:

2.1   Can the DFSS process provide a structured framework for designing of stress corrosion tests? This question focuses on the assessment of the DFSS model and the tools and methods available within its framework. In this thesis, the DCOV model is used to develop the SCC test method which stands for Definition, Conceptualisation, Optimisation and Validation. Each stage is then modified according to the scope of the parameters and requirements and assessed. Finally, a novel methodology is developed and followed to design and develop the SCC test method.

2.2 What is the potential of using the designed methodology for further development of industry-relevant corrosion test methods? This question critically analyses the developed methodology for designing SCC tests, including the advantages and disadvantages of using this methodology. It also compares the novel method to conventional test development methods to establish whether this methodology can be used in the future as a standardisation approach to develop other industry-relevant corrosion test methods.

1.2. Research Approach

As mentioned above, the main DFSS framework model used in this thesis is the DCOV model. In the Definition phase, the analysis of the automotive lifecycle and the design of the SCC test method are structurally broken down through DFSS tools into functional requirements. These functional requirements are then converted into tangible technical requirements which are in turn converted to design parameters of the SCC test method. Since there are several design parameters, they are clustered into two principal categories: Environmental and Mechanical. Each category is then studied separately in the next phases, which are the conceptualisation and the optimisation phase. In order to analyse the metallurgical aspect, four alloys, each with varying contents of Zn, Mg and Cu, are analysed throughout this thesis. Each alloy was tempered to T4, T6 and T7 tempers, hence providing a broad spectrum of SCC susceptibility of materials for testing.

The environmental influences on the SCC behaviour of the 7xxx alloys are evaluated in order to answer Question 1.1 mentioned above. An automobile gets exposed to several kinds of environments depending on its location in the world. [18] Depending on the region, it is exposed to different temperature ranges, humidity, pH and salt contents of exposed precipitations. [19] This could lead to different SCC behaviours of the 7xxx alloy in different climates. One of the key challenges addressed in this thesis is to scientifically study the synergistic effect of parameters and represent them successfully in an accelerated corrosion test cycle. This was done by analysing the critical environmental conditions occurring in an automotive lifecycle and then representing them in an initial design of a novel cyclic corrosion test environment. In

the next step, the influence of the critical environmental parameters effecting the SCC susceptibility is analysed by varying these parameters in the developed corrosion test cycle and scientifically analysing their influence through Design of Experiment (DoE). This data is then used to determine the optimal environmental conditions.

Secondly, the mechanical influences on the SCC behaviour of the 7xxx alloys are evaluated in order to answer the research question 1.2. An automobile is also exposed to a varied range of stresses and forces depending on the automobile part and the load conditions. These include dynamic as well as static stresses in various forms which can be induced from production processes, real-time loading, or other factors. In this thesis, two critical load conditions are analysed to represent the critical stresses which can be endured in the automotive lifetime. Parallelly, through DFSS tools, the design parameters are used, and three mechanical specimens are chosen for further experimental analysis to determine the optimal mechanical specimen. Qualitative experimental analysis is then used to determine the optimal mechanical parameters. The results from testing in each of these stages were incorporated to develop a novel test method, the Mercedes Benz Stress Corrosion Test (MBSC).

Finally, to validate the results obtained from the designed test, an outdoor exposure test is conducted, in which stressed materials were exposed outdoors to four critical climatic conditions for a duration of one year. The behaviour of the alloys in the different climatic conditions is assessed and compared to the results of the novel developed test to assess their correlation and scientifically understand the behaviour of the alloys in the real-world complex environment. Through use of DFSS and the systematic study and understanding of the influencing parameters, this thesis aims to gain a deeper understanding of the SCC behaviour of the 7xxx and move a step closer to assess the usage of this alloy in the automotive industry.

Chapter 2 THEORETICAL BACKGROUND AND LITERATURE REVIEW

2.1. Statistical Analysis by Design for Six Sigma

Six Sigma methodology is a systematic approach toward process improvement using analytical and statistical methods, which is used to eliminate defects in products and processes.[20] Multiple researches have showed that the implementation of the six sigma methodology could lead to improvement in the performance of a company in terms of efficiency, resources and economic benefits .[16, 21-23] The six sigma approach aims to make the performance of processes measurable with the help of key figures.[24] A six sigma process, is a process which has 3.4 defects per million parts.[25] If the scatter of data is too high, six sigma methodologies identify the causes of the process deviation by cause-effect relationship analysis and then proceed towards optimizing the process to reduce or eliminate these causes and achieve the aforementioned level of defects to be qualified as a six sigma process. The six-sigma methodology is not only useful for quality improvement but can also be implemented in all the processes of a company. The most popular approach for the six-sigma process is the DMAIC approach which stands for Define, Measure, Analyse, Improve and Control. [26-28]While the classical six sigma process, aims to eliminate errors and failures in existing products or processes, the Design for Six Sigma is a product generation process (PGP), which aims to support the design and development of a new product or process in such a way that cross-functional, technical requirements are processed in a methodical manner to produce a product with minimized defects and variations at the root level. [16, 29, 30]

The DFSS process is not a fixed methodology like the six sigma, rather a more flexible approach to be used to design or re-design new products or processes in a systematic manner, which are measured by the customers and critical to quality measures.[31] There are several advantages of using the DFSS approach for the design and development of new processes and products.[17] Firstly, the DFSS approach focuses greatly on the customer requirements and orients the project towards systematically

fulfilling the requirement. The DFSS methodology also has the capability of predicting the quality of design at the start of the project, allowing for better planning and implementation. The DFSS approach provides strategic tools to allow integration of cross-functional design requirements. Moreover, the methodology focuses on quantitative measurements in the early design phases and uses process capabilities to make final decisions. [32] However, there are also certain challenges faced in the implementation of the DFSS process. It can be tedious and require extensive time and require extensive resources, in terms of time and money, for the implementation.

Unlike the Six Sigma process, the DFSS process is far less standardized and contains various phase models to choose from.[33] Although, there are several published DFSS methods in literature, there is no single established structure which can be used by companies, which in turn also makes it difficult for the companies to implement the methodology. [34] However, this also gives companies the flexibility to establish their own methodology which would fit their needs. The Mercedes Benz standard model for DFSS is the Definition-Conceptualisation-Optimisation-Validation or DCOV model, which will also be used for this thesis. The DCOV process consists of 4 main steps which will subsequently be explained.

Definition Phase: The aim of the definition phase is two-fold. Firstly, in this phase the problem statement, the aim, and the exact scope (in-scope and well as out-of-scope) of the project and the project benefit is identified and defined. Each of these points are discussed, analysed and are documented into a project proposal. The project proposal also contains administrative information such as the project team, budget and timeline of the project. This information acts as a guideline for decision making throughout the project, with every decision aimed at being in line with the defined goals of the project and within the scope of the project.

The next steps are to recognize the customer requirements (Voice of Customer) and convert them into tangible, measurable functional requirements. These functional requirements will be used in later stages to develop the design parameters. The advantage of this phase is that the fundamentals of the project, which is the problem statement, the scope and the outline of the project is clearly structured and documented. This acts as a guideline throughout the project and can be referred back

to at each stage of the project. Each customer requirement is taken into consideration and converted into measurable functional requirements, which are in-turn used to develop design parameters in the next phase.

Conceptualisation Phase: In the Conceptualisation phase, various concepts of the new product or process are identified using various creativity tools such as brainstorming, morphological analysis and Walt Disney Method. This identified concepts are then filtered and rated based on the functional requirements, which are determined in the previous stage. Analysis and ranking tools such as quality function deployment are used to compare and assess the chosen concepts with respect to the customer requirements which are defined in the definition phase. Once the choice of concept is made, risk assessment of the concept is carried out by breaking down the functions into sub-functions and each possible risk factor that could occur in the sub-function is listed and categorized into risk levels. Precautions to avoid or reduce the risk of errors are also determined in this step. This step helps to identify the potential error variables and reduce the probability of occurrence of these risks at the root level during the design process. In the next step of this stage, the design parameters that could influence the output of the concepts are listed using tools such as fish-bone analysis. The conceptualisation phase ends with the final chosen design concept of the process or product along with listing of the design parameters which influence the output of the designed process or product.

Optimisation Phase: In the optimisation phase, the design parameters are filtered using tools such as Pareto and the filtered parameters are then analysed in detail via Design of Experiment (DoE). The aim of the DoE is to find the optimized parameters for the designed product or process, which fulfil the target value which is defined in the earlier stages and fulfils the customer requirement which is determined in the definition phase. The first step towards optimisation is measurement system analysis (MSA). MSA is a tool used to determine the initial reproducibility and repeatability of the designed system or process, so as to choose the direction of optimization. The aim of this tool is to determine the influence of the operator on the output of the system or the process (reproducibility) and the influence of the scatter of data when the same operator repeats the test (repeatability), which is represented by %GRR value, which is further described in section 3.4.5.[35] Once the Gage R&R value is determined and

the direction of optimisation is determined, design of experiment is carried out in order to determine the optimal parameters. DoE is a tool which is used to solve complex problems in which multiple variables influence the output of the response and two or more variables interact with each other. [36] The DoE is superior to other traditional methods such as 'one variable at a time' (OVAT) method since it uses resources effectively to analyse the influence of variables on the output [36] The process of design of experiment is further discussed in section 3.3.3.

Validation Phase: The last step of the DFSS methodology is the validation phase. The aim of this phase is to validate the outcome of the newly developed process or design and achieve maximum process capability with respect to the earlier defined customer requirements and functional requirements. This is done weighing the designed outcome against the earlier defined requirements and completing the Scorecard which was filled in the definition phase. Tools such as process capability test, reliability test and lifespan tests are used to determine the robustness and process capability of the designed process. Once this is achieved, the newly designed product is handed over to the responsible bodies for further use. Further steps to be carried out is determined and feedback is also carried out to determine the 'lessons learnt' from the project. Finally, the project is ended by acceptance of the output by the customer, which is validated by completion and confirmation on the project proposal.

2.2.   Aluminium 7xxx Alloys

Aluminium offers a wide range of beneficial properties such as high strength-to-weight ratio, good corrosion resistance in comparison to the traditional ferrous alloys and good machining properties. Due to these properties, it has become an important choice of metal in the aerospace industry, construction industry and the automotive industry.[9] However, pure aluminium, has low mechanical strength and almost always needs to be alloyed for engineering applications. Based on the alloying elements, the aluminium alloys are divided into different categories, which is detailed in the section below. Due to its high strengths, the Al-Zn-Mg-(Cu) alloys, also called the 7xxx series alloys are extensively used in the aerospace industry.[37, 38] However, higher strength 7xxx alloys are susceptible to SCC making it difficult to be used in the automotive industry.

Since this thesis focuses on the 7xxx series, the subsequent sections will focus on the properties and corrosion behaviour of the 7xxx aluminium alloy.

2.2.1. Nomenclature of Aluminium Alloys

The primary alloying elements added to aluminium in order to increase its mechanical strength are copper, magnesium, manganese, silicon, zinc, and tin. The alloys are classified according to these alloying elements into groups which are shown in the table below. According to the European norm DIN EN 573:2005, [39] the nomenclature for the aluminium alloys is 'EN AW-alloy group' where EN stands for European Norm, A for aluminium and W for wrought alloys. For e.g., EN AW-7075 is an alloy in the 7xxx series. Through this thesis, the complete nomenclature is represented by just the alloy group name (e.g., EN AW-7075 is mentioned as 7075), for ease of reading. Besides the alloying elements, the mechanical properties of aluminium alloys are also determined by mechanical and thermal treatments. Table 2.1 shows the major alloying elements, their strengthening methods, and their strength ranges. [9, 39-41]

TABLE 2-1:   OVERVIEW OF GROUP OF ALUMINIUM WROUGHT ALLOYS [9,39-41]

Wrought Alloy Groups	Major Alloying elements	Strengthening Methods	Strength Range [MPa]
1xxx	Min 99% Al	Cold Work	70-175
2xxx	Cu	Heat treatment	170-319(1-2.5 wt.% Cu) 380-520 (2.5-6 wt.% Cu)
3xxx	Mn	Heat treatment	140-280
4xxx	Si	Cold work and Heat Treatment	105-350
5xxx	Mg	Cold work	140-280 (1-2.5 % wt. Mg) 280-380 (2.5-6% wt. Mg)
6xxx	Mg, Si	Heat treatment	150-380
7xxx	**Al Zn Mg (Cu)**	**Heat treatment**	**380-520 (Al-Zn-Mg)** **520-620 (Al-Zn-Mg-Cu)**
8xxx	Li Cu Mg	Heat Treatment	280-560

The principle focus of this thesis is the aluminium 7xxx (Al-Zn-Mg-Cu) series. With zinc as its primary alloying element, and magnesium or magnesium and copper as secondary alloying elements, the aluminium 7xxx series is the strongest aluminium alloy group with a yield strength of above 500MPa [9]. Other elements such as chromium and zirconium are added to the alloy to improve its mechanical properties. The mechanical properties of 7xxx alloys can be enhanced by means of precipitation strengthening by different aging processes.

2.2.2. Microstructure of 7xxx Aluminium

The mechanical and chemical properties of the 7xxx alloys can be modified by the precipitation strengthening through different aging processes. The high strength of the alloy comes from the precipitation of finely dispersed metastable $MgZn_2$ precipitates, or $Mg(Zn,Cu)_2$ precipitates in the copper containing 7xxx alloys.[41] The supersaturation of vacancies allows diffusion and hence leads to the formation of Guinier-Preston Zones (GPZ). The general precipitation formation sequence of 7xxx alloys on aging is as follows:

$$\alpha \rightarrow \alpha + GPZ(I \ and \ II) \rightarrow \alpha + \eta' \rightarrow \alpha + \eta$$

where α is the supersaturated solid solution, η' is a semi-coherent intermediate $MgZn_2$ phase or Mg(Zn, Cu) phase and η is incoherent equilibrium $MgZn_2$ or $Mg(Zn, Cu)_2$ phase [42, 43]. Once precipitation initiates, the saturated solid solution first develops solid clusters. These solid clusters enable the formation of non-equilibrium precipitates. The final structure consists of equilibrium precipitates, whose contribution to precipitation strengthening becomes minimal. The 7xxx alloys follows a three-step heat treatment process. In the first step, solution annealing is carried out on the alloy to dissolve all the alloying elements in the matrix. This is carried out at temperatures ranging from 450°C to 550°C. Once the alloy is solution annealed, it undergoes quenching, wherein the alloy is exposed to high cooling speeds, which result in the formation of precipitates within the matrix. Once the alloy is quenched, it undergoes the aging process in which finely distributed precipitates are formed, leading to the increase in strength. [44] Aging can take place at room temperature, called natural aging which is depicted by the designation T4.[45] Artificial aging can also take place

at moderate temperatures of about 140°C to 190°C, leading to higher strengths. During aging, two aging peaks are achieved which can be attributed to coherent high density GP zones and semi coherent ή phases.[46] The high density GP zones formed in the first aging peak are weak and soft and they determine the strengths achieved in the first peak. Aging the alloy beyond this point results in dissolution of the GP zones and reduction in strengths. The second peak is caused due to the high density of the semi coherent ή phases, according to the Orowan mechanism. [44] Larger volume fractions of ή precipitates results in more difficulty in movement of dislocation and hence higher strengths. Once maximum strength is achieved, the alloy is peak aged, depicted by T6. The high strength of the alloy at the T6 condition is attributed to finely dispersed ή ($MgZn_2$) or $Mg(ZnCuAl)_2$ precipitates, which tend to obstruct the movement of dislocations in the matrix.[10] Tempering an alloy beyond peak age is called over-aging which is depicted by the nomenclature T7. In this stage the coherent η phase is the main precipitate. Over-aging the alloy changes the precipitation sequence and corrosion properties of the alloy.[47] A summary of the nomenclature of tempering used in this thesis is described below.

TABLE 2-2:   THE MAIN TEMPER DESIGNATIONS AND DESCRIPTIONS OF RESPECTIVE TEMPER TREATMENTS ACCORDING TO DIN EN 515:2017-05 [45]

Temper Treatment	Description
T4	Solution heat treated and naturally aged
T6	Solution heat treated and artificially aged to maximum strength
T7	Solution heat treated and overaged

2.3.   Forms of Corrosion Influencing Aluminium

According to the DIN EN ISO 8044 [48] corrosion is defined as "*physiochemical interaction between a metallic material and its environment that results in changes in the properties of the metal, and that may lead to significant impairment of the function of the metal, the environment or the technical system, of which these form a part*". There are multiple types of corrosion based on their electrochemical nature.[48] However, since the focus of this thesis is mainly aluminium, this section will focus

mainly on the various corrosion types on aluminium. Although aluminium is an electrochemically active material, it exhibits excellent corrosion resistance due to a natural barrier oxide layer formed on its surface. The oxide film is stable at pH 4 to 8.5 and is naturally self-healing, hence any damage to it is rapidly repaired.[9, 49, 50] However, aluminium is not completely free of corrosion attack and undergoes specific forms of corrosion. A brief description of some of the localised corrosion occurring in aluminium alloys is given below.

Pitting Corrosion: This form of corrosion results in localised cavities or "pits" on the metal surface due to micro flaws in areas of the stable oxide layer on the aluminium surface. [51, 52]These micro flaws leads to localised depassivation of oxide layer and adsorption of chloride ions within the stable oxide layer. The contact of aluminium ions with the metal outside the hole results in a reduction reaction, which in turn increases the pH of the solution outside the hole. Meanwhile, there is a reduction in the pH within the hole due to higher hydrogen and chloride ion concentration. The localised region becomes anodic to the surrounding area which acts as a cathode. A localised galvanic reaction is formed between the two regions resulting in formation of deep, acidic pits. [53]

Intergranular Corrosion (IGC): Intergranular corrosion is a selective corrosion that generally occurs on or around the regions of grain boundaries in the matrix of polycrystalline metals. This type of corrosion is mainly observed in the 2xxx, 5xxx, 6xxx and 7xxx series.[54] Intergranular corrosion occurs due to differences in electrochemical potential between phases (or precipitates) at the grain boundaries and matrix resulting in microgalvanic corrosion along grain boundaries. This leads to dissolution of precipitates on grain boundaries or the regions adjacent to it depending on which has the higher electrochemical potential. The precipitates on the grain boundary could be anodic to the matrix, such as the Mg_5Al_6 in the 5xxx series which would corrode preferentially over the matrix. [55-57] The precipitates could also act as a cathode as in the case of $CuAl_2$ of the 2xxx series alloy, which results in the corrosion of area surrounding the precipitate, leaving a precipitate free zone at the grain boundary.[58]

Environmentally Induced Cracking: Environmentally induced cracking (EIC) is a failure arising from a combined action of corrosive environment and tensile stresses on a susceptible material leading to a brittle mechanical failure. [59] Based on the failure mechanism, EIC can be further classified into stress corrosion cracking, corrosion fatigue cracking, liquid-metal embrittlement and hydrogen induced cracking (HIC) [59]. Although the nature of these failures appears similar, the underlying mechanisms in each of these types of corrosion varies. Stress corrosion cracking belongs to the category of environmentally induced cracking, where mechanical stress also plays a role in the mechanism of the corrosion. It varies from other forms of EIC corrosion due to variation in mechanism and stressing conditions for e.g., static, or dynamic stressing. Since this thesis focuses mainly stress corrosion cracking, the following sub-section discusses details of stress corrosion cracking, especially of the aluminium 7xxx alloys.

2.4.   Stress Corrosion Cracking

Stress corrosion cracking is the synergistic effect of three parameters (i) susceptible material, (ii) specific corrosive environment and (3) stresses (residual or applied).[60] For stress corrosion cracking to occur, all three factors must act simultaneously. [59, 61] Stress corrosion cracking can be critical with respect to an automotive perspective, since it can lead to a sudden brittle failure of material, which is stressed much below its yield limit. The aluminium 2xxx, 5xxx (with high Mg) and the 7xxx series show the highest susceptibility to this form of corrosion among all the aluminium series. Stress corrosion cracking was responsible for multiple system failures in the aerospace industry in the 1960s and 1970s, which is why it needs to be thoroughly studied and understood before the 7xxx alloy is utilized in the automotive industry.[62]

2.4.1.   Crack Initiation and Morphology

In order for stress corrosion cracking to occur the three parameters, stress, material and environment must act parallelly.[63] Stresses can be in the form of applied or residual stresses, which are induced by means of machining, heat treatment, cold working or grinding. Stresses could be in the form of direct static loading or low-amplitude cyclic loading. [59, 60]. Along with critical stresses, environmental

parameters play an important role in stress corrosion cracking. Temperature, pH, salt concentrations and compositions etc. can influence the SCC susceptibility of the material. It should be noted that SCC is an environment specific phenomenon, which means that an environment could be critical to SCC for a certain alloy but not for another alloy. Lastly, the stress corrosion cracking is also material specific. Material properties such as microstructure, precipitation, grain size and structure could have a huge impact on the SCC susceptibility [61].

Stress corrosion cracks cause low-deformation and brittle fractures, which usually take place without the formation of corrosion products. It could lead to sudden, unforeseeable crack initiation and propagation, leading to component failure which cannot be detected earlier. A predominantly intergranular crack course is characteristic to the aluminium materials. [64] Figure 2.1 (a) shows a typical SCC crack in an AlZn9Mg2.2Cu alloy. Cracks begin on the surface orthogonally to the applied stresses and initially runs perpendicular before branching out into tuft-like sub-cracks. The number and characteristics of the branches are proportional to the level of applied stresses.[65] Crack initiation requires the presence of all three factors, critical stress, critical environment and a susceptible microstructure in order to initiation a cracking nucleus. Surface inhomogeneities such as pre-existing crack-like defects, metallurgical homogeneities such as inclusion from porosity, hot tears, weld defects etc. could act as initiation points for the SCC crack to initiate. Other forms of corrosion, such as intergranular corrosion, crevice corrosion could also act as crack initiators.[60] [66]

The transition from localised corrosion sites to SCC depends on various factors such as the pit depth and shape and local stress factors. After the initial incubation period, once the threshold stress is reached, crack propagation occurs. When there are multiple crack initiation sites close to one another, these sites coalesce to form one large crack initiation site before crack propagation starts to occur. Cracks continue to initiate and coalesce, until a minimum threshold stress at the crack tip is achieved which is expressed in terms of stress intensity factor (K) in fracture mechanics. [60]

A typical stress corrosion crack growth curve is seen in Figure 2.1(b) [67]. The first region, labelled region 1, is K_I dependent. It also shows that stress corrosion crack growth does not initiate until it reaches a critical stress intensity factor of K_{ISCC}. Once K_{ISCC} is reached, the crack propagates quickly as a function of K and reaches region 2. This region is independent of K implying that the corrosion mechanism in this region is only time dependent [67]. This region may be a chemical or diffusion rate limiting process [61]. Finally, region 3 is reached where the crack growth is dependent on K once again. This sudden surge in crack growth can be attributed to the fact that it is soon approaching K_{IC} which is critical stress intensity factor, leading to final failure [67].
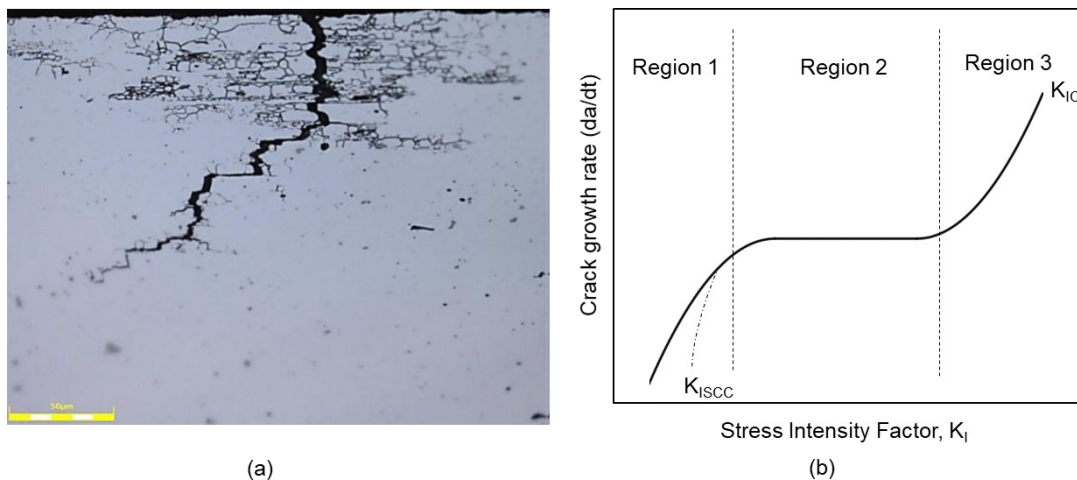
FIGURE 2-1: (A) SCC WITH INTERGRANULAR CORROSION IN ALZN9MG2.2CU (WHICH WILL BE LATER KNOWN AS KK18-T4) ALLOY (B) SCHEMATIC OF CRACK GROWTH RATE WITH RESPECT TO STRESS INTENSITY FACTOR [MODIFIED FROM [67]]

2.4.2. Mechanisms of Stress Corrosion Cracking in Aluminium 7xxx alloys

There are various SCC mechanisms proposed for different SCC systems. These include Hydrogen Enhanced Local plasticity (HELP), hydrogen enhanced decohesion, corrosion enhanced local plasticity (CELP), hydride formation, slip dissolution, adsorption induced dislocation emission (AIDE) and film induced cleavage. [60] For high strength Al-Zn-Mg-(Cu) alloys, there are three widely published SCC mechanisms. The earliest accepted mechanism was the anodic dissolution assisted cracking (ADAC), which causes embrittlement due to grain boundary weakening. However, in recent years, the role of hydrogen induced cracking has been widely accepted as a mechanism for SCC in aluminium alloys. Furthermore, theories of

synergistic effects of HIC and ADAC have also been researched in the recent years. Each of these mechanisms have been discussed in detail below.

Anodic Dissolution Assisted Cracking: One of the theories explaining the SCC phenomena in high-strength Al-Zn-Cu-Mg alloys is the anodic dissolution assisted cracking. [57, 60, 62] According to this theory, localized decomposition occurs at grain boundaries resulting in electrochemically active paths. Corrosion along these paths produce fissures with normal components of tensile stress concentrated at the tip of the fissures. When a threshold stress is reached, there is localised plastic deformation at certain grain boundaries which in turn causes the fissures to propagate. This results in exposure of fresh unfilmed metal to be exposed to the corrosive electrolyte leading to further corrosion. [68] This type of cracking characteristically displays an intergranular mode of failure.

This theory was supported by several studies such as Choi et al. [69] who suggested initiation of SCC by electrochemical dissolution of grain boundaries on a 7039 alloy. Uesaki et al. who carried out TEM analysis and observed the precipitates aligned along the grain boundaries showed a tendency to dissolute during exposure to the test environment indicating an anodic dissolution mechanism for failure.[70] Kannan and Raja observed anodic grain boundary precipitates which caused the dissolution and crack propagation, and the microstructure of alloy with peak aged state suggested an intergranular stress corrosion cracking mechanism (IGSCC). Although this theory is consistent with many experimental observations, some of the experimental observations cannot successfully be explained by this theory. Speidel noted that this theory does not account for the materials that are susceptible to intergranular corrosion but are not susceptible to stress corrosion cracking and vice versa. [71]

Hydrogen Induced Cracking (HIC): Although in earlier studies, the anodic dissolution model was widely accepted as the SCC mechanism for the 7xxx alloys, it was later accepted that the brittle nature of environmentally induced fractures can be accounted for by a hydrogen embrittlement mechanism. One of the main pieces of evidence supporting this mechanism was due to the observation that degradation can occur from a moist environment at humidity levels well below that required for condensation at a crack tip. Without condensation it is difficult to perceive how preferential anodic

dissolution mechanism of stress corrosion cracking can occur. [72] Crack arrest markings and striations observed in various studies further indicated towards a hydrogen induced embrittlement process. [73-77]. There are several other studies conducted pointing to the [78, 79]

Holroyd and Scamans [78] studied the activation energies cracks under sustained-load of AA 7xxx alloy series exposed to moist air and distilled water. They proposed that the crack propagation in these alloys were dominated by hydrogen-related process, which are formed due to chemical or electrochemical reactions within the material. Albrecht et al. [79]   also studied the hydrogen-assisted fracture of charged and uncharged 7075 aluminium alloy in various temper conditions. Their study also indicated toward hydrogen embrittlement mechanism. The hydrogen embrittlement was influenced by the aging conditions, with underaged displaying maximum embrittlement and overaged showing the least. Other evidence includes reversal of hydrogen as demonstrated by Hardie et. al. [80] and evidence of higher hydrogen concentration at grain boundaries found by Smiyan et al. [81]

There is no consensus on a single mechanism by which hydrogen induced cracking occurs. Currently, the most suggested mechanisms are decohesion, hydride formation, dislocation theory and pressure theory. The decohesion model is described as the weakening of binding energy and cohesive forces due to the dissolved hydrogen, resulting in a gap fracture with brittle crack propagation.[62, 63, 68, 82, 83].Stress induced hydride formation leading to cleavage fracture of the brittle hydride phase has also been reported as a hydrogen embrittlement mechanism. [62, 68, 84]. The pressure theory, hydrogen is accumulated in areas of increased energy such as pores, inclusions, and precipitates without recombination due to the presence of promoters. Once the hydrogen is in the material, it recombines resulting in pressure within the specimen causing formation of localized cracks and bubbles within the specimen when critical stresses are reached.[85] Finally, the dislocation theory suggests that dislocations within the material get pinned due to hydrogen atoms, which causes lower mobility of dislocations resulting in reduced ductility. [86] There are also theories of synergistic effects of SCC and HIC which have been suggested by researchers such as Najjar et. al. [87], Magnin et. al.[88] and Schnatterer et. al.[51]

2.5. Factors influencing Stress Corrosion Cracking of 7xxx Alloys

Stress corrosion cracking is a combined effect of material, environment, and stress factors. A change in any one of them can have a great influence on the SCC properties and can also impact the influence of other factors. It is due to this interdependence that it is essential to systematically study these individual factors.

2.5.1. Environmental Factors Influencing SCC

Through the lifecycle of an automobile, it is exposed to a variety of environmental conditions which causes varied corrosion damage to the vehicle. The variation in environmental parameters such as temperature, pH, humidity, and salt composition in the climate of a region could also influence the SCC susceptibility of the materials, if they are exposed to these variations for a long term. Thus, it is essential to analyse the presence of these factors in the automotive lifecycle and its influence on the SCC susceptibility of high strength 7xxx alloys individually.

One of the main factors found in nature is the different kinds of salt compositions, which is different cations and anions, which could have a significant effect on SCC susceptibility. Bhaskar et al. studied the concentration of various ions in rainwater such as SO_4^{2-}, NO_3^-, Cl^-, NH_4^+ and the pH at various GAW stations in India for a period of 31 years from 1981 to 2012. [86] A maximum concentrations of about 500 µeq/l of Cl^-, 300µeq/l of SO_4^{2-}, 308µeq/l of NO_3^-, 100 µeq/l of NH_4^+ and 734 of HCO_3^- concentration was found at the sites in India. Santos et al. [87] also analysed the rainwater for the above-mentioned ions at the Portuguese west coast (Aveiro) from 2008 to 2009. They found a maximum of 200 µeq/l of Cl^-, 31.5 µeq/l of SO_4^{2-}, 39.5µeq/l of NO_3^- and 18 µeq/l of NH_4^+. Xu et al.[88] carried out the similar analysis in Beijing and Chizhou, China from the period 2011 to 2012 and found that the predominant ions present in the rainwater were SO_4^{2-} and NH_4^+, with a maximum of 798 µeq/l of SO_4^{2-} and 545 µeq/l of NH_4^+. The NO_3^- concentration showed a maximum of 86 µeq/l. Rainwater analysis in Harz, Germany in 2013 and 2014 also that maximum content of ions which were observed were 68.5 µeq/l for SO_4^{2-}, 101 µeq/l NO_3^-, and 185 µeq/l NH_4^+ [89]. There are several other research conducted in various parts of the world

indicating significant presence of the ammonium, nitrates, and sulphate ions in the rainwater. [90-92] The reader is directed to a global study conducted by Vet et al. [93] which gives a complete overview of the rainwater and precipitation analysis of various parts of the world. This analysis makes it an important aspect to study these ions with respect to its influence on SCC and incorporate them into the development of the SCC testing, to recreate the critical environmental parameters in the SCC test.

Speidel and Hyatt observed that the susceptibility of the 7xxx alloys had the same effect when it is exposed to 100% relative humidity as it is in distilled water, thus showing the significant of aqueous solutions on the SCC susceptibility. They observed that the following cations: Li^+, Na^+, K^+, Rb^+, Cs^+, Ca^{++}, Al^{3+} and NH^{4+}, did not influence the crack growth rate of the stress corrosion crack, however, indirectly could influence the susceptibility by affecting the solubility product of the anions.[71] Braun's study contradicted the data above with regard to Ammonium cation, observing that ammonium cation significantly increased SCC susceptibility for 7475-T651 plate material.[89]

With regard to the influence of anions, it is well-known that halides accelerate the SCC susceptibility of 7xxx alloys. [62, 71]. Due to the abundance of chloride in the environment it is used as a standard solution in testing of SCC susceptibility of 7xxx alloys. Besides the halide ions, which have the highest influence of SCC susceptibility on the 7xxx alloys, studies have shown that other ions such as sulphates, nitrates, bicarbonates, ammonium and other ions could substantially influence the SCC susceptibility.[77, 89-91]. Braun studied the effect of behaviour of various aluminium alloys, including 7475-T651 and 7075-T7351, under constant load test in 0.6M chloride solutions with various additional salts, with anion to chloride ratio of 0.1.[89] The study concluded that the addition of sulphates, nitrates, hydrogen carbonates, hydrogen phosphates, sulphite and carbonate promoted the susceptibility of 7475-T651 to SCC. The 7075-T7351 was immune to SCC failure in all solutions apart from chloride-nitrate. This was attributed to increased pitting and transgranular SCC. [89] Nguyen et al. [92] studied the crack chemistry of 7075-T6 alloy in 1M NaCl, $NaNO_3$ and Na_2SO_4 solutions, respectively. They observed a reduction in crack growth rate in sulphate and nitrate solutions at open circuit and anodic potentials, but the rate increased significantly in

the cathodic range. The acceleration of crack growth rate in the $NaNO_3$ was attributed to the formation of ammonia within the crack.

Another important factor influencing SCC susceptibility is the form of environment around the material. Speidel and Hyatt observed the behaviour of various 7xxx alloys in various gaseous environments to study their influence on the stress corrosion crack propagation. It was observed that, in the absence of humidity, the exposure of 7xxx alloys to hydrogen, nitrogen, argon or dry air has no significant difference in SCC susceptibility.[71, 93] However, on exposure to even a small amounts of humidity, stress corrosion cracking will initiate. [71] The studies conducted by Speidel and Hyaat showed that there is linear dependence of the double logarithmic plot of the stress corrosion crack velocity and the relative humidity and increasing the humidity in air shifts the V-K curve to lower stress intensities. [71]

Temperature also plays an important role in influencing the SCC properties of the 7xxx alloys. Depending on the region the automobile is present in, it could get exposed to extreme temperatures ranging from extreme high to extreme low. Moreover, there are also internal components and processes taking place in the automobile, which results in higher temperatures observed in certain parts of the vehicles. [94, 95]. Mercedes Benz internal analysis on the temperatures observed in the body-in-white (BIW) of the cars reveals, that the surface of the BIW could reach maximum temperatures of up to 80°C. This factor should also be considered while recreating the critical environmental parameters in the design of the SCC testing.

Speidel and Hyatt observed that an increase in temperature lowers the minimum stress intensities in region I, as well as increases the speed of crack propagation in region II. [71] They approximated the correlation between the crack velocity and temperature in region II to be exponential with a factor of activation energy and the same with region I with the addition of experimental constants to their empirical formula. [71]However, it was experimentally determined that with varying alloys, the activation energy also varied. This could indicate that there could be different rate-controlling processes in different alloys. Onoro and Ranninger [96] also found a linear relationship between the log of stress corrosion crack growth rate and reciprocal of the temperature on 7075 alloys. They claimed that temperature influences the chemical reactions at the crack

as well as the rate of diffusion of corrosion product from corrosion environment to the material. Young and Scully studied the effect of temperature on the crack growth rate of 7050 alloy and found an Arrhenius-type temperature dependence. [97]

pH also plays an important role in influencing the SCC, due to the variation in pH of solutions that the automobile is exposed to in various parts of the world. Bhaskar et. al. studied the pH in various parts of India and found the annual pH ranged from 4.77 up to 7.31 from all the stations. [98] Xu et al.[99] carried out the similar analysis in Beijing and Chizhou, China from the period 2011 to 2012 and found that the average pH range was highly acidic ranging from 3.78 to 5.67. Rainwater analysis in Harz, Germany in 2013 and 2014 also revealed an acidic average pH ranging from 4.4 to 6.8. [100] There are several studies carried out on the effect of pH on the SCC susceptibility of 7xxx alloys. There is a common consensus in the studies of the 7xxx alloys that with increasing acidity, SCC susceptibility also increases. [10]However, this effect varies with the different regions of V-K curve as observed by Speidel and Hyatt. [71] Research also shows variation in the chemistry of the bulk solution from within the narrow crack.[101, 102] Rout et. al. [103] carried out potentiodynamic polarisation and slow strain rate test (SSRT) on 7150 alloy (6.3 wt.% Zn, 2.4 wt.% Mg, 2.3 wt.% Cu) in NaCl solution at various pH levels. They observed that SCC susceptibility was greater at a pH of 1 and 12, as compared to that of pH 7. These results could also be attributed to the fact that the protective oxide layer of aluminium is unstable, accelerating other corrosion forms.

2.5.2. Mechanical Factors Influencing SCC

The nature and magnitude of stresses that the metal is exposed to in the automobile also has a significant influence on the SCC initiation and propagation, making it an important aspect to analyse for development of an SCC test. Although it has been generally accepted, that a tensile stress is required for SCC to occur, there have been studies that show that other modes of stress could also cause SCC. Chu et al. [104] investigated the SCC behaviour of 7075 alloy under compressive stresses and concluded that when the compressive displacement exceeds a critical value, SCC could occur. John et al. observed that due to the triaxial stress field in Mode I (tension), which provides a driving force for hydrogen embrittlement, it is more critical to hydrogen

embrittlement as compared to Mode III (torsion), where the triaxiality is absent. [105] Similar observations were found by Pickens et al. who studied the hydrogen embrittlement properties of 5083 alloy under different load conditions and found higher HE susceptibility in Mode I (tension). [106] Zhang et al. observed that the incubation time for an SCC crack to occur was significantly affected by prior application of tensile overload or compressive underloads. [107] Endo et al. concluded that specimen thickness determined whether the crack propagated in plane stress or plane strain condition and thus had an influence on the threshold stress and the crack growth rate in stage II. [108]

The load direction with respect to the grain flow plays an important role in SCC susceptibility. Since the stress corrosion cracks in 7xxx aluminium alloys are generally intergranular in nature, they follow the path of grain flow. Speidel et al. observed that the threshold stress is the lowest at the short transverse direction, since SCC takes the shortest path to failure and tensile stresses are nearly perpendicular to the grain boundaries in this path.[62] This is followed by the transverse direction and then the longitudinal direction. Sprowls and Brown also studied the effect of grain orientation and stress direction with respect to SCC susceptibility [109] on extruded 7075-T6 samples and concluded that short transverse was most susceptible and longitudinal had the highest resistance to SCC.

Residual stresses caused by various production processes such as forging, rolling etc. cause a significant increase in localised tensile stresses within the material. They may also result from quenching the materials after solution heat treatment. Quenching complicated designs and geometries with varying cooling rates in different regions of the body, could also cause residual tension stresses that would be carried on without further machining as well. Another source of sustained tensile stresses is the formation of voluminous corrosion products within the cracks itself. [71] These stresses could overlap with the external stresses and influence SCC susceptibility. Hyatt studied the effect of residual stresses on the stress corrosion crack growth rate of 7079, 7075 and 7175 alloys. [110] They observed that residual stresses effectively lower threshold stresses, therefore increase chances of initiating stress corrosion cracks. They also accelerate the average growth rate of the stress corrosion cracks.

During the lifecycle of an automobile, the loads which the vehicle experiences are varied and complex in nature.[111] In order to safely design a component, it is important to consider these load cases. Two such critical local load cases at Mercedes Benz AG are the towing assembly and the door assembly, which is also analysed in detail within the scope of this thesis. The towing assembly consists of a hook which is bolted onto the frame of the vehicle through a towing hook pipe, passing through front protection plates and reinforcement plates to the anti-collision plates. [112] Varying load cases are tested on the towing assembly to simulate the actual towing event, which could be done in multiple angles. Wang et al. carried out the FEM simulation on the assembly with varying load scenarios of magnitude and angle. High stresses and localised plastification were observed in the towing hook and towing pipe as well as the reinforcements. [112] Raj et al. also carried out FEM simulations on the towing assembly using various alloys and found that use of aluminium in the assembly, resulted in large strains in the components.[113] Other research carried out on the towing assembly also shows localised stresses and large strains occurring in mostly in angular loading of the assembly.[114]

The door assembly is not only one of the most vital parts of the automobile, but also critical to the safety of the passengers in the vehicle. Therefore, it is important to ensure that there is no critical loading on the door assembly. [115] There are various scenarios in which the door and the door hinges which are attached to the door and the car body undergo localised stresses, such as door slamming or door lowering. Darwish et al. conducted numerical simulations on the various load conditions on the door and showed high stresses that could occur in the door at various conditions.[115]

2.5.3. Metallurgical Factors Influencing SCC

Stress corrosion cracking is a material specific phenomenon. Therefore, factors such as alloy composition and microstructural modifications in the material can influence the SCC susceptibility substantially. [10, 60, 62]

Effect of Zn and Zn/Mg Ratio: Zn, Mg and Cu are the primary alloying elements constituting the 7xxx series and have the highest effect on the SCC susceptibility of the alloys. Lin et al. [116] explains the mechanism of corrosion in the 7050 alloy. Zn

and Mg form $MgZn_2$ precipitate, known as the η, which are attributed to give the high strength to the 7xxx alloys. Since Zn and Mg are more electrochemically active compared to aluminium in the salt solution, addition of Zn and Mg to the solid solution shifts the corrosion potential of the aluminium towards the anodic region. Since the Mg and Zn diffuse from the matrix to the grain boundaries, there is lower $MgZn_2$ concentrations in the matrix resulting in the matrix being shifted towards the cathodic direction. This causes localised intergranular corrosion and weakens the grain boundaries, resulting in easier crack propagation under tensile stress conditions. Similar theories have also been suggested by other researchers [62, 117, 118] Gruhl carried out TEM and EDX analysis on materials with varying alloying compositions and heat treatments, to study its influence on the SCC susceptibility. One of the most significant observation from the study was that with increasing Zn content at the grain boundary, the time to fracture clearly reduced. [117]

Gruhl's extensive studies on various alloys with varying Zn and Mg content showed that along with the sum of Zn and Mg, even the ratio of Zn/Mg had an influence on the SCC susceptibility. The study concluded that with a sum of 8 wt.% of Zn and Mg, maximum SCC resistance was observed at an Zn/Mg ratio of 2.7 to 2.9 , which approximately corresponds to Zn:Mg mole ratio of 1. [117, 119] Chen et al. also investigated the SCC susceptibility of Al-Zn-Mg alloys with Zn/Mg ratio varying between 4.53 and 12.65 and Zn+Mg ≈ 7 wt.%. They observed an increase in SCC resistance with decreasing Zn/Mg ratio. This phenomena was attributed to the narrowing of PFZ and lower concentration of solute Zn in the matrix, hence enhancing the SCC resistance.[120] Rao et al. claimed the optimal Zn:Mg ratio depended on the total solute content in the matrix. SCC resistance for alloys with Zn+Mg of 4.5-6.0 wt.%, was maximum at a Zn:Mg ratio of ~2.5, whereas for the total content of above 8 wt.% had maximum SCC resistance at a Zn:Mg ratio of above 3. [10]

Effect of Mg: The selective absorption of hydrogen in microstructure can play a crucial role in the SCC susceptibility of the matrix. Vishwanadham et al. conducted AES, argon sputtering and plasma-loss energy measurements on 7075-T6 alloys to study the grain boundary segregations. They concluded that there was a significant segregation of Mg and Zn on the grain boundaries. The segregated Mg could facilitate hydrogen entry and preferentially attract the hydrogen to form MgH and MgH_2 complexes, which in

turn affects the SCC susceptibility. [121] Song et al. studied the effect of Mg and H segregation on 7175 alloy plates and seconded this theory. They proposed that Mg segregation to the grain boundaries is inevitable and its affinity for hydrogen, which is greater than that for aluminium, results in Mg absorption of hydrogen at grain boundaries, leading to intergranular hydrogen embrittlement. [46] Similar theory was also proposed by Scamans et al., Chen et. al. and Wei et. al. [122-124]

Effect of Cu: The addition of Cu enhances the mechanical properties of the Al-Zn-Mg alloys by precipitation hardening.[11] However, addition of Cu could result in susceptibility of the alloys to various forms of localised corrosion such as pitting and IGC as well as SCC susceptibility of the alloys.[97, 125-128] Rometsch et al. observed that aging of Cu- rich 7xxx alloys lead to the increase of Cu in the grain boundary precipitates. This in turn reduces the anodic nature of the grain boundary precipitates with respect to matrix and hence enhances SCC resistance.[11] Speidel et. al [62] observed that over-aging of higher Cu alloys (7075 and 7178) substantially decreased crack growth rates, whereas over-aging of the low-Cu alloys did not have any significant effect on the SCC. It must however be noted that the Zn and Mg content of the investigated alloys varied, which could also contribute to the variation in SCC behaviour. Sarkar et al. found similar results [125] on varying the Cu content of Al-6Zn-2Mg-X Cu alloys from 0.01 to 2.1 wt.% showing that increasing Cu content reduced the crack velocity in stage II. Over-aging the high-Cu alloys, further reduced the plateau crack velocity. Similar observations were made by Birnbaum et. al and Hardwick et. al.[128, 129]

Effect of other alloying elements: Besides the main alloying elements, other secondary alloying additions such as chromium and zirconium have also known to influence SCC susceptibility. Scamans et al. carried out pre-exposure embrittlement tests on Al-6%Zn-3%Mg alloys and found that an addition of 0.14% Cr and 1.7% Cu reduced the rate of pre-exposure embrittlement. [130] They attributed this to the increased grain boundary regions due to grain refinement caused by the chromium. Similarly, Shi et al. observed that the addition of Sc and Zr reduces the area fraction of grain boundary precipitates, thus reducing SCC susceptibility. [131] Similar studies were carried out to study the effect of addition of minor alloying elements such as Sc, Yb and Er, which also influenced the SCC susceptibility of the 7xxx alloys. [131-136].

Effect of heat treatment and microstructure: It is not only the alloy composition that has a substantial influence on the SCC susceptibility, but also the heat treatment and their resulting microstructures.[137] SCC susceptibility can be decreased either by disintegrating the continual precipitates on the grain boundaries or by decreasing the potential difference between the grain boundary precipitates and the matrix. [10] Once the 7xxx alloy reaches peak-age, it is seen to have finely dispersed ή precipitates along the grain boundaries, which attribute towards the high strength of the alloy.[138] These precipitates, which mainly constitute the $MgZn_2$ precipitates are anodic to the matrix. Therefore, they enhance the intergranular corrosion at the grain boundaries.[139] This intergranular corrosion could then lead to acceleration of hydrogen transportation, which results in embrittlement of the grain boundaries.

Due to this, SCC susceptibility is greatly influenced by the dispersion of precipitates in the matrix and their size and type. [140] Albrecht et al.[79] tested 7075 plates for hydrogen assisted fracture in underaged, peak-aged and over aged conditions. The underaged alloy was most susceptible to hydrogen, which they attributed to the coherent GPZ which are formed. Strengthening occurs by shearing of these GPZ by passing dislocations which in turn softens the slip plans and concentration of slip bands. This leads to increased hydrogen dislocation transport and local hydrogen accumulation at grain boundaries. At peak-aged, there is a mixture of GPZ and some semi-coherent η' precipitates which results in inhomogeneous slip distribution, which causes SCC susceptibility. Once the alloy is overaged, the grain boundaries are covered with large coherent η precipitates which are discontinuous in the grain boundary and therefore enhance SCC resistance.[79]

Sun et al. suggested that SCC susceptibility of Al-Zn-Mg alloys first decrease and then increase with the increase in grain boundary precipitate fraction.[141] Similarly, Puiggali et al. [142] attributed SCC resistance of aging of 7010 alloy to volume fraction and alternating distribution of MgZn precipitate. Rometsch et al. suggested that the aging resulted in the increase of Cu content on the grain boundary precipitates, effectively reducing the potential difference between the matrix and grain boundary precipitates. Thus, on over-aging Cu-rich 7xxx alloys, there is a large improvement in SCC resistance.[11] Precipitate free zones (PFZ), which are formed during aging are also shown to have an influence on the SCC susceptibility. [143, 144] [145] The

softness of the PFZ could enhance localized plasticity within the matrix, hence increasing SCC susceptibility. [145] Tsai et al. also showed that grain size plays a role in influencing the SCC resistance, with finer grain size showing better resistance to SCC. [146]

In order to overcome SCC problems, researchers have been extensively working on heat treatment methods which could reduce the SCC susceptibility of the alloy without influencing its mechanical strengths. The retrogression and re-aging heat treatment, created by Cina [147] is a popular heat treatment method for this purpose. The heat treatment involves subjecting a peak aged material to a retrogression treatment for a very short time and then again re-aging to peak age, which would result in coarsening of η particles and its discontinuation on the grain boundaries. There are also several other two-, three- step aging treatments which are being studied. [122, 148-150]

2.6. Test Methods for testing Stress Corrosion Cracking

Due to its complex nature, there is a plethora of test methods available in the form of international, national standards and unstandardized test methods, which are used for various applications.[15] However, no single method is markedly superior to the other. Depending on the testing objective and the information required, the selection of specimen forms and testing conditions are extremely important to ensure the reliability of the test. The following section discusses the factors that influence testing of SCC, with respect to the mechanical aspects and the environmental aspects.

2.6.1. Influence of Mechanical Factors on SCC Testing

An important aspect of testing in SCC is the selection of an appropriate test specimen. Specimens can be of two forms, smooth or pre-cracked specimens.[151] A smooth specimen does not contain any pre-existing flaws, whereas a pre-cracked specimen accounts for the probability of physical defects by introducing a defect during the fabrication of the specimen. The specimens could range from simple smooth tensile specimens to pre-cracked double cantilever beam specimens.[15] Both the categories of specimens can be stressed in different kinds of stressing systems, such as constant total strain, constant total load, constant strain rate, incremental step load etc. [14]

The constant total strain or constant displacement specimens are popular due to their economic viability and ease of preparation of specimens and stressing frames. They can simulate the failures in service which are caused by fabrication stresses which are incorporated into the structure. [152] They can be in several forms with varying stress distributions and stress magnitudes such as U-bend,[153] bend-beam specimens such as 3-point bending or 4-point bending [154], tensile specimens or C-ring specimens[155] to name a few. Despite their ease of preparation and economic advantages, they have certain disadvantages such as the stress relaxation that is caused in the specimen once a crack is initiated in the specimen, due to the fixed straining. This relaxation could diminish the mechanical forces and could also lead to ceasing of the crack growth. The extent of relaxation depends on the size of specimen, stiffness of the frame, loading mode and also variation in nature and number of crack formations. [12] [152] These differences in relaxation behaviour could cause variations in reading of the results since time-to-failures would be varied.

The constant load test overcomes this problem of stress relaxation. On the contrary, once crack initiates in a constant load sample, there in an increase in stress concentration of the sample due to the effect of constant load and leads to faster failure of the specimen. [151, 156] The constant load test gives results in terms of time-to-failure which can be used to determine the threshold stress of the alloy, below which failure does not occur. However, carrying out a constant load test is relatively difficult in comparison to the constant strain test, due to the need for heavy machinery and lever systems, depending on the strengths of the materials being tested. However, use of springs could reduce the bulkiness of the experimentation.

The constant strain rate or slow strain rate test is another popular testing method to test SCC susceptibility. [157] Slow strain rate technique is defined by the ASTM G129-00(2013) norm as "*a dynamic slowly increasing strain imposed by an external means on the gauge section or notch tip of a uniaxial tension specimen or crack tip of a fatigue pre-cracked specimen for purpose of material evaluation*" [158] The advantage of this method is reduction in time for delivery of results and that the samples always end with failure, unlike the other two loading modes mentioned above, where an arbitrary experimentation time is set. [15] However, there are certain disadvantages to the test. One of the main disadvantages is its poor correlation to actual service conditions and

dependence on the strain rate of the testing.[159-161] It is imperative to find an optimal strain rate in the testing since, higher strain rates could lead to ductile residual failures since the hydrogen atoms can neither diffuse nor be carried by dislocations and lower strain rates could lead to higher corrosion influences or the hydrogen atoms at trap sites is reduced by diffusional escape. [157, 159]

2.6.2. Influence of Environmental Factors on SCC Testing

Stress corrosion cracking is an environment specific phenomena. Thus, it should be taken into consideration that the environment the material is being tested in plays a very important role in the outcome of the results and the interpretation of the level of SCC susceptibility of the alloy. There are certain standard solutions which are used to test for SCC over the years. For e.g., NaCl solution for aluminium or boiling $MgCl_2$ for stainless steel. However, small changes in environmental factors such as salt concentration, pH of the solution or temperature and humidity can significantly modify the SCC results. [162]

Studying the effect of changing wet-dry cycle is imperative with respect to automobile, since the vehicle inevitably undergoes a wet-dry cyclic condition in its lifetime. The alternating immersion test is a popular test method for testing SCC of aluminium 7xxx alloys. According to the ASTM G44-99 [163] , the specimen is immersed in 3.5 wt.% NaCl solution for 10 minutes, followed by 50 minutes of drying cycle. This environment is popularly used as a standard in the aerospace industry for testing 7xxx alloys. However, the parameters of the alternating immersion can also significantly influence the SCC results. Onoro carried out a comparison test, in which he exposed the 7xxx alloys to salt spray fog tests and to alternating immersion test and found that the results were comparable to the standard alternating immersion test. [164] Yu et al. [165] studied the influence of dry: wet ratio on 7050-T7451 by conducting slow strain rate tests and electrochemical tests. The study concluded that with increasing dry: wet ratio, the SCC susceptibility decreases. They also concluded that wet-dry cycle led to higher SCC susceptibility of the alloy as compared to continuous immersion.

Various other environments can also be used to test SCC susceptibiltiy, which could yield different results, as seen in Magaji et al.[13] Multiple standard and non standard

test environments are tested in this study and the results are compared to show a significant variation in the SCC susceptibility results in each environment. Lifka et. al. [90] also exposed three different aluminium in three different outdoor atmospheres. The correlation between the outdoor exposure with the standard alternating immersion test is shown to be poor. Onoro also studied the SCC behaviour of 7075 alloy in a modified salt spray fog chambers with vapourised solutions of 0 and 5% NaCl and found good correlation with the results of standard alternating immersion environment. [164] These studies show that when choosing a test environment, the influence of environmental parameters on the test results must be considered and accounted for based on the application.

Chapter 3 DESIGN STRATEGIES AND EXPERIMENTAL METHODS

This section describes the experimental methods used in the thesis as well as explains the design strategies which were implemented using the DFSS methodology.

3.1. Selection of Materials and Characterisation

3.1.1. Selection of Materials

The materials for this thesis were strategically selected to include a wide spectrum of SCC susceptibility. A key research questions to be addressed in this thesis is how variation of alloy content and temper state effect SCC susceptibility of 7xxx alloys. As discussed in detail in section 2.5.3, the three main alloying elements, Zn, Mg and Cu and their ratios have the highest influence of SCC on the 7xxx alloys. In line with this research, quadrants based on the Cu content and Zn+Mg as well as Zn/Mg ratio were created as shown in Figure 3-1. The Cu content boundary was chosen at 0.3 wt. % since this is a Daimler specific internal limit for permitted Cu content in the aluminium alloy. According to Gruhl when the combined content of Zn and Mg in the 7xxx alloy is above 8.5 wt.% , the ideal SCC ratio is 3 for the best SCC resistance.[117] Therefore, a Zn+Mg boundary of 8.5 wt.% was considered a limit for the Zn+Mg content and a Zn to Mg ratio of 3 was considered as a limit. One alloy in each quadrant was then
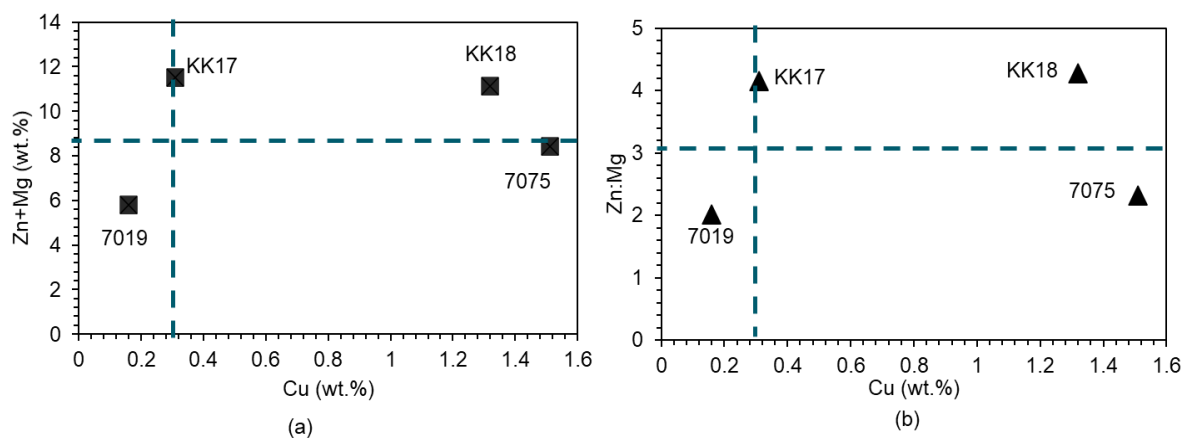

FIGURE 3-1: SPECTRUM OF ZINC, MAGNESIUM AND COPPER CONTENT CHOSEN IN THE ALLOY WITH RESPECT TO (A) ZN + MG CONTENT (B) ZN:MG RATIO

selected. The first alloy with the lowest alloy content was EN AW-7019 (which will be called simply 7019 further in the thesis). The second is the EN AW-7075 (which will also be called 7075 henceforth), which is a popular high Cu alloy used in many industries. Two non-standardized alloys with high alloying element content were also chosen, identified as the KK17, with lower Cu content and the KK18 with higher Cu content.

While Zn, Mg and Cu are the main alloying elements of the 7xxx alloys, other alloying elements may have a secondary influence on its SCC properties. The chemical composition of the selected alloys was determined by the wet chemical analysis technique, the results of which are shown in Table 3-1.

TABLE 3-1: CHEMICAL COMPOSITION OF THE ANALYSED ALLOYS

Alloy Name	Si	Fe	Cu	Mn	Mg	Cr	Zn	Ti	Zr	Zn/Mg	Zn+Mg
7019	0.17	0.19	0.13	0.19	1.87	0.04	3.97	0.03	0.12	1.87	5.84
7075	0.07	0.19	1.36	0.04	2.46	0.20	5.88	0.02	0.02	2.46	8.34
KK17	0.10	0.18	0.30	0.06	2.18	0.02	8.74	0.03	0.12	4.01	10.92
KK18	0.08	0.17	1.31	0.02	2.18	0.02	9.08	0.02	0.12	4.17	11.26

Since heat treatment also has a significant influence on the SCC behaviour, each of these alloys were tested in three temper states: naturally aged (T4), peak-aged (T6) and over-aged (T7). The T4 temper was produced by solution heat treatment and water quenching followed by storage at room temperature. The temper treatment process of T6 and T7 is described in Table 3-2. The alloys were mill-finished and delivered by the suppliers in the form of 1500 x 1500mm sheets with a thickness of 2mm.

TABLE 3-2: SPECIFICATIONS OF HEAT TREATMENT CYCLE ON THE RESPECTIVE ALLOYS

Alloy	T6	T7
7019	95°C 12h + 150°C 17h	107°C 6h + 165°C 24h
7075	125°C 24h	107°C 6h + 165°C 24h
KK17	125°C 24h	107°C 6h + 165°C 24h
KK18	125°C 24h	107°C 6h + 165°C 24h

The materials were stored in a controlled room-temperature atmosphere with a humidity ranging from 50-60% RH throughout the duration of this work. The materials were characterised with various techniques to study its mechanical and microstructural properties. Each characterisation technique has been discussed in this section.

3.1.2. Mechanical Testing

Figure 3-2 shows the modified A30 specimen, with and without a hole in the middle, which was used to carry out the tensile testing. This specimen dimension was specifically chosen since it would be used consequently in other SCC tests. Tensile testing was carried out to determine the important mechanical properties such as the yield strength ($Rp_{0.2}$), ultimate tensile strength (R_m), and elongation of the materials(A_{30}). Tensile testing was also carried out on modified A30 samples with holes to determine the maximum force to failure (F_m), which will be subsequently used in SCC tests. The tensile testing was carried out according to DIN EN ISO 6892-1:2009-12.[166] Each test was repeated at least thrice, to ensure reproducibility of the results.
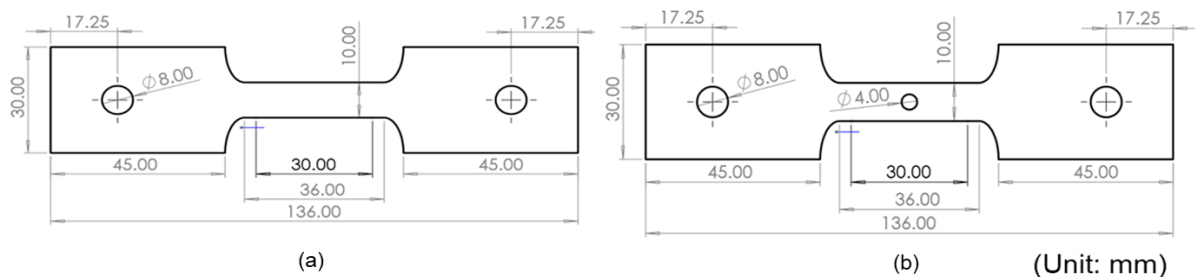

FIGURE 3-2: DIMENSIONS OF THE MODIFIED A30 TENSILE SPECIMENS (A) WITHOUT HOLE (B) WITH HOLE

3.1.3. Microstructural Characterization

Microstructural characterization of the as-received materials was done by means of optical microscopy and scanning electron microscopy (SEM) to determine the nature of grains and orientation. Samples were cut in a cross-section and cold mounted with an acrylic resin, which was made using KEM 30® powder and KEM 30® binder from the company QATM®. The mounted samples were then ground up to 2000 grid, followed by polishing up to 0.06µm (Episol®) from the company QATM®. This was followed by etching of the sample by immersing the sample in 10 wt.% phosphoric acid for a period of 30 minutes. The samples are then cleaned with acetone and dried and

observed under the laser microscope, Olympus LEXT OLS4100.

Microstructural characterization was carried out by scanning electron microscopy and EDX analysis of each material. One sample of each material were examined in as-received state to determine the microstructure of the tested materials. Samples were cut using automatic cutting machines and brought to appropriate sizes for the mounting. Samples were cut parallel to the rolling direction. The samples were then cold mounted with the electrically conductive cold mounting resin from the company QATM® called KEM 70®. The samples were then polished up to 2500 grain size and polished with diamond suspension and then analysed under the Zeiss 1540 XB Scanning electron microscope (SEM)

3.1.4. Constant Load Test According to ASTM G47- 98

 The constant load test in an alternating immersion environment according to ASTM G47-98 [167] is a standard test method to test the SCC susceptibility of 7xxx aluminium alloys. Since this test is the most widely used as industry standard qualifying tests across industries such as aerospace, this test has been used as a standard reference test for testing SCC susceptibility of the materials in this thesis.

TABLE 3-3   ENVIRONMENTAL PARAMETERS FOR THE CONSTANT LOAD TEST ACCORDING TO ASTM G47-98 FOLLOWING THE ASTM G44-99 EXPOSURE **[163]**

Control Parameter	Value
Solution Conditions	
Temperature	23°C ± 2°C
Solution Concentration	3.5 wt.% NaCl
pH	6.5-7.5
Air Conditions	
Temperature	23°C ± 2°C (anomaly from the norm which states 27°C ± 2°C)
Relative Humidity	45% ± 5%

Tensile specimens were milled to the dimension showed in Figure 3-2. They are then uniaxially stressed up to 75% of its yield strength ($Rp_{0.2}$) and exposed to the alternating immersion environment. The tensile samples are then exposed to an alternating immersion environment according to the ASTM G44-99. [163] This test employs a 1-hour cycle which includes 10 minutes in an aqueous solution of 3.5 wt.% sodium chloride followed by 50 minutes in air, during which the specimen is allowed to dry. This cycle continues for 24 hours/day for a period of 30 days. A summary of the test environment is given in Table 3-3.

3.2.   Structuring Through DFSS

In order to structure the complex array of parameters and systematically design the test method, the framework of a strategic product development methodology called Design for Six Sigma (DFSS) has been used in this thesis. The DFSS methodology followed in this thesis is adapted to follow a four-phase process as outlined in section 2.1. Within each phase, suitable tools and methodologies are used to structure the study and navigate through the complex range of parameters. The DFSS framework used in this thesis is carefully assessed to become the potential standardized framework for development of future corrosion test methods, particularly SCC tests.

This section describes the first phase called the definition phase. The aim of this phase is to define the overall objective and scope of the project and establish constraints of the proposed design by converting customer requests to tangible functional requirements. This phase consisted of three steps, namely, establishing project proposal, gathering of customer requirements, and finally converting them into functional requirements. The project proposal contains a defined problem statement, a defined objective of the project and the project scope. The purpose of defining a scope and an objective for the project is that it acts as a basic guideline throughout the steps of the project. Table 3-4 shows the outcome of the project proposal which was established for this thesis.

TABLE 3-4 CONTENTS OF THE PROJECT PROPOSAL

Section	Description
Problem Statement	There are multiple tests available for testing the SCC susceptibility of 7xxx alloys. However, there is no accepted standardized test method for testing the SCC susceptibility of 7xxx alloys especially for the automotive application. Due to this, the 7xxx alloys cannot be successfully tested for automotive use and hence cannot be released.
Objective	Development of a defined test method to test the SCC susceptibility of the uncoated sheet metal 7xxx alloys for automotive purpose. With this test, a reliable assessment of the risk of stress corrosion cracking for the automotive structural applications should be carried out.
Benefits	The 7xxx alloys have the highest potential for lightweight construction among aluminium alloys. This offers a highly competitive advantage over other aluminium alloys and high-strength steels. With a better knowledge of the resistance to stress corrosion cracking, it would be possible to use this alloy for the automotive purpose.
Project Metrics (Y)	-Time-to-failure -Time to start of crack -Maximum stress until failure -Residual elongation -Optical microscopy -Fracture surface analysis
Defect Definition	The Gage R&R value of the test is above 20%

In the next step, a list of requirements in the form of Voice of Customer were gathered. The gathered requirements were weighed using pairwise comparison, which is a tool used to rank multiple options relative to each other. In pairwise comparison, entities are generally compared in pairs, whether one option is preferred over the other or whether they are identical. Once each option in the pool is compared, a ranking of the various options is created. Finally, following the Pareto rule, the top 20% of the requirements were used to select the highest weighing customer requirements which are listed in Table 3-5.

TABLE 3-5   FINAL CUSTOMER REQUIREMENTS FOR THE COMPLETE MBSC TEST

Customer Requirement	Weightage	Rank
The developed test method must clearly indicate the stress corrosion cracking susceptibility level of aluminium 7xxx alloys	60	1
The test must be reproducible and repeatable	56	2
The test method should be applicable independent of the alloy content	54	3
The test should show differentiation between the SCC susceptibilities of different 7xxx alloys	53	4
Critical stresses and environmental conditions should be accounted for	50	5
The test method should be able to determine the time-to-failure of material with respect to the critical stress	46	6
The test method should be able to determine the critical stress with respect to the time-to-failure	45	7
The automotive process and lifecycle should be reproducible on the tested specimen	44	8

Once the customer requirements are shortlisted, they are converted into functional requirements using the scorecard. The scorecard is used to convert customer requirements (Voice of Customer) into tangible, measurable and quantifiable functional requirements, which are later used in the design process. The customer requirements in their first stage can be vague, unspecific, and qualitative in nature. Through tools such as '5 why's', these customer requirements are then converted into clearly defined customer needs in the scorecard. These defined needs are then clustered based on their functions to create a final list of customer needs. Once the customer requirements are clustered, they are transformed into quantifiable and measurable functional parameters. The metrics and the target values for each parameter are also defined in the scorecard. These functional parameters are later used to design a product or process. An example of the transformation of one of the customer requirements is given in Table 3-6.

TABLE 3-6   CONVERSION OF CUSTOMER REQUIREMENT TO FUNCTIONAL PARAMETERS USING SCORECARD

Customer Requirement	Functional Requirement	Design Parameter	Category of Functional Parameter
Critical stresses and environments should be accounted for	Critical test temperature for SCC should be determined	- Test temperature - Temperature cycle w.r.t. time	Environmental parameters
	Critical Humidity conditions for SCC should be determined	- Humidity (RH) - Humidity cycle (dry/wet cycle)	
	Critical salt conditions for SCC should be determined	- Salt composition - Salt concentration - pH - Oxygen saturation -Salt-spray cycle w.r.t. time - Mode of salt solution contact (Spraying, raining etc.)	
	Critical mechanical load conditions need to be mirrored in the test specimen	- Load Magnitude - Stress Distribution - Load Propagation w.r.t. time	Mechanical parameters

This conversion was carried out for all the customer requirements and a list of design parameters were listed. A clear distinction between environmental and mechanical parameters were noticed and the design parameters were bundled accordingly. For the ease of designing the test and analysing each design parameter individually, the conceptualisation step of the thesis was divided into two parts, i.e., the analysis of influence mechanical parameters on the SCC susceptibility and the environmental parameters. They were individually studied and combined at a later stage to form the final SCC test. The next sub-sections focus on the strategies and techniques used with the help of DFSS to design the concepts of the corrosion test cycle followed by the conceptualisation of the mechanical test specimen.

3.3. Designing of the Corrosion Test Cycle (MBSC Test Cycle)

A key research question for this thesis, as described in section 1.1, is to scientifically analyse the key environmental factors occurring in an automotive lifecycle which can influence the SCC susceptibility of 7xxx alloys. Due to the complexity of environments that an automobile is exposed to in its lifetime, a strategic flowchart was created using DFSS tools to categorically identify the SCC parameters, study them individually as well as synergistically and then implement the findings into a novel accelerated corrosion test environment, the MBSC test. This step-by-step flowchart is shown in Figure 3-3 and has the potential in the future to be used as a template to design future SCC corrosion test environments. Conceptualization phase for initial designing of the MBSC test was done through the brainstorming. In this step various climatic conditions that the automobile is exposed to are analysed and represented in the design of the corrosion test cycle. The next DFSS optimization, optimization, was carried out by filtering the important environmental parameters that influence the MBSC corrosion test cycle and analysing its influence experimentally through Design of Experiment (DoE). Through this phase, the optimal environmental parameters for the MBSC test cycle were established. Finally, in the validation phase, the results generated from the optimized test cycle was validated by comparing to outdoor exposure test environment.

3.3.1. Conceptualization of the MBSC Corrosion Test Cycle

The automobile goes through several stages in its lifetime and in each stage, it is exposed to a different environment that could influence the SCC susceptibility in a different manner. The primary objective while conceptualizing the corrosion environment was to encompass these stages and critical factors that occur in an automotive lifecycle. The lifecycle was divided into three phases and each phase was analysed for factors that could be critical to SCC susceptibility and reproduced in the corrosion test cycle. It should be noted that the effects of factors in the production phase have been excluded from scope of this thesis. The three phases included a pre-customer lifecycle phase, which is a storage and transportation phase, customer lifecycle phase and an extreme climate phase. Since the storage and transportation occurs once in the lifecycle, this complete phase occurs once during the whole

corrosion test cycle. Each of these phases has been described in detail below. Figure 3-3 depicts flowchart of the strategy used to design the test cycle.
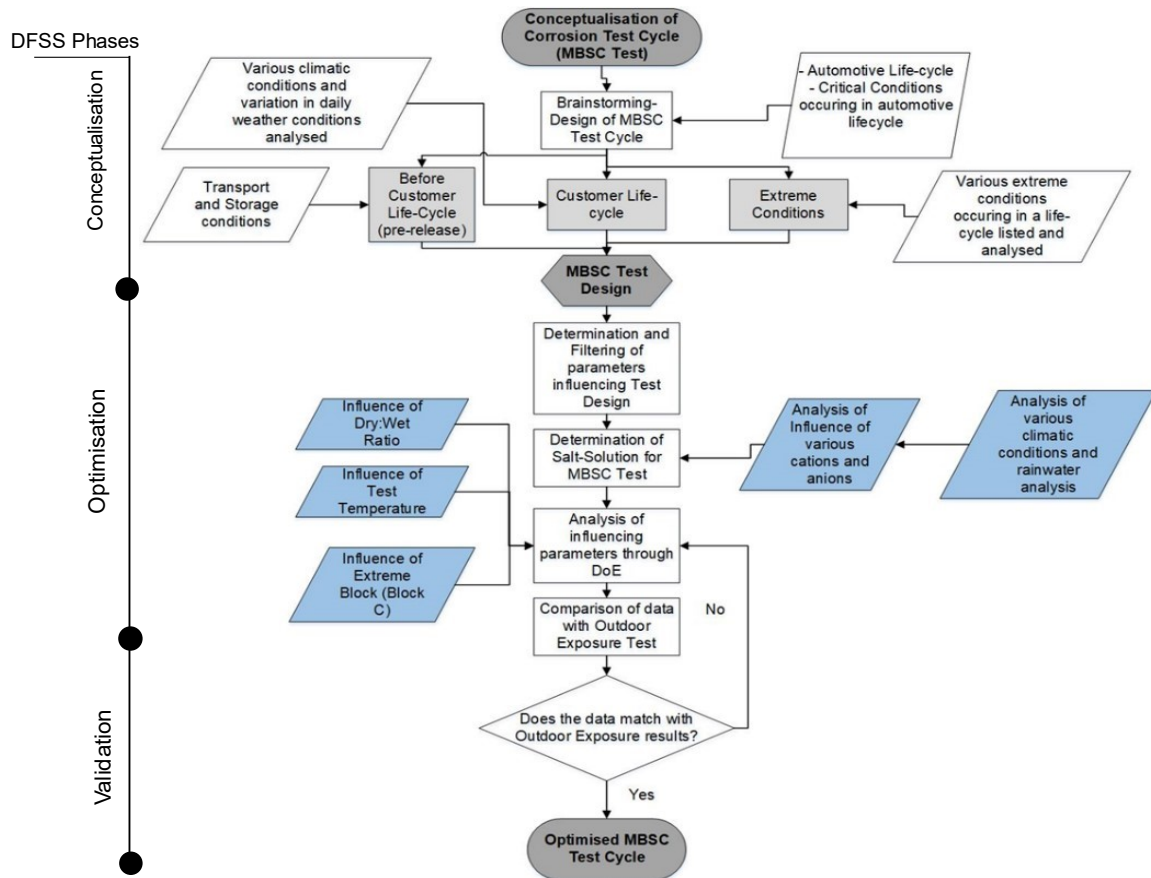

FIGURE 3-3: FLOWCHART OF THE STRATEGY USED FOR THE DESIGN AND OPTIMIZATION OF MBSC TEST CYCLE.

Storage and Transportation (Block A): After the production of the automobile and before it is handed over to the customer, each automobile goes through a storage and transportation phase. Some of the automobiles from the production go through the testing tracks. When the testing is done during winters or rains, there is a chance of splashing of rainwater from the road onto the vehicle. This water contains de-icing salts and other impurities that could concentrate and crystallise onto the vehicle during the next phase, which is the transportation of the automobile via train to the respective harbour. During the train transportation, room temperature and dry climate is maintained within the storage compartment, enhancing the drying process. This effect is reproduced in the test by a salt-spray phase which is carried out at normal room temperature, followed by a drying phase which is also carried out at room temperature with a relative humidity of 50% RH.

Once the automobiles are transported to the harbour, they are loaded into merchant ships for overseas transport. The temperatures within transport carriages could reach up to 40°C and humidity of around 80% RH*. The duration of overseas transport can last up to 6 weeks. This is followed by the storage of the automobile on the harbours for up to six months. Due to its proximity to sea water, the automobile is exposed to atmospheres of higher salt content. The conditions of the various storage and transportation phases mentioned above have been represented by Block A as shown in Figure 3-4.
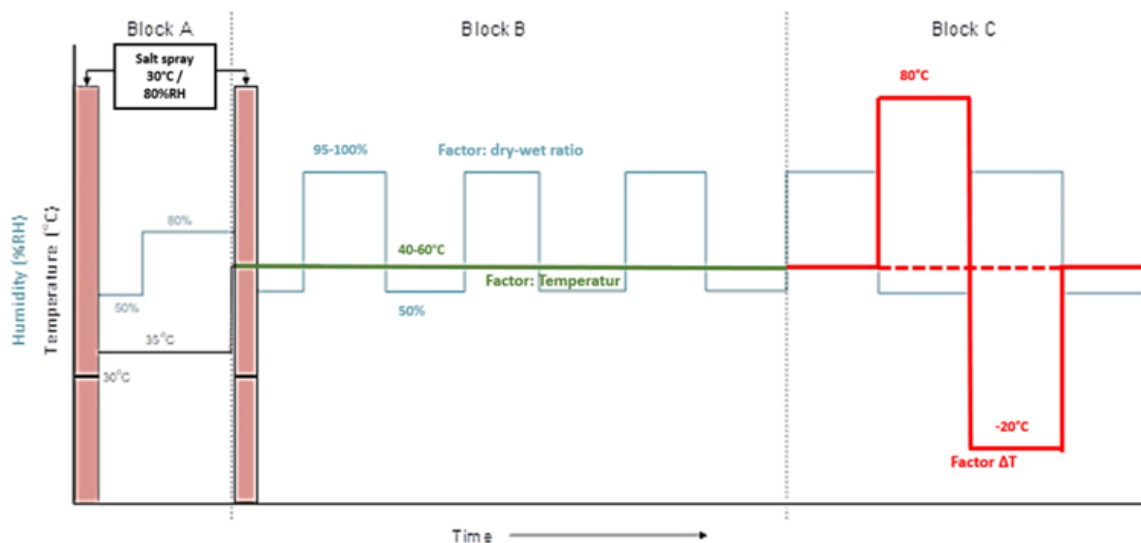

FIGURE 3-4: FINAL DESIGN OF THE MBSC CORROSION TEST CYCLE

In-service Phase (Block B): This is the phase which represents the automobile comes into actual on-road operation. In this phase, the automobile is exposed to a considerably broad range of climatic conditions depending on the location of the automobile. This includes exposure to various temperatures, humidity levels, pollutants in the air which in turn effects the ions and its concentrations in the rainwater, etc. There are two aspects that are critical during the on-road stage of the automotive lifecycle. Firstly, the yearly seasonal climatic changes that occur in most parts of the world. These climatic changes, result in a cyclic dry and wet condition for the automobile depending on the season. Secondly, the daily change in weather conditions is to be considered. Temperature and humidity variations during the day and night also produce a dry-wet cycle which has an influence on the SCC susceptibility. These two phenomena together can be reproduced in a corrosion test cycle with a dry-wet cycle, which is represented as phase B in Figure 3-4. An optimal

dry-wet ratio, with respect to time, is to be achieved here to replicate the field conditions. This study is done as part of the Design of Experiment which will be discussed in section 4.2.

Extreme Conditions Phase(Block C): During its on-road service, the automobile could come across extreme conditions which are infrequent but could have a significant influence on the SCC susceptibility. For e.g., internal investigations carried out at Daimler showed that the temperature on the car body could reach up to 80°C when exposed to a harsh hot climate which could negatively impact SCC susceptibility*. Similarly, in extremely cold regions, temperatures could fall drastically in sub-zero range. In these cold conditions, it is frequent that the car body is exposed to salt-water due to de-icing salts on the roads. These wet automobiles then enter and are stored in climate-controlled garages resulting in a sudden change in temperature of the car. This results in drying and concentration of solute on the vehicle body, making it critical to SCC susceptibility. These extreme conditions have been represented in Block C of the corrosion test cycle as seen in Figure 3-4, which are represented by a hot phase with 80°C and a cold phase with -20°C. Due to extreme variations in temperature, it could possibly have a harsh influence on the SCC susceptibility of the materials tested. To study this influence further, the temperature difference between the hot phase and the cold phase of this block was analysed as part of the DoE carried out and is discussed further in section 4.2. The sequence of each block was also designed to represent the frequency of the exposure of the alloy in the actual automotive lifecycle. Thus, the Block A occurs only once at the start of the test for a period of 72 hours (3 days). This is followed by a rotation of the Block B and C, with the block B repeating for a period of 144 hours (6 days), followed by the Block C for 24 hours (1 day). The total test duration is 31 days.

The study of influencing parameters was carried out in two stages. The first was to determine the influence of cation and anions on the SCC susceptibility in order to determine the salt solution which would be used in the MBSC test. Once the salt solution was determined, in the second stage further parameters were tested through

*Data obtained from Daimler Internal Research

46

DoE analysis to determine their influence on the SCC susceptibility. The procedure for these two steps is discussed in the subsequent sections.

3.3.2. Influence of Anions and Cations

In the course of brainstorming to design the MBSC test cycle, focus was also put on the exposure of various solutes on the automobile during its lifecycle. Rainwater analysis and internal case study analysis was carried out to determine all the possible anions and cations which the vehicle could be exposed to has been discussed in section 2.5.1. From these studies, the ions that are most frequently found overlapping with the ions having highest influence on the SCC susceptibility were shortlisted for further testing. Four options were shortlisted for further testing which are given in Table 3-7. To test these solutions, constantly loaded samples were exposed to the MBSC test cycle with the above varying salt solutions and the results were compared.

TABLE 3-7: SALT COMPOSITIONS AND CONCENTRATIONS ANALYSED FOR THE MBSC TEST

Option	Main Salt	Salt Addition	Concentration of the addition [mg/l]
A	NaCl (3.5 wt. %)	-	-
B	NaCl (3.5 wt. %)	Na_2SO_4	500 [SO_4^{2-}]
C	NaCl (3.5 wt. %)	NH_4NO_3	100(NH_4NO_3)
D	NaCl (3.5 wt. %)	NH_4NO_3	500 (NH_4NO_3)

Tensile samples without hole were constantly loaded to a stress of 75%$Rp_{0.2}$. The procedure to stress the specimen will be described in section 3.4.3. Once the specimens were stressed, they were exposed to the MBSC Test cycle shown in Figure 3.4. The parameters and scope of the test is described in Table 3-8

TABLE 3-8 PARAMETERS OF THE TESTING OF VARIOUS CATIONS AND ANIONS

Parameter	Value
Materials Tested	7019, 7075, KK17, KK18
Temper States	T4, T6, T7
Replications	4

Test Temperature (Block B)	50°C
Dry: Wet Ratio	1:1 (6 hours: 6 hours)
Temperature Difference in Block C (ΔT)	100°C
Test Duration	28 days

3.3.3.   DoE to Determine the Influence of Environmental Factors

The design of experiment is a tool which is used to determine the influence of more than one variable on the output of a process and analyse the interaction between two or more variables.[36] The first step in design of experiment is to determine the desired output and the quality of the output, which could be in the form of a variable or an attribute.[168] Once the outputs are defined, the design parameters are selected which influence the output of the process or product. It is important to identify all the variables that could influence the output in order to improve the accuracy. Once the variables are selected for further analysis, a design matrix is established which gives a complete overview of the factors and the various levels and order of running the experiment.[169] The most commonly used design matrix are full or fractional factorial with 2-level or 3-levels. The full factorial design includes all the possible combinations of all the levels of factors. Carrying out a full factorial program allows for the analysis of impact of each individual factor on the output as well as the interdependencies between the factors.[170] For a full factorial program, if n is the number of factors in an experiment with 2 levels, the total combination of experiment is given by 2^n. [170]

Three main parameters of the MBSC test cycle were chosen to be analysed further with a Design of Experiment tool, namely test temperature (in Block B), dry-wet ratio (block B) and temperature difference in Block C. DoE is carried out in order to determine and analyse the influence of these parameters on the SCC susceptibility of the materials being tested. The parameters chosen for the DoE and their values are given in Table 3-9.

TABLE 3-9 DOE PARAMETERS FOR TESTING THE INFLUENCE OF ENVIRONMENTAL PARAMETERS

Parameter	Value	
Materials Tested	7019, 7075, KK17, KK18	
Temper States	T4, T6, T7	
Replications	4	
Salt Solution	$3.5\%NaCl + 100mg/l\ NH_4NO_3$	
Test Duration	31 days	
DoE Parameters		
Test Temperature (Block B)	40°C	60°C
Dry:Wet Ratio	1:1 (3h: 3h)	1:5 (1h :5h)
Temperature Difference in Block C (ΔT)	0 (elimination of Block C and continuation of Block B)	100 (-20°C to 80°C)

Tensile samples are constantly loaded to **75%Rp$_{0.2}$** using the procedure described in Section 3.4.3. A general 2-step full-factorial program is generated using the 3 DoE factors which are determined in the concept phase of the DFSS. The number of test scenarios created using the three factors is calculated by 2^n, where n is the number of factors. Thus, there were 8 possible test conditions (work packages) with all the combinations of the factors and a 9th test condition with a central point, which is shown in detail in Table 3-10.

TABLE 3-10 DETAILED EXPERIMENTAL PLAN FOR THE DOE OF ENVIRONMENTAL PARAMETERS OF MBSC TEST

Work Package	Temperature [°C]	Dry:Wet Ratio	ΔT [°C]
1.1	40	1:1	100
1.2	40	1:5	100
1.3	40	1:1	0
1.4	40	1:5	0

3.1	60	1:1	100
3.2	60	1:5	100
3.3	60	1:1	0
3.4	60	1:5	0
2.1 (central point)	50	1:3	50

3.3.4.   Analysis of Test results

Once the samples fail or pass the maximum duration of the test, the samples are unstrained, cleaned with distilled water and the following analysis takes place.

I.   The day of failure is noted for failed samples.
II.   Tensile testing is carried out, following the procedure described in section 3.1.2, on the samples that passed the maximum duration of the test to determine the remaining mechanical properties after corrosion of the samples.
III.   Fracture surface is observed under scanning electron microscope to determine nature of fracture surface.
IV.   Optical microscopy of one sample per alloy system is carried out to determine the presence and nature of cracks. Optical microscopy was also carried out to determine the presence of other forms of corrosion.
V.   Apart from the mechanical and microstructural analysis, in the DoE study, statistical analysis is also carried out using Minitab 18 ®.

Once the experiments are carried out, the results are analysed by multiple methods. One way of determining the influence of a particular factor on the output is the p-value. The p-value tests the null hypothesis and checks the probability of occurrence of a result as extreme as the result observed with the assumption that the null hypothesis is true. [169] For a confidence interval of 95%, a p value of below 0.05 means, that the factor has a statistically significant effect on the output. Based on the given population data, Minitab automatically calculates the P-value and determines whether the factor is statistically significant or not.

Another representation of the DoE results is the Pareto diagram, which demonstrates the magnitude of influence of each variable on the output of the process being tested. The diagram can show the absolute value of the standardized effect from the maximum to the minimum effect, with a reference line (denoted by α) marking the statistical significance of the effect on the output. The reference value of standardized effect was

taken as 1.968 was considered in this thesis which corresponds to a confidence interval of 95%. Variables that cross the reference line are considered statistically significant and those below the line are considered insignificant.[36]

3.4. Influence of Mechanical Factors on SCC susceptibility

This section discusses the methodology and structure which was used to answer the research question 1.2 related to the influence of critical mechanical parameters on SCC susceptibility. The DFSS methodology was adapted here to conceptualise mechanical specimens as shown in Figure 3-5. Detailed stages of selection and analysis are elaborated in this section.

3.4.1. Design and Selection of Test Specimen

The strategy for selection and optimizing the mechanical test specimen for the MBSC test was also tailored to get the optimal specimen, taking into factor all the possible conditions that could occur in the automotive lifecycle concerning the mechanical variations. The conceptualization phase was carried out by using the morphological box tool, where the concept of mechanical specimen was divided into various functions and all the relevant options for each function were listed. Parallelly, real-life load cases were analysed as input to determine the nature of actual stresses that occur in an automobile. Through QFD analysis, the three most fitting mechanical specimens were selected for further study. These selected specimens were studied experimentally for the influence of the most significant mechanical parameters. Finally, a measurement system analysis was carried out for the whole mechanical test setup in order to determine the reproducibility and repeatability of the setup. Each of these steps will be discussed in detail in the sub-sections below. The flowchart depicting the step-by-step process is shown in Figure 3-5.

Morphological Box Analysis: Morphological Box analysis is a tool, developed by F Zwicky, [171] which is used to breakdown and systematically evaluate complex processes successfully. Using this tool, complex processes are broken down into sub-functions and concepts for each sub-function are independently developed. Once all the concepts are listed, analysis of all combinations of the concepts are analysed and

filtered to get the best concept. The function of stressing of the test specimens was first divided into four distinctive sub-functions. These were specimen cutting, specimen form, load propagation with respect to time, and nature of stress. In the next step, all relevant concepts or designs for each function were analysed and a comprehensive list of these concepts was created for each function. In the last stage, all combinations of concepts under each function were listed and filtered according to their relevance to deliver a list of feasible and favourable concepts.
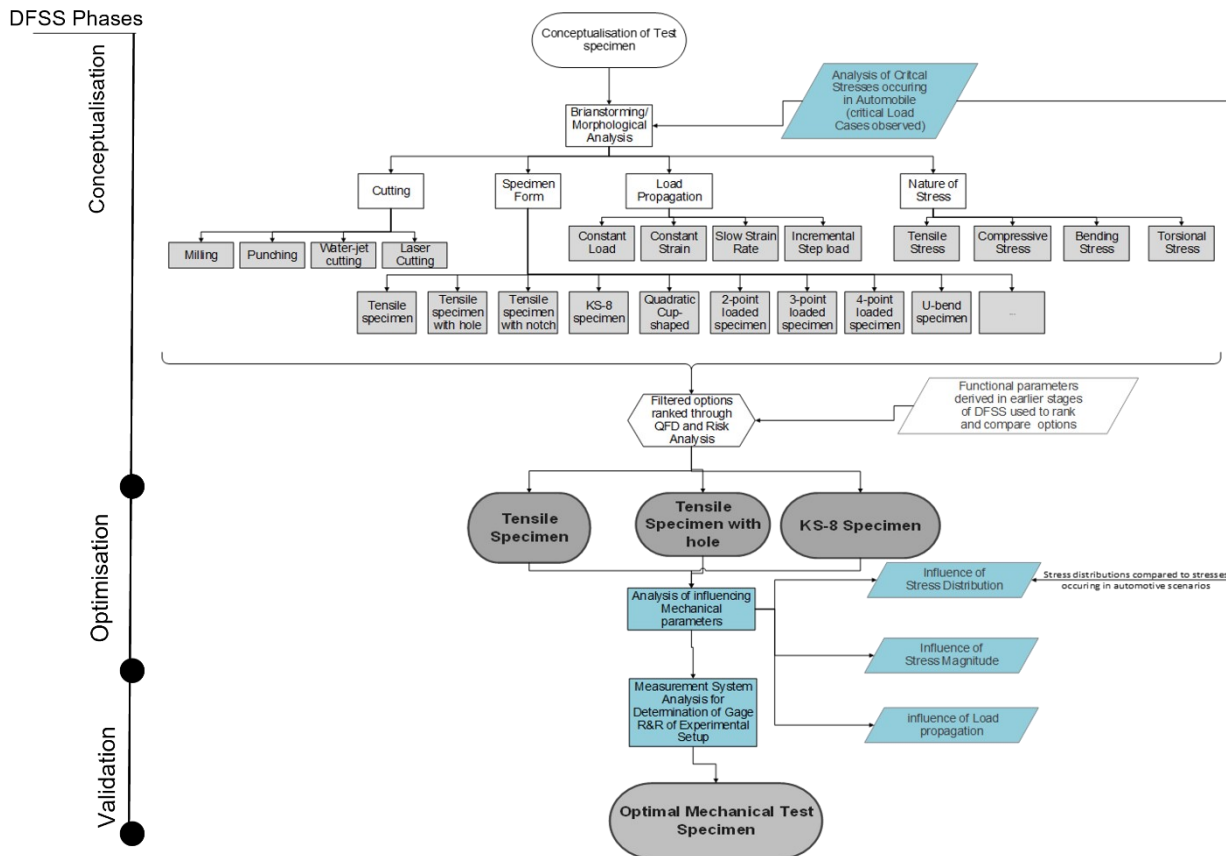
FIGURE 3-5 STRATEGY USED FOR CONCEPTUALISATION OF OPTIMAL MECHANICAL SPECIMEN

QFD and Risk Analysis: The final relevant concepts which were developed from the morphological analysis were then subjected to QFD analysis in order to select the final specimens. Each customer requirement which was determined in the second step of the DFSS cycle was first ranked by using pairwise comparison. A weightage for each of the customer requirement was derived. In the next step, each filtered concept from each function of the morphological analysis was weighed against the customer requirements. The points given to each concept were multiplied by the weightage of the respective customer requirement to determine the *Technical Value/Technical*

Weightage of each concept. Apart from technical weightage an initial risk assessment of the highest weighed concepts was also carried out in order to identify and address the risks at an early stage and aid in selection of the mechanical test specimen.

Finally, three specimens with the highest technical weightage with reasonable risk levels were crystallised as shown in Figure 3-6. These specimens incorporated all the critical variations of stress parameters. The tensile specimen has the principal advantage of its uniaxial stresses, ease of preparation and stress calculation as well as flexibility in application. However, it was seen from the simulation of automotive load cases that the stresses occurring on the vehicle parts were localized and multiaxial and generally concentrated on the bolting regions around the holes. To represent this phenomenon, the tensile specimen with hole was chosen as the second specimen.
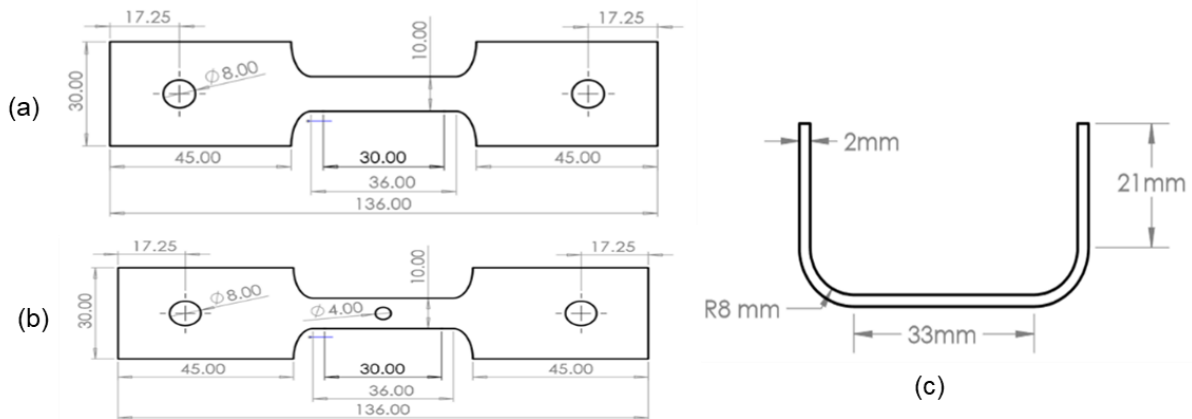
FIGURE 3-6 ILLUSTRATION OF THE THREE SELECTED SPECIMENS (A) TENSILE SPECIMEN WITHOUT HOLE (B) TENSILE SPECIMEN WITH HOLE (C) KS-8 SPECIMEN

Finally, the third specimen chosen was the novel developed KS-8 specimen which had the advantage of having plastic deformation and bending stresses in the specimen, which is also similar to the stresses observed in the automobile. Each of these specimens vary greatly in terms of mechanical influences. Factors such as load propagation mode, stress magnitude and stress distribution could have a significant influence on the SCC test results. Therefore, in order to avoid pitfalls of the false interpretation of the test results, it is important to understand the influence of these factors on the SCC susceptibility and consequently choose the right specimen with the right mechanical parameters.

Once the specimens were determined, the factors influencing the specimens were analysed through fish-bone analysis. The most important factors that have an influence on the mechanical specimens were load propagation mode, stress distribution and stress magnitude. Each of these influencing factors were then experimentally analysed in order to determine the optimal influencing parameters. Parallelly, stresses that occur in certain critical load cases in the automobile were also analysed to determine the nature of stresses that actually occur in the automobile. The detailed testing carried out to determine the influence of the parameters will be discussed in the next sub-sections.

3.4.2.   Simulation of Stresses Occurring in Automobile

The first step towards studying the influence of mechanical factors on the SCC susceptibility of the chosen alloys was to determine the actual nature of stresses occurring in the automobile during its lifecycle. There is an exhaustive list of critical loading conditions that occur in an automotive lifecycle. Among them, two critical load conditions with critical stresses were analysed in this thesis, in order get further insight into the nature and magnitudes of stresses that occur real-time in the automobile. The first load condition was the towing assembly and the second was the door override assembly. This was done by simulating the loads that would occur on these assemblies and analysing the resulting simulated stresses. The analysis of the simulation was carried out using ANSA ® as the pre-processor and ABAQUS ® as the solver.

Towing Assembly: Strength simulations were carried out on the towing assembly of a passenger car (BR 205) with towing done according to three different conditions listed in Table 3-11, where the internal standards 1 and 2 were higher load cases compared to the TÜV standards. The simulation was carried out on the front module of the towing assembly, where maximum stresses are obtained, and the assembly was simulated to be fixed to a rigid body by constraining all the degrees of freedom. Figure 3-7 illustrates the different parts which were analysed, and the materials used for each part. The strength simulation was carried out by applying the load in the x-y plane with respect to the towing hook as shown in Figure 3-7(a). For each simulation, 5 load cycles were initiated for each direction of force at a speed of 1KN/s. The cyclic load

simulation is shown in Figure 3-7(d). The test loads are calculated according to the permissible total weight of the vehicle and an additional gravity load.
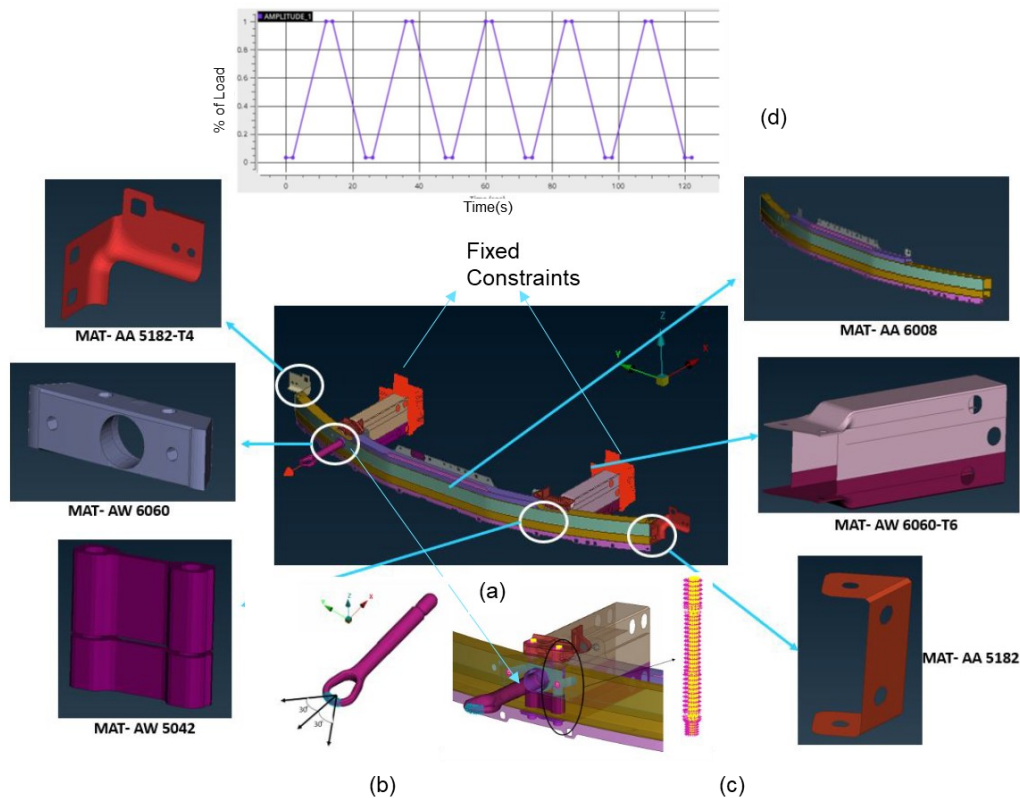

FIGURE 3-7: (A) TOWING ASSEMBLY SHOWING THE DIFFERENT PARTS AND ALLOYS USED FOR EACH PART (B) DIRECTION OF LOADING (C) BOLT CONNECTION (D) APPLIED LOAD CYCLE

The above load cycle is applied on the towing assembly according to three different standards, which are the TÜV standard and Daimler internal standards 1 and 2, the loads of which are summarised in Table 3-11. With the TÜV standard, the linear tensile load is applied only along one direction which is at 0°C with respect to the towing hook. The internal standards 1 and 2 contain three step simulations in which the first step is only a linear tensile load of 5 cycles as shown in Figure 3-7(d). After this step, an angular tensile load at an angle of 30° (with respect to x-axis) is applied on the inside and then on the outside direction.

TABLE 3-11: MAGNITUDE AND DIRECTION OF LOAD APPLIED ON THE TOWING ASSEMBLY

Test	Tensile Load	Direction of Load
TÜV Standard	$0.5^*m_{zul}^*g$	0°
Internal Standard 1	$K1^*m_{zul}^*g$	0° and ± 30°
Internal Standard 2	$K2^*m_{zul}^*g$	0° and ± 30°

Where, g = acceleration due to gravity; m_{zul} = total weight of the car with the driver (75kg); K1 and K2 = load factors, where K2>K1

Door Lowering Assembly: This assembly simulates the stresses that occur onto the door assembly when a load is experienced on it in the Z direction after the door has been opened slightly, i.e., 5-10° in the lock area. This causes localized stresses on the A- and B- pillars and to an extent also plastification. Figure 3-8 shows the door assembly, which was analysed, and the various individual parts, which were studied along with the materials and their respective yield strengths. Unlike in the towing assembly, the load in this case was a static load with a magnitude of 1000N along with gravitational load. The total run time of the load was 1s.
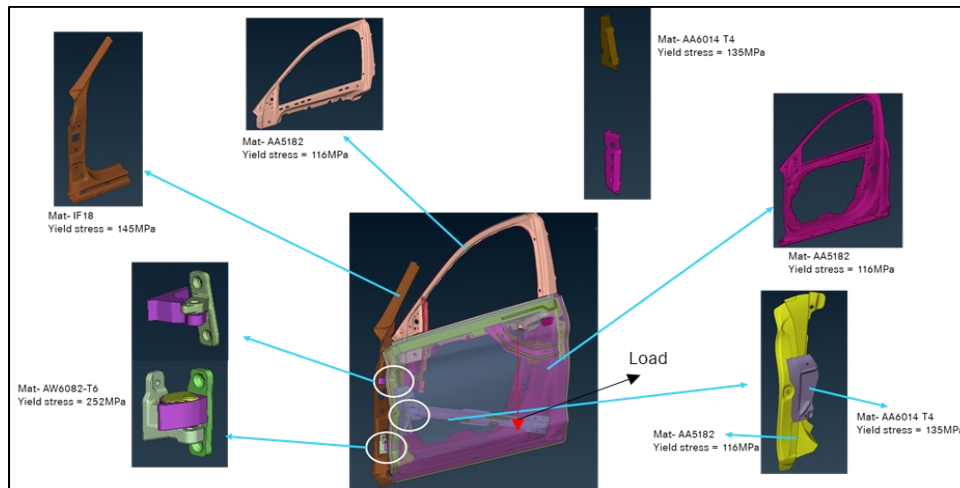
FIGURE 3-8 DOOR LOWERING ASSEMBLY AND THE INDIVIDUAL PARTS ANALYSED IN THE SIMULATION

3.4.3. Influence of Stress Distribution and Stress Magnitude

Once the specimens were chosen according to the strategy mentioned in section 3.4.1, the specimens were subjected to various tests in order to analyse the influence of the mechanical parameters on the test specimens. Three main mechanical parameters were chosen to be studied: Stress distribution, stress magnitude and load propagation mode. This section describes the procedure followed to determine the influence of stress distribution and stress magnitude on SCC susceptibility of 7xxx alloys.

(i) Preparation and Stressing of Specimens

Constant Load Specimen (with and without hole): The tensile specimens, with and without hole used in this thesis were modified A30 specimens which were prepared by milling. Figure 3-6 (a) and (b) shows the dimensions of the sample used. The specimens were specifically made for the specially designed spring-loaded stressing frame which is shown in Figure 3-9. The stressing frame was made of EN AW-6082 aluminium, whereas the bolts and connecting rod were made of Zinc-Nickel coated steel. These steel parts along with the disc springs, which were also made of spring steel, were protected from corrosion before exposure to a corrosive environment by covering it with a thermoplastic resin and the disc springs with a PVC pipe.
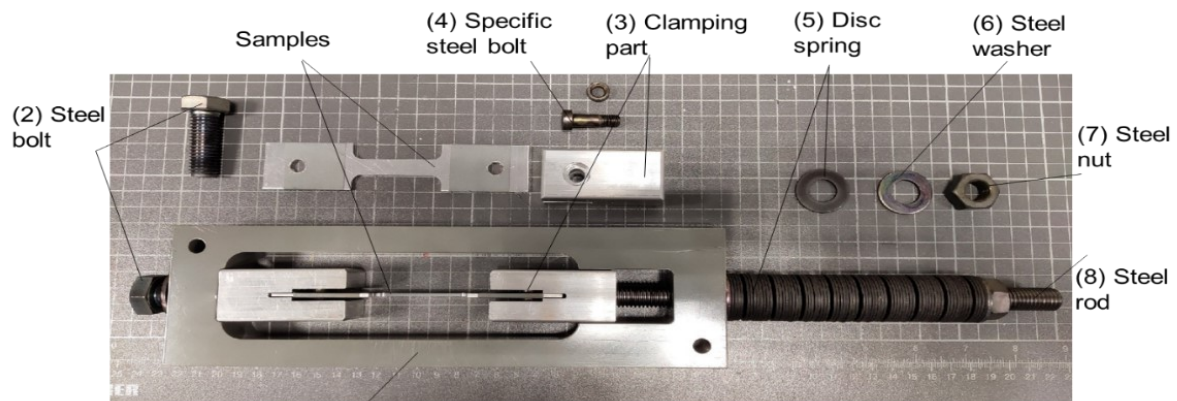
FIGURE 3-9: TENSILE TESTING SETUP FOR CONSTANT LOAD TEST

The force on the specimen was achieved by employing disc springs which were stressed manually to achieve the desired force on the spring. The exact force to be generated onto the specimen was determined with the help of an extensometer, as shown in Figure 3-10 (a) (Epsilon axial-extensometer with a gauge length of 30mm) The displacement required to achieve the desired force was calculated for each material from their yield curve. The extensometer, which measures the displacement, was clipped onto the sample and the sample was stressed with a ring spanner until the desired displacement was achieved. The validity of extensometer readings was also verified with standard spring calculations as well as by comparison of these readings with standard UTM machine readings.

The samples were stressed to a maximum of 24 to 48 hours before the specimen was exposed to the test chambers in order to avoid variation in load timings among specimens and to have minimum gap between stressing and exposure. Additional precautions were taken into consideration to prevent the setup from getting corroded, including covering the disc springs with PVC pipe and sealing the interface with tape and protecting the bolt connections within the setup with a polymer coating. The samples were placed in the corrosion chamber at an angle of approximately 15° with respect to the vertical, such that they have equal exposure to the environment without any shadowing effect on each other as illustrated in Figure 3-10(b).

FIGURE 3-10 (A) ILLUSTRATION OF STRESSING OF SPECIMEN USING EXTENSOMETER (B) FINAL EXPOSURE OF SPECIMEN IN THE CORROSION CHAMBER

Constant Strain Specimen (KS-8) : KS-8 samples are constant strain samples, which have been modified by the original KS-2 samples, which were developed in the University of Paderborn together with Fraunhofer Institut für Werkstoffmechanik(IWM). [172] The original samples had a bending radius of 2mm, which were difficult to achieve on very brittle materials which were part of this work. Therefore, the KS-8 sample was redesigned to a bending radius of 8mm. Specimens were punched with a cutter and then holes were drilled on both side with a drilling machine. The schematic of the dimension of KS-8 sample is shown in Figure 3-11. The rolling direction was chosen such that the bending is parallel to the rolling direction, i.e. the specimen is stressed in the long-transverse direction, which is more critical to SCC compared to the longitudinal direction [109]. Since the samples KK17 and KK18 in T4 and T6 temper

states were extremely brittle, the edges of these samples were roughly ground using a belt grinder to remove any sharp corners on the edge surface.
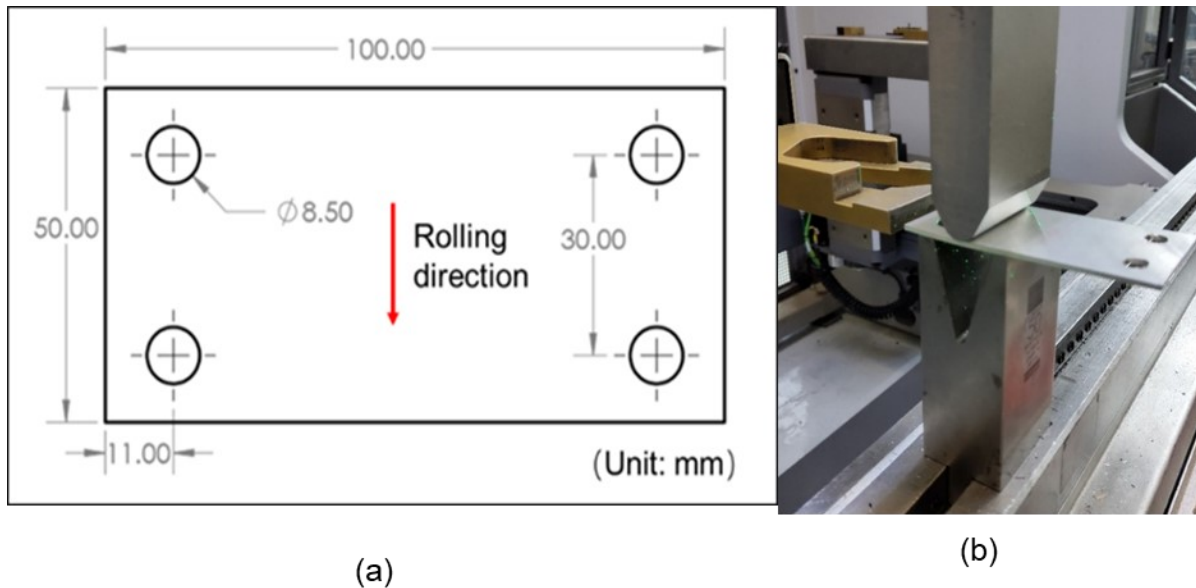

(a)   (b)

FIGURE 3-11 (A) DIMENSIONS OF THE KS-8 SAMPLE AFTER CUTTING AND DRILLING (B) THE BENDING PROCESS BY AN ANGLED HYDRAULIC PRESS

After the punching and drilling of the samples, they were bent to the final dimension with a two-step bending process. In the first step, the samples were bent by an angled hydraulic press, as shown in Figure 3-12(b). Both sides of the samples were bent up to 100°±1°. The spring-back effect was adjusted by corrector angles and varying velocities for different materials. In second step, the samples were manually bent to the final position, i.e., 90° using bolts connection, the different steps of bending and the final dimensions after bolting are shown in Figure 3-12.
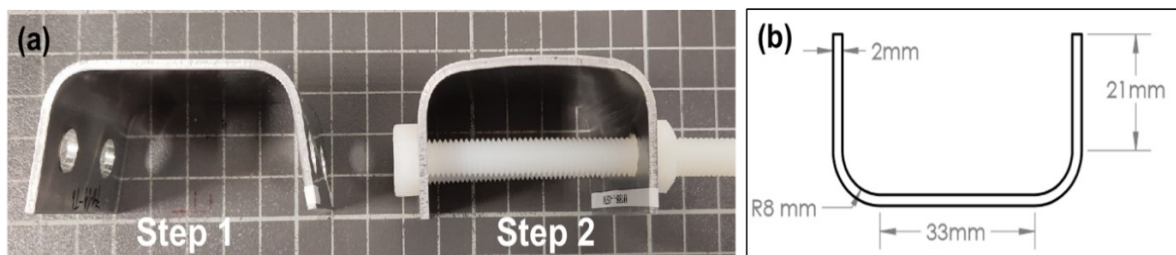
FIGURE 3-12 (A) TWO-STEP BENDING PROCESS OF KS-8 SPECIMEN (B) FINAL DIMENSIONS OF THE KS-8 BENT SPECIMEN

As with the constant load specimen, the samples underwent the final stressing step maximum of 24 to 48 hours before it was exposed to the corrosion environment in order to avoid premature and uncontrolled SCC influence. The samples were again

kept at an angle of approximately 15° with respect to the vertical and exposed evenly to the corrosion climate for the designated period of time. In order to study the influence of stress magnitude and stress distribution the tensile specimens with and without hole were exposed to the environments under various stress magnitudes which are summarized in Table 3-12.

TABLE 3-12 PARAMETERS USED TO STUDY THE INFLUENCE OF STRESS DISTRIBUTION AND STRESS MAGNITUDE ON SCC RESULTS

Specimen	Stress Magnitude	Environments Tested
Tensile Specimen	50%, 75% and 90% of $Rp_{0.2}$	DIN EN ISO 11997-1:2016-05
Tensile Specimen with hole	50% and 75% of Fm	ASTM G85-11: A2
KS-8 Specimen	Undefined	MBSC Test

(ii)   Corrosion Environments used to expose stressed specimens

Once the tensile specimens (with and without hole) and the KS-8 specimens were stressed following the procedures described above, they were exposed to two standardized environments for the testing of mechanical influences, the DIN EN ISO 11997-1:2016-05 and the ASTM G85-11: A2 (MAASTMAASIS). This was done for two main objectives. Firstly, since the mechanical specimens were the prime focus in this section, testing in standardized corrosion test cycles enabled testing a larger sample space in controlled and validated test environments, thus eliminating the influences of the novel developed test. Secondly, the results obtained from the testing of these specimens in standard environments were later used to compare the results obtained when the samples were exposed to the MBSC test.

DIN EN ISO 11997-1:2016-05 [173] contains various cyclic corrosion tests, in which the samples were confronted with salt-spray fog, dry phase and humidity, alternatingly. In doing so, aggressive conditions which may occur in open environment was simulated. Various cycle combinations are described in the norm, of which Cycle B is followed in this thesis. A schematic of the cycle is shown in Figure 3-13. The salt solution used in this test had a composition of 5 wt.% NaCl, with a maintained neutral pH ranging from 6.5 to 7.2. The duration of the testing was 31 days.
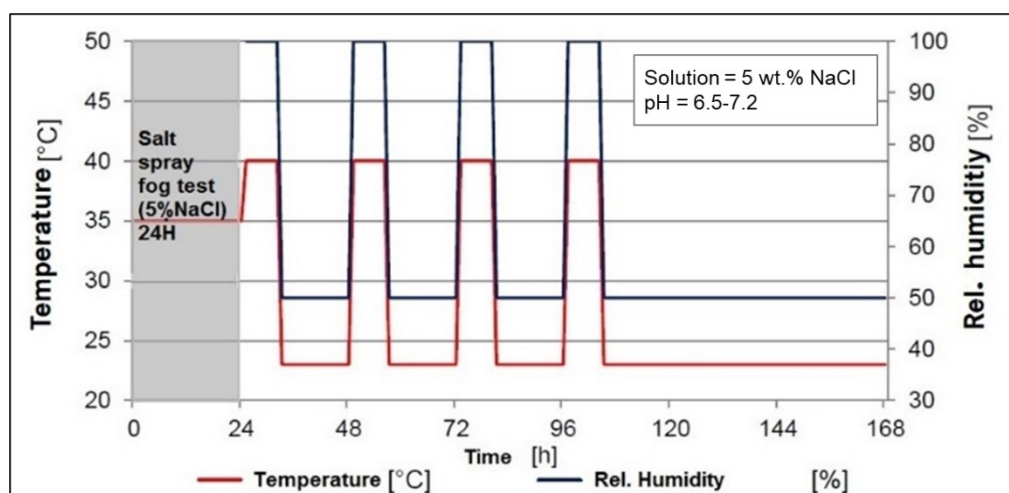
FIGURE 3-13: SCHEMATIC OF DIN EN ISO 11997-1:2016-05

ASTM G85-11: A2 (MAASTMAASIS) is a cyclic acidified salt spray test. [117]. It is a method in which samples are exposed to atomized acidified 5 wt.% NaCl solution under a controlled environment. The solution was prepared by dissolving the sodium chloride in distilled water to make its concentration of 5 wt.%. The pH-value was obtained by adding the acetic acid and was checked before the test. Each test cycle lasts 6 hours and contains salt spray for 45 minutes, dry-air purge for 2 hours and soak at high relative humidity (95% RH) for 3 hours and 15 minutes. In the thesis the repetition of the cycles was 4 cycles daily and for 21 days. The condition of the samples was checked daily as well.

MBSC Corrosion Test Environment: The MBSC Corrosion Test environment is the test environment which is specifically designed within the scope of this thesis as described in detail in section 3.3. Once the initial design of the MBSC corrosion test underwent optimization loops through DoE the final parameters were established. These parameters were used while exposing the various test specimens to the MBSC test in order to study the influence of mechanical parameters on these specimens in the MBSC Test Cycle. The test cycle followed is as shown in Figure 3-4 with the parameters summarized in Table 3-13 The salt spray solution used for testing was 3.5 wt.%NaCl+100mg/l NH_4NO_3.

TABLE 3-13   PARAMETERS OF MBSC TEST FOR TESTING OF MECHANICAL FACTORS

MBSC Test Block	Parameter	Value
Block A (72h)	Test Temperature	35°C
	Dry:Wet Period	20h:50h
Block B (144h)	Test Temperature (Block B)	40°C
	Dry:Wet Period	3h:3h
	Salt-Spray	3.5 wt.% NaCl + 100mg/l NH_4NO_3
Block C (24h)	Test Temperature	-20°C & 80°C
	Hot:Cold Period	15h:6h

(iii)   Analysis of Test Results

Once the samples failed or passed the maximum duration of the test, the samples were unstrained, cleaned with distilled water and the following analysis were carried out:

   I.   The day of failure was noted for failed samples.
  II.   Fracture surface was observed under scanning electron microscope to determine nature of fracture surface.
 III.   Optical microscopy of one sample per alloy system was carried out to determine presence cracks to determine presence of microcracks and nature of the cracks.

3.4.4.   Influence of Load Propagation Mode

Researchers have shown that load propagation is also shown to have a significant influence on SCC testing. [152] [15] In order to find the appropriate load propagation mode, various modes were tested and the results were compared. These included slow strain rate test, incremental step load test, constant load test according to ASTM G47-98 and the constant strain test using the KS-8 specimen as mentioned in section 3.4.3. The description of the test methods is described in this section.

Slow Strain Rate Test

The slow strain rate test uses dynamic straining on a tensile material to determine the SCC resistance of the material tested. The specimens were milled into tensile

specimens following the DIN 50125:2009-07 [174] , to the dimensions shown in Figure 3-14(a). The tensile samples were then subjected to a tensile straining in the UTM with a constant strain rate of 4.167 x 10^{-7} s^{-1}. One sample was subject to this straining in air, while two other samples were constantly immersed in a neutral NaCl solution of 3.5 wt.% concentration. An image of the setup with sample immersed in solution is given in Figure 3-14(b). The force-strain curve was noted for each specimen.
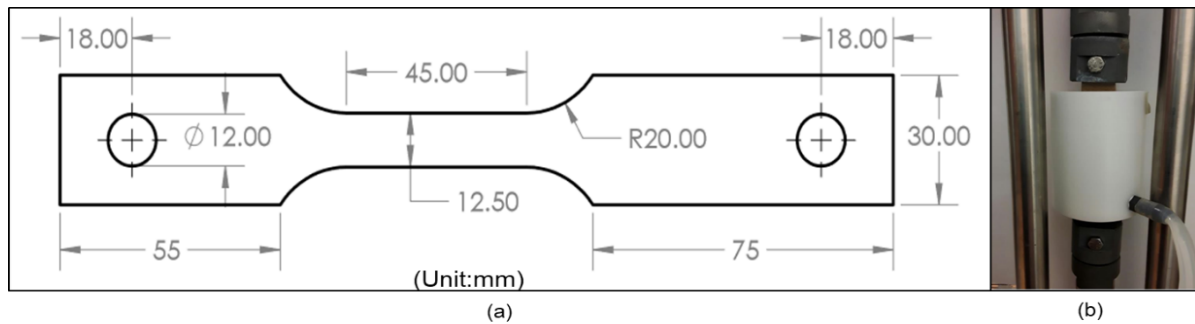
FIGURE 3-14: (A) DIMENSIONS OF THE SLOW STRAIN RATE TEST SAMPLE **(B)** SETUP OF THE SLOW STRAIN RATE

Once the samples were subjected to the test, they were cleaned with distilled water and dried. Analysis of test result was carried out in order to determine the SCC susceptibility of the materials. Firstly, the force-strain curve for each of the samples were noted and the results of the test carried out in air were compared to that of the test carried in the immersed medium to determine the loss in elongation of the samples. Fracture surface analysis of the specimens was carried out using scanning electron microscopy to determine the nature of failure and the nature of crack surface. Moreover, optical microscopy was carried out to determine other forms of corrosive influences on the specimens.

Incremental Step Load Test

The incremental step load test follows a similar procedure as the slow strain rate test, with the exception of loading conditions, wherein, the specimens are exposed to stepwise incrementing load until failure. The specimens were milled to the dimensions shown in Figure 3-14(a), which was also used in the slow strain rate test. The specimens were then subjected to a load cycle which is given in Figure 3-15, while

being continuously immersed in a neutral NaCl solution with 3.5 wt.% concentration and pH ranging from 6.5-7.5.
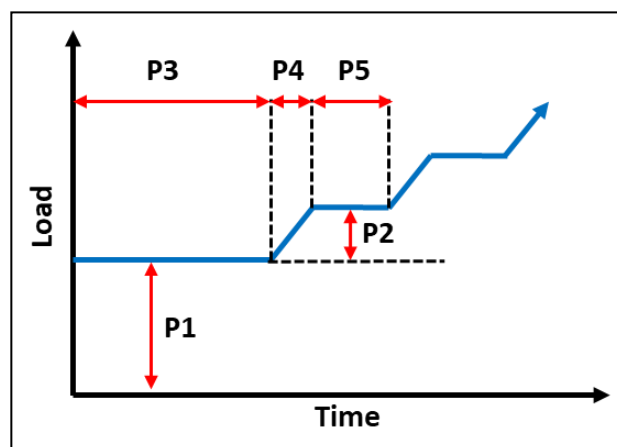

FIGURE 3-15 LOAD CYCLE USED IN INCREMENTAL STEP LOAD TEST

The parameters of the load cycle are described in Table 3-14. Varying values of Pre-load time (P3) and duration of each load step (P5) were tested in order to study the influence of these parameters on the test result and to determine the optimal parameters to get the optimal SCC susceptibility results.

TABLE 3-14 TEST PARAMETERS OF THE INCREMENTAL STEP LOAD TEST

Condition	P1 (Pre-Load)	P2 (Loading step)	P3 (Pre-load time)	P4(Load change time)	P5 (Duration of each load step)
A	50%F_{max}	5% F_{max}	96h	30s	1h
B	50%F_{max}	5% F_{max}	96h	30s	8h
C	50%F_{max}	5% F_{max}	168h	30s	1h

The maximum load to failure of each sample was noted and compared to maximum load to failure in air. Moreover, metallographic analysis was also carried out in order to determine the nature of failure and the corrosion influences. SEM fractographic

analysis was also carried out on the fracture surface to determine the nature of cracking.

3.4.5.　　Measurement System Analysis of Tensile Test Setup

In order to analyse the reproducibility and repeatability of the constant load setup explained in section 3.4.3, a measurement system analysis of the complete setup was carried out. MSA is carried out in order to determine the error in the output of the process or product due to the operator and the equipment. It is measured by a value called Gage R&R which stands for reproducibility and repeatability. The reproducibility and repeatability are represented by Gage R&R (GRR) value. The %GRR value is calculated using the Equation 3.1.[175] The aim of the MSA is to achieve a system with %GRR under 20% since it is considered a tolerance limit until which the operator and equipment influence of the system is not large enough to significantly influence the output of the system. With the help of Minitab ®, a statistical analysis software tool, an experimental plan is setup wherein the operator and the variable parameters are randomized. The experimentation is done according to the randomized order given in the table and the output is noted in the software. Once the data is fed to the software, it calculates the Gage R&R (GRR) of the system being tested. In this thesis, the MSA was carried out for the constant load setup in three steps.

$$\%GRR = \sqrt{EV^2 + AV^2} \qquad\qquad \text{(Equation 3.1)}$$

Where, EV =Equipment variation; AV = Operator variation

Operator Influence: 3 operators carried out the loading of the specimen following the steps explained in section 3.4.3 on the same material(7075-T6) and the same sample. Each operator was to load the specimen by rotating the ring spanner to 6 different number of rotations (1,2,3,4,5 and 6 rotations), leading to 6 different stresses on the specimens and readings on the extensometer. For e.g., 1 rotation corresponds to a certain displacement reading on the extensometer whereas 4 rotations correspond to a higher displacement reading. Four repetitions of each trial were carried out. These readings were then noted for each trial and the Gage R&R value was calculated using MINITAB ®.

Specimen Influence: In this trial, 3 operators tested 6 different specimens of the same material (7075-T6) with correspondingly 6 different rotations. For e.g., specimen 1 was with 1 rotation, specimen 2 was with 2 rotations and so on. Each trial was repeated 4 times and the displacement readings were noted in Minitab®. The Gage R&R value was then calculated by the Minitab software. In order to ensure that the clamping conditions remain the same for each of the trial, the zero level from which the disc spring was compressed with each trial were recorded by marking on the thread of the rod. Secondly, a laser pointer was fixed to provide a reference point for the rotations of the ring spanner.

Material Influence: In this trial,3 operators tested 3 different materials, 7019-T4, 7019-T6 and 7019-T7, each for 3 different rotations (1, 2 and 3 rotations each). Each trial was repeated 4 times. The idea of this trial was to determine the variation in readings with respect to varying materials.

Since this trial was carried out with multiple variables, linear regression analysis was carried out on the output of these trials using Minitab ®. The regression analysis determined the statistical significance of the influencing parameters on the results, which in this case was the displacement readings on the extensometer. The influencing parameters being operator, materials, and rotations.

3.5.   Outdoor Exposure Test

The research question 1.3 is addressed here which compares the susceptibility of alloys in the developed test method to their behaviour in the natural weathering conditions. In order to compare the results of SCC testing in the laboratory to natural weathering conditions, an outdoor exposure program was carried out as part of this thesis. The materials were stressed in two forms, uniaxially and U-bend, and then exposed to various climatic conditions. It should be noted that the total duration of the outdoor exposure is two years, however, due to time constraint, the data in this thesis will be based on one year of exposure. A detailed description of the procedure of the outdoor exposure test is given in this section.

3.5.1. Selection of Outdoor Exposure Locations

Three main parameters were considered while selecting the climatic regions of exposure, namely, temperature, relative humidity, and salt concentration. Based on the Köppen-Geiger climate classification, four locations were selected such that the samples were exposed to a variety of weathering conditions that are critical to SCC susceptibility. Table 3-15 shows the Köppen-Geiger Climate classification of the selected locations. [18]

The location at Sindelfingen, Germany was taken as a reference climate representing the warm temperate climate of a majority of the European region. Chennai, India was considered due to its hot climate with heavy monsoons, making the alternating dry and wet scenario ideal for SCC. Layton, USA was chosen due to its coastal location, leading to high humidity all year round as well as higher salt-content exposure. Saguenay, Canada was chosen to represent cold climates which could be critical to SCC due to the de-icing salts used in these cold regions. In order to replicate the exposure to de-icing, the samples at the Sindelfingen and Saguenay location were sprayed with 1 wt.% NaCl salt solution for the winter months from November until March with a frequency of once every week.

TABLE 3-15: LOCATIONS OF OUTDOOR EXPOSURE AND THEIR RESPECTIVE CLIMATIC CONDITIONS [DATA ADAPTED FROM [18]]

Location	Köppen-Geiger Classification	Main Climate	Key Feature for SCC testing
Sindelfingen, Germany	Cfb	Warm Temperate	Reference Climate
Chennai, India	Am	Equatorial	Hot summers and monsoonal
Long Key, USA	Aw	Equatorial	High humidity and high salt-content
Saguenay, Canada	Dfc	Snow	Cold climate

3.5.2. Setup of Outdoor Exposure Tests

Two differently stressed samples were used in the outdoor exposure test, the uniaxially stressed tensile specimen and the U-bend specimen.

Preparation of Tensile Specimen: The same modified A30 dog-bone sample (Figure 3-6(a)) as in the laboratory tests were also used in the outdoor exposure test for direct correlation. The stressing-jig used were the same as that in the laboratory tests for constant load stressing as shown in Figure 3-9. Samples were stressed up to 75% of its yield strength ($R_{p0,2}$), which was achieved by stressing of disc-springs following the procedure described in section 3.4.3. The disc-springs were then protected from corrosion by PVC casings. Once the specimens were prepared, they were mounted on racks and exposed to the atmosphere at an angle of 15°.

(a) (b)

FIGURE 3-16 (A) FINAL SETUP OF TENSILE SPECIMENS AT FLORIDA SITE (B) HOUR METER DISPLAY RECORDING THE TIME-TO-FAILURE OF THE SPECIMENS.

An in-house time-to-failure detection system was designed and connected to the samples since some of the sites could be manually observed a maximum of only once a month. Each stressed jig was connected to an individual proximity induction sensor, which was in-turn connected to an operating hour meter. These sensors acted as failure-detection system, in which when failure occurs in the specimen, the stressed jig loses contact with the induction sensor, resulting in stoppage of the operating hour meter. The hour at which the meter stopped was recorded, thus the exact time-to-failure was established. Figure 3-16 shows the final setup of the tensile specimens, and the hour meter displays which record the time-to-failure of the specimens.

Preparation of U-bend specimen: The U-bend specimens were prepared in a two-step process according to the ASTM G30-97(2016) [153]. In the first step, the specimens were clamped at one end and roll-bent on a 32mm diameter roller. In this stage, the sample was bent up to ~80-90% of 180°. Due to the spring-back effect, the sample dimensions change and the sample springs back some degrees. In the second stage, the samples were all connected in a row and stressed together with the help of screws on both ends of the rows. Figure 3-17 shows the stages of preparation of the

U-bend specimen. Once the specimens were stressed, they were connected to the failure detection sensor as shown in Figure 3-17 (c) and (d). These sensors were in contact with the surface of the leg of the U-bend specimen and once the sample fractures, due to a spring inserted into the bolt of the specimen, the contact of the sensor with the sample was broken and the timer on the connected hour meter stops, recording the time-to-failure of the specimen.
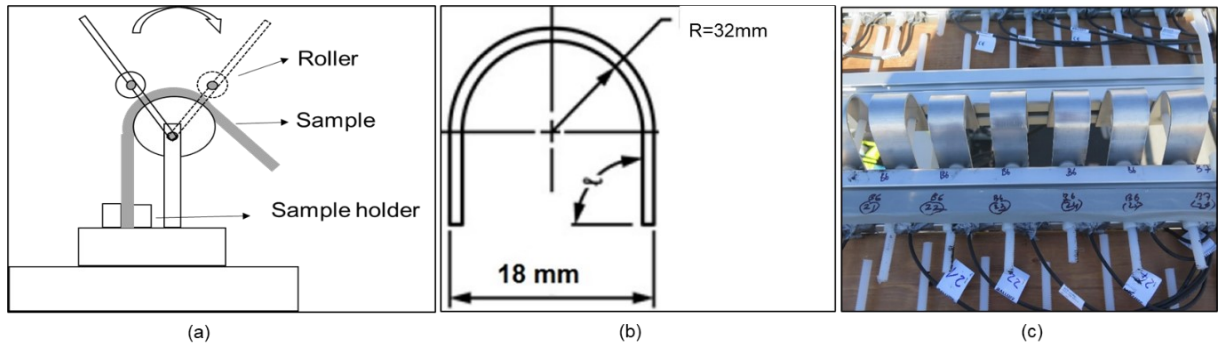

FIGURE 3-17 U BEND SPECIMEN PREPARATION (A) BENDING STEP 1 (B) FINAL SPECIMEN DIMENSIONS (C) FINAL SETUP OF U-BEND SPECIMENS AT THE OUTDOOR EXPOSURE SITE

3.5.3.   Analysis of Test Results

The time-to-failure for each sample were recorded based on the operating hour meter. Through this, the day of failure were determined, and an SCC susceptibility index was established in order to compare the SCC susceptibility in the different sites and among each material. The SCC index was calculated using Equation 3.4.

$$SCC\ Susceptibility\ Index\ (SCC\ Index) = \sum_{q=1}^{n=number\ of\ samples} \frac{Days\ to\ failure_{(sample\ q)}}{Total\ number\ of\ days\ of\ Exposure}$$ (Equation 3-4)

Once the samples failed, they were removed from the setup and dismantled. The samples were cleaned with distilled water and stored in a dry area for transportation. The failed samples were then analysed by the following methods in order to get further information on the nature of failure. Optical microscopy was carried out to determine the nature and magnitude of corrosion on the failed samples. Optical microscopy was also carried out to determine the presence of cracks and determine the nature of stress corrosion cracking. Fracture surface of the failed samples were analysed to determine the nature of failure.

Chapter 4   RESULTS

4.1. Material Characterization

4.1.1.   Mechanical Properties

Tensile testing was carried out on the materials received from the supplier in order to determine its mechanical properties. The result of the tensile test is given in Figure 4-1. The EN AW-7019 alloy had the lowest mechanical strengths, with the ultimate tensile strength at T6 of about 400MPa. The elongation (A_{30}) was the highest at T4 temper state at about 20.87 %, which was then reduced to 14.57% with the T6 tempering. The 7075 alloy, which has a higher Cu content, had a maximum ultimate tensile strength of about 550MPa. The elongation achieved at this high strength T6 phase was 15.73% which was slightly higher than the 7019 alloy, which can be attributed to the higher Cu content in this alloy. The KK17 and KK18 are novel 7xxx alloys which showed extremely high strengths of about 600MPa at T6 temper states. It is also seen that the strength of the material reduced on over-aging the alloy to T7 temper state. However, these high strength alloys exhibit lower ductility at T6 as compared to the standard alloys with elongation of KK17-T6 as low as 10.9%. KK18-T6, which again contains higher Cu as compared to KK17 alloy, has a higher elongation of 14.43%.
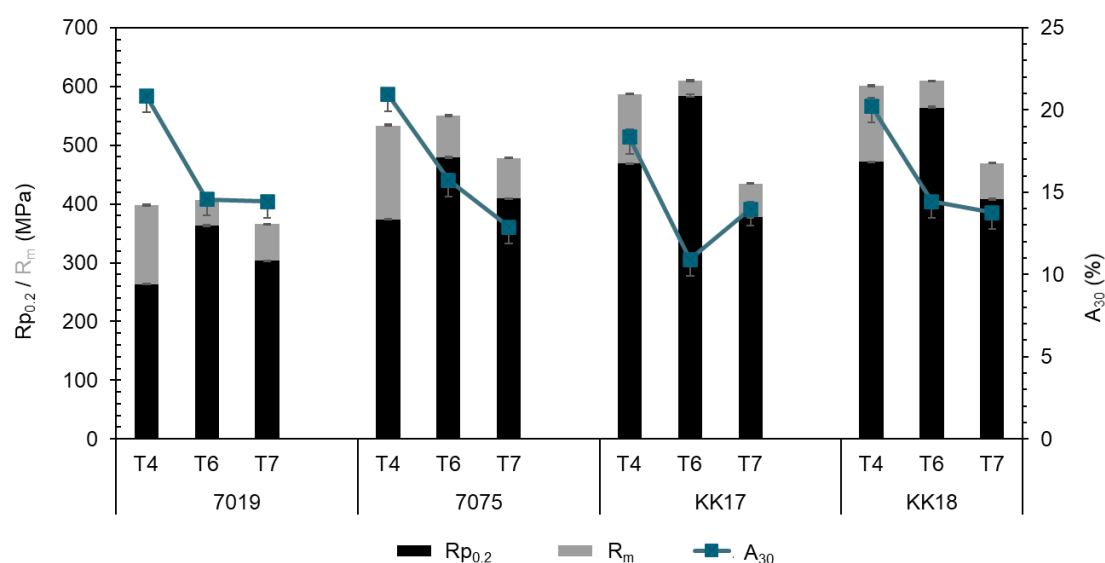
FIGURE 4-1:   RESULTS OF THE INITIAL MECHANICAL TESTING OF AS RECEIVED MATERIALS

4.1.2. Microstructural and Morphological Properties

As it is mentioned in section 3.1, the selection of the alloys was done in order to encompass a wide range of alloy contents and microstructures, which in turn provides a large range of SCC susceptibility. The four alloys chosen range over a wide spectrum of Cu and Zn+Mg content, resulting in different mechanical, microstructural and SCC properties. This section compares the microstructural and morphological variations in the chosen alloys.

The 7019-T6 alloy showed a uniform microstructure throughout the width of the samples. The grains were uniformly recrystallized near the surface of the sample as well as in the center of the samples. The 7075-T6 sample, on the other hand, showed unevenness in the grain size from the edge of the sample to the center. As shown in Figure 4-2, it was seen that grains at the edge of the sample, closer to the surface had fine recrystallized grains whereas the grains in the central region were not crystallized or elongated.
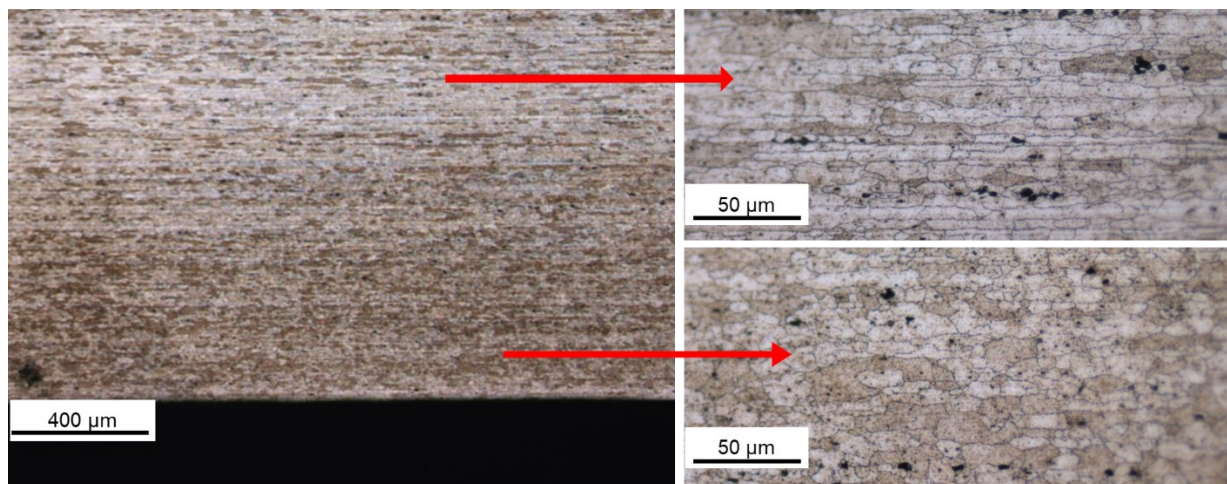
FIGURE 4-2: MICROSTRUCTURE OF THE 7075-T6 ALLOY SHOWING THE DIFFERENCE IN GRAIN ORIENTATION IN THE CENTRE OF THE SPECIMEN AND NEAR THE SURFACE

The microstructure of the KK17-T6 and KK18-T6 alloys were also found to be an inhomogeneous grain structure. It was seen that the grains were unevenly recrystallized throughout the width of the specimens. Moreover, it was observed for

both the alloys that the grains were highly elongated in the rolling direction. Figure 4-3 shows the microstructure of KK17-T6 which shows the uneven grain size.
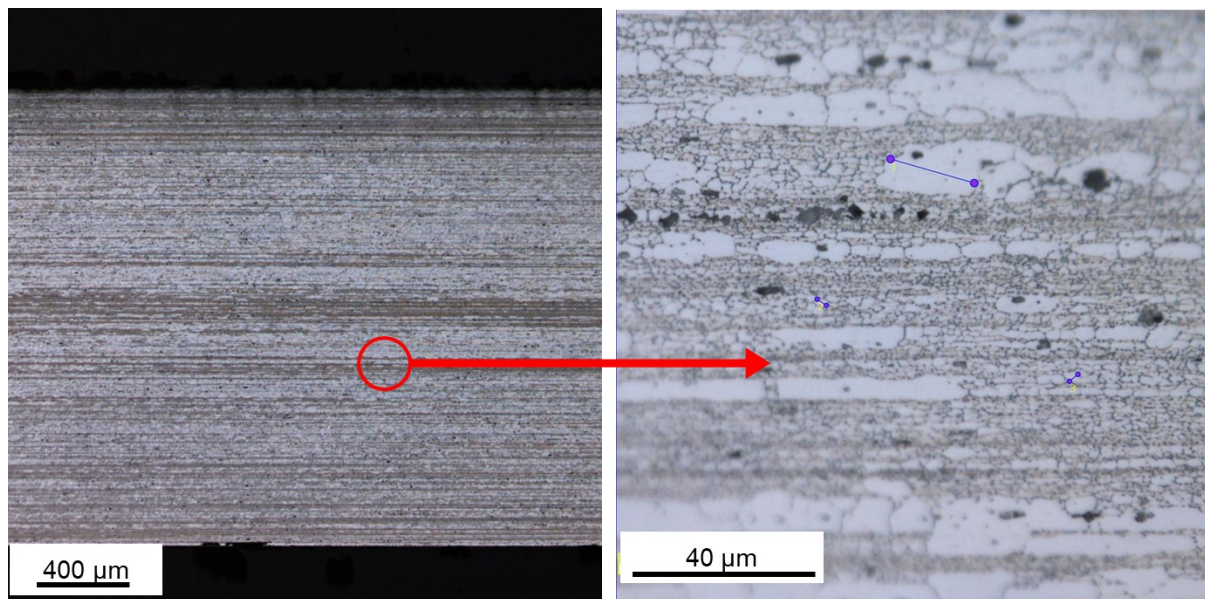
FIGURE 4-3: MICROSECTION OF KK17-T6 SAMPLE SHOWING UNEVEN "BANDED" GRAIN STRUCTURE WITH VARIATION IN GRAIN SIZES

The uncorroded samples were also observed in the scanning electron microscope to get further information on the distribution of precipitates and the grain orientation. The distribution of precipitates was also observed and compared with each alloy, with changing temper treatment. Figure 4-4 shows the microstructure of EN AW-7075 in the three temper states. It was seen that there is an increase in the number of precipitations on the grain boundaries at the peak aged condition, as compared to the naturally aged conditions. The precipitates in the 7075-T6 alloy, which are indicated by the small bright dots at the grain boundaries, were encompassed by a visible precipitate free zone which is recognised by the colour contrast, indicating a potential
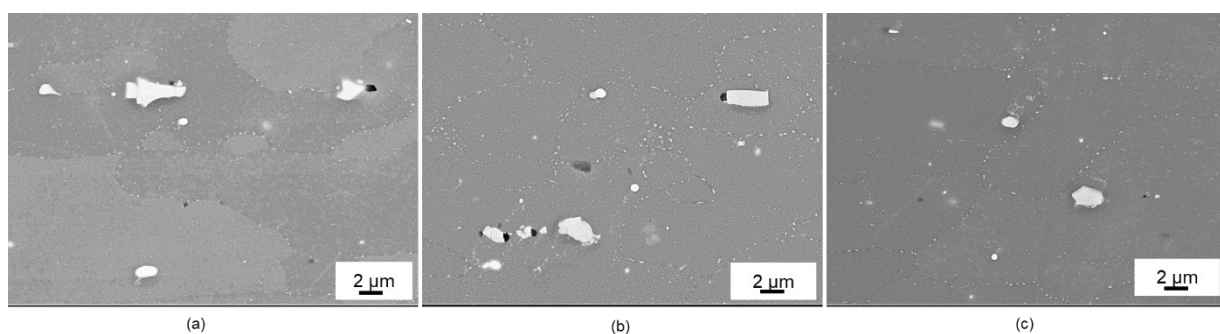
FIGURE 4-4: MICROSTRUCTURE OF EN AW-7075 IN TEMPER STATES (A) T4 (NATURALLY AGED) (B) T6 (PEAK AGED) (C) T7 (OVER AGED)

difference in the grain boundary compared to the matrix. On observing the 7075-T7 microstructure, a much-reduced number of precipitates could be observed as compared to the 7075-T6 alloy and the distance between the precipitates were also increased. Some larger primary precipitates were also observed which on EDX simulation were mostly AlFeCu and AlFeSi particles.

Figure 4.5 shows the microstructure of the KK17 and KK18 in the various temper states. The unevenness of the grain size observed in the optical microscopy was verified in SEM analysis for both the alloys. With the KK17-T4 alloys, larger precipitates were seen along the grain boundaries, which were then surrounded by precipitate free zones. The number of precipitates observed were lesser in the KK17-T6 alloy, and larger gaps between the precipitates were observed. The precipitates observed in the KK17-T7 were again continuous and larger in number and surrounded by larger precipitate free zones. The same trend was observed in the KK18 alloy. However, higher number of primary particles containing Cu were observed in the KK18 alloy compared to the KK17 due to the higher Cu content.
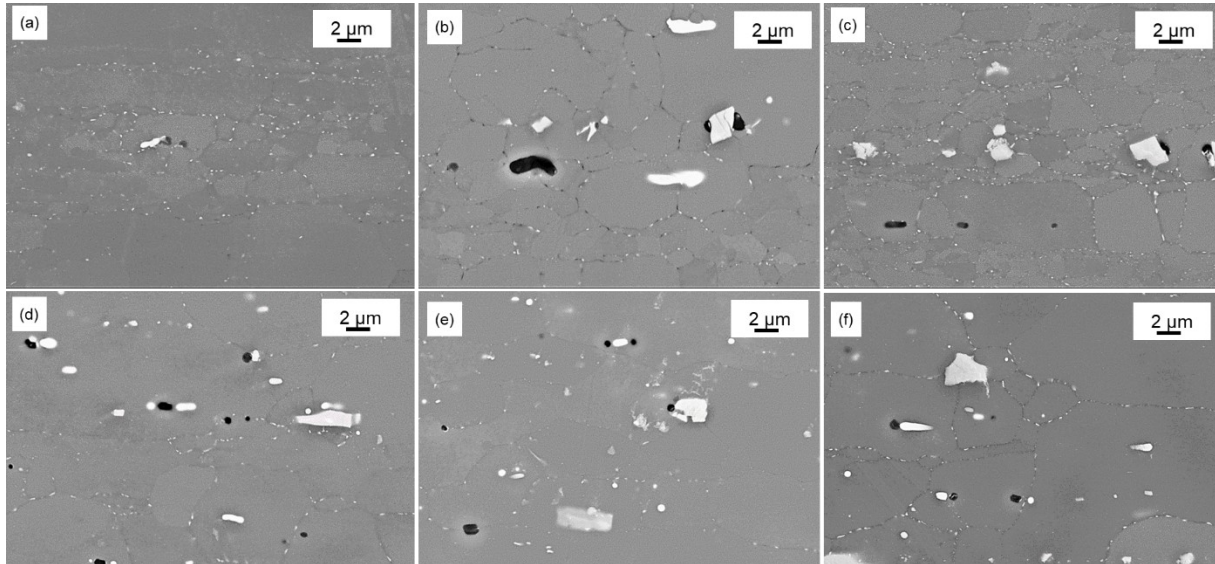
FIGURE 4-5: MICROSTRUCTURE OF THE KK17 IN TEMPER STATES (A) T4 (B)T6 AND (C) T7 ALLOY AND KK18 IN TEMPER STATES (D) T4 (E) T6 AND (F) T7

SEM fracture surface analysis of the uncorroded samples after tensile testing was also carried out in order to characterise the fracture surface for comparison with corroded specimens. The 7019 and 7075 alloys in all temper states showed relatively

homogeneous ductile fractures with honey-comb structures throughout the surface. The KK17-T6 , which has the least ductility among all the alloys, showed a brittle region at the edges of the sample towards the surface. However, towards the centre of the sample, honey-combed structures with dimples were observed, indicating ductile fracture. The KK18 alloy on the other hand showed relatively uniform ductile fracture surface with honey-comb structure observed throughout the thickness of the sample.

4.2. Influence of Environmental Parameters on SCC Susceptibility

The following section analyses the influence of environmental factors on the SCC behaviour of the 7xxx alloys. The strategy for designing of the corrosion test cycle (MBSC test) and analysis of the influence of environmental parameters is given in section 3.3.1. Once the MBSC test was designed, the next step was to study the influence of the environmental parameters on SCC susceptibility. The first step towards this was to study the influence of anions and cations in order to determine the composition of the salt-spray solution. Once this was done, the next step was to carry out DoE to determine the influence of other environmental parameters. This section describes the results of these two stages.

4.2.1. DoE for Influence of Environmental Parameters on MBSC Test

After the initial MBSC test design and the composition of salt-spray solution was determined, the next step was to determine the influence of the various parameters on the output of the test, i.e., the SCC susceptibility of the materials. This was done through the process of DoE where each chosen parameter was individually and codependently analysed. The execution of the DoE and the steps towards the statistical analysis has been described in section 3.3.3. The following section analysis the influence of the three DoE factors (temperature, dry-wet ratio, ΔT).

A general full factorial regression analysis of all the materials was carried out to determine the influence of all the factors on the SCC data using the ANOVA method. Apart from the three influencing factors, the material was considered as a factor to get a complete overview of the significant influencing parameters. Moreover, the co-
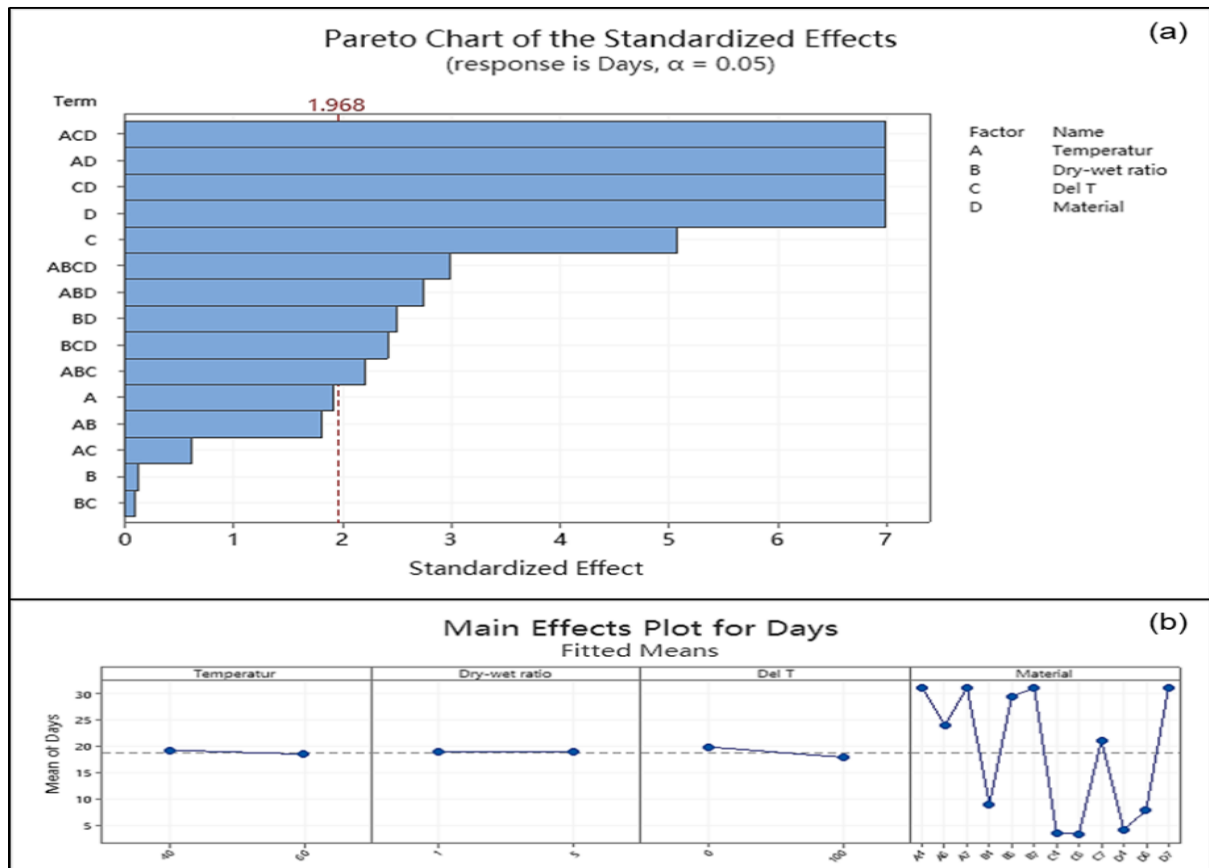
FIGURE 4-6 (A) PARETO CHART OF THE STANDARDIZED EFFECTS OF THE FACTORS ON THE MBSC TEST RESULTS (B) MAIN EFFECT PLOT OF THE 4 FACTORS (DAYS TO FAILURE)

dependent effects of these factors were also analysed. Figure 4-6 (a) shows the Pareto chart of the standardized effects of these parameters. The standardized effect indicates the strength of a relationship between influencing factors. It can be calculated as the mean difference of the pool observed divided by the standard deviation of the pool observed. [189] The minimum reference value of the standardized effect was calculated directly by Minitab as 1.968, which corresponds to a P value of below 0.05. Beyond this, the factors are considered to have a significant influence on the output. It can be observed that material, as a factor has the highest influence on the results, which is the average days to failure. This result is also expected since the material pallet was chosen to have a varied range of susceptibilities, hence giving varied results. The second most influencing factor was seen to be ΔT, which is the temperature difference between the hot and cold phase of the extreme block. Temperature showed a standardized effect factor just short of the reference, however individual material analysis revealed that it has a significant influence on most of the alloys. The dry-wet

ratio factor showed the least significance in influencing the output with a very low standardized effect factor.

This effect is mirrored also in the main effects plot, where all the mean days to failure of all the four effects were plotted against the maximum and minimum input of each factor. It can be seen that the factor 'material' had the highest influence on the mean days to failure. Following that, variation in ΔT also can be seen to have an influence on the mean days to failure with mean days to failure reducing from 19.86 to 17.88, on changing ΔT from 0°C to 100°C. Meanwhile, the mean days to failure showed a slight change in mean days to failure from 19.2 days to 18.5 days, with change in temperature from 40°C to 60°C. The change in dry-wet ratio from 1:1 to 1:5 was negligible, with average days to failure of 18.89 and 18.85, indicating no apparent influence on the test result

Based on the average days to failure of the specimens, the specimens were divided into four susceptibility categories. The alloys KK17-T4, KK17-T6 and KK18-T4 failed within 4 days of failure and were hence indicated as "high susceptibility" alloys. The 7075-T4 and the KK18-T6 alloys failed within an average range of 4 to 10 days and were categorised as "medium susceptibility". The 7019-T6, 7075-T6 and the KK17-T7 alloys which have mean days to failure ranging from 20 to 31 days were categorised as "low susceptibility" materials. Finally, the materials which passed the complete 31 days of the test without any failure such as the 7019-T4, 7019-T7 and KK18-T7 were considered as "no susceptibility". Table 4-1 shows a summary of mean days to failure of all the tested alloys and their respective categories. These categories will be later used to discuss the influence of each of the tested parameters on the individual categories.

TABLE 4-1 MEAN DAYS TO FAILURE OF THE ALLOYS TESTED AND THE RESPECTIVE SUSCEPTIBILITY CATEGORIES

Alloy	Temper State	Mean days to failure	Susceptibility Category
7019	T4	31.00	no susceptibility
	T6	23.84	low susceptibility

	T7	31.00	no susceptibility
	T4	8.59	medium susceptibility
7075	T6	29.50	low susceptibility
	T7	31.00	no susceptibility
	T4	3.53	high susceptibility
KK17	T6	3.40	high susceptibility
	T7	22.00	low susceptibility
	T4	3.35	high susceptibility
KK18	T6	7.81	medium susceptibility
	T7	31.00	no susceptibility

4.2.2.   Influence of Anions and Cations on SCC susceptibility

The first step towards optimisation of MBSC test was to determine the influence of anions and cations, which the vehicle is exposed to in its lifetime, on the SCC susceptibility. The aim of this series of experimentation was to determine the composition and concentration of a salt-spray solution containing the ions which are critical to SCC susceptibility as well as presence in the field. The material pallet was exposed to MBSC test cycle with four different test solutions, which is listed in Table 3-7. Results in the form of average days to failure and metallographic analysis were analysed.

Figure 4-7 shows a summary of the results obtained from testing the material pallet with the different test solutions. The most susceptible alloys were the KK17-T4, KK17-T6, KK18-T4 and KK18-T6 which all failed within 5 days of testing. There was also no significant difference in the average days to failure of the materials exposed to solutions with or without additives for these highly susceptible alloys. The 7075-T4 also failed within 3 days when exposed to solution with additives. However, the average days to failure of the same material exposed to salt solution without additive was around 9 days. Moreover, the standard deviation for the 7075-T4 alloy was higher

compared to the specimens exposed to solutions with additives. This was followed by the 7019-T6 and the KK17-T7 alloys which failed between 10-15 days of testing. A significant difference of average days to failure was observed for the 7019-T6 which failed at an average of around 16 days when exposed to salt solution without any additional ions, which is about 5 days later compared to the ones exposed to salt solution with additive. Once again, the standard deviation of the specimens exposed to pure 3.5 wt.% NaCl was higher than those exposed to solutions with additives. The 7019-T4, 7019-T7, 7075-T7 and KK18-T7 did not show any failure in any of the exposed solutions, with a few exceptions. On comparison of average days to failure between the three solutions with three varying additives, it was seen that the difference was negligible in most of the alloys except 7019-T6 and 7075-T4, where the additives accelerated the SCC failure.
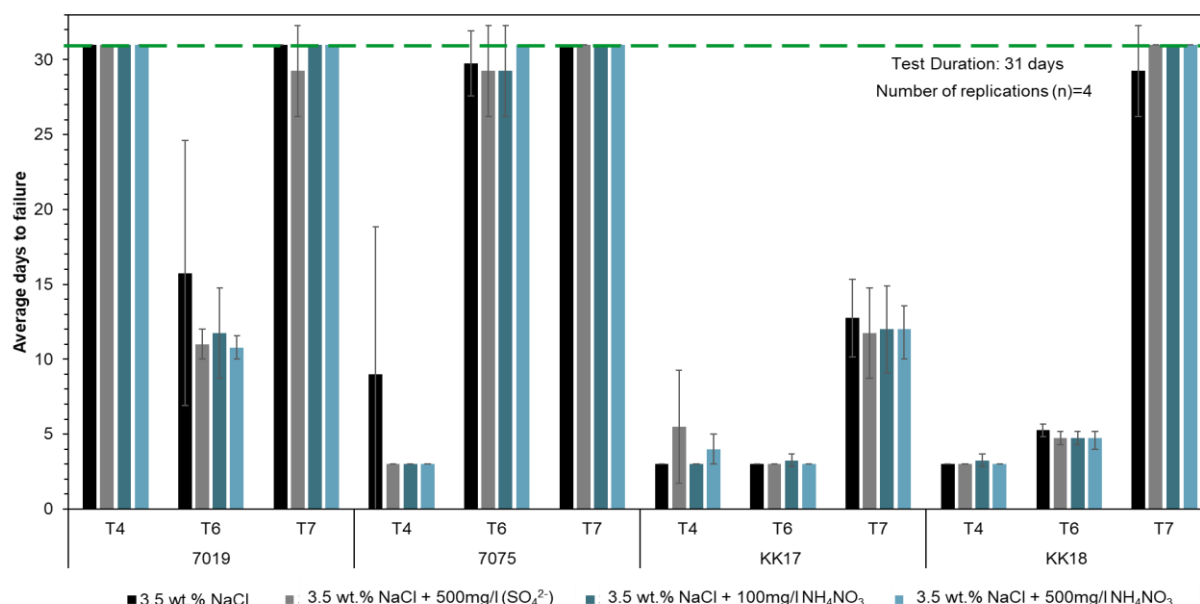
FIGURE 4-7: COMPARISON OF TIME-TO-FAILURE OF ALLOYS EXPOSED TO MBSC TEST WITH VARYING SALT SOLUTION COMPOSITIONS

The metallographic examination of the samples revealed that the additives had a significant corrosion influence on the materials. It was generally observed that the additives increased localised corrosion such as intergranular corrosion and pitting corrosion on the materials. Moreover, it was seen that the addition of NH_4NO_3 also resulted in more and deeper secondary SCC cracks on the surface of the samples along with higher corrosion influence. Figure 4-8 shows the micrograph of 7075-T4 exposed to the four different solutions. The samples exposed to pure NaCl solution showed intergranular and pitting corrosion on certain parts of the surface. However,

the corrosion was lesser compared to that observed in the solution with Na_2SO_4, where severe intergranular corrosion was to be seen. The specimens exposed to the NH_4NO_3 of different concentrations also showed intergranular and pitting corrosion and also secondary SCC cracking as shown in Figure 4-8(c) and (d).

 In summary, it was generally observed that the specimens exposed to salt solution with additives, showed a marginally higher SCC susceptibility as compared to that exposed only to 3.5 wt.% NaCl solution. Micrographs also showed larger microcracks and more intergranular and pitting corrosion in specimens exposed to solutions with additives. To test the influence of the added salts, potentiodynamic polarisation of the alloys in T6 condition was carried out to in the above-mentioned solutions and compared. A marginal increase in the anodic current density was observed, especially on the addition of NH_4NO_3, indicating towards higher corrosion susceptibility with the additive.
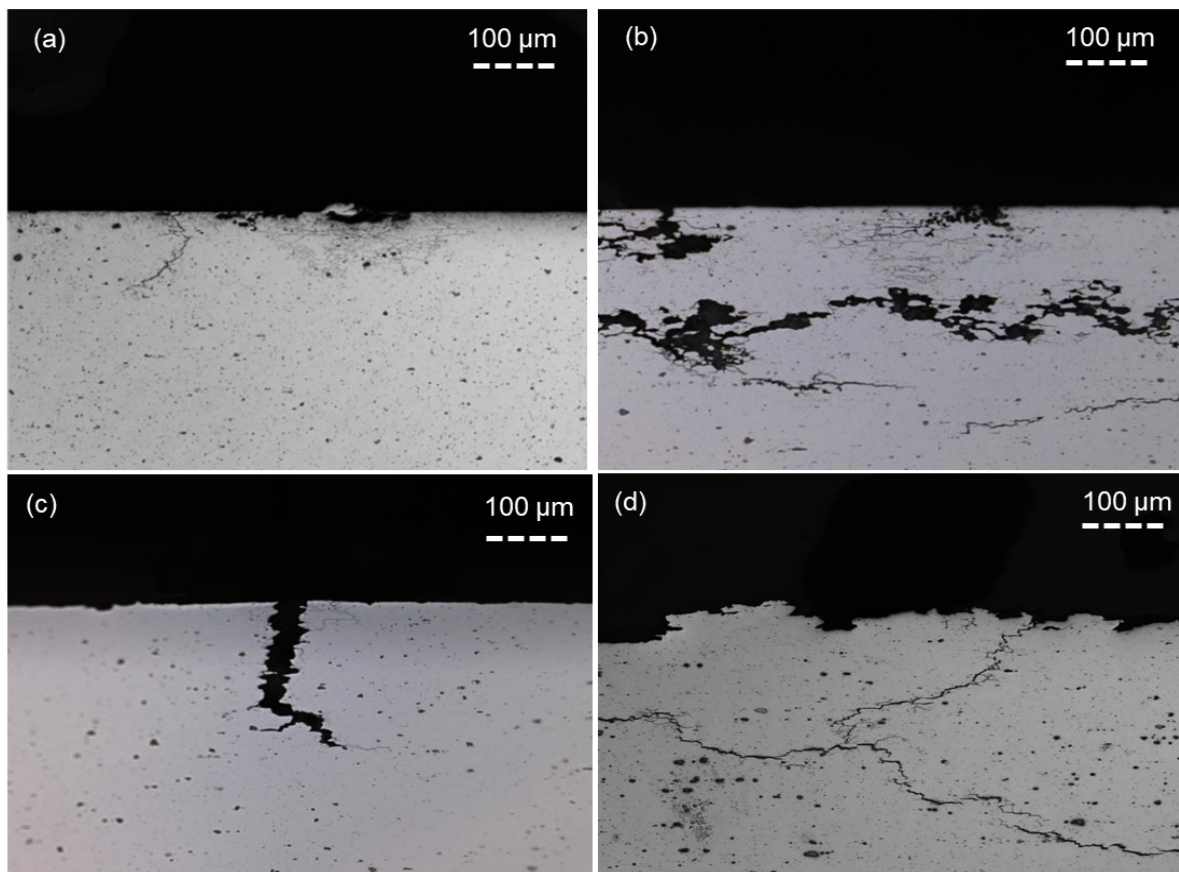
FIGURE 4-8   7075-T4 EXPOSED TO (A) 3.5 WT.% NACL(B) 3.5 WT.% NACL + 500MG/L SO$_4$ $^{2-}$ (C) 3.5 WT.% NACL + 100MG/L NH$_4$NO$_3$ (D) 3.5 WT.% NACL + 500MG/L NH$_4$NO$_3$

The addition of NH_4NO_3 showed the higher corrosion on the alloys and also showed lesser variance in the SCC failure. Due to this evidence of influence of NH_4NO_3 on the SCC susceptibility and its significant presence in the environment, it was chosen to be added as an additive in the salt solution for the MBSC test. Since there was no significant difference in the results with respect to the amount of additive used, 100mg/l NH_4NO_3 was chosen and used for further testing of MBSC in the DoE.

4.2.3. Influence of Temperature

Figure 4-9 shows the comparison of SCC susceptibility at 40°C and 60°C at varying dry:wet and ΔT values. Figure 4-9 (a) with dry:wet ratio 1:1 and ΔT is 100°C does not show a significant difference in the average days to failure in any of the tested alloys. However, changing the dry:wet ratio to 1:5, shown in Figure 4-9(b), showed a larger reduction in average days to failure, with increasing temperature for the 7019-T6, KK17-T7 and the KK18-T6 which were classified as medium and low susceptible alloys. This difference in result indicates that the variation in SCC susceptibility with varying temperature is dependent on the other two factors. In order to analyse the influence of the temperature the co-dependency of temperature with the other two factors must also be analysed.
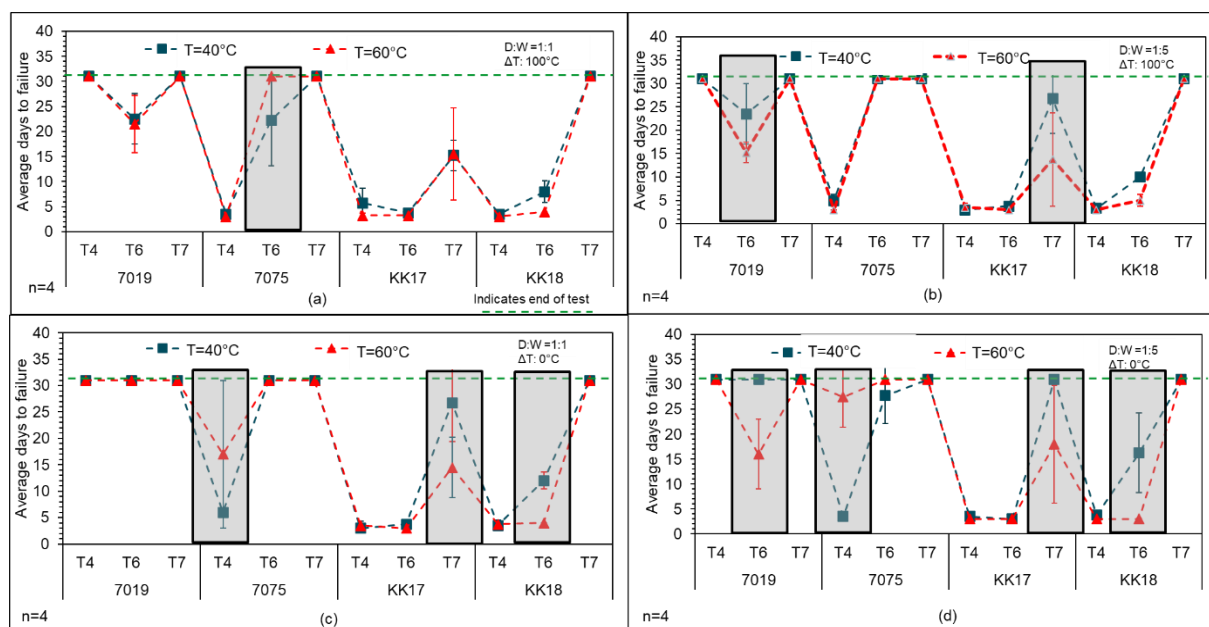
FIGURE 4-9   INFLUENCE OF TEMPERATURE ON AVERAGE DAYS TO FAILURE ON EXPOSURE TO MBSC TEST

Similarly, observation of the data from Figure 4-9(c) where the dry:wet ratio was 1:1 but the ΔT is 0°C showed a significant difference in the SCC susceptibility of alloys exposed to 40°C and 60°C, respectively. The alloys KK17-T7 and KK18-T6 showed a drop in the average days to failure on increasing the temperature from 40°C to 60°C. However, the 7075-T4 showed a contrary result, wherein, the average days to failure increased with increase in temperature. When the dry:wet ratio was changed to 1:5 and T to 0°C, as in the Figure 4-9 (d), a difference in average days to failure was again observed in 7019-T6, KK17-T7 and KK18-T6, where the SCC susceptibility increased, with increase in temperature. On the contrary, 7075-T4 and 7075-T6 showed an increase in SCC susceptibility with increase in temperature.
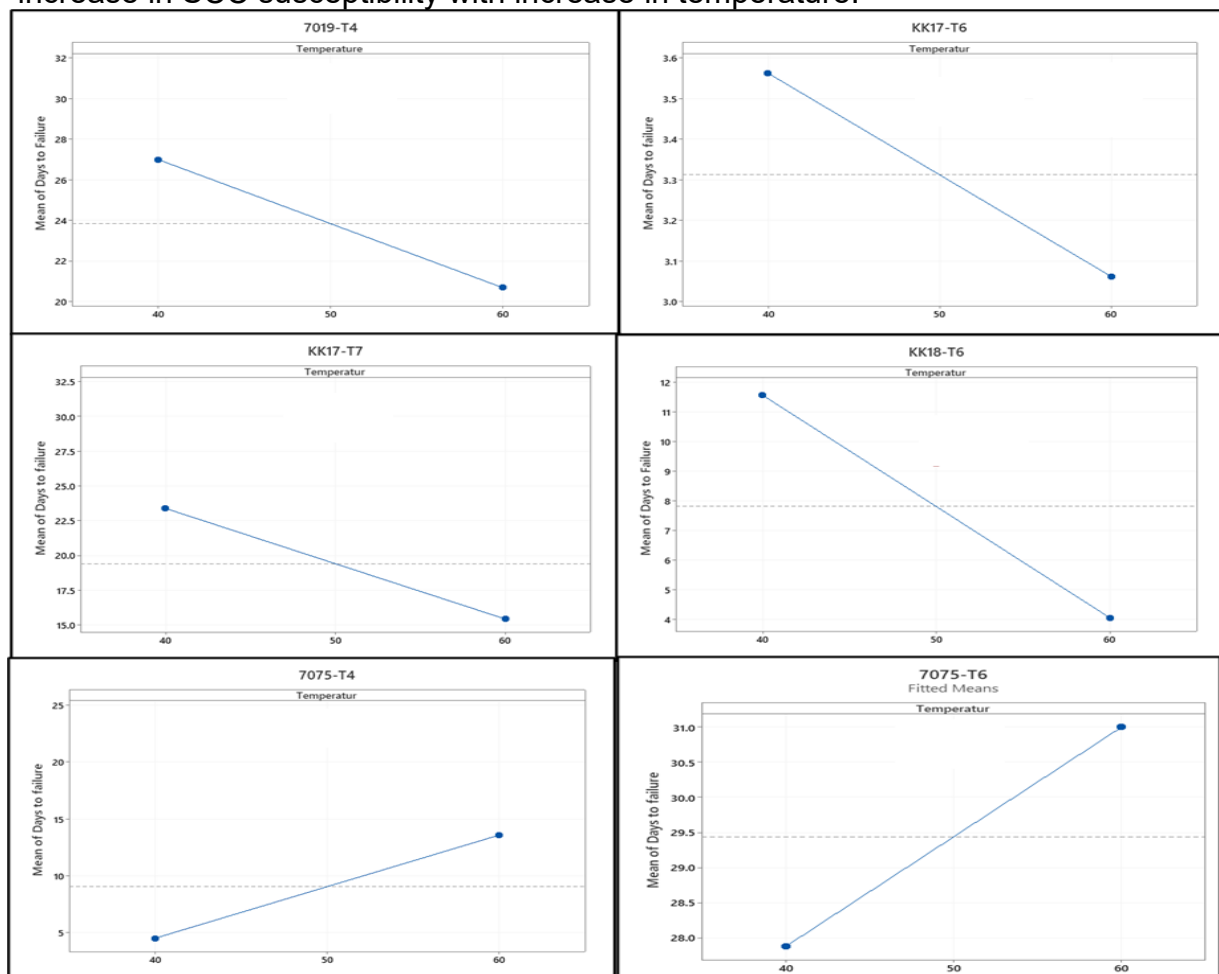
FIGURE 4-10: MEAN EFFECT OF TEMPERATURE ON DAYS TO FAILURE FOR INDIVIDUAL MATERIALS

In summary, it can be seen that the SCC susceptibility of the high susceptible and the non-susceptible alloys did not change considerably with the change in temperature. However, the medium and low susceptible alloys showed a considerable increase in SCC susceptibility, with increase in temperature, with the exception of 7075-T4 and

7075-T6, which shows the opposite trend. The influence of temperature on the SCC susceptibility is also dependent on the other parameters. In order to study the individual effect of the temperature on the materials and its statistical significance, a full regression analysis was carried out on the data gathered from the testing. As shown in Figure 4-6(a) it can be seen that the temperature has a very slight influence on the SCC test results, with its standardized effect value just short of the reference value. However, detailed analysis of the influence of temperature on individual materials, revealed that temperature has a significant influence on the alloys 7019-T4, KK17-T6, KK17-T7, KK18-T6, 7075-T4 and 7075-T6. The mean difference of these alloys is depicted in Figure 4-10. In all of these alloys except 7075-T4 and T6, with an increase in temperature from 40°C to 60°C, there is a significant decrease in the days to failure. For e.g., the mean days to failure reduced from approximately 27 days to 21 days in the 7019-T4 alloy and 12 days to 4 days for the KK18-T6 alloys. As also seen in the previous results, there is an increase in the average days to failure when the temperature increases from 40°C to 60°C in the 7075-T4 alloy and 7075-T6 alloy. This exception of increase in susceptibility with decrease in temperature is discussed further in section 4.2.6. The difference in the other alloys were statistically not significant.

4.2.4.   Influence of Temperature Difference in Extreme Block (ΔT)

The influence of temperature difference between the hot phase and the cold phase of the extreme block, called ΔT, was also examined in the scope of the DoE. Two conditions were considered as minimum and maximum for the DoE, wherein minimum ΔT was 0°C, corresponded to elimination of the extreme block C and the continuation of the Block B instead. The maximum ΔT was taken as 100°C, where the temperature of the hot phase was 80°C and that of the cold phase was -20°C, making a temperature difference of 100°C. The central point was taken as 50°C, where the temperature in the hot phase was 50°C and in the cold phase it reduced to 0°C.

Figure 4-11 shows the difference in average days to failure with varying ΔT, in various combinations of dry:wet ratio and test temperature. On observation of Figure 4-11(a), where the dry:wet ratio is 1:1 and temperature is 40°C, there was a significant drop in average days to failure observed with increase in ΔT from 0°C to 100°C in the 7019-T6, 7075-T6, KK17-T7 and 7075-T4 alloys. In Figure 4-11(a), (b) and (c) it is observed

that with ΔT=0 no failure of 7019-T6 is observed at all, although the alloy is susceptible. Similarly, 7075-T4 alloy, which is a significantly susceptible material has much delayed fracture in the with ΔT=0. Therefore, it can be concluded that the ΔT generally plays a
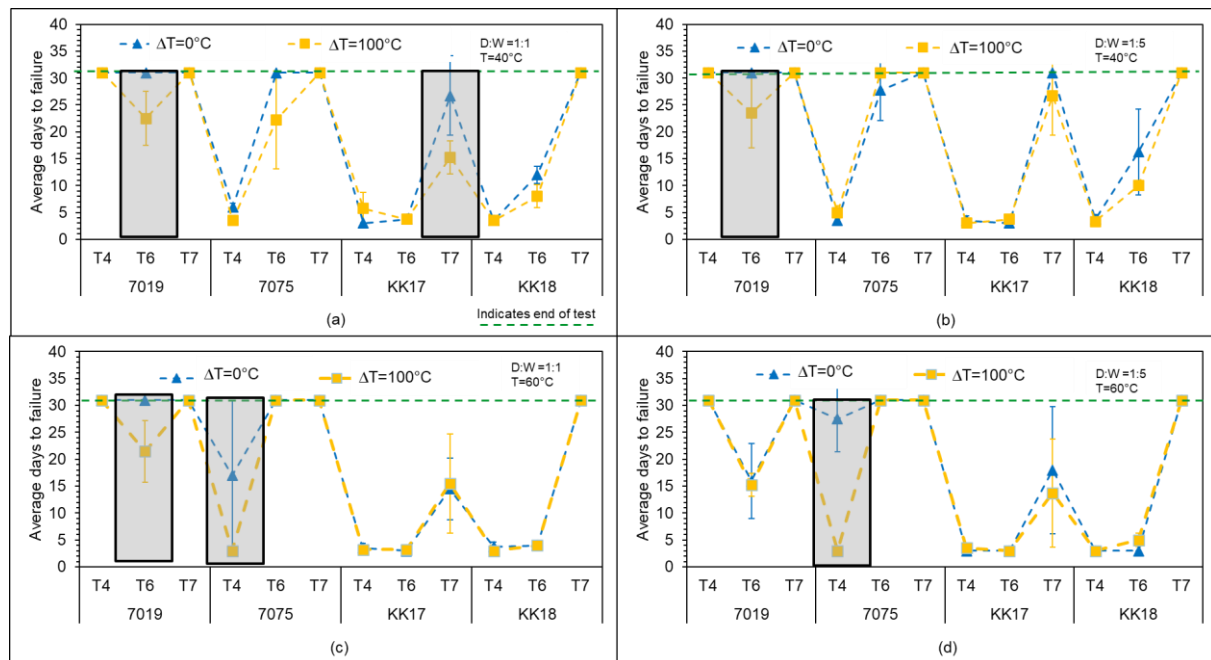

FIGURE 4-11: INFLUENCE OF ΔT ON THE AVERAGE DAYS TO FAILURE OF ALLOYS EXPOSED TO MBSC TEST

crucial role on identifying the SCC susceptible materials and thus, needs to be considered within the design of the MBSC test.

The complete full regression analysis, also with material as a factor, described in section 4.2 showed ΔT to have the most significant influence on the average days to failure after the material itself. Individual material analysis revealed that ΔT had a statistically significant influence on three materials, 7019-T6, 7075-T4 and KK17-T7. As it can be seen in the Figure 4-12, with increasing ΔT from 0°C to 100°C, there was a reduction in mean days to failure for all the three alloys. For 7019-T6, the mean days
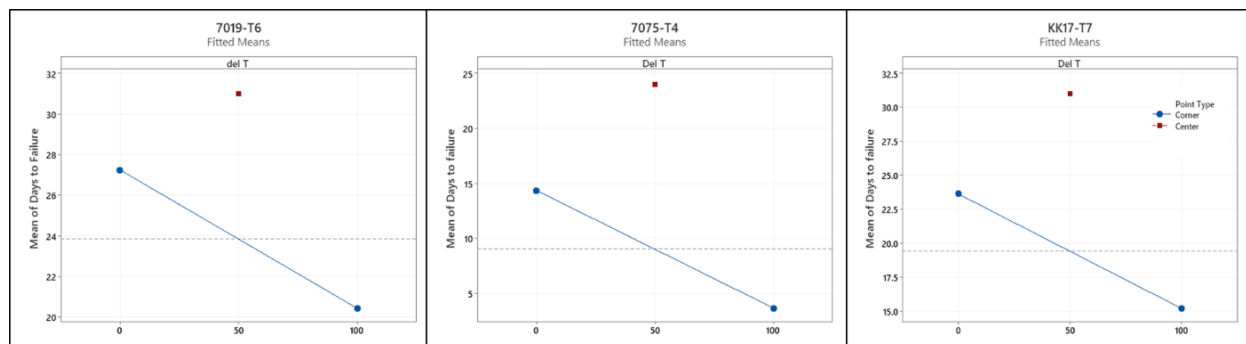
FIGURE 4-12 MEAN EFFECT OF ΔT ON THE MEAN DAYS TO FAILURE FOR INDIVIDUAL MATERIALS

to failure reduces from around 27 days at 0°C to about 21 days at 100°C. The drop in 7075-T4 is also noteworthy, showing a drop from 15 days at 0°C to less than 5 days when ΔT increased to 100°C. KK17-T7 also showed a drop from about 23 days to 15 days with change in ΔT

4.2.5. Influence of Dry:Wet Ratio

The dry:wet ratio has also shown to significantly influence on the SCC susceptibility of 7xxx alloys, making it an important parameter to analyse in the MBSC test.[165] Dry:wet ratios of block B were considered as DoE parameters with a minimum value of 1:1, corresponding to 3 hours: 3 hours of dry and wet cycle. A maximum value of 1:5 was set which corresponded to 1 hour of dry period and 5 hours of wet period. The dry phase was characterised by a relative humidity level of 50% and the wet phase was characterised by a relative humidity level of above 95%. The results are compared for different values of temperature and ΔT as shown in Figure 4-13.
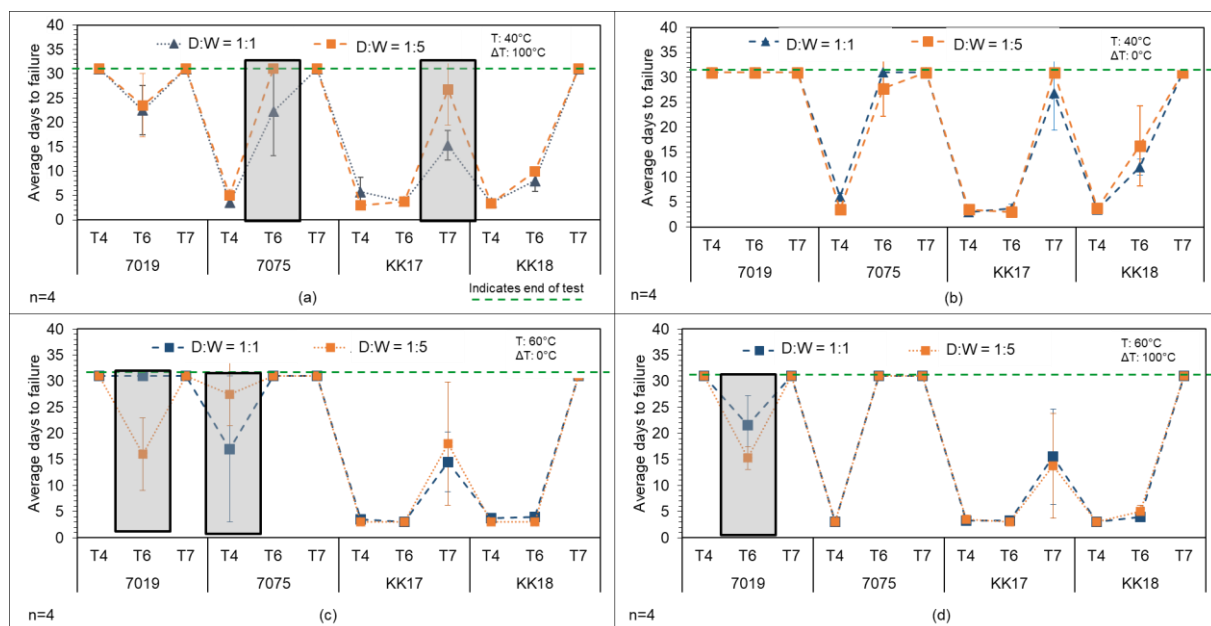
FIGURE 4-13 INFLUENCE OF DRY:WET RATIO ON AVERAGE DAYS TO FAILURE ON EXPOSURE TO MBSC TEST

When test temperature was 40°C and ΔT is 100°C, as in Figure 4-13(a), a difference was observed in 7075-T6 and KK17-T7 where sample failed with a dry:wet ratio of 1:1 whereas it passed the test with a dry:wet ratio of 1:5. Similarly, the KK17-T7 alloy also showed a delay in failure when the dry:wet ratio changes from 1:1 to 1:5, showing that the dry:wet ratio 1:1 is more critical. A difference in SCC susceptibility was again observed when test temperature was 60°C and T is 0°C, with the 7019-T6 and 7075-

T4 alloys as shown in Figure 4.13(c). With 7019-T6, a dry:wet ratio of 1:5 was observed to be more critical compared to the ratio of 1:1 and the vice versa trend for the 7075-T4 alloys. However, the rest of the alloys did not show any significant difference in SCC susceptibility with change in dry:wet ratio.

The full regression analysis, shown in Figure 4-6 confirmed the results seen above that the factor dry:wet ratio was below the reference line of standardized effect factor in the pareto chart, indicating that the influence it has on the average days to failure is not statistically significant. Individual material regression analysis also revealed that the variation in dry:wet ratio did not show a statistical significance on the average days to failure, which translates to the SCC susceptibility, of all the materials tested, with the exception of 7019-T6. In this alloy, it can be seen that with change in dry:wet ratio from 1:1 to 1:5, the days-to-failure decreases from an average of around 26 days to 21.5 days.

4.2.6.   Selection of Optimal Parameters for MBSC Test

Table 4-2 gives the complete overview of the results obtained from the DoE. It can be seen from the analysis above and the table below, that the individual environmental parameters have a significant effect on the SCC susceptibility of the materials. The primary results from analysis of the individual factors revealed that the parameter ΔT and temperature have a significant influence on the materials. These parameters influence each material differently and in different magnitudes. The dry:wet ratio was not a statistically significant parameter as observed in the full regression analysis and on individual material level only influenced the 7019-T6 alloy. The general trend to be seen was that with the increase in T from 0°C to 100°C, there was a reduction in the mean days to failure for most alloys observed, indicating an increase in the SCC susceptibility. An increase in test temperature resulted in the decrease in mean days to failure for most alloys, indicating higher SCC susceptibility, except for 7075-T4 and 7075-T6. On observation of individual materials, it was seen that different materials react differently to the variation in these environmental parameters, and it is important to individually analyse the influence on materials in order to determine the optimal parameters.

The alloys rated as 'highly susceptible,' generally failed within a period of 3 to 5 days. This includes the KK17-T4, KK17-T6, KK18-T4 and KK18-T6 alloys. Variations in the environmental parameters, did not considerably change the susceptibility of these alloys. Similarly, on the other end of the spectrum, in which alloys are considered 'not susceptible,' such as the 7019-T4, 7019-T7, 7075-T7 and KK18-T7, did not fail in any of the variations. The most observable differences were found in the 'medium' and 'low' susceptible alloys, especially the 7019-T6, 7075-T4, 7075-T6 and the KK17-T7 alloys which are the deciding factor to determine the optimal test parameter and thus will be discussed further.

TABLE 4-2 COMPLETE OVERVIEW OF THE AVERAGE DAYS TO FAILURE IN EACH TESTED CONDITION OF THE DoE [ALLOYS WITH MOST OBSERVABLE DIFFERENCES HIGHLIGHTED IN RED]

Work Package		1.1	1.2	1.3	1.4	2.1	3.1	3.2	3.3	3.4	Average
Temperature|D:W|ΔT		40°C|1:1|100°C	40°C|1:5|100°C	40°C|1:1|0°C	40°C|1:5|0°C	50°C|1:3|50°C	60°C|1:1|0°C	60°C|1:1|100°C	60°C|1:5|0°C	60°C|1:5|100°C	fracture
Material	Temper										days
7019	T4	31	31	31	31	31	31	31	31	31	31
	T6	22.5	23.5	31	31	31	31	20.5	16	15.25	23.84
	T7	31	31	31	31	31	31	31	31	31	31
7075	T4	3.5	5	6	3.5	24	17	3.25	27.5	3	8.59
	T6	22.25	31	31	27.75	31	31	31	31	31	29.5
	T7	31	31	31	31	31	31	31	31	31	31
KK17	T4	5.75	3	3	3.5	3.5	3.5	3	3	3.5	3.53
	T6	3.75	3.75	3.75	3	3.5	3	4	3	3	3.40
	T7	15.25	26.75	26.75	31	31	14.5	29.25	18.75	13.75	22
KK18	T4	3.5	3.333	3.5	3.75	3	3.75	3	3	3	3.35
	T6	8	10	12	16.25	9.25	4	4.25	3	5	7.81
	T7	31	31	31	31	31	31	31	31	31	31

The 7019-T6 alloy underwent fracture in work packages 1.1, 1.2, 3.2 and 3.4 while passing the test without failure in other work packages. The general trend was that with ΔT=100°C, failure was observed in this material, whereas with ΔT=0°C the materials did not fail in any condition, apart from Work package 3.3, with 60°C and 1:5 dry:wet ratio. Therefore, the cause of failure was important to be determined in order to assess whether the failure was actually caused due to SCC failure or whether it was residual failure due to thermal changes in the material. To confirm the nature of failure of this alloy, SEM fracture surface analysis was carried out, as shown in Figure 4-14. A mixed ductile-brittle fracture was found with secondary cracks and embrittlement on the edges of the sample. Figure 4-14 (b) shows the edges of the specimen, showing intergranular brittle structure with SCC cracks within the surface. Figure 4-14 (c) shows the transition from brittle to ductile failure, indicating that the initiation of the failure could be embrittlement due to SCC and the failure is then continued as residual strength decreases. With the confirmation of SCC on the 7019-T6 alloy, it was seen

that the extreme block, ΔT, plays a very important role in filtering out the susceptible materials from the non-susceptible material.

The 'medium susceptible' alloys, 7075-T4 showed a failure in all the 9 variations. The parameters which were statistically significant for this alloy were the test temperature
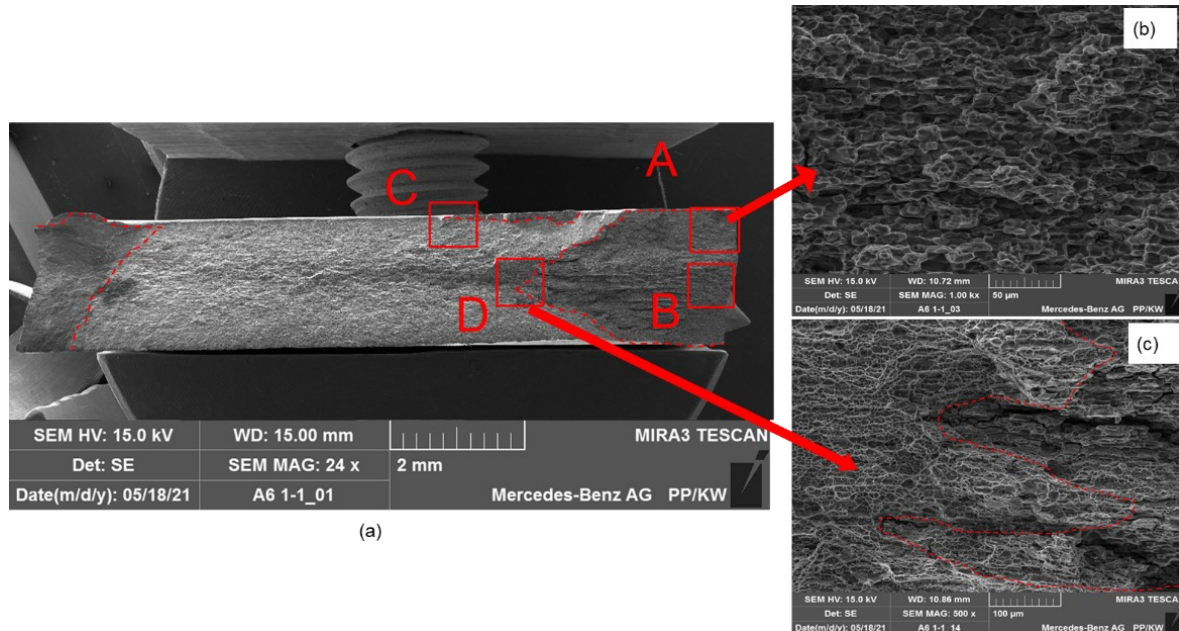

FIGURE 4-14 SEM FRACTURE SURFACE ANALYSIS OF FAILED 7019-T6 AFTER EXPOSURE TO MBSC TEST (WP 1.1) SHOWING (B) EMBRITTLEMENT ON THE EDGE SURFACE AND (C) TRANSITION FROM BRITTLE TO DUCTILE

and the ΔT. The fastest failure was observed at 60°C, 1:5 dry:wet ratio and ΔT as 100°C. With the same parameters, but a change in ΔT to 0°C, the mean days to failure drastically increase from 3 days to 27.5 days, once again highlighting the importance of the Block C on the SCC susceptibility of the alloys. However, when the test temperature is 40°C, the decrease in mean days to failure between ΔT of 0°C and 100°C is from 6 days to 3 days. This implies the co-dependent nature of ΔT and the test temperature. This co-dependency is also shown to be statistically significant, on carrying out a regression analysis.

The 7075-T6 alloy is of special interest to the thesis due to its high strengths, good ductility, and its wide use in various industries. However, the 7075-T6 alloy is known to be SCC susceptible. Due to this, the behaviour of the 7075-T6 alloy was closely studied, to determine the influence of the environmental factors on its susceptibility. Interestingly, it is observed that the 7075-T6 alloy only shows failure in two work packages, 1.1(40°C|1:1|100°C) and 1.4(40°C|1:5|0°C). The alloy passed the 31 days

of all the other test environments without any failure. The residual strength analysis of the passed alloys was compared, as shown in Figure 4-15. The residual elongations for samples exposed to 40°C, as in WP 1.2 and 1.3 reduces considerably from an original elongation of 15.6% to 2.5%. On the contrary, the 7075-T6 alloy, which were exposed to a temperature of 60°C, show very slight loss of elongation to range of 10 to 13% elongation. This indicates that contrary to the other failed alloys, the SCC susceptibility of the 7075-T6 alloy decreases with increase in test temperature.
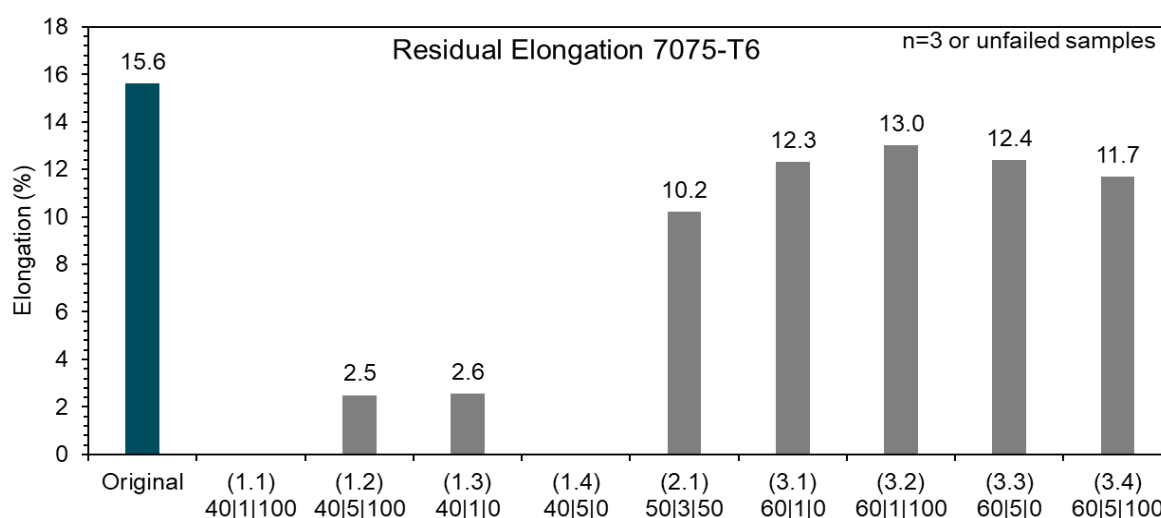
FIGURE 4-15 RESIDUAL ELONGATION OF 7075-T6 EXPOSED TO THE VARIOUS WORK PACKAGES OF MBSC TEST SHOWING SIGNIFICANT LOSS OF ELONGATION IN WP 1.2 AND 1.3

The SEM analysis of the failed 7075-T6 alloy also revealed partial embrittlement and secondary cracks within the specimen. Figure 4-16 (a) shows the fracture surface of the 7075-T6, failed after 17 days after exposure to work package 1.1(40°C|1:1|100°C). Embrittled intergranular fracture surface is observed on the edges of the specimen, with secondary cracks, indicating SCC failure. Similarly, Figure 4-16 (b) shows the fracture surface of 7075-T6 after exposure to work package 1.4 (40°C|1:5|0°C) for 18 days. Complete embrittlement with secondary cracks running parallel to the surface are observed in the edges of the specimen and the central area shows mostly intergranular brittle structure, with small regions of residual ductile regions. The SEM analysis confirms the SCC related fracture of the specimens.

In general, the over-aged alloys tend to be less susceptible to SCC compared to the peak-aged variant. [10] However, in the DoE conducted, the KK17-T7 alloy, showed failure in most of the tested environments and was classified as a 'low susceptible

alloy'. It also showed considerable variation in time-to-failure with respect to the change in environmental conditions. WP 3.4 showed the lowest time-to-failure of 13.75 days, followed by WP 3.1 and 1.1, with 14.5 and 15.25 days, respectively. As in the previously discussed alloys, the test temperature plays an important role in the days to failure of this alloy as can be seen comparing WP 1.2 and 3.4, where the dry:wet ratio is 1:1 and ΔT is 100°C for both, however, the test temperature is 40°C and 60°C, respectively. The increase in test temperature reduces the average days to failure in this case from 26.75 days to 13.75 days. However, surprisingly, a reverse trend was observed with the WP 1.1 and 3.2, where the increase in test temperature is shown to increase the average days to failure from 15.25 days to 29.25 days. ΔT is also seen to have a significant influence on the results, with increasing ΔT from 0 to 100°C , there is an increase in the average days to failure as observed in the WP 1.1 comparing with WP 1.3, where test temperature and dry:wet ratio remains constant , but ΔT varies. Regression analysis also showed the influence of the two parameters, test temperature and ΔT on the susceptibility of this alloy.
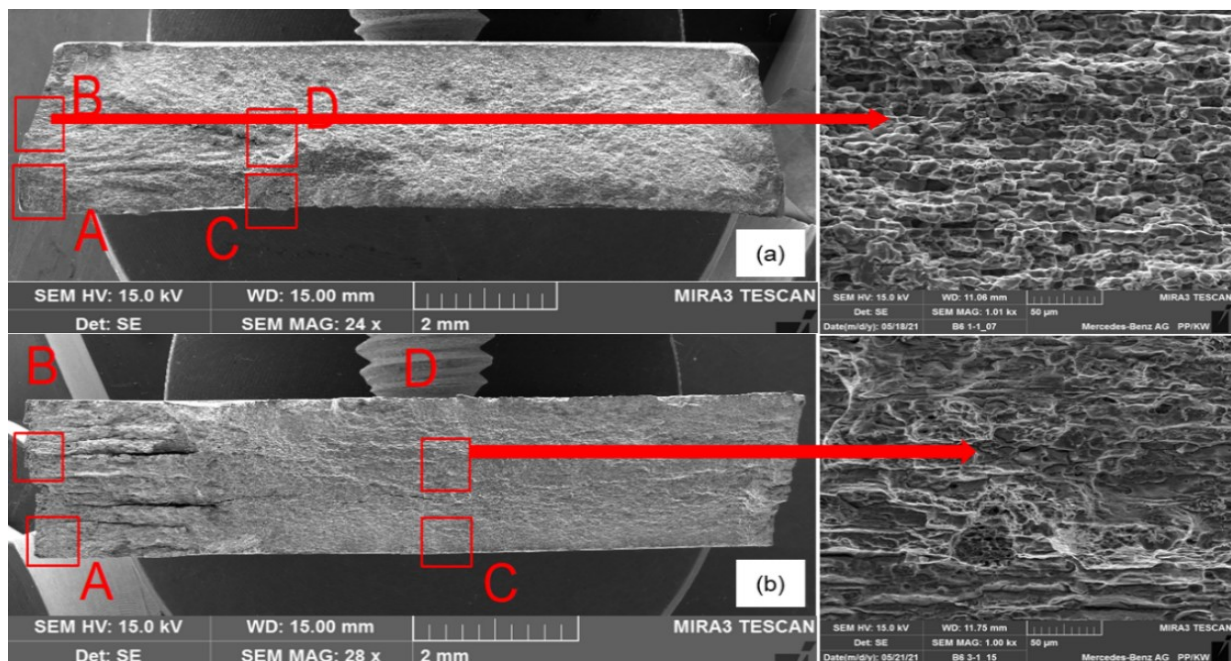
FIGURE 4-16 (A) FRACTURE SURFACE ANALYSIS OF 7075-T6 AFTER EXPOSURE TO MBSC TEST (WP 1.1) (B)) FRACTURE SURFACE ANALYSIS OF 7075-T6 AFTER EXPOSURE TO MBSC TEST (WP 1.4)

The SEM analysis of the KK17-T7 alloy also revealed intergranular brittle structure, as shown in Figure 4-17, where the KK17-T7 alloy was exposed to WP 1.1 for 15 days until failure. Intergranular brittle surface along with secondary cracks running parallel to the surface confirm SCC embrittlement of the specimen. Interestingly, there is also

a level of stepwise structure to be observed in this fracture surface, which could indicate crack-arrest due to hydrogen embrittlement.[122] This confirmed the SCC susceptibility of the KK17-T7 alloy and the ability of the MBSC test to differentiate and crystallize also low susceptible materials.
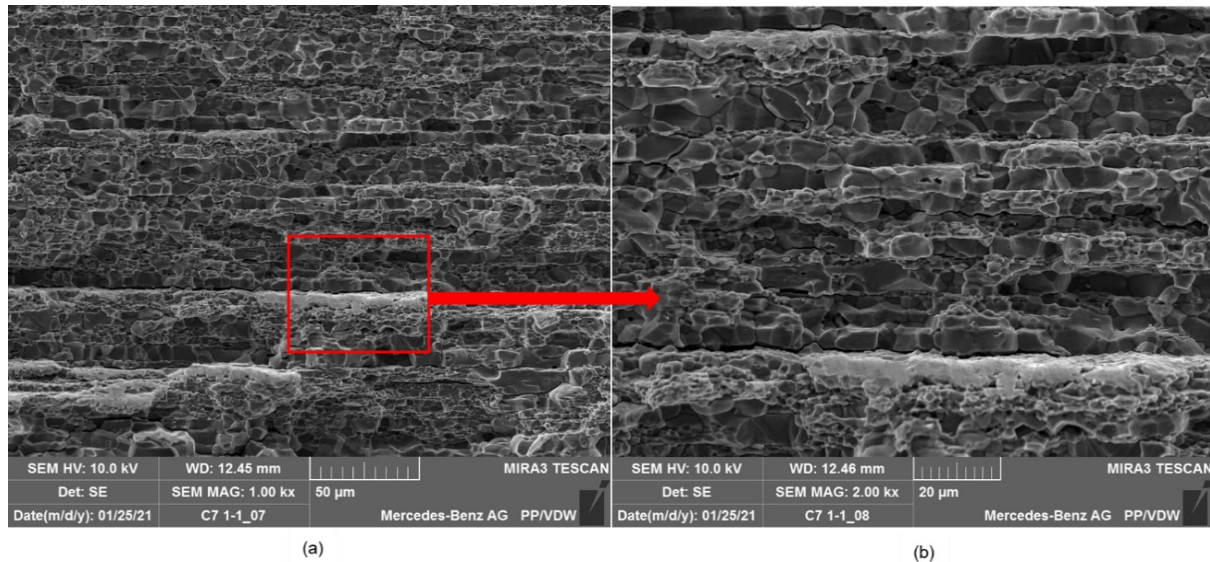
FIGURE 4-17 FRACTURE SURFACE OF KK17-T7 AFTER EXPOSURE TO MBSC TEST (WP1.1)

In summary of the all the results above, it can be seen that the test temperature and ΔT play the most important role in determining the average days to failure, hence the SCC susceptibility of the materials. The variation of ΔT of 100°C, represents the extreme temperatures (80°C in the hot phase and -20°C in the cold phase) that could occur in the lifecycle of an automobile. It was observed that the presence of block C results in the failure of medium and low susceptible alloys, which do not fail in the absence of this block. Due to this significant influence on the material differentiation and its similarity to 'real-time' environment, it is important to retain this block within the MBSC test.

The test temperature also showed a significant influence in the SCC susceptibility of the tested alloys. While 7019-T6 and KK17-T7 alloys showed a reduction in SCC susceptibility with increase in test temperature, 7075-T4 and 7075-T6 showed an opposite trend. This was also observed in the residual tensile elongation where an increase in temperature from 40°C to 60°C increased the residual elongation, hence reduced embrittlement, showing that 40°C was more critical to the 7075 alloy as

compared to 60°C. This result shows the importance of finding the optimal temperature which would be critical to all the alloys.

On combined analysis of the results discussed above, it was considered that the environmental parameters in the work package 1.1, with test temperature of 40°C, dry:wet ratio of 1:1 and ΔT of 100°C was the most appropriate parameters. This work package showed early failure of within 10 days in the most critical alloys such as the 7075-T4, KK17-T4 and T6 and KK18-T4 and T6. The low susceptible alloys also showed failure with this parameter, especially the 7019-T6, 7075-T6 and the KK17-T7 alloys. Moreover, the alloys which are not susceptible to SCC, also did not show any failure in this work package. This indicates that this combination of environmental parameters also revealed a good range of spectrum for the susceptible and non-susceptible alloys.

4.3.   Influence of Mechanical Factors on SCC Susceptibility

This section focuses on the research question 1.2 which focuses on the influence of the critical mechanical parameters on the SCC behaviour of the 7xxx alloys. The strategy to determine the influence of mechanical factors has been discussed in Section 3.4.1. The following section discusses the conceptualization of the test specimen using DFSS tools such as morphological analysis. After the selection of specimens, the influence of various mechanical parameters was studied. These were load propagation with respect to time, stress magnitude and stress distribution. Finally, measurement system analysis was carried out on the chosen setup to determine its reproducibility and repeatability.

4.3.1.   Analysis of Critical Stresses Occurring in Automobile

To assess the nature and magnitude of critical stresses that occur in automobile, two critical sub-assemblies were chosen to be simulated and analysed. The first was the loads acting on a towing assembly and the second is the door lowering assembly. These assemblies were subjected to various load conditions which conform to TÜV standards and Daimler internal standards (internal standard 1 and internal standard 2). The description of the load conditions is mentioned in section 3.4.2. Each local

component in the assembly was individually analysed for the nature of stresses in various load conditions which will be summarized in this section.

Towing Assembly: The towing sub-assembly consists of the towing hook which is bolted to the support block through the bumper beam. The support block is in turn connected to the crash box, via bolt connections. The entire towing sub-assembly was simulated to be fixed to a rigid wall, by constraining the ends of the crash-box by using single point constraints (SPC). When the tensile load was applied to the assembly according to the internal standards, the load was applied in three directions, linear and angular direction (30° inward and outward). The point of application of load was on the towing hook, which was in turn connected to the support block, leading to the transfer of load onto the support block.

On the application of a linear load, the displacement of the support block was restricted by its connection to the crash-box via bolt connection. This caused a high stress concentration around the bolting region of the support block as shown in Figure 4-18. When angular loads were applied onto the towing hook, there was contact force between towing hook and support block, resulting in stress concentrations in the point of connection of towing hook and support block. Stresses as high as 124 MPa were seen near the bolting regions. From the stress vector figure, the direction of the stresses was in XY plane when the load is applied in negative X axis.

Since the support block is connected to the crash-box, a part of the load was also transferred onto the flanges of the crash-box in the bolting region. This load caused a displacement in the crash-box in the X direction. However, since the crash-box was restricted, the displacement was restricted, resulting in a stress concentration at the bolting regions. On application of angular loads, the crash box underwent a displacement in XY plane. However, due to its constraints, the displacement was restricted, resulting in high stresses developing on the bent region of the crash-box, as shown in the Figure 4-18(b). The stresses could exceed 220MPa and localized plastification was observed on application of highest loads according to the internal standard 2.
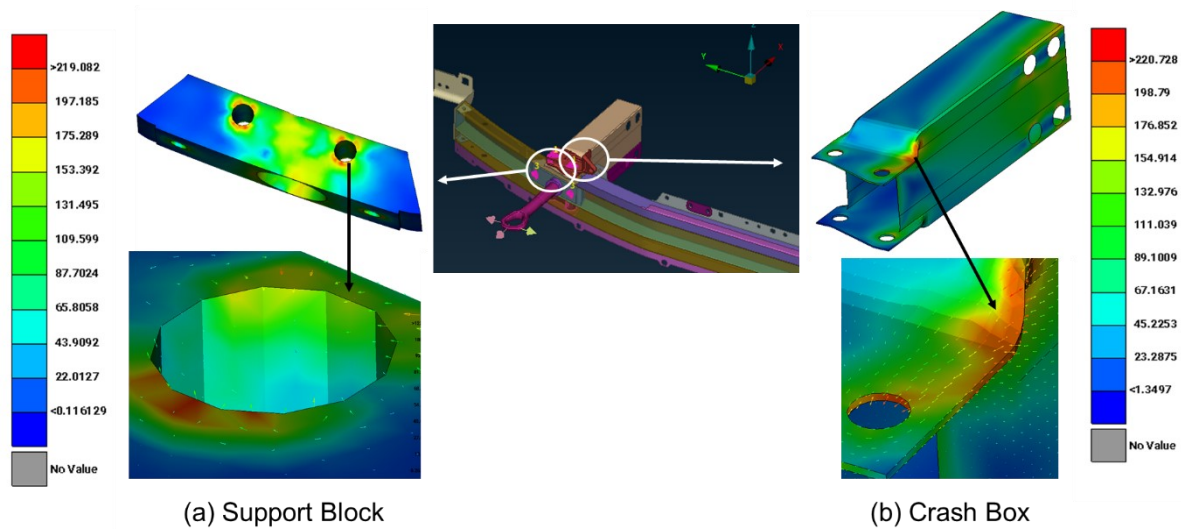
FIGURE 4-18 STRESS SIMULATION OF PARTS OF TOWING ASSEMBLY (A) SUPPORT BLOCK (B) CRASH BOX

Door Lowering Assembly: A similar effect, as in the towing assembly load case was observed in the stress concentration of the door lowering assembly, shown in Figure 4-19. In this assembly, the door was opened by 5-10° and then a load was applied in the Z-direction. The Z- movement was restricted by the door hinges (upper and lower) which are bolted to the A-pillar by the upper and lower brackets. This caused a stress onto the A-pillar in the bolted regions. The stresses were in seen in XY plane and were concentrated around the bolting regions as well as the bending regions. The stresses on the A-pillar exceeds 300MPa and shows localized plastification. Similarly, the door hinge reinforcement also showed localized plastifications and stresses exceeding 140MPa around the bolting regions.

The nature and magnitude of these stresses provide important information which can be used as an input for the designing of the test specimens. From both the load cases, it was observed that the high stresses were seen in localized areas, which also leads to localized plastification near the regions of bolt connections around the holes. With respect to stress corrosion cracking, these localized stresses can exceed the critical SCC threshold and result in crack initiation and propagation of the cracks, leading to failure of the part. These stresses are also multi-axial and have varying magnitudes in

different parts, according to varying load conditions. These conditions are taken as input during selection of the test specimen with the aim of mirroring these stresses on the test specimen and studying their behavior.
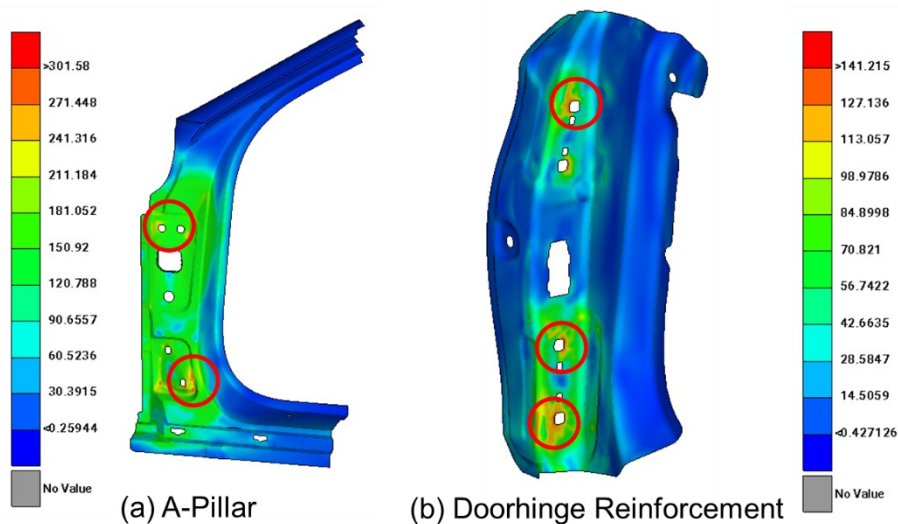
FIGURE 4-19 STRESS SIMULATION OF THE PARTS OF THE DOOR LOWERING ASSEMBLY (A) A-PILLAR AND (B) DOOR HINGE REINFORCEMENT

4.3.2.   Influence of Load Propagation Mode

In order to study the influence of load propagation on the SCC test results, four modes of load propagation were tested on all the four materials of T6 variant. Constant load mode, constant strain mode, slow strain rate test and incremental step load test were the four chosen load propagation modes, the results of which are discussed and compared in this section.

As shown in Figure 4-20(a), tensile samples loaded in constant load mode with a load of 75% $Rp_{0.2}$ showed the most differentiability in the results, with the KK17-T6 alloy failing within 3 days of exposure to the DIN 11997-1(B) environment. This was followed by the KK18-T6 which failed within 10 days of exposure. The 7019-T6 and the 7075-T6 alloys were resistant to failure in the 30 days of testing in this environment. The reproducibility of the results was also very good with negligible standard deviations for the failed samples. The optical microscopy and SEM fracture analysis revealed brittle fracture surface with intergranular cracking mode.

The constant strain test (CST) was carried out by exposing KS-8 samples to the DIN 11997-1(B) climate, which is a neutral salt-spray fog climate for a period of 35 days. Only KK17-T6 incurred failure within 12 days of exposure, whereas the other three materials passed the test, without failure. There is also a higher variation in individual results observed in the failed KK17-T6 KS-8 specimens. Optical microscopy of the failed KS-8 sample showed multiple crack branching and multiple secondary crack formations. The SEM fracture surface of the failed KS-8 samples in constant strain mode also showed intergranular SCC cracks and complete embrittlement of the fracture surface.

 The results of the slow strain rate test shown in Figure 4-20(a) illustrates the loss of elongation of samples tested in immersed 3.5 wt.% NaCl solution as compared to air. It can be seen that there is no significant loss observed for the 7019-T6 and 7075-T6 alloys. There is a loss of elongation observed in the KK17-T6 alloy from 3.9mm to 2.4mm which is approximately a 38% loss in elongation. The KK18-T6 also shows a loss in elongation from 6.3mm to 3.15mm, which is 50% loss in elongation. However, with KK18-T6, a higher standard deviation can be seen, which indicates the low reproducibility of the result. The SEM fracture analysis of the SSRT samples show a partly brittle fracture surface on the 7019-T6, KK17-T6 and KK18-T6 failed samples.

The incremental step-load test was conducted in air and with three varying conditions of time which are mentioned in Table 3-13. As seen in Figure 4-20 (b), the results show that for all the conditions, there is no loss in maximum load to failure for all the materials, with the exception of KK17-T6 for condition C. However, SEM fracture analysis of the failed KK17-T6 specimen for condition C showed brittle fracture surface only in localized regions towards the edges of the specimen, whereas the maximum surface was ductile in nature. All other samples showed no difference in fracture surface compared to the fracture surface on testing in air, which is complete ductile surface.
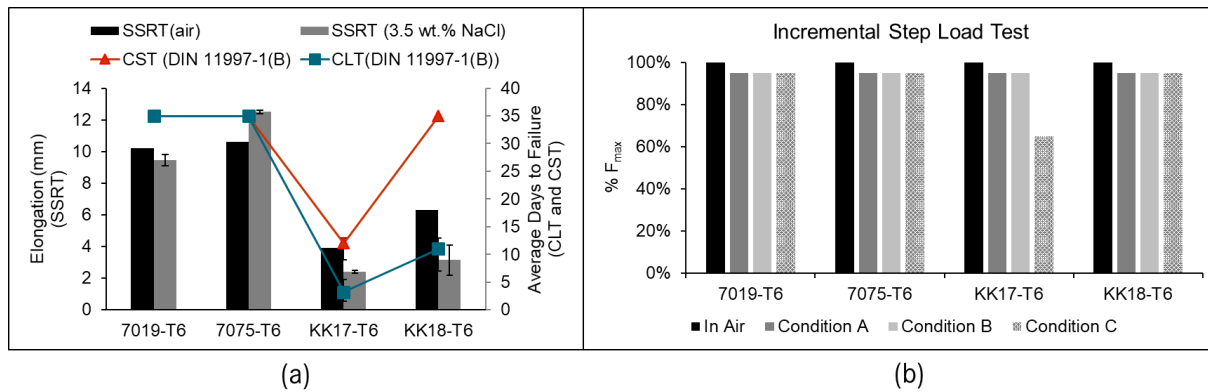
FIGURE 4-20 COMPARISON OF RESULTS OF VARIOUS LOAD PROPAGATION MODES: (A) THE RESULTS OF SLOW STRAIN RATE TEST AND CONSTANT LOAD TEST AND CONSTANT STRAIN TEST (B) SHOWS THE RESULT OF THE INCREMENTAL STEP LOAD TEST

By comparing the results of the various load propagation modes, it was clearly observed that the constant load test showed the best identification and differentiation to SCC susceptibility. This was followed by the constant strain mode and the slow strain rate mode which managed to show differentiability for the extremely susceptible alloys. However, the constant strain mode achieved by the KS-8 sample had the advantage of being easy to implement and compact. The incremental step load test, however, did not manage to show any differentiability. Due to these results and other factors which were considered in order to choose the load mode, including ease and feasibility of testing, the constant load mode and constant strain mode were chosen to be investigated further, whereas the SSRT and ILT mode were eliminated as possible options. The comparison of these tests will be discussed in detail in section 5.3.2 in detail.

4.3.3.   Influence of Stress Distribution

The three specimen concepts chosen in the concept phase of the DFSS were tensile specimen, tensile specimen with hole and the KS-8 specimen. These specimens were strategically chosen in order to cover a range of stresses with respect to its nature, the distribution and concentration, as discussed in section 3.4.1. The first step to determine was to determine the stress distributions occurring in these chosen specimens and compare them to those occurring in the automobile load cases, which were studied in section 4.3.1. This analysis was followed by experimental analysis of the various specimens in the MBSC corrosion test cycle.

FEM Simulation of chosen specimens: FEM simulation analysis was carried out on the three chosen specimens, tensile sample, tensile sample with hole and the KS-8 sample and the stress distribution was compared to the auto parts in the loaded cases discussed in section 4.3.1 and represented in Figure 4-21. Figure 4-21(a) shows the stress distribution in tensile sample without hole. As expected, it is observed that the stress is evenly distributed in the narrow region of the tensile sample. The stresses observed in this sample are uniaxial. This specimen form is advantageous due to its uniformity in stress distribution and ease of calculation of stresses applied onto the specimen.
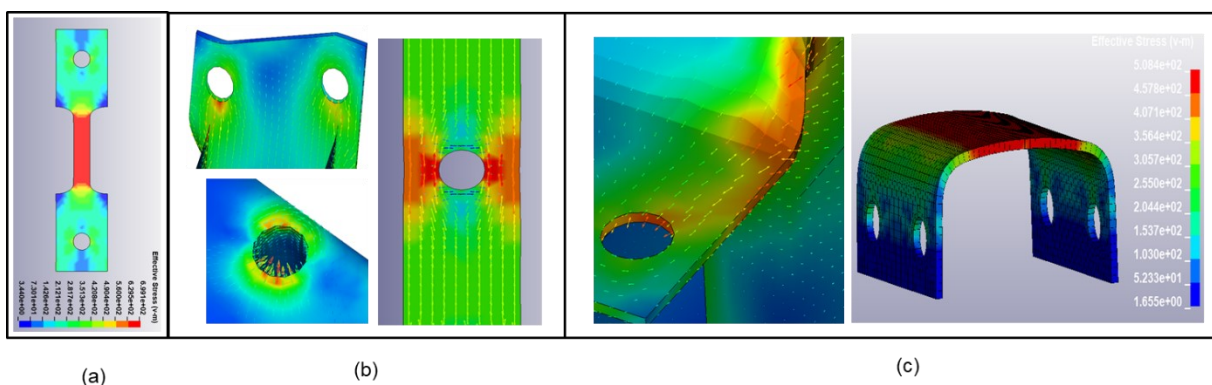
FIGURE 4-21 FEM STRESS SIMULATION OF LOADED (A) TENSILE SAMPLE WITHOUT HOLE (B) TENSILE SAMPLE WITH HOLE AND (C) KS-8 SAMPLE

Figure 4-21 (b) shows the FEM simulation of the tensile sample with hole under load. It can be seen that the hole, acts as a notch for the specimen, resulting in higher concentrations of stress around the hole. Moreover, the hole also causes stress distribution of the specimen to change from uniaxial to biaxial. This stress concentration effect mirrors the effect shown in the auto parts such as support block and bumper beam, where it was observed that the stresses were also concentrated around the bolting regions and were multiaxial in nature.

Lastly, Figure 4-21 (c) shows the stress distribution within the KS-8 specimen. It is seen that due to the structure of the specimen, the highest bending stresses, are observed on the top flat flange of the KS-8 specimen. There were also some stresses observed at the bending angles of the KS-8 specimen, where plastification is observed. The stresses in this specimen can be comparable to the stresses observed in the crash box, which are also concentrated due to the thinning of samples caused at the bending.

From the results above it can be seen that each of the three specimens, with their variations in stress distribution and stress concentration, mirror the critical stresses that occur in the automobile load cases. Therefore, they cover all the possible stress distribution scenarios that could be critical to the automobile and to the SCC susceptibility. These three specimens were further experimentally tested in MBSC test to analyse its influence on the SCC susceptibility of the tested alloys.

Experimental observation of chosen specimen: Initial testing was carried out by exposing the three sample variations to the standard environmental conditions, DIN 11997-1(B) and the ASTM G85- 11(A2) in order to generate the SCC susceptibility difference. This was done with all four alloys, with T6 temper. Figure 4-22 illustrates the results obtained. The main observation seen was that the samples with hole, generally failed earlier as compared to without hole, which was expected due to its reduction in surface area. On exposure to DIN 11997-1(B), the KK17-T6 alloy showed little difference on comparing the time of failure of the various specimens. The tensile samples with and without hole failed within the first 5 days and KS-8 in 10 days. The KK18-T6 showed considerable difference with fastest failure observed in tensile samples with hole, followed by without and no failure in the KS-8 samples. Similar observations were made in the ASTM G85-11(A2) environment. However due to the
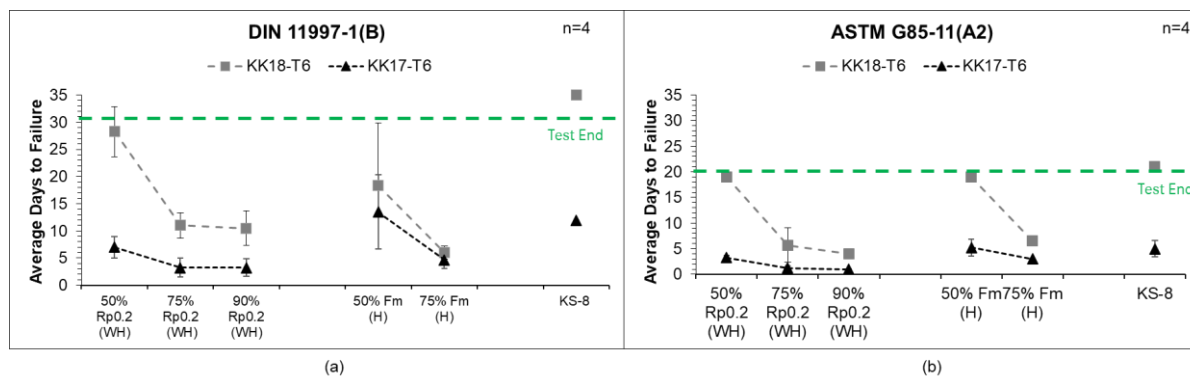
FIGURE 4-22 COMPARISON OF DAYS TO FAILURE OF THE VARIOUS SPECIMENS OF KK17-T6 AND KK18-T6 EXPOSED TO (A) DIN 11997-1(B) AND (B) ASTM G85-11(A2)

high corrosivity of the environment, faster failures and higher corrosion were observed in the samples.

After the initial results, further testing was done with the whole material profile on the three samples with 75%$Rp_{0.2}$ and 75% F_{max} since they showed the best differentiability. The results, illustrated in Figure 4-23, showed that the KK17-T4 and T6, KK18-T4 and

T6 and the 7075-T4 were the most susceptible materials, which fail within 5 days of exposure both for the tensile specimens, with and without hole. This is followed by the 7075-T6, KK17-T7 and 7019-T6, which failed at an average ranging from 11 days to 22 days of exposure for the tensile samples with and without hole, thus falling in the medium range of SCC susceptibility. Lastly, the 7019-T4 and T7, 7075-T7 and the KK18-T7 did not show failure for the tensile samples without hole and very delayed failures for the tensile samples with holes.

On closer observation of the tensile samples with holes, it was observed that the average time-to-failure of these specimens was less than that of the tensile samples without hole. This result is also expected to due to the stress concentration created on the tensile specimen due to the hole in the center, which acts as a notch for the specimen once the crack is initiated. It was also observed that all the 12 materials, at least 2 or more of the 4 replications, underwent failure within the test time of 30 days. The highly susceptible materials showed little to no difference in the average time-to-failure comparing the tensile specimens with and without hole. The medium susceptible alloys showed some difference in results, for e.g., the tensile sample without hole of 7075-T6 alloy, which failed at average of approximately 22 days, failed at around 16 days for tensile specimen with hole. Similarly, the 7019-T6 alloy also failed at 23 days for the tensile specimen without hole, in comparison to the 12 days for the tensile specimen with hole. An important observation to be made is that the alloys, which were generally resistant to SCC failure, also failed with tensile specimen with hole. This includes the materials such as 7019-T4, 7019-T7, 7075-T7 and KK18-T7, which are generally resistant to SCC. This leads to questioning the criticality of the test. Another important consideration of the results of the two samples is the differences in standard deviation. It is seen that the standard deviation of the tensile specimens with hole tend be greater than that of tensile specimens without hole, showing lower reproducibility of the results.

On the contrary to the critical result of the tensile samples with hole, the constant strain specimens, KS-8 did not show failure in some of the susceptible materials. In Figure 4-23 it can be seen that failure is observed in the KK17-T4 and T6 and the KK18-T4 and T6 specimens. However, the 7075-T4 specimen, which failed in the tensile form, both with and without hole within 5 days, did not show any failure for the KS-8 specimens. Similarly, for the medium susceptible alloys such as 7019-T6, 7075-T6 and KK17-T7 also showed no failure for the KS-8 specimens, whereas they failed with the tensile specimens.
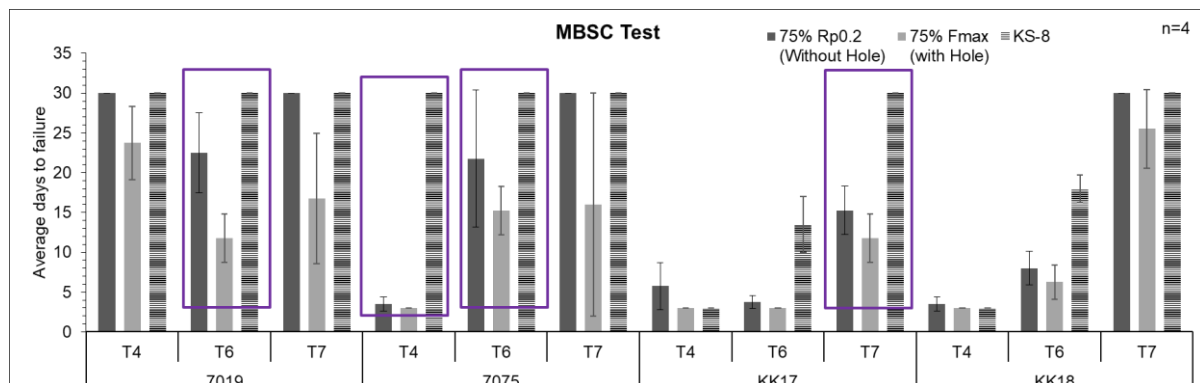
FIGURE 4-23 COMPARISON OF AVERAGE DAYS TO FAILURE OF THE DIFFERENT SPECIMENS EXPOSED TO MBSC TEST HIGHLIGHTING THE DIFFERENCE OBSERVED IN 7019-T6, 7075-T4 AND T6 AND KK17-T7

The SEM fractographic analysis of the samples was also carried out in order to determine the difference in the behavior of the failed samples. An interesting observation made is shown in Figure 4-24 showing that the KK17-T6 tensile sample without hole loaded to 75%$Rp_{0.2}$ failed after 3 days and showed a completely brittle fracture surface as seen in Figure 4-24 (a). The nature of the fracture surface is brittle and intergranular cracks are observed on the surface which is indicative of SCC failure. This is confirmed by the optical microscopic images, where secondary cracks are observed initiating from the surface of the specimen, running perpendicular and branching out in the material.

Figure 4-24 (b) shows the fracture surface of the 7075-T7 tensile sample with hole, loaded to 75%Fm, which also failed after 3 days of exposure. The fracture surface shows a classic honey-combed structure indicating a ductile fracture surface. This fractographic image indicates that the failure of the 7075-T7 sample with hole could not be SCC, rather residual elongation of the sample due to high stress concentration,

leading the sample to failure. Microscopic examination of the sample also observed no secondary cracks or corrosion to be seen on the specimen. The comparison of this image shows that although the two samples failed on the same day, it is important to carry out further analysis to determine the exact cause of failure.
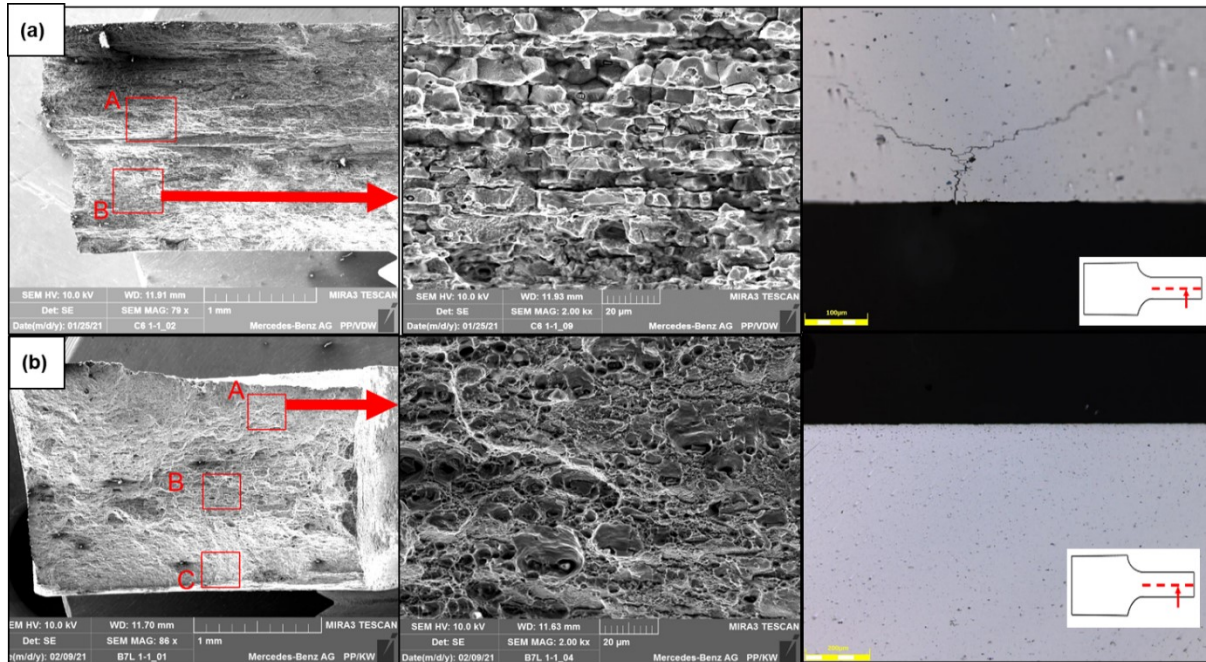
FIGURE 4-24 FRACTURE SURFACE OF (A) KK17-T6 AND (B) 7075-T7 AFTER 3 DAYS OF EXPOSURE TO MBSC TEST

In summary of the results discussed above, it can be concluded that the specimen form, and the nature of stresses on the specimen can play a vital role in SCC test results and in turn identifying the SCC susceptibility. It was seen from the results above, that the tensile specimen with hole in the MBSC test was extremely critical and caused failures in materials which were not susceptible to SCC. Further investigation of the cause of failure revealed that the failure was due to stress concentration and not due to SCC failure. Moreover, it was observed that in some cases, the results of the tensile samples with hole had large standard deviations, indicating non-reproducibility of results. Contrary to the tensile specimen with hole, the KS-8 specimen, was less critical and did not show failure in otherwise SCC susceptible alloys, as in 7075-T4. The tensile specimen, without hole showed the most distinct results among all the three specimens, in all the environments tested. The extremely susceptible alloys failed within the first 5 days of testing, followed by the alloys which were medium susceptible. The alloys which are not SCC susceptible, did not fail the test.

4.3.4. Influence of Stress Magnitude

The influence of stress distribution of the tested specimens revealed that the tensile specimen was the most appropriate specimen for testing SCC susceptibility. The next step was to determine the influence of stress magnitude on the SCC susceptibility and the test results. This was done by exposing the tensile specimen under various load magnitudes in a two-stage testing. Initial testing was carried out with the T6 samples of all four alloys in the DIN 11997-1(B) and the ASTM G85-11(A2) environment, in the load condition 50%, 75% and 90% of $Rp_{0.2}$. Since the mechanical parameter was the prime focus in this section, testing in standardized corrosion test cycles enabled testing a larger sample space in controlled and validated test environments, thus eliminating the instability of the novel developed test. Secondly, it gave a reference for the behavior of the samples when exposed to the MBSC test. The next step was to expose the samples to the MBSC test with the filtered load conditions in order to determine the appropriate load magnitude.

On exposure to the DIN 11997-1(B) and ASTM G85-11(A2), the 7019-T6 samples and the 7075-T6 samples did not undergo failure under all the tested load conditions. Figure 4-25 compares the result of the KK17-T6 and KK18-T6 samples in the various environments. It can be noted that by changing the force load from 50%$Rp_{0.2}$ to 75%$Rp_{0.2}$, the average time to failures reduced significantly, for both the materials. The average time-to-failure of KK18-T6 sample in the DIN 11997-1(B) environment reduced from 28.3 days to 11 days and that of KK17-T6 reduced from 7 days to 3.25 days, which was greater than 50% reduction in average time-to-failure. A similar observation can be made for the KK18-T6 specimens exposed to the ASTM G85-11(A2) environment. However, the average time-to-failure by increasing the load from 75%$Rp_{0.2}$ to 90% $Rp_{0.2}$ almost remained the same, as can be seen in Figure 4-25 (a) and (b) where the average days to failure of KK18-T6 specimen changed from 11 to 10.5 days in DIN 11997-1(B) environment and from 5.7 to 4 days in the ASTM G85-11(A2) environment. For the KK17-T6 materials, there was no change in average days to failure for specimens exposed to DIN 11997-1(B) environments and only a marginal decrease in specimens exposed to the ASTM G85-11(A2) environment. The results for the KK17-T6 and KK18-T6 indicate that at 75%$Rp_{0.2}$, a minimal critical or initiation stress could be achieved, for both materials, which, if exceeded, does not necessarily

accelerate the SCC initiation in the materials. However, stresses lower than that, such as 50%$Rp_{0.2}$, which were tested here, could be less than the critical mark for the identification of SCC susceptible materials. It was also seen that the 90%$Rp_{0.2}$ stress was too high and showed results similar to that of 75% $Rp_{0.2}$, indicating that the 75% mark was the threshold to initiate the SCC susceptibility. The 90% $Rp_{0.2}$ stress also showed lower differentiability of test results, thus making it inappropriate for further use.
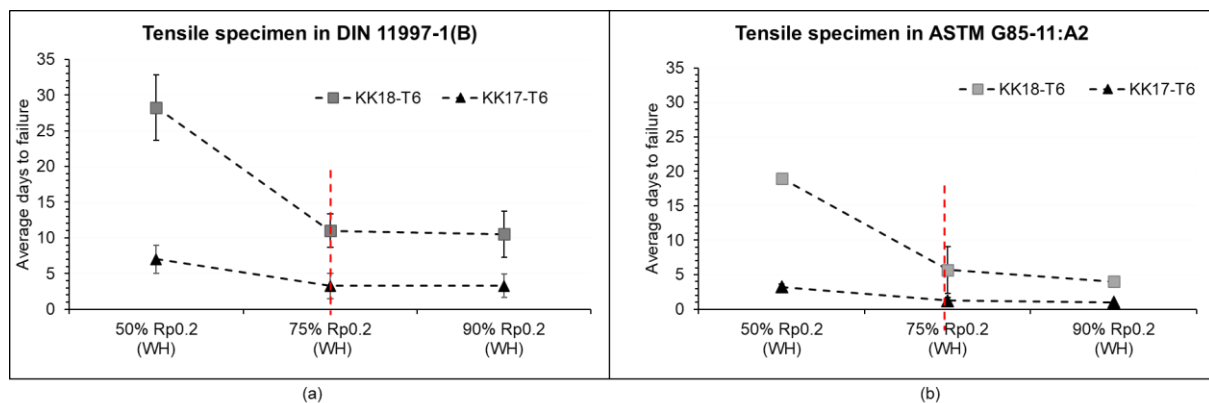
FIGURE 4-25 AVERAGE DAYS TO FAILURE OF KK17-T6 AND KK18-T6 IN VARYING LOAD MAGNITUDES EXPOSED TO (A) DIN 11997-1(B) AND (B) ASTM G85-11:A2

To further study the influence of stress magnitude on the SCC susceptibility of the 7019-T6 and 7075-T6 alloys, which did not fail within the stipulated test period of the constant load test conducted above, the corroded specimens were subjected to residual tensile testing in order to determine the residual strains of the corroded specimens. It was observed that the difference in the loss of ductility for samples stressed at different stress magnitudes was minimal in both environments.

The initial testing showed that the influence of load magnitude also depends on the testing environment. There is a difference in average time-to-failure, which in turn indicates SCC susceptibility, on comparison of specimens exposed to DIN 11997-1(B) and the ASTM G85-11(A2) environment. Therefore, the next step was to study the influence of load magnitude in the MBSC test. The tensile samples without hole were exposed to MBSC Test cycle at 50%$Rp_{0.2}$ and 75%$Rp_{0.2}$. All the four materials, 7019, 7075, KK17 and KK18 in three temper states were tested and the results are compared, as shown in Figure 4-26.

The results indicate that an increase in load magnitude from 50%$Rp_{0.2}$ to 75%$Rp_{0.2}$ results in a significant decrease in average days to failure in certain alloys which are tested. The most noteworthy difference in average days to failure is to be seen in the 7019-T6, 7075-T4, 7075-T6 and KK17-T7 alloys. The 7075-T6 alloy passed the test when loaded to 50%$Rp_{0.2}$ with no failure of samples being observed. However, on increasing the load to 75% $Rp_{0.2}$, samples showed failure at an average of 20 days. Similar observations were made for the 7019-T6 and the KK17-T7 samples, which showed no failure for the 50%$Rp_{0.2}$ load but failed when the load was increased to 75%$Rp_{0.2}$. This indicates the importance of load magnitude in order to identify SCC susceptible materials and differentiate them from the materials, which are not susceptible to SCC.
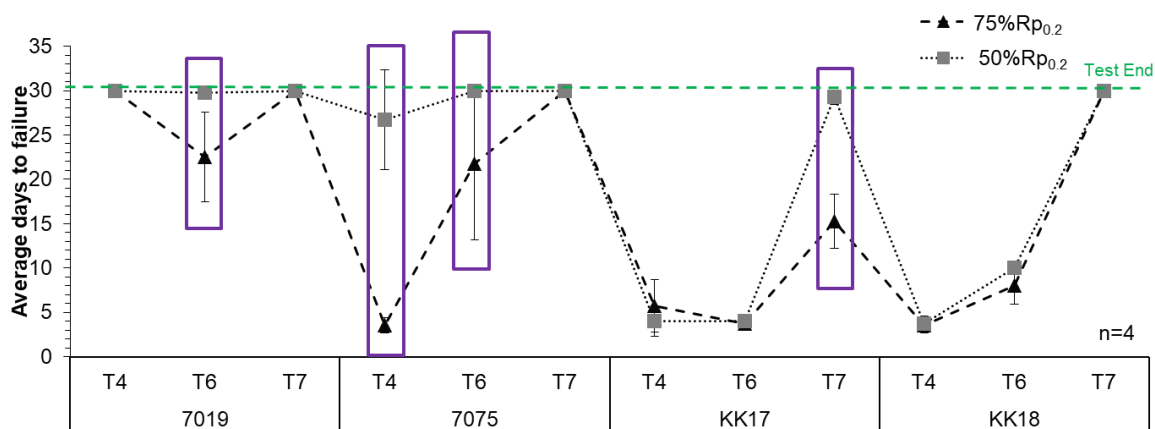
FIGURE 4-26 TENSILE SAMPLES EXPOSED TO MBSC TEST IN VARYING LOAD MAGNITUDES

The time-to-failure for highly susceptible alloys, such as KK17-T4, KK-T6, KK18-T4 and KK18-T6 did not vary with regard to the load magnitude. The SEM fractography of the samples also did not show any considerable differences with varying load magnitude. However, metallographic observations showed that the length of the secondary cracks found in samples loaded to 75%$Rp_{0.2}$ were longer than the cracks found in samples loaded to 50%$Rp_{0.2}$. This observation can be seen in KK17-T4 samples, as shown in Figure 4-27, which were exposed to the MBSC climate under both load conditions and failed after three days. The length of the crack under 50%$Rp_{0.2}$ load was approximately 182µm, whereas that under load of 75%$Rp_{0.2}$ was approximately 233µm.
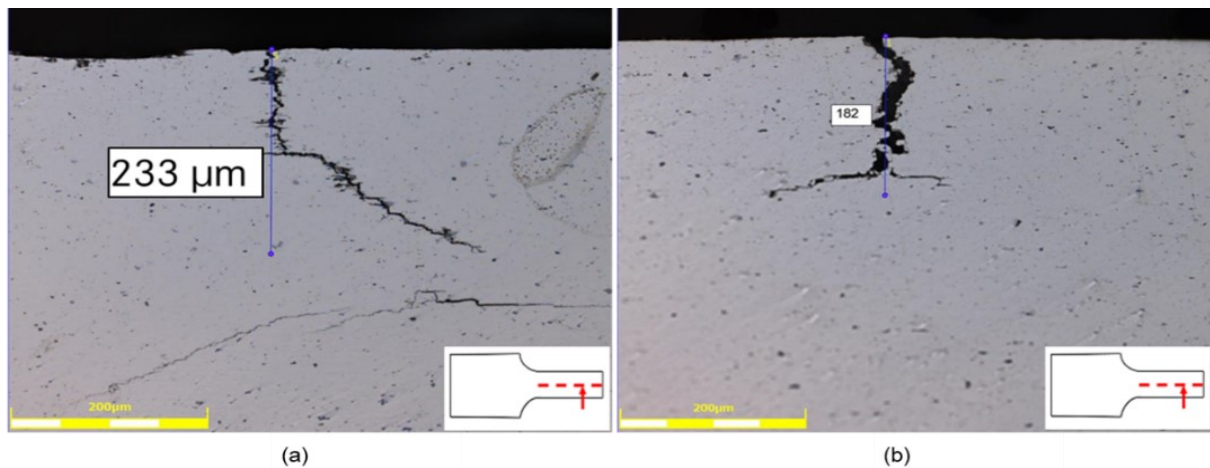
FIGURE 4-27 DIFFERENCE IN CRACK LENGTH OBSERVED IN KK17-T4 WHEN LOADED TO (A) 75%$RP_{0.2}$ AND (B) 50% $RP_{0.2}$ AFTER EXPOSURE TO MBSC TEST

In summary of the results of the tests conducted above, it can be concluded that the change in load magnitude, has a significant influence on the average time-to-failure of the susceptible specimens up to a critical stress, which in the above case was 75%$Rp_{0.2}$. Below this stress, it was observed that the certain susceptible alloys showed delayed or no failure. For e.g., the 50%$Rp_{0.2}$, the KK18-T6 specimens, which is SCC susceptible, showed a delayed failure at around 28 days in the DIN 11997-1(B). On the contrary, increasing the load to 75%$Rp_{0.2}$ load magnitude showed considerably faster failure of the same material. Similarly, on exposure to the MBSC test, the 7019-T6, 7075-T6 and KK17-T7 alloys showed no failure with a load of 50%$Rp_{0.2}$, but on increasing the load to 75%$Rp_{0.2}$, resulted in failure of the specimen. This could indicate that the 50%$Rp_{0.2}$ load magnitude may not be sufficient threshold stress to detect SCC in medium susceptible alloys. Therefore, the 75%$Rp_{0.2}$ load could be considered as the threshold stress for the SCC to initiate in the materials tested.

Beyond this threshold stress, the increase in stress magnitude does not accelerate the SCC susceptibility. Moreover, apart from the length of secondary crack observed in the MBSC test, there were no significant differences observed in the microstructure and the fracture surface of the specimens, with respect to varying load magnitudes indicating that the mechanism of failure remained the same at all load magnitudes. There were also no differences observed in the residual elongation of the 7019-T6 and 7075-T6 specimens, in response to the varying load magnitude.

4.3.5.   Measurement System Analysis of Tensile Test Setup

Once the concepts are selected, the first step in the optimising phase of DFSS is to carry out the measurement system analysis of the experimental setup. This step determines the variations caused by the system and the process itself and helps determining the influence of these variations on the results. In other terms, measurement system analysis determines the reproducibility and repeatability of the system. If the process variation is large, the results obtained are distorted due to these variations and must be optimised to reduce these variations. The MSA for the tensile testing setup was carried out in three steps. The first step was to determine the influence of operator by varying the operator and the number of rotations on the same sample and determine the variation in displacement. The second step was to determine the influence of specimen, by varying the specimen of the same material. Finally, to determine the influence of material, three different materials were tested with varying rotations and varying operators.

The key value to determine the influence is the Gage R&R value which represents the gage variation in the data and hence indicates the reproducibility and repeatability of the system. Repeatability of the system measures the variation that occurs when the same operator carries out measurement of the same object repeatedly. Reproducibility is the variation that occurs when different people measure the same item. The general rule is to keep the Gage R&R value as low as possible, with acceptable values being below 30%. The goal value of Gage R&R for this system was established as below 20% in the first step of the DFSS

Operator influence: The first trial in this thesis was carried out to determine the operator influence by keeping the specimen constant and varying the operator only. The results are shown in Figure 4-28. The total Gage R&R value, which represents the combined effect of reproducibility and repeatability of the experimental setup was determined to be 9.48%. The individual repeatability value was 8.22% and the reproducibility was at 4.72%. The variance of all the three operators were below 0.009mm and the reproducibility in each of the 6 rotations was high as shown in Figure 4-28. These low Gage R&R values show that the system variation with respect to

operator influence was not significant. The Gage R&R value was significantly lower than the target value of 20%.
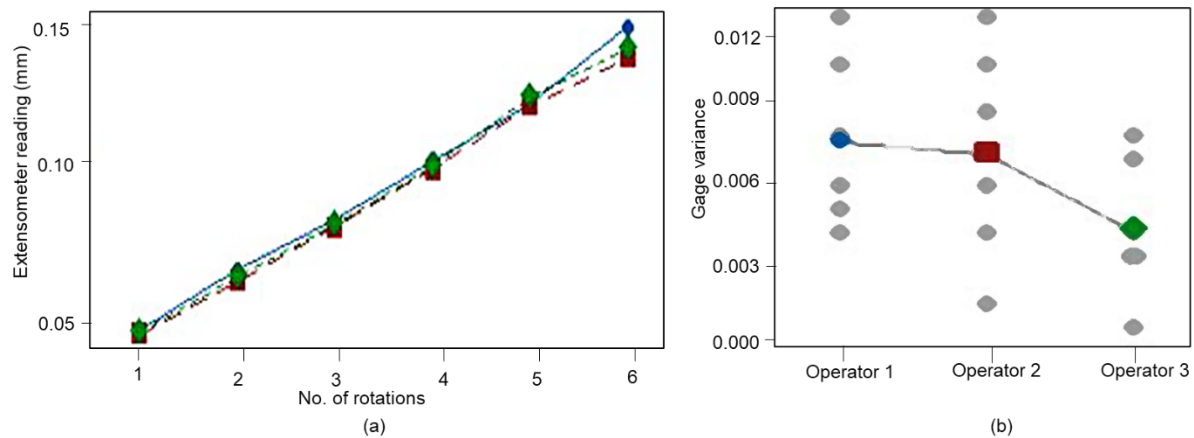
FIGURE 4-28 RESULTS OF THE MEASUREMENT SYSTEM ANALYSIS OF THE OPERATOR INFLUENCE SHOWING (A) REPRODUCIBILITY (B) REPEATABILITY

Specimen Influence: The second trial, which tested the variation of result with respect to specimen showed a Gage R&R value of 19.7% which was just below the target value of 20% and within the range of acceptable variance. This indicates that the variance in displacement readings caused by the change in specimen was not significant. The reproducibility of the setup was high with a low variation rate of 5.5%. From the Figure 4-29(a) it is observed the reproducibility is good apart from some slight deviations observed in specimens C and D. The repeatability of the sample showed a higher variance of 18.92%, As observed in Figure 4-29(b), there were certain points with exceptionally large variances, which could have resulted in the higher variance rate. However, despite the larger variances it was still within the acceptable range of variance.

Material Influence: The last set of trials were carried out varying specimen, material as well as operator in order to include the variance caused by change of material being tested. The variance in results were measured using linear regression analysis, due to the multiple factors involved in this trial. The analysis of variance measured for each individual factor revealed that the influence of operator and the material was insignificant with the P-value being above 0.05. This indicates that the displacement of

the sample remains the same with each rotation, irrespective of the material within the elastic zone.

(a)
(b)
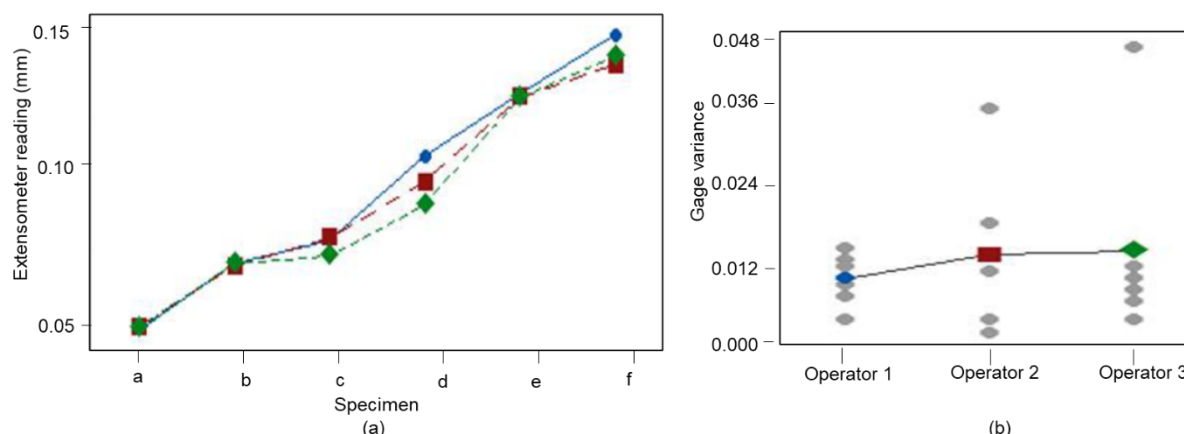
FIGURE 4-29 RESULTS OF THE MEASUREMENT SYSTEM ANALYSIS OF THE SPECIMEN INFLUENCE SHOWING (A) REPRODUCIBILITY (B) REPEATABILITY

These trials concluded that the stressing of the specimen with the current tensile setup described in section 3.4.3 is measurement system capable. The displacement indicated by the extensometer, which in turn indicates the load on the specimen is reproducible on the samples, irrespective of the operator, the sample, as well as the material being stressed as long as it is in the elastic region. Thus, fulfilling the criteria determined in the first step of the DFSS of reproducibility and repeatability.

4.4.   Results of Outdoor Exposure Tests

This section focuses on answering the research question 1.3, which focuses on the validation of the developed test method to the outdoor exposure. The outdoor exposure test was carried out with the objective of providing a reference data to compare the results of SCC failure generated in the laboratory tests. Different climatic conditions were chosen to gain information on the SCC behaviour of the tested alloys in different climatic conditions. This information was then used to compare the results of the MBSC test to validate the results.

The outdoor exposure test was carried out in four different regions, with four varying climates. The regions chosen were (i) Saguenay, Canada, (ii) Long Key, United States of America, (iii) Chennai, India and (iv) Sindelfingen, Germany. Two specimens, the U-bend and the constant loaded tensile specimen were exposed to the climates. The following section compares the behaviour of the material pallet, with respect to SCC

index which is calculated based on the time-to-failure of the specimens with the varying climates. Fractographic analysis and metallographic analysis of the failed samples are also discussed to confirm the cause of failure and corrosion influences on the specimen.

4.4.1.   Environmental Conditions in Test Regions

Before discussing the SCC results at the various sites, the climatic conditions of each of the sites is highlighted in order to correlate the results to the climatic conditions.

Chennai, India was chosen for its Equatorial Monsson (Am) climate according to the Köppen-Geiger classification. The high temperatures and seasonal rainfall would be an ideal critical climate for SCC susceptibility. The temperatures of the region generally remain high throughout the year. The temperatures ranged from a minimum of around 23°C to maximum temperatures reaching 38-40°C. The relative humidity ranged from 50%RH to 75%RH, with cyclic variation throughout the year. It is important to note that the start of the testing coincided with the monsoon season of this site and experienced very high average rainfall. After the monsoon season, around December, the precipitation drastically reduced and with the onset of summer temperatures reached the maximum.

Long Key, Florida, USA, also classified as Equatorial (Aw) was especially a critical environment, due to its proximity to the sea and high humidity, precipitations, and temperatures throughout the year. The average annual temperature of this place is generally high, ranging from 25°C to 30°C. This site also experiences constant high humidity of approximately 75% RH throughout the year. Due to the coastal proximity, this site also experiences significant rainfall with around 300mm around September to December and lowers to below 100mm during January through March and rose again in April until September.

The Saguenay site in Canada was chosen as a representation of the cold polar climates (Dfc). Temperatures here dropped to below 10 degrees in the winter season, with heavy snowfall from December until early March. This period was coincided with the application of salt spray on the specimens in order to recreate the de-icing of roads

condition on the samples. The humidity of this site ranges from 60%RH to around 80%RH throughout the year. Saguenay also experienced considerable rainfall throughout the testing period ranging from 50mm up to a maximum peak of 200mm in July 2020.

Finally, the Sindelfingen site was taken as a reference site, representing the warm temperature climate. The temperatures of this site varied from around 20°C in the summer season to around 0-5°C in the winter season. The samples at this site were also sprayed with NaCl solution to represent the de-icing salts on the roads, since region also experiences snow. The rainfall was lower compared to the other sites with maximum rainfall of around 200mm in February 2020, but generally lower than 100mm rainfall throughout the year.

4.4.2. Test Results

Figure 4-30 (a) and (b) shows the SCC index of the tensile and U-bend specimens, respectively. The SCC index was calculated using the Equation 3-4. On nearer observation of the SCC index of the tensile samples, it was seen that the 7019 alloy in all the three temper states were not susceptible to failure in any of the climatic conditions. With an SCC index of 5, all the samples passed the one-year mark without any cracking or failure. The 7075-T4 alloy tensile sample showed a variation in behaviour with respect to the various climates. The alloy showed early failure in the Long Key and Saguenay sites, with SCC index below 1 in each of them. However, in the Chennai and Sindelfingen sites, the specimens passed the one-year mark without any failure in specimen. The 7075-T6 specimen showed no failure in any of the sites except for Saguenay, Canada, where it had an SCC index of 3.78. The 7075-T7 alloy did not fail in any of climates. The KK17-T4 and KK17-T6 alloys were the most susceptible alloys which showed earliest failure, with extremely low SCC indexes of below 0.25. The KK18-T4 also showed very low SCC indexes of below 0.3, in the Long Key, Saguenay and Sindelfingen site. There was a delayed failure observed in the Chennai site with an SCC index of 4.2. The KK18-T6 alloy also showed varying susceptibility, with an SCC index of 0.73 in Long Key, 0.26 in Sindelfingen and delayed failures in Chennai and Saguenay, with SCC index of 3.32 and 3.6, respectively. The

KK17-T7 and KK18-T7 alloys also showed no failure within the period of one year in any of the four climates
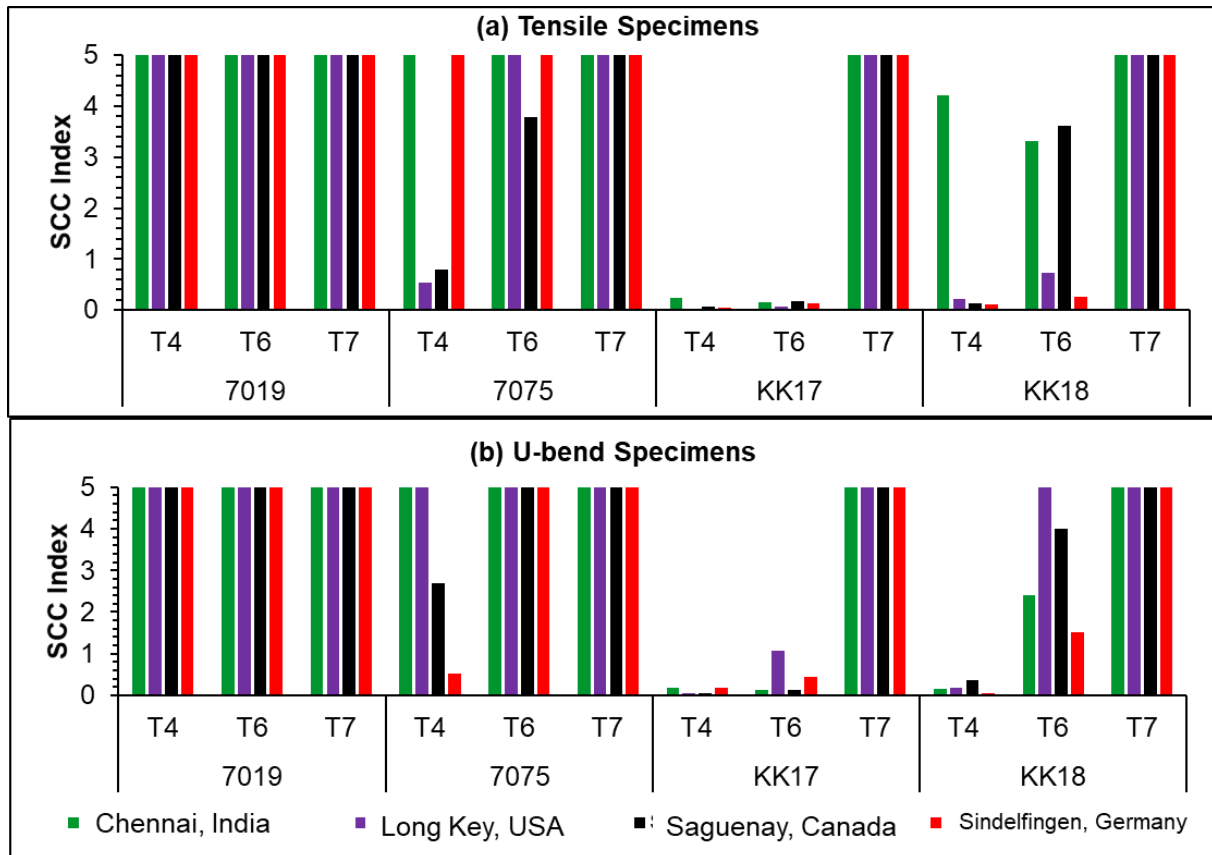
FIGURE 4-30 RESULTS OF THE OUTDOOR EXPOSURE TEST OF (A) TENSILE SPECIMENS AND (B) U-BEND SPECIMENS

The U-bend specimens results were also similar to that of the tensile specimens, with a few exceptions. With the U-bend specimen also there was no failure of the 7019 alloy of any temper states. The 7075-T4 alloy showed failure in Saguenay and Sindelfingen, with SCC indexes of 2.69 and 0.6, respectively. Meanwhile the result of the 7075-T6 varied from that of the tensile sample, by showing no failure in any of the sites. The KK17-T4 and KK17-T6 U-bend samples also showed higher susceptibility with SCC index below 1 in all the climates. Similarly, the KK18-T4 also shows high susceptibility with SCC index values lower than 0.5, which is comparable to that of the tensile specimens. The KK18-T6 specimens showed delayed failure with lowest SCC index in Sindelfingen of 1.53, followed by 2.41 in Chennai and 4.01 in Saguenay. The material showed no failure in the Long Key site. As in the tensile specimen, the KK17-T7 and the KK18-T7 also did not show any failure during the period of testing in any of the sites.

In summary of the results discussed above, the general trend of susceptibility among the material pallet to be seen is that the KK17-T4, KK17-T6 and KK18-T4 were the highest susceptible materials, showing early failure in all of the tested locations. This was followed by the 7075-T4 and the KK17-T6 alloy, which showed delayed failure in some of the sites. Finally, the 7019 alloy in all three temper states and the 7075-T7, KK17-T7 showed no failure in the duration of testing in any of the four locations.

On comparing the results obtained in the various locations, it can be observed that the trend of susceptibility is similar at all the four sites tested. Most samples show early failure at the Long Key site, which could be attributed to the high temperatures, high humidity, and the salt content in the air due to its proximity to the sea. The Saguenay site, which represents the cold-salty climates also shows considerable harshness towards the SCC failure. Most importantly, the 7075-T6 tensile samples uniquely showed failure at this site. The Chennai site showed the most delayed failure among all the four sites, this could be attributed to the fact that the time of installation of the specimens coincided with the yearly monsoon season occurring in this region. This resulted in continual rains washing away of any salts and impurities on the sample.

To validate the cause of failure of the fractured samples and determine the influence of corrosion on the materials, SEM fractographic analysis and metallographic examinations were carried out on the failed samples. The fractographic images of the KK17-T4 and KK17-T6 alloys from all the locations showed complete brittle fracture surface with intergranular brittle failure and secondary cracks running through the surface of the materials. This confirms the SCC susceptibility of these materials in all the environments tested. Figure 4-31 shows the fracture surface of the 7075-T6 sample failed at the Saguenay site. It was noticed that the edges of the sample show a brittle nature with smooth quasi-cleavage structures and secondary cracks whereas, as shown in Figure 4-31(a) and the central regions show a mixed ductile-brittle fracture with honey-combed structures mixed with smooth step-like structure, illustrated in Figure 4-31(b). The KK18-T4 alloy and KK18-T6 alloy also showed complete brittle

failure, with intergranular fracture surface and secondary intergranular cracks within the fracture surface.

(a)   (b)
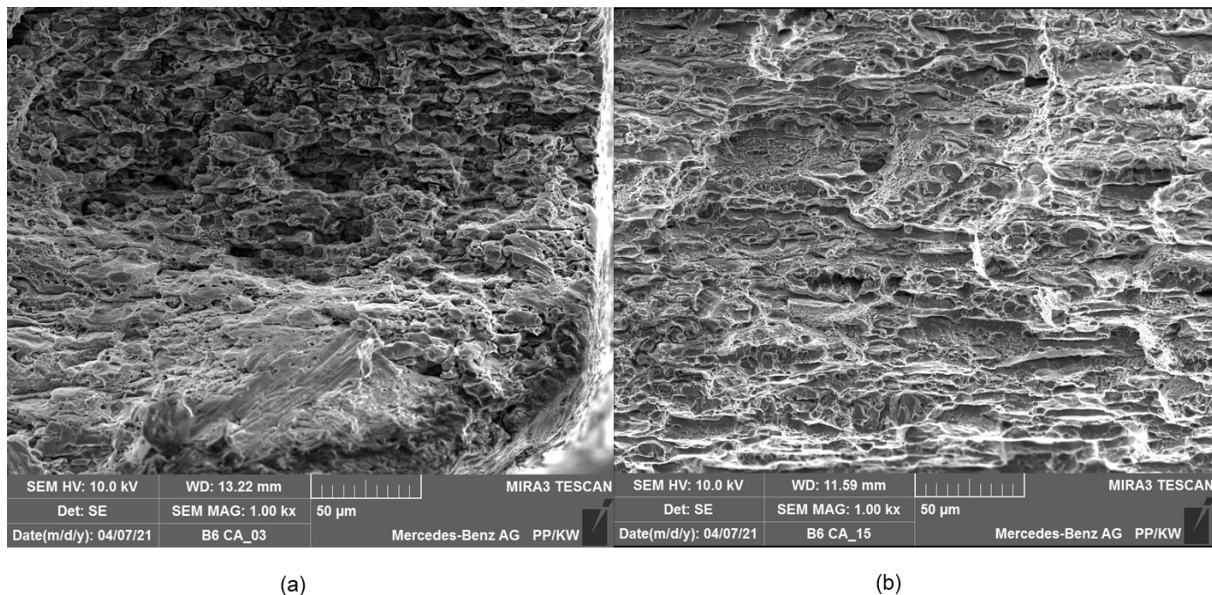
FIGURE 4-31 SEM FRACTURE SURFACE IMAGE OF FAILED 7075-T6 AFTER EXPOSURE TO THE SITE AT SAGUENAY, CANADA (A) BRITTLE STRUCTURE AT THE EDGES (B) MIXED STRUCTURE IN THE CENTRE

4.5.   Risk Assessment of MBSC Test

Once the concept/s were chosen, a detailed risk assessment was carried out for each of the chosen concepts. The DFSS methodology emphasizes on a risk assessment once the main concepts are established. The principal advantage of carrying out a risk assessment at this stage was to enable the selection of the right concept with all the information which was gathered through the analysis done and weigh the risks or uncertainties of each concept in order to optimize the concepts at an early stage. The first step for the risk assessment was to breakdown the complex system or process into sub-functions or sub-processes. Each sub-function was individually analysed for the failures or errors that could possibly occur within the sub function and listed. In the next step each failure was rated according to its 'probability of occurrence' and its 'impact' on the test design from a rating of 1,3,5,7 and 9. The rating of these two factors are then multiplied to determine the risk level of the particular failure. Risk levels are divided into 3 Categories- Low risk, Medium Risk and High-Risk categories depending on the final score. The final risk assessment is shown in Table 4-3.

The risk assessment of the MBSC test was divided into two categories: specimen and corrosion test cycle. The test cycle in turn was classified into the three blocks of the test since each block has different environmental conditions and therefore different levels of risk and impact of various factors. The risks related to specimen were mostly related to the positioning and risks related to the transfer of specimens from one chamber to another, when the cycle is carried out in multiple chambers. These positioning errors could lead to uneven corrosion exposure on the specimens and could influence the SCC test results. The measures to be taken to avoid these errors was to determine and document specifications for the positioning of the samples. The operators must be made aware of the specifications and trained accordingly. Another important error that could occur related to specimen is with the detection of failure and failure time. Measures to automate the detection of the failure in the specimens or specifications should be determined and documented to avoid this error.

TABLE 4-3   RISK ASSESSMENT OF THE MBSC CORROSION TEST CYCLE

Category	Risk Description	Probability of Occurance			Impact			Risk Level		
Specimen	Specimen does not conform to specifications	3			9			Medium Risk		
	False positioning in climate chamber leading to coverage of specimen and uneven exposure	3			5			Medium Risk		
	Unplanned cleaning of specimens leading to uneven corrosion exposure	1			7			Medium Risk		
	Use of different climate chambers for different cycles, causing disrupted corrosive exposure and possible false positioning of specimen during transfer of specimen	5			5			Medium Risk		
	Failure time not detected or not documented	3			9			Medium Risk		

Category	Risk Description	Block A			Block B			Block C		
		Probability of Occurance	Impact	Risk Level	Probability of Occurance	Impact	Risk Level	Probability of Occurance	Impact	Risk Level
Climate Cycle	Phase does not occur due to technical failure	1	7	Medium Risk	1	9	Medium Risk	5	9	Top Risk
	Salt-Spray does not occur due to technical failure	3	7	Medium Risk	3	9	Medium Risk	n/a	n/a	-
	Temperature does not conform specifications	3	7	Medium Risk	1	9	Medium Risk	5	9	Top Risk
	Humidity does not conform specifications	3	7	Medium Risk	3	5	Medium Risk	3	5	Medium Risk
	Variation in temperature change slope	5	5	Medium Risk	n/a	n/a	-	5	7	Medium Risk
	Variation in humidity change slope	5	5	Medium Risk	5	3	Medium Risk	3	5	Medium Risk
	Time of each phase does not conform to specifications	3	9	Medium Risk	5	5	Medium Risk	3	7	Medium Risk
	Salt concentration does not conform to specification	3	7	Medium Risk	3	7	Medium Risk	n/a	n/a	-
	Salt composition does not conform to specification (Addition of NH4NO3)	3	9	Medium Risk	3	9	Medium Risk	n/a	n/a	-
	pH not according to specification	5	7	Medium Risk	5	5	Medium Risk	n/a	n/a	-
	Precipitations content not according to specification	7	5	Medium Risk	7	5	Medium Risk	n/a	n/a	-

The possible risks involving the climatic cycle were categorized into the three blocks and rated accordingly. The most probable cause for error in this category would be caused due to technical failures in the corrosion chambers used for testing. This includes failures in conforming to the specification of temperature, humidity, time of each phase, rate of change of temperature and humidity and failure in executing the complete phase itself. It is seen that the Block C has the top risk in not carrying out the phase and non-conformity to the temperature specifications, due to the very high and low temperatures which are present in the block C, which could strain the climate chambers. These failures can be controlled by usage of appropriate climatic chambers that can control the technical specifications of the MBSC test. Another important measure to be taken to avoid these risks is real-time online monitoring of the temperature and humidity cycle, in order to ensure that the climatic chamber conforms to the programmed cycle. Risks involved in regard to the salt-solution include non-conformity to the specifications regarding salt composition and the concentration. This risk can also be controlled by using appropriate mixing techniques, measuring, and documenting the weights of the salts used during the mixing. Thus, through this risk assessment, the novel design of the MBSC test was evaluated based on the possible errors that could occur. This assessment could be utilized in the future for further enhancement of this test method.

4.6.   Validation of MBSC Test

4.6.1.   Validation of MBSC Corrosion Test Cycle

After the complete analysis of the designed MBSC corrosion test cycle and the selection of optimal test parameters, the final test design was compared to the customer requirements which were defined in the first stages of the DFSS to determine the level of fulfilment of requirements of the design. Table 4-4 gives an overview of the level of fulfilment. Green indicates complete fulfilment of requirement, yellow indicates partial fulfilment or potential to be fulfilled and red indicates not fulfilled.

It is seen that the MBSC test cycle, with the chosen parameters shows a high degree of fulfilment of requirements. The chosen parameters are from the Work package 1.1, which is test temperature of 40°C, dry:wet ratio of 1:1 and ΔT of the extreme block as

100°C. The test indicates SCC in the susceptible alloys, which are verified by optical microscopy and SEM fracture surface analysis. The Gage R&R testing of the corrosion test cycle is not carried out in the scope of this thesis; however, it has the potential, due to which it is marked yellow. The MBSC test is used for the whole material pallet and shows a good differentiability as can be seen in results discussed above. The MBSC test accounts for critical environmental conditions, including extreme conditions, therefore fulfilling that requirement. The test cycle along with the mechanical specimen can determine the time-to-failure of the material with respect to the critical stresses, however, the critical stresses with respect to time-to-failure was out of scope of the project. Lastly, the cycle allows for automotive processes and lifecycle to be reproduced in the test cycle with the test parameters. Therefore, the MBSC test has a good degree of fulfilment of customer requirement.

TABLE 4-4   LEVEL OF FULFILMENT OF MBSC TEST WITH RESPECT TO CUSTOMER REQUIREMENTS

Customer Requirement	Level of fulfillment		
The developed test method must clearly indicate the stress corrosion cracking susceptibility level of aluminium 7xxx alloys	🟩	🟨	🟥
The test must be reproducible and repeatable	🟩	🟨	🟥
The test method should be applicable independent of the alloy content	🟩	🟨	🟥
The test should create good differentiation between the SCC susceptibilities of different 7xxx alloys	🟩	🟨	🟥
Critical stresses and environmental conditions should be accounted for, in the test	🟩	🟨	🟥
The test method should be able to determine the time-to-failure of material with respect to the critical stress	🟩	🟨	🟥
The test method should be able to determine the critical stress with respect to the time-to-failure	🟩	🟨	🟥
The automotive process and life-cycle should be reproducible on the tested specimen	🟩	🟨	🟥

4.6.2.   Validation of Specimen Concept

After complete analysis of the three test specimen concepts and the parameters which influence the mechanical specimens, it was concluded that the tensile specimen without hole, loaded to a stress of 75%$Rp_{0.2,}$ was the optimal specimen for the testing of SCC susceptibility of the material pallet. This specimen concept along with the mechanical parameters showed clear SCC susceptibility in the critical materials and showed the highest differentiability among all the possibilities. The risk assessment also showed least risk scenarios among the three specimen concepts for the tensile

specimen due to its ease of preparation and straightforward execution procedure and analysis of results.

TABLE 4-5 LEVEL OF FULFILMENT OF TENSILE SPECIMEN WITHOUT HOLE AT 75%RP$_{0.2}$ STRESS

Customer Requirement	Level of fulfillment		
The developed test method must clearly indicate the stress corrosion cracking susceptibility level of aluminium 7xxx alloys	🟩	🟨	🟥
The test must be reproducible and repeatable	🟩	🟨	🟥
The test method should be applicable independent of the alloy content	🟩	🟨	🟥
The test should create good differentiation between the SCC susceptibilities of different 7xxx alloys	🟩	🟨	🟥
Critical stresses and environmental conditions should be accounted for, in the test	🟩	🟨	🟥
The test method should be able to determine the time-to-failure of material with respect to the critical stress	🟩	🟨	🟥
The test method should be able to determine the critical stress with respect to the time-to-failure	🟩	🟨	🟥
The automotive process and life-cycle should be reproducible on the tested specimen	🟩	🟨	🟥

The final step towards the selection of this specimen for further use was to verify whether this concept fulfils the initial customer requirements that were defined in the definition phase of DFSS. This was done by comparing each customer requirement to the chosen concept and determining the level of fulfilment for each requirement as shown in Table 4-5.

It is seen that the chosen concept, which is tensile specimen without hole stressed at 75%Rp$_{0.2}$ clearly indicates stress corrosion cracking susceptibility of susceptible alloys in the MBSC test as well as good differentiability between less susceptible and more susceptible alloys. The Gauge R&R value of the stressing of the specimen was also under the target value of 20%, indicating a good reproducibility and repeatability of the specimens. The critical stresses were developed in the chosen concepts and analysed to get the most appropriate stressing. Time-to-failure of the material with respect to critical stresses were also determined in the study of stress magnitude. Finally, the results of the tensile specimen were comparable to that of the tensile specimen with hole and the KS-8 specimen, which are closer to the 'real-world' application. Due to its simple and flexible form, the tensile specimen has the potential to be further modified to incorporate the effects of other automotive processes such as welding, thus fulfilling the condition of being able to reproduce the automotive processes and lifecycle. The good level of fulfilment of the chosen concept with respect to the customer requirement indicates that this chosen concept is appropriate for the testing of SCC susceptibility of the 7xxx alloys for the automobile purpose.

Chapter 5 DISCUSSION

5.1. Using Design for Six Sigma for Designing of MBSC Test

There are several product development techniques researched which can be used to systematically design and optimize new processes or products. Among them the design for six sigma methodology is gaining popularity in recent years, especially in the automotive sector. After its introduction, many design success stories on the usage of DFSS led it to becoming popular especially among automotive companies and led many of them to establish the DFSS as a state-of-the-art design process for product development. Due to its several advantages, including its focus on customer requirement and its cross-functional approach, the DFSS methodology has been used in this thesis for the first time to design and develop a corrosion test, the MBSC test. A key matter of this thesis was to assess the usage of the DFSS methodology for the designing of SCC test methods, as discussed in chapter 1. The key research questions which are discussed in detail in this section is whether the DFSS successfully provides a structured framework for designing of SCC tests and does the DFSS in the adapted form used in this thesis have potential of becoming a template for future SCC test developments.

The DFSS approach is not a standardized approach rather a flexible approach used to design new products in a systematic method, through various available methodological models[31, 33]. There are several models of DFSS available in literature of which, the Mercedes Benz standard DFSS model, the DCOV model is used for this thesis. The DCOV model consists of four phases: Definition, Conceptualisation, Optimisation and Validation. Each of these phases will be individually discussed and reviewed below.

Definition Phase: When designing a complex test method, such as the SCC test for automobile, one of the biggest difficulties is to define a clear goal and scope of the project. Due to the complex array of parameters involved and the cross-functional nature of designing an automobile it is also a challenge to structure all the requirements from the various teams and implement them into the test design without losing scope of the project. Thus, the definition phase addresses these gaps and aims at defining

the foundation of the project in terms of its aim and scope, gathering and analysis of the customer requirements and its conversion to tangible functional requirements and design parameters. Tools such as project proposal and scorecard aided to define the exact problem statement (business case) and the objective of the project, which were used as guidelines to determine the specific requirements of the project.

The next step was to determine the Voice of Customer (VoC) or customer requirements. The customers in this case were the end-users of the test method. This stage is critical for the success of a DFSS project and is increasingly being used in product development processes in order to efficiently design customer-oriented products.[176] [177] The requirements of the MBSC Test cycle were cross-functional in nature, ranging from replication of automotive lifecycle in the test phase to material considerations such as applicability of the test method independent of alloy content. The customer requirements were then filtered and prioritized using the pairwise comparison tool and using the Pareto rule, the most important customer requirements were chosen as shown in Table 3-5. The filtered customer requirements were then transformed into tangible and measurable functional requirements as shown in Table 3-6. This stage is important to understand the ambiguous customer needs and thoroughly analyse and interpret them into design parameters which are later used in designing and optimizing the test method. [177, 178] After every stage of designing, the test design is validated by weighing the design against these customer requirements to establish their degree of fulfilment. This feedback loop facilitates for the orientation and focus of the design on the customer requirement.

Conceptualisation Phase: Due to the complexity of the test, the designing was divided into two parts, the environmental test cycle, and the mechanical test specimen. Each of these were tackled with different strategies as shown in the flowcharts Figure 3-3 and 3-5. This illustrates the flexibility of the DFSS process. For the design of the mechanical specimen, the use of morphological box analysis, helped in breaking down the complex features into simple sub-functions and analyse the sub-function individually. The various outputs were then strategically compared to the functional requirements determined in the definition phase to crystallise the best designs for further analysis. For the environmental aspect, the use of brainstorming with Daimler internal design experts was a more appropriate tool to reconstruct the complete

automotive cycle and mirror it onto the corrosion test cycle, resulting in a test cycle that represents the most critical environmental parameters. This stage was followed by filtering of the design parameters which were determined in the definition phase. The conceptualisation phase was vital in bringing together a vast area of multiple factors and ideas and channelling it structurally into a customer-oriented design. Contrary to traditional design techniques, the DFSS conceptualisation phase was customer requirement-centric and provided the right structure to use creativity techniques to reach the most optimal and creative solutions efficiently. Moreover, ranking and weighing of the designs with respect to the customer requirements supported the efficient designing of the test method by incorporating the most important cross-functional requirements.

Optimisation: Once the design concepts of both the environmental corrosion test cycle and the mechanical test specimens were fixed, the next phase was to scientifically study the influence of the chosen design parameters on the SCC susceptibility and eventually filter the optimal parameters for the designed test. In-depth scientific analysis of the various factors enabled a complete picture of the influence of the various parameters on the SCC susceptibility. Qualitative findings of test parameters provided the foundation for the test design. In parallel, quantitative analysis such as MSA supported in optimising the test design. It validated the test results and eliminated the error factors caused by variation in experimental setup and operator conditions which could lead to false results. Similarly, DoE carried out to determine the influence of the environmental parameters threw deep insight on the factors effecting SCC susceptibility and their co-dependencies. Through all this information the optimal parameters were chosen which were again compared to the requirements and the goals set in the definition phase. Moreover, as the next step of the DFSS in the optimisation phase, a detailed risk assessment was carried of the optimized concept. Carrying out a risk assessment at this stage helped to identify the critical factors that could potentially be a risk for the designed test and the risk level of each of these factors. This awareness in turn helped to determine the measures to be taken in future optimisation to prevent these risk factors.

Validation: Since the designed test method is novel, it is important to validate the results it generates to determine the reliability of the test method. The validation phase

was carried out in two parts. The first was by comparing the results to the outdoor exposure results to get a scientific validation of the results. Thus, by comparing it to the results generated from actual outdoor exposure tests, the results obtained from the MBSC test results were proved to be reliable and had good correlation to the actual automotive lifecycle. The second stage was to validate the designed test method with respect to the customer requirements determined in the first stage. Thus, closing the loop successfully of confirming that the developed test method fulfils the requirements which were determined in the definition stage and thus fulfils the goals set in the definition stage.

There were several advantages which were observed by the usage of DFSS methodology for the designing of the MBSC test method. Designing of complex products, such as the SCC test, has several multi-faceted aspects to it that need to be addressed to parallelly. This could easily result in disorientation in the design process and lead to errors or neglect of certain aspects. This could also lead to diversion of focus from the main objectives of a design project. The DFSS process provided a structured template in the designing of the complex test method. This structure was objective, and requirement oriented which were already established in the first step of the DFSS. Each phase was designed such that the primary objectives and requirements were always verified, thus always ensuring requirements were fulfilled in each design phase. This is contrary to many other waterfall design techniques that lack the customer-centric focus and feedback loop for crosschecking with requirements. Moreover, the DFSS process enabled thorough scientific analysis of all the cross-functional influencing factors that influence SCC susceptibility in the complex automotive lifecycle. The main advantage of this was the ability to study these influencing factors as an integrated whole, rather than individual parameters under carefully controlled laboratory conditions as in most scientific studies. Methodical identification and analysis of all influencing parameters ensures that all the important parameters are considered and incorporated into the test design. Another important advantage of using the DFSS process is the use of various tools for various stages of the DFSS process. Innovative tools such as the morphological box analysis or ranking and weightage tools such as QFD, pairwise comparison, etc., are commonly used in many design processes and have proven to be beneficial to structurally reach decisions in designing the process. The DFSS methodology provides the guideline of

using the right tool in the right step. Moreover, using these tools also results in methodical documentation of each step. This helps not only in retracing the steps but also documents the reasons behind each decision, which could otherwise get lost in a complex project such as this. Finally, as it can be seen in this thesis, the DFSS is a flexible process. It provides a structure and a pallet of tools which can be used for the design and optimisation process. However, the user is free to choose which path and which tool suits the situation best. The DFSS structure used in this thesis was adapted to enable the best test design with all cross-functional parameters of the automotive lifecycle to be taken into consideration. Environmental parameters, mechanical parameters and material parameters were methodically analysed and incorporated into the SCC test design in a cross-functional and efficient manner and then validated by outdoor exposure tests. Due to the efficiency of this structure, it has the potential to be used as a template for future SCC corrosion test designs.

Although there were several advantages to use the DFSS method to design the MBSC test, there are also certain limitations and disadvantages that are worth mentioning. For the designing of a complex product or process, the DFSS could be an extremely long and tedious process since it requires to analyse every minute influencing parameter and document them systematically. This could prove to be very time and resource consuming. Thus, the time and resource planning should take this factor into consideration depending on the complexity of the project. Another point to be considered in the DFSS is that due to the complexity of the designing process, it is not possible to experimentally verify each parameter or aspect and thus decision-making is often done based on trusted knowledge or experience or in companies usually through top-down management decisions. This could be advantageous since the decisions are discussed intensely with the project group and taken unanimously. However, it must be carefully considered to not allow personal biases or exceptional experiences to be considered while making such decisions.

There are certain differences between DFSS and other traditional product development approaches such as the the product development method from VDI 2221-1-2019-11[191] which are to be highlighted in order to understand the advantages of the DFSS methodology. Firstly, the definition phase of both traditional and DFSS methodology involve in defining the needs and exact objectives of the

product to be developed. This is done by gathering the requirements and converting them into functional, tangible requirements. The traditional design approach provides tools to focus on understanding these requirements and converting them into tangible functions. The DFSS methodology, however, focuses intensively on a customer-centric approach. The DFSS tools emphasises on weightage to customer requirements, thus providing a customer-centric focus throughout the development process. For the development of an SCC test method, there are several multifaceted requirements which could easily lead to loss of focus on the main objective. Providing a main list of customer requirements as in Table 3-5, proved advantageous in maintaining the objective of the development efficiently. Tools such as the Scorecard used in DFSS enabled to track the customer requirements to functional parameters which in turn were linked to the design parameters. Similarly, in the next phase of conceptualisation, the traditional approach creates concepts based on the derived functions and select suitable concepts accordingly, whereas the DFSS approach focuses on understanding these functional requirements and selecting concepts with weightage of the functional requirements in mind. Finally, unlike the traditional systematic design approaches which have been studied and modified extensively over several years and standardized, the DFSS is a relatively young and evolving methodology, giving the flexibility to modify it as required. A complex multifunctional test development such as this one, benefited from this flexibility, while holding the key framework of product development throughout the project.

In summary, for the purpose of designing the MBSC test, the DFSS proved to be a valuable tool, which provided a structured guideline to disintegrate the complex automotive lifecycle and SCC process with several influencing parameters into tangible sub-functions. A critical challenge faced in development of accelerated corrosion tests, especially those that represent real-life conditions are the complexity of several cross-functional influencing factors. A trial-and-error approach or single parameter approach could not only lead to tedious efforts and significant resources, but also lead to misguided results. By using the DFSS, all the crucial cross-functional parameters were studied holistically. Appropriate DFSS tools and innovative and flexible concept creation methods enabled the designing of the MBSC test efficiently. Moreover, the DFSS process also focused on the reproducibility and repeatability of the designed test which is also an important aspect of designing a new product and determines the

validity of the results obtained. Keeping all these factors in mind, it is recommended to adapt the DFSS methodology used in this thesis as a standardized framework to design future accelerated corrosion test methods, especially SCC test methods.

5.2. Influence of Environmental Factors on SCC Susceptibility

In the lifetime of an automobile, it undergoes a range of environmental conditions. A key research question addressed in this thesis is to scientifically understand the influence of environmental factors that occur in the automotive lifecycle on the SCC behaviour of the 7xxx alloys and successfully transfer this knowledge into designing an accelerated corrosion test cycle. Several attempts were been made to model complex environmental conditions into one accelerated corrosion test [179-181]. The tests are generally designed to expose the specimens to a range of different temperatures, humidity and salt sprays in repeated cycles. The aim of these tests is to correlate the corrosion behaviour to the 'field' environment. However, the corrosion behaviour is highly dependent on the parameters such as temperature, humidity, concentration, and pH of the salt spray solution, among others, making it very difficult to replicate and validate the actual field environment. The goal of this thesis was to analyse the complex interactions of real-world environments occurring in the automotive lifecycle, rather than the influence of individual environmental parameters. This section discusses the influence of the environmental parameters on SCC behaviour of 7xxx aluminium alloys and the incorporation of this knowledge into the accelerated corrosion test cycle, the MBSC test.

5.2.1. Design and Optimisation of the MBSC Test Cycle

To ensure the correlation of the designed test to actual field results, the designing of the MBSC test cycle followed three steps. The first was to conceptualise the structure of the test cycle. This was done by analysing the complete automotive lifecycle and identifying the conditions, which would be most critical to the SCC susceptibility of the materials and replicating these conditions into the test. This was done with the aid of internal expertise and literature research. This was followed by scientifically analysing the influencing environmental parameters individually as well as synergistically. Qualitative as well as quantitative analysis was done using DoE. Finally, the results

obtained from the developed test were validated by qualitatively comparing them to the results obtained from outdoor exposure tests. A range of outdoor environments were tested and compared to encompass all scenarios critical to SCC.

Since stress corrosion cracking differentiates itself from other forms of corrosion due to its specific nature, the process of designing a new corrosion test cycle, instead of using an already existing test cycle, was advantageous due to the thorough analysis carried out of the complete automotive lifecycle with the principal focus on SCC susceptibility of the material. Moreover, the design of the new cycle also gave the freedom to individually analyse the critical environmental test parameters such as temperature and dry:wet ratio with respect to its influence on the SCC susceptibility and optimise the designed test cycle accordingly. While designing the MBSC corrosion test cycle, all the key scenarios that occur in an automotive lifecycle were factored in and replicated within the test cycle. To do so, each stage of the automotive lifecycle was individually analysed, and all the critical phases of the lifecycle were listed. The cycle was divided into three phases: (1) Storage and Transportation, (2) In-service (3) Extreme, which are detailed in section 3.3.1. The storage and transportation phase encompassed the critical scenarios that occur before the vehicle is handed over to the customer. Internal studies conducted by Daimler revealed the extreme humidity and temperature conditions that the automobile is exposed to during the overseas transport, which could last for 6 to 8 weeks, thus already influencing the corrosion susceptibility of the exposed parts. These along with train transport and harbour storage are incorporated into the first stage of the MBSC test cycle. The focus of the in-service test cycle focused on the daily weather change as well as the yearly climatic changes which causes an alternating wet-dry cycle on the automobile. This wet-dry cycle could cause a thin film of corrosive solution on the surface, which could initiate corrosion on the surface. The aim of this cycle is to achieve the optimal wet-dry cycle which is critical to the SCC susceptibility. Finally, the third phase, the extreme phase, incorporated all the extreme environmental conditions that could possibly occur in the automotive lifetime.

Once the initial design of the test cycle was defined, the key environmental parameters were scientifically studied to determine their influence on the SCC susceptibility. In most research studies on SCC susceptibility individual parameters are studied in

carefully controlled laboratory conditions and conclusions are derived based on these results. However, this kind of studies is less close to real automotive lifecycle conditions in which several environmental factors react simultaneously on the exposed alloy. This thesis covers that gap and approaches the study in a novel manner, where focus on real-world parameters was given while designing the corrosion test and synergistic behaviour of environmental parameters was studied along with individual parameters. This has the advantage of identifying SCC behaviour in the real-world conditions. The influence of each crucial environmental parameters is discussed below:

Influence of Cations and Anions: In the course of its life, the automobile is exposed to a several kinds of environments and thus several kinds of solutions, such as rainwater, seawater, and residual water from the roads. Depending on which part of the world, the solutions vary in parameters such as chemical composition, salt concentration and pH, among others. Studies showed that not only the cations, especially halides have an influence on SCC susceptibility of the 7xxx alloys[62], but also certain anions have a significant effect [89]. Further state-of-the art on rainwater analysis of different regions suggested the significant present of the sulphates, nitrates and ammonium ions depending on the regions. [19, 98-100, 182, 183] A detailed analysis carried out by Braun on the influence of anions on the SCC susceptibility of the 7xxx alloys [89] showed that anions such as sulphates, nitrates, hydrogen carbonates, and also ammonium ions could promote the SCC susceptibility of the 7474-T651, thus making it imperative to study the influence of these ions with respect to the test method and determine the optimal composition of the salt-spray solution.

Correlating with the study conducted by Braun, alloys exposed to MBSC test in different salt-solutions showed lower average time-to-failure of the SCC susceptible on the addition of Na_2SO_4 as well as the different concentrations of the NH_4NO_3 solutions, compared to only NaCl solution as seen in Figure 4-7. The influence was more evident in the medium susceptible alloys such as 7019-T6 and 7075-T4 alloys. Metallographic observations also revealed higher localised corrosion influences on the materials exposed to salt-solutions with the additives. Especially with NH_4NO_3, higher pitting and intergranular corrosion was observed, which could act as initiation points for SCC and thus resulting in increased susceptibility to SCC. Braun also observed an increase in

the SCC susceptibility of the 7475-T651 plate on exposure to sulphates, nitrates, and ammonium which he attributed to modification of chemistry within the cracks. Similarly, Nguyen et al. [92] attributed the increase in crack propagation rate of the 7075-T651 alloy exposed to $NaNO_3$ solution to the formation of ammonium within the crack surface. The exact mechanism for the acceleration in corrosion of the 7xxx alloys needs to be further investigated, however, due to the conclusive evidence showing the increase in SCC risk with the addition of the ions and its clear presence in the field environment, the NH_4NO_3 additive within the standard 3.5 wt.% NaCl solution was chosen as the composition of the salt spray solution in the MBSC test.

After selection of the salt-spray solution, a full factorial DoE analysis was carried out to analyse the influence of the three main parameters on the SCC susceptibility of the tested materials and determine the optimal parameters. The three chosen parameters to be tested were test temperature, dry:wet ratio and the influence of the extreme block of the MBSC test. The complete Pareto chart of the standardized effect of all the factors, shown in Figure 4-6, shows which of the factors have a statistically significant influence on the average days to failure of the specimens. Naturally, the material itself had the highest influence on the SCC susceptibility, which will be discussed in Section 5.4. Following this, the temperature difference in the extreme block (ΔT) and temperature were shown to have a significant influence, which are discussed below.

Influence of Temperature: Several studies have been conducted to study the influence of temperature on the SCC susceptibility of the 7xxx alloys. The consensus is that there is an increase in the crack growth rate, and hence increase in SCC susceptibility with increase in temperature. [71, 96, 97] This influence of temperature was attributed by the researchers to the changes in chemical reactions at the crack surface and the rate of diffusion of the corrosion products from the corrosive environment to the material. [96] The average results from the complete DoE showed a tendency for the reduction in average days to failure with increase in temperature from 40°C to 60°C, as shown in Figure 4-10. An individual analysis of the materials revealed, shown in Figure 4-10 that for the alloys 7019-T6, KK17-T7 and the KK18-T6 there was a reduction in average days to failure, when the temperature was increased, which correlates to the results of the state-of-the-art.

However, an anomaly in this pattern was observed with the 7075-T4 and the 7075-T6 alloy, which showed slower failure on increase in temperature, especially when the temperature difference ΔT was 0°C. Moreover, comparison of the residual strengths of the 7075-T6 alloys which did not fail within the test, also showed that the residual elongations for samples exposed to 40°C, as in WP 1.2[40°C|1:5|100°C] and 1.3 [40°C|1:1|0°C], shown in Figure 4-15, reduces considerably from an original elongation of 15.6% to 2.5%. On the contrary, the 7075-T6 alloy, which were exposed to a temperature of 60°C, show very slight loss of elongation to range of 10 to 13% elongation. Thus, the increase in temperature seemed to have a positive effect on the 7075-T6 alloys. A possible explanation of this phenomena is that exposure to the high temperature of 60°C for a long period of 30 days along with exposure to short duration of extreme temperature in the extreme block could possibly result in microstructural changes in the material which could have led to a slight overaging of the material and thus improving its SCC properties. On observing the behaviour of individual alloys to temperature it was seen that exposure to 40°C showed the best differentiation among the alloys and successfully differentiated the susceptible alloys from the non-susceptible alloys. It must also be noted that individual analysis of the temperature was not sufficient to determine the behaviour of the tested alloys, since there was a significant co-dependency of the temperature on the other parameters, especially the ΔT.

Influence of Temperature Difference in Extreme Block(ΔT): The extreme block is a vital component in the complete design of the MBSC test cycle since it represents the extreme conditions which the automobile could be exposed to in its lifetime. However, the sudden change in temperature within the block could have a significant influence on the materials. Therefore, DoE of this parameter was carried out to observe the impact on this phase had on the tested materials and whether this phase was actually required within the test and to which extent. The results of variation in the ΔT parameter, which is the difference of temperature between the hot phase and the cold phase in the extreme phase was shown to have a significant influence on certain medium susceptible alloys. With a ΔT of 100°C, the specimens failed significantly faster, compared to a ΔT of 0°C (which was the absence of the extreme phase itself and continuation of the In-service phase) as shown in Figure 4-11. Moreover, it was observed that certain medium or less susceptible alloys such as the 7019-T6, 7075-T6

Discussion

and the KK17-T7 did not fail, when the ΔT was 0°C in some work packages and failed when the ΔT was 100°C. These alloys showed a statistically significant influence of the extreme block on the SCC susceptibility results. The increase in temperature to 80°C in this phase could lead to acceleration of crack initiation and crack propagation.[71, 96]. This combined with the residual and thermal stresses caused by the sudden drop in temperature to -20°C could result in the complete failure of the embrittled specimens. The evidence of embrittlement found from the SEM fracture surface analysis of the 7019-T6 and 7075-T6 alloys exposed to the extreme block confirmed SCC initiation followed by residual failure which could be the result of thermal stresses. This indicated that these alloys are indeed susceptible to SCC and the extreme block with ΔT of 100°C was required by the MBSC test cycle to identify these susceptible alloys and to filter them. Moreover, these sudden changes in temperature could also be a possible scenario that occurs in the lifetime of the automobile and thus, should be encompassed within the test.

Influence of Dry:wet Ratio: Finally, the dry:wet ratio in the block B (in-service) block was the third parameter which was studied in the DoE for the optimisation of the MBSC test cycle. The dry:wet cycle in the block B represents the daily as well as yearly weather changes that an automobile experiences in its lifetime. There are of course limitations to be considered in the mirroring of this effect due to the extreme variations in climates depending on the various regions in the world. However, the through the optimal dry:wet ratio, the aim was to achieve an optimal dry:wet ratio which could identify the SCC critical alloys and differentiate them from the alloys which are not critical. The DoE results showed a relatively insignificant change in the SCC susceptibility of the alloys with change in dry:wet ratio. The exception was the 7019-T6 for which the susceptibility increased on changing the dry:wet ratio from 1:1 to 1:5. These results contradicts the study conducted by Yu et. al. which showed a decrease in susceptibility, with increase in dry:wet ratio. [165] Since, for most other alloys the difference in dry:wet ratio did not show significant changes and for the 7019-T6 the ratio 1:1 was the critical ratio, this ratio was preferred to be further used in the MBSC test cycle.

On detailed quantitative as well as qualitative analysis of the DoE, it was evident that the parameters studied had a significant influence on the SCC susceptibility of the

tested alloys as described above. The influence was not only individual parameters but also co-dependent on each other. These scientific findings were then correlated to the customer technical requirements to determine the optimal test parameters. The requirements indicated that the test method should be able to distinguish the susceptible alloys from the non-susceptible alloys. Table 4-1 shows the mean days to failure of all the tested samples. The highly susceptible alloys such as KK17-T4, KK17-T6 and KK18-T4 showed early failure in all the tested environments. There was also no significant difference in the time to failures with respect to the parameters observed for these alloys due to the extremely early failure of the alloys. Similarly, the non-susceptible alloys such as the 7019-T4, 7019-T7, 7075-T7 and the KK18-T7 showed no failure in any of the tested environments and thus, showing no difference with respect to the parameters. The key was to identify the differences in the SCC behaviour of the other alloys which were classified as medium and low susceptible alloys. It was seen that these alloys were susceptible to SCC and failed in certain environmental conditions, while surviving without failure in others.

SEM analysis of these alloys also confirmed failure due to stress corrosion cracking , confirming their susceptibility. Thus, it was important to choose an environment which indicated failure of these susceptible alloys. The fastest failure within these categories of alloys were seen in the work package 1.1, which had a test temperature of 40°C, dry:wet ratio of 1:1 and the ΔT of 100°C. In this package, the 7019-T6 alloy failed at an average of 22.5 days and the KK17-T7 alloy failed at an average of 15.25 days. The 7075-T6 alloy, which is a very important alloy in this study due to its good mechanical properties and its popularity in the other industries, showed also showed failure in this work package at an average of about 22.5 days. These alloys did not show failure in most other environments. Moreover, on comparing the days to failure of all the alloys, this work package shows a significant differentiation of the different categories of susceptibility of the tested alloys. Comparing the results of this work package with the rest of them, the mean days to failure of this work package was the lowest for most of the alloys making it the most critical test condition for the tested materials. However, this approach of choosing the most critical test condition was favoured, since the test cycle is supposed to represent a complete automotive lifecycle of about 15 years. This includes all the conditions which were mentioned above, including the extreme conditions. Considering that these alloys could be used in parts which are safety

related in the automobile in the future, it is important to take a conservative approach while selecting the test parameters. This work package also includes the extreme block with a ΔT of 100°C, thus representing the extreme conditions that could be possible in the real lifecycle of the automobile. Thus, keeping all these factors in mind, the environmental parameters of the work package 1.1, with temperature at 40°C, dry:wet ratio at 1:1 and ΔT at 100°C, was the preferred among all the other parameters. However, to finalise these parameters, it was important to validate these results by comparing them with the outdoor exposure test. The comparison is discussed in the next section.

5.2.2.   Comparison of Outdoor Exposure Results with MBSC Test

Different areas in the world have extremely varying climates, thus resulting in varied influences on the automobile with respect to corrosion. The research question 1.3 was to determine the correlation of the susceptibility of the 7xxx alloys in the developed test method to the outdoor exposure conditions. To do this, the most critical outdoor environments with respect to SCC were identified and various mechanical specimens were exposed to these environments. This gave an understanding of the difference in SCC behavior of the tested alloys in the different climates and also compared the results generated from the newly designed MBSC test to the outdoor exposure test. Figure 5-1 compares the results of the outdoor exposure test of the tensile samples to that of the MBSC test with the chosen optimal parameters discussed above and the ASTM G47-98 results which is a commonly used standard to test the SCC susceptibility of 7xxx alloys, especially in the aerospace industry.

When it comes to the extremely resistant alloys, such as 7019-T4, 7019-T7, 7075-T7 and the KK18-T7 there seems to be a good correlation between the outdoor exposure results, ASTM G47-98 results and the MBSC Test results. None of the alloys failed in any of the exposures, showing high resistance to SCC. Similarly, a good correlation was observed for extremely susceptible alloys, such as the KK17-T4, KK17-T6, KK18-T4 and KK18-T6. These alloys failed in all of the tests and had an extremely low SCC index. With the help of these results, it can be concluded that the MBSC test has the capability to recognize and distinguish the alloys which have extreme susceptibility as well as extreme resistance. However, this is a comparatively easier task, which could

be easily achieved through other tests as well, as shown with the results of the ASTM G47-98.

However, referring back to the customer requirements which were gathered during the
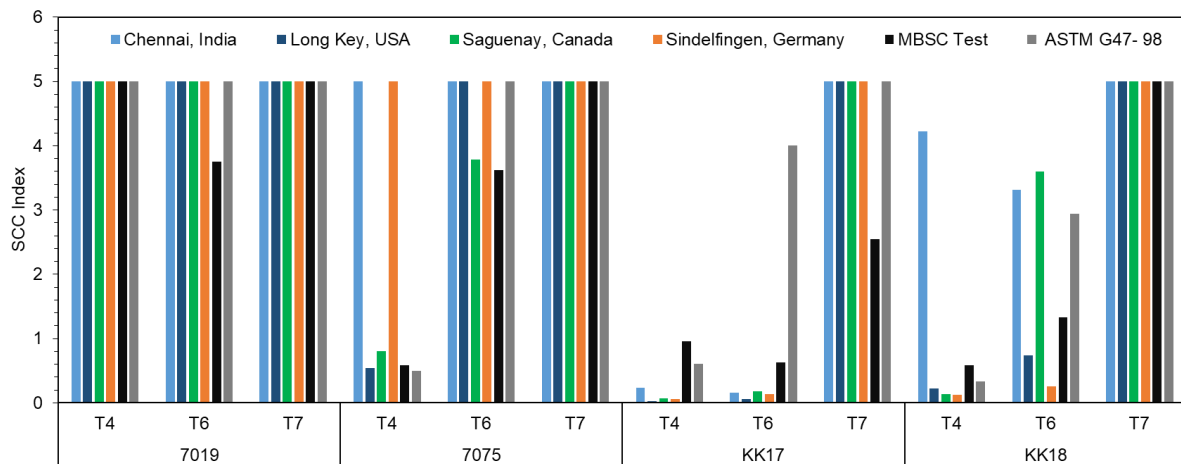

FIGURE 5-1 COMPARISON OF THE OUTDOOR EXPOSURE TEST RESULTS WITH THE MBSC TEST RESULTS AND THE ASTM G47-98

definition phase of the DFSS project, the requirement clearly states that '*The test should show differentiation between the SCC susceptibilities of different 7xxx alloys*. Thus, a nearer observation of these alloys is required to determine whether the test is successful in fulfilling these requirements or not. Starting with the 7019-T6 alloy, it was seen that there was no failure observed in any of the outdoor exposure sites as well as the ASTM G47-98, but failure was observed in MBSC test. However, the SEM analysis of the 7019-T6 alloy, as shown in Figure 4-14, showed the presence of embrittlement and secondary cracks on the fracture surface, which are a typical indication of SCC susceptibility.[64] Similarly, for the 7075-T6, late failure was observed in the Canada site with an SCC index of 4. This is also reproduced in the MBSC test, where the 7075-T6 alloy undergoes failure and has an SCC index of about 3.7. However, this failure is not reflected in the rest of the outdoor exposure sites, nor with the ASTM G47-98 test. With the KK17-T7, was also the same contrast of results observed. Thus, a deeper dive into the microstructure of these alloys was required to determine the cause of failure of these alloys. However, observing the fracture surface of these alloys, it was also clearly seen that an embrittlement had taken place leading to a brittle fracture with little to no corrosion influences on the surface as shown in

Figure 4-16 and Figure 4-17. These results clearly indicate an SCC susceptibility in these alloys which led to the failure of these samples in the MBSC test.

Thus, comparing the results of the outdoor exposure tests and the ASTM G47-98 with the MBSC test results, it was clearly seen that the MBSC test was more critical. The time period of the outdoor exposure test in the scope of this thesis was a period of one year, which could probably be insufficient to identify the medium and low susceptible alloys. Moreover, the MBSC test was able to identify the medium and low susceptible alloys which could not be identified in the ASTM G47-98 test, showing that the test environment has a huge influence on the SCC susceptibility, and it is important to interpret the results of testing carefully. As mentioned earlier as well, the decision to go move towards a conservative test method (which is more critical than less) is warranted due to the risks involved in the usage of this material in the automobile. The comparison of the test results with the outdoor exposure results as well as the ASTM G47-98 results, clearly indicated that the MBSC test with the chosen parameters is appropriate to test the SCC susceptibility of the 7xxx alloys.

5.3. Influence of Mechanical Factors on SCC Susceptibility

5.3.1. Selection of Optimal Mechanical Specimen

Mechanical parameter variations in SCC testing such as specimen form and loading mode can have a significant influence on the SCC susceptibility, which could correspond to variations in interpretation of SCC test results. These variations have been extensively researched by Turnbull et. al [151], Parkins et. al.[14] and Dietzel et. al. [15], who have extensively studied and compared the variations in SCC test results, with changing mechanical parameters. The research question 1.2 focuses on gaining a scientific understanding of these parameters and incorporating them into the test method. As in the environmental parameters, the focus was to study the influence of the mechanical parameters on the SCC behaviour of 7xxx alloys holistically and synergistically. Through morphological analysis, described in section 3.4.1, the critical mechanical parameters, which influence the SCC test were filtered out and individually studied. The initial assessment of the three chosen specimens is discussed below.

Tensile specimen: The classic tensile specimen, as shown in Figure 3-2(a), is the most commonly used specimen to carry out SCC testing of 7xxx aluminium, especially in the aerospace industry using standards such as the ASTM G47-98 [167]. This specimen has the obvious advantage that the stresses induced in this specimen are almost homogeneous until the point of necking and also uniaxial, making it the easiest to calculate the exact stresses in the specimen. This can be particularly helpful to determine the exact threshold stresses that induce SCC in the material. Moreover, being a universally accepted specimen form, it is easy to prepare this specimen by means of cutting or milling. This specimen type also has the advantage that it could facilitate the testing of weld specimens or other joint specimens. However, observing the real-world conditions such as the load cases of door overloading and the towing assembly, it is observed that the stresses induced are generally multiaxial in nature and localized.

Tensile specimen with hole: The tensile specimen with a hole in the provides a multiaxial stress variant in the specimen which is closer to the stresses that occur in an automobile. The stress concentration in the specimen due to reduced surface area also makes this specimen also results in the control of initiation point of the cracking, at the hole, which acts as a notch. The tensile specimen with hole is the closest specimen to mirror the real-time stress conditions that were observed in the automotive stress simulations described in section 3.4.2, due to its localization of stresses near the hole and the multiaxial nature of stresses.

KS-8 specimen: This is a novel test specimen which was developed by modification of the KS-2 specimen, which were developed in the University of Paderborn with Fraunhofer Institut für Werkstoffmechanik(IWM) designed to test weld-specimens of steel.[172] This specimen was designed to test the SCC susceptibility in a constant strain mode. The advantage of this specimen is the presence of plastic deformation, which represents the plastic stresses that occur in the automobile parts. Moreover, the specimens are easy to prepare and bending takes place in a mechanized, controlled manner, making its preparation a reproducible process.

5.3.2. Influence of Load Propagation Mode

Once the mechanical specimens were determined, the next step was to analyse the influence of mechanical parameters which could have an influence on the SCC susceptibility. From fish-bone analysis, several mechanical parameters were listed, and the most important parameters were crystallized for detailed analysis which were: load propagation mode, load magnitude and stress distribution, which is discussed in detail in this section. In the first step, the load propagation modes were analysed. The load propagation modes: constant load, constant strain, slow strain rate and incremental step-load, were compared and analysed in this thesis in order to determine its influence on the SCC susceptibility and in turn, the SCC test results.

Observing the results in section 4.3.2, the constant load samples show the highest failure in the SCC test and shows relatively better differentiability and ranking of SCC susceptibility compared to the other tests. The KK17-T6 and the KK18-T6 alloys, which are SCC susceptible alloys, showed early failure in both the environments. This was earlier than the constant strain mode which could be attributed to the effective reduction in cross-section of the samples in the constant load mode when the crack initiates. The constant load mode has a considerable disadvantage of being bulky and requiring heavy equipment and machinery while testing high strength alloys. [14] However, with the help of the in-house designed small scale, mobile constant load setup, the practicability and flexibility in implementation of the experiments also played to the advantage of this test method. Moreover, the samples that did not fail could be subjected to tensile testing after the test to determine the loss in ductility.

On the contrary, the constant strain mode was less critical. The constant total strain mode is by far the most popular form of SCC testing due to its ease of implementation. However, they have certain drawbacks including poor reproducibility of strains on the specimens which could lead to poor reproducibility of results.[14] Additionally, calculation of loads on these specimens are also difficult due to the complicated nature of stresses that are observed in these specimens. This lead to the development of certain standard specimens such as the 2-point, 3-point and 4-point bend specimens which were developed to obtain calculable stresses on the specimens.[154] The KS-8 specimen, which was a modification of the KS-2 specimen [172] had the advantage of

controlled bending, which was mechanically operated, considerably reducing variability in bending. However, the results showed that the constant strain mode was not as critical as the constant load mode. On observing the results of the KK17-T6 and the KK18-T6 specimens, it is seen that these alloys exposed to the DIN 11997-1(B) environment, shows slower failure compared to the tensile specimen also exposed to the same environment, as shown in Figure 4-20(a). This can be attributed to the stress relaxation that is caused in the constant strain mode, on the initiation of a crack which results in the gradual decrease in velocity or possibly cease in the crack propagation.[152] This phenomenon could lead to variations in determination of the threshold stresses, showing lower threshold stresses in the constant load mode, compared to the constant strain mode, which is also observed by experimentation conducted by Brenner et. al. [156] Moreover, there can also be variations in the individual test results observed in failed KK17-T6 samples, which could be the result of crack branching and multiple secondary crack formations.

The slow strain rate test provides a controlled crack propagation process by loading the sample with a controlled increase in extension. The aim of this test is to replicate the morphology which is obtained from the constant total strain or the constant load mode at an accelerated rate. [157] This is done by gradually exposing the opening of the crack to corrosive solution which could lead to SCC on the crack surface and thus enhances further SCC as the crack opens up.[157] However, this load mode also requires bulky, expensive test devices which created practical limitations of testing, such as limited range of test environments, in which it can be tested. Results showed a loss in ductility of the KK17-T6 and KK18-T6 materials. However, when the standard deviations are taken into consideration, the differentiability of SCC susceptibility was reduced. Moreover, one must consider the importance of strain rate on the test results, which could also considerably influence the SCC test results. [159, 184] Therefore, it is important to find the optimal strain rate, which is individual to every material, depending on its material properties. Due to the several disadvantages faced in this method, including low correlation to real-life stress conditions, low differentiability of SCC susceptibility, high efforts, and equipment in carrying out test, this load propagation mode proved to be an unsuitable candidate.

Discussion

The incremental step load mode was also considered in this thesis due to its ability to show hydrogen embrittlement in high-strength steels as investigated by Kröger et al. [185] . Moreover, earlier tests conducted by Magaji et. al. [13] on the SCC susceptibility of 7075 alloys, showed that this test could have potential due to its clear advantage of a defined end period. However, the chosen parameters have a large influence on the test results and thus the test was conducted in varying conditions of load time and duration of load step. However, no loss of %F_{max} observed in any conditions, showing no loss in ductility. This was again contradictory to the results of the constant load test, which showed SCC susceptibility for KK17-T6 and KK18-T6 materials. Similar to the SSRT test, the incremental step load test required tensile machines to carefully control the increase in step load, making it a bulky test setup, which is difficult to test with this load in various environments. Due to these disadvantages, the incremental step load mode was also deemed unsuitable to

Deploying DFSS strategy again to compare the above load conditions and the results obtained from them, a QFD (Quality Function Deployment) analysis was carried out to weigh each of these tests with respect to the relevant functional requirements determined in step 3 of the DFSS process. The incremental step load test scored the lowest for functional requirements, which were focused on interpretation of results such as '*Identification of SCC susceptible material through time-to-failure analysis*', '*differentiability of time-to-failure/SCC susceptibility ranking*' and '*identification of SCC failure through fracture surface analyses*. The constant load test, due to its fast failure of susceptible materials, as well as clear ranking of susceptibility of materials, scored the highest in the QFD analysis. The constant strain test also scored low compared to the other load conditions, for functional requirements of interpretation of results. However, due to its ease of experimentation and sample preparation, constant strain test scored higher in requirements which were based on the practicability and factors considered for execution of the experiment such as 'least preparation steps', 'higher possibility of automation', 'high reproducibility' and 'high flexibility of sample preparation'. The weightage of the slow strain rate test followed the constant strain test due to its lower score in identification and differentiation of SCC as well as difficulty and inflexibility in carrying out the experiment. Lastly, the incremental step load test had the least scores due to its inefficiency in ranking SCC susceptibilities of the materials tested and the tediousness of the experimental setup.

TABLE 5-1   QFD ANALYSIS OF THE VARIOUS LOAD PROPAGATION OPTIONS

Functional Requirements	Technical Weightage	Constant Load Test	Constant Strain Test	Incremental Step Load Test	Slow Strain Rate Test
High Reproducibility	9.7	8	8	6	9
High Automation	2.8	9	9	7	7
Stress distribution easy calculable	8.3	9	7	5	3
Less difficulty in experimental setup	1.7	8	9	5	5
Load applied on the sample reproducibly	7.9	9	7	9	9
Identification of SCC susceptibility through time-to-failure analysis	10.0	9	5	2	4
Identification of SCC through fracture surface analysis	8.6	9	4	2	4
Test Duration	6.9	6	5	8	9
Technical Weightage		261.72	231.03	198.62	211.03

The comparison and analysis of the SCC results of the different load conditions along with the QFD analysis, gave a clear ranking to the different load conditions. Constant load test, which had showed the best SCC differentiability and had highest weightage according the QFD was carried forward for further testing. The constant strain test, which had the second highest weightage was also further analysed due to its significant advantages mentioned above. The slow strain rate test and incremental step load test were not considered for further testing due to their difficulty in carrying out the experiment, lower differentiability of SCC susceptibility and overall lower scores in QFD analysis.

5.3.3.   Influence of Magnitude and Nature of Load

In the course of an automotive lifecycle, the car body undergoes various stresses which are varied and complex in nature. These stresses could have a significant influence on the SCC susceptibility. Mechanical changes on the vehicle body, such as notches or defects, could act as localised stress raisers and if the minimal threshold stress is exceeded, these points could result in being initiation points for the SCC to occur. In

order to understand and replicate these stresses, two critical load scenarios were analysed. These were the towing assembly and the door lowering assembly which are described in section 3.4.2.

The towing sub-assembly has been known to be a critical assembly with respect to mechanical stresses in the vehicle body. Several studies have been conducted to determine the nature and magnitude of the stresses experienced in the assembly and to optimize the design of the assembly accordingly.[112-114, 186] For e.g., Wang et al. [112] analysed the structural integrity of the towing hook assembly on application of angular loads. The simulation showed that there was localised plastic deformation at the towing hook and the anti-collision box. On removal of the load, residual deformation was also observed, making this sub-assembly critical with respect to load stresses.

Similarly, the simulation of the towing assembly in this thesis also revealed high localised stresses around the bolting region of the support block. Angular loads applied on the towing hook also created multiaxial stress concentrations and localised plastifications on the point of contact of the towing hook, support block and the flanges of the crash box. Similarly, the door assembly, on the application of a load in Z direction, also showed high localised stresses on the bolting regions with stresses exceeding 300MPa on the A-pillar and localised plastification. This indicated that these localised high-stress regions could also be critical areas for SCC initiation. The simulation study revealed that in the vehicle body, there are several critical load scenarios to be considered, which could have a critical influence on the initiation of SCC cracks. The above load conditions showed high localised stresses and localised plastification in certain regions which could act as stress raisers for the SCC initiation to occur. Therefore, these phenomena were incorporated into selection of the mechanical specimens.

The three chosen specimens, tensile specimen, tensile specimen with hole and the KS-8 specimen were strategically chosen to encompass a wide range of stress distributions and magnitudes, including the stress conditions found in the automotive load cases described above. FEM simulation of the loaded specimens, shown in Figure 4-21, show the localisation of stress in the tensile specimen with hole, which mirrors the critical stresses observed in the support block and bolting regions of the towing

hook. The bending stresses of the KS-8 specimen, observed in Figure 4-21(c) replicates the bending stresses on the crash box flanges, which are observed on the application of angular loads. These stresses are also multiaxial in nature, as observed in both the analysed load cases.

Exposure of these three specimen types to the DIN 11997-1(B) environment and the MBSC test environment revealed variations in the time and nature of failures in the specimens. The tensile specimen with hole showed fastest failures among the three tested specimens. This result was also expected due to the high concentration of stresses at the hole region, leading to achievement of threshold stresses in the localized high stress regions. This would initiate the SCC crack faster and the constant load mode would result in increase of stress on crack initiation due to reduction in cross-sectional area and thus complete failure of the sample. However, it was observed that materials which are not susceptible to SCC, such as the 7075-T7 exposed to MBSC test, also showed failure in this specimen. However, observation of the fractographic images of the specimen revealed no embrittlement or cracks on the surface, indicating that the probable cause of failure could be residual stresses rather than stress corrosion cracking failure. On the contrary, the KS-8 specimens did not show failure, also in the SCC susceptible materials. For e.g., the 7075-T4 material, which is an SCC susceptible material and shows early failure in other test specimens did not fail with the KS-8 specimen form on exposed to the MBSC test as shown in Figure 4.21. Similarly, the medium susceptible alloys such as 7019-T6 and 7075-T6 alloys did not fail in the KS-8 specimen form on exposure to the MBSC test. The underlying cause of this difference in result is again due to the stress relaxation mode, which occurs on the crack initiation in a constant stain mode specimen as also established by Brenner et al. [156]

These results indicate that the stresses occurring in the tensile specimen with hole and the KS-8 specimen are not suitable for the identification of SCC susceptible materials. While the tensile sample with hole is too critical and could lead to false assessment of susceptibility on otherwise resistant materials, the KS-8 specimen does not induce enough stresses to show SCC failure, also in susceptible specimens. In comparison to these specimens, the tensile specimen without hole showed the most appropriate results on exposure to the various environments, with respect to differentiability and

recognition of SCC susceptibility. It was seen that with the tensile samples exposed to the MBSC test, extremely susceptible alloys failed within the first 5 days of testing, followed by the medium susceptible alloys. The alloys which are SCC resistant such as the 7019-T4 and 7075-T7 did not show any failure within the testing period. The key factor in this sample was that it was able to differentiate the medium and low susceptible alloys such as the 7075-T6 and the KK18-T7. SEM fractographic analysis as well as optical microscopic imaging confirmed showed SCC cracking and embrittlement, confirming the cause of failure to be SCC. Moreover, the reproducibility of these specimens was also considerably better than the other two specimens, with lower standard deviations of time-to-failure compared to the other two specimens. The main customer requirements listed in Table 3-5, included clear indication of SCC susceptibility on failure and the reproducibility and repeatability of the test results. Thus, the tensile specimen fulfills these criteria making it a suitable choice for the MBSC test. Moreover, risk assessment of the various specimens carried out toward the last stage of the DFSS concept phase revealed the lowest risk levels in the tensile specimen due to its standardized preparation methods and even distribution of stresses within the specimen. All these factors combined, made the tensile specimen in the constant load mode the most appropriate choice for the testing of SCC susceptibility. This decision was also favored by the in-house designed constant load testing specimen made the implementation of testing easier and more feasible.

Once the influence of specimen distribution was established and the appropriate specimen was chosen, the next step was to determine optimize the specimen in order to select the appropriate load magnitude. It has been established that crack initiation requires the presence of all the three factors, which are susceptible material, critical environment and lastly a minimum threshold stress. The typical stress intensity curve, as shown in Figure 2-1 (b), shows that a minimum threshold stress intensity factor (K_{ISCC}) is to be reached for cracks to initiate. [67] . This initial stress could be in the form of stress raisers such as metallurgical inhomogeneities or mechanical processing defects such as weld defects or porosities. [60, 66] It was observed from the real-time load cases analysis, that the load magnitudes vary for different automotive body parts in different load conditions. Localized stresses reach very high magnitudes and could also lead to localized plastification, which could result in the initiation of SCC in these regions. Thus, a conservative approach to choosing the appropriate stress is to

determine the minimum load stress, which could occur within the automotive body, and which could initiate SCC within the material.

Tensile samples without holes of all the four alloys in T6 temper state were exposed to the DIN 11997-1(B) and the ASTM G85-11(A2) environments under three load magnitudes, which corresponded to 50%, 75% and 90% of yield strength. The results of the time-to-failure of the KK18-T6 and the KK17-T6 samples exposed to the DIN 11997-1(B) and ASTM G85-11(A2), as shown in Figure 4-25, showed significant reduction in time-to-failure at 75%$Rp_{0.2}$ as compared to 50%$Rp_{0.2}$ load. Whereas there was no significant change in time-to-failure with increasing the stress to 90%$Rp_{0.2}$. Comparison of the fracture surfaces of the specimens also showed no significant differences among the three surfaces. This indicated that the 75%$Rp_{0.2}$ load was an appropriate threshold load for the samples tested, in order to induce SCC susceptibility in the specimens which are SCC susceptible. Verification of the load influence was carried out by comparing the whole material pallet of all the 12 materials in 50% and 75% $Rp_{0.2}$ corresponding loads after exposure to the MBSC test. The results indicated a significant difference in the time-to-failures of the two load magnitudes. The difference was most prominent in the medium susceptible alloys such as the 7016-T6, KK17-T7 and the 7075-T6 alloys which showed failure with the 75%$Rp_{0.2}$ load but did not show failure with 50%$Rp_{0.2}$ load. Moreover, the 7075-T4, which is otherwise also a very susceptible alloy showed much delayed failure with the 50% load conditions. This could indicate that the load corresponding to 50%$Rp_{0.2}$ may not be a sufficient threshold load for the medium susceptible alloys for SCC initiation in the time frame of the test carried out.

The maximum true stresses observed in the simulated load conditions were seen to be around 220MPa in the towing assembly and around 300MPa in the A-pillar of the door lowering sub-assembly. These correspond to around 50% of yield strength of the high strength alloys such as 7075-T6, KK17-T6 and KK18-T6, which ranged from around 250MPa to 300MPa. However, a safety factor must also be considered while testing since the test is an accelerated version of the complete lifecycle of the test. Unforeseen high stresses could occur within the automobile for a short period of time, or dynamic or cyclic stresses could occur of lower magnitudes, but longer periods of time. Therefore, the load corresponding to the 75% or yield strength, which ranges

from 360MPa up to 440MPa for the high strength alloys such as 7075-T6, KK17-T6 and KK18-T6 was elected as the most appropriate load magnitude for testing.

The final step of the selection of the tensile specimen for the MBSC test was to determine the reproducibility and repeatability of the tensile specimen preparation setup by carrying out measurement system analysis. Measurement system analysis, gives insight into the variability of a system caused by the operator, the measuring equipment or the measuring object itself, indicating up to which extent the results obtained are accurate and reliable. [187] The process of preparation and stressing of the tensile specimen could have induced variations in the stresses which are carried onto the specimens. These variations could be due to operator influence, material influence or the setup influence and these stress variations could lead to variations in time-to-failure of the specimens. The gage R&R value is the indication of the reproducibility and repeatability of the system as described in section 4.3.5 and the objective for the tensile specimen setup was to have a %GRR value of below 20%. This was achieved in all the three levels of MSA testing carried out, with respect to operator influence, material influence and specimen influence. Thus, fulfilling the criteria of reproducibility and repeatability of the specimen setup and validating the results obtained from these specimens.

5.4.   Influence of Metallurgical Properties

Numerous research has conclusively shown that the metallurgical properties of the 7xxx alloys have a significant influence on the SCC susceptibility of the 7xxx alloys. The research question 1.4 aims to understand this influence by analysing the SCC behaviour of 7xxx alloys with varying alloy content and temper states. Therefore, it was imperative to choose a material pallet which included a broad spectrum of SCC susceptibility of the materials achieved by varying the alloy composition and the temper state. Alloys with a variation in the Zn, Mg, and Cu composition of the alloy were selected as shown in Figure 3-1., since these alloying elements show the highest influence on the SCC susceptibility.[10, 60] Apart from composition, each of the four chosen alloys were also tested in three temper states, since microstructural changes in within the material due to heat treatment also has a significant influence on the SCC

susceptibility of the 7xxx alloys. [60]. On carrying out the DoE, it was clearly seen that the material has the largest influence on the variation of SCC susceptibility as shown in Figure 4-6. Considering the mean days to failure of the specimens, they were divided into four susceptibility categories as shown in Table 4-1, thus showing a wide range of susceptibility as expected. The mechanisms and detailed influences of the metallurgical parameters on the SCC susceptibility of the material is discussed in this section.

5.4.1. Influence of Alloying Elements

One of the main alloying elements of the 7xxx series is zinc. In this thesis, four different alloys were chosen with varying levels of zinc, starting at 3.97 wt.% of the 7019 alloy , 5.88 wt.% for the 7075 alloy, 8.74 wt.% for the KK17 alloy and finally the highest Zn content of 9.08 wt.% in the KK18 alloy. On observing the average time-to-failure of these alloys, as shown in Table 4-1, in the T4 state, the 7019 alloy was the most resistant, followed by the 7075 alloy. The KK17 and KK18 in the T4 state show very high susceptibility with failure times of less than 4 days. Therefore, a direct correlation is observed between SCC susceptibility and the Zn content of the alloy in the T4 temper state. This result agrees to the research carried out by Gruhl [117] who observed the microstructure of varying alloy compositions through TEM and EDX analysis and found that with increasing Zn content at the grain boundaries, the time to fracture significantly reduced. However, rather than Zn alone, its relative content with respect to the Mg also is shown to have an influence on the SCC susceptibility. Zn and Mg form the characteristic $MgZn_2$ precipitate within the alloy, which gives the 7xxx alloys its characteristic mechanical properties. [41-43] However, these precipitates, segregate in the grain boundaries and due to their anodic nature compared to the matrix they could weaken the grain boundary strength by localised corrosion and thus making the alloy susceptible to fracture. [62, 116, 118]. On observing the microstructure of the four alloys in this thesis, it was observed that the higher alloy content alloys such as KK17 and KK18 showed higher number of precipitates on the grain boundaries, compared to the lower alloy content 7019 and 7075 alloys, as shown in Figure 4-5. The higher SCC susceptibility of these alloys could possibly be attributed to these grain boundary segregations and the surrounding precipitate free zones. However, detailed TEM

analysis of the alloys is to be carried out in order to determine the exact mechanism of corrosion and the composition of the grain boundary precipitates.

The total Zn and Mg content as well as the Zn/Mg ratio is also an important aspect with respect to SCC susceptibility, since it determines the amount of precipitate formation within the matrix. As shown in Figure 3.1, the four chosen alloys have varying Zn+Mg content and varying Zn:Mg ratio. In the T4 temper state the 7019 alloy with a Zn:Mg ratio of 1.87 is the least susceptible to SCC followed by the 7075 alloy with a ratio of 2.46. KK17 and KK18 with higher Zn:Mg ratios of 4.01 and 4.17 respectively are highly susceptible to SCC. This could be attributed to the expansion of the PFZ and higher concentrations of solute Zn in the matrix, resulting in higher SCC susceptibility as hypothesised by Chen et. al.[120]

Additional to the Zn and Mg alloy, a third alloying element, copper, has a significant influence on the mechanical and the corrosion properties of the material. Addition of Cu has shown to strengthen the mechanical properties of the 7xxx alloys, however leads to an increase in susceptibility of various other forms of corrosion.[54, 97, 127] To incorporate this effect in the thesis, the four chosen alloys also varied in copper content as shown in Figure 3-1. The four alloys were divided into two groups, first a low copper group, with 7019 (0.13 wt.%) and KK17 (0.30 wt.%) and secondly, a high copper group of 7075 (1.36 wt.%) and KK18 (1.31 wt.%). The division between low and high was decided due to Daimler internal standards of allowable Cu content in the aluminium alloys. The mechanical properties of the materials were clearly enhanced with the addition of the Cu, which can be seen in the 7075 alloy and the KK18 alloy. With respect to SCC susceptibility, it was observed that in the T6 temper state, the 7075 alloy showed a higher average days to failure as compared to the 7019-T6 alloy, which has a similar Zn+Mg content and the Zn/Mg ratio. Similarly, the KK18-T6 alloy had a higher value of mean days to failure compared to the KK17-T6 alloy, which could also be attributed to the Cu content, due to their similar Zn:Mg ratio and the Zn+Mg weight content. These results agree with the findings of Rometsch et al. who observed that aging of Cu-rich 7xxx alloys lead to increase of Cu in the grain boundary precipitates, which in turn reduces the anodic nature of the grain boundary precipitates with respect to the matrix and enhances SCC resistance. [11]

One of the main requirements which were listed in the customer requirement was that the developed test method should be applicable independent of the alloy content, as shown in Table 3-5. Thus, with variation of these main alloying elements, a large spectrum of SCC susceptibility of the materials was achieved and observed, fulfilling this customer requirement. However, alloy content alone was not enough to determine the SCC susceptibility level of the material. The temper treatment leading to microstructural variation within the same material also plays an important role in determining the SCC susceptibility and testing these four alloys in various temper state also broadened the spectrum of SCC susceptibility, while throwing light on its variation. The detailed influence of these parameters on the SCC susceptibility is discussed in the next section.

5.4.2. Influence of Microstructure and Heat Treatment

The mechanical and chemical properties of the 7xxx alloys can be modified by precipitation strengthening through different aging processes. With each stage of aging, the stage of precipitate sequence formed changes, changing the microstructure of the specimen and the composition and amount of segregation at the grain boundaries, thus influencing the SCC susceptibility of the alloys. The general representation of the effect of aging time on the strength and stress corrosion cracking is explained in section 2.5.3. [60] The alloys tested in this thesis showed a general trend in which the naturally aged material (T4) showed the highest susceptibility, followed by the peak-aged state, with the exception of the 7019 alloy. The over-aged materials were most resistance to SCC. These results correlated with the results of Albrecht et al. [79] which hypothesized, that the underaged alloy was most susceptible to SCC due to the soft coherent GP zones that can be sheared easily for strengthening by passing dislocations, which in turn softens the slip planes and concentration of the slip bands. This leads to easier hydrogen dislocation transportation and local hydrogen accumulation at grain boundaries, leading to higher SCC susceptibility. On reaching the peak-age a high density of finely dispersed semi-coherent $\acute{\eta}$ phases (Mg Zn$_2$) or Mg(ZnCuAl)$_2$ are formed, which tend to obstruct the movement of dislocations in the matrix. [10, 138] These semi-coherent phases are generally found along the grain boundary, forming a continuous anodic region in the grain boundary, thus weakening the grain boundaries through accelerated hydrogen transportation, making the material

more susceptible to SCC.[139] Finally, in the over-aged state, coherent η phases are precipitated. [47] These coherent phases, break the continuous cycle of anodic precipitates formed at the grain boundaries in the peak-aged state, thus enhancing the SCC resistance of the alloy. [79] This theory was also seen in the microstructure of the tested materials in this thesis as shown in Figure 4.4. The figure shows three temper states of 7075 ,namely, T4, T6 and T7 state. A high number of continuous precipitates were observed in the grain boundaries of the 7075-T6 microstructure surrounded by a continuous precipitate free zone, which could lead to the susceptibility of the material. On over-aging the material to T7, the number of precipitates on the grain-boundaries reduced and were discontinuous, which could attribute to its SCC resistance. The same trend was also observed in the KK17 and the KK18 alloy, which showed continuous precipitates and PFZ in the T6 temper state and discontinuous precipitates in the T7 state. The T4 microstructure showed a lower grain boundary precipitates compared to the T6, however the mechanism of SCC susceptibility in this state is hypothesized to be related to the soft semi-coherent GP zones which would require TEM analysis for the further analysis.

Although the trend was similar in all the 4 alloys, a difference in the SCC susceptibility with aging was observed with the Cu-rich and the Cu-poor alloys. A direct comparison of the Cu-rich KK18 alloy and the Cu-poor KK17 alloy, with similar Zn+Mg content and almost identical Zn/Mg ratio. It was observed that at T4 stage, both the alloys behaved similarly, with mean days to failure of under 4 days. On aging it further to peak-aged, the KK17 alloy showed higher SCC susceptibility compared to the KK18 alloy, with the average days to failure of KK17-T6 still remaining under 4 days, whereas that of T6 was improved to 7.8 days. Finally, in the over-aged condition, the KK17-T7 was still susceptible to SCC with a mean days to failure at about 22 days whereas the KK18-T7 showed no failure at all in any of the tested conditions, showing high SCC resistance. These results agree with the research conducted by Rometsch et al. [11] who suggested that on aging the Cu-rich alloys, there is an increase in the Cu content of the precipitates at the grain boundaries which are otherwise anodic in nature. Due to the increase in Cu content, which is cathodic to the matrix, these precipitates become less anodic and result in increasing the SCC resistance of the matrix. This phenomenon is however not possible in the Cu-poor alloys, thus showing lesser improvement in SCC resistance with aging. Similar theories on the influence of Cu

content on the SCC resistance were also proposed by other researchers such as Sarkar et al. [125], Speidel et. al. [71], Birnbaum et. al.[129] and Hardwick et al. [128], thus showing the importance of Cu content in the SCC resistance of the material.

Grain size is also shown to be a factor that has an influence on the SCC resistance of the 7xxx alloys, as demonstrated by Tsai et al.[146]. They showed that finer grain size results in higher SCC resistance. Further studies carried out by other researchers on the influence of grain refining minor alloying elements such as Cr, Zr, Sc, Yb and Er also showed that finer grain size resulted in better SCC resistance. [130-136] On comparing the microstructure of the 7019-T6 and the 7075-T6 alloy to the KK17-T6 and KK18-T6 alloy, it was seen that the latter showed inhomogeneous grain structure, with "banded" recrystallized and non-recrystallized grains. Moreover, it was observed in the KK17-T6 and the KK18-T6 alloy, that the grains were highly elongated in the grain direction. This unevenness in the grain size of the KK17 and KK18 alloy could be attributed to its processing methods, since these alloys are novel and were not optimally processed with respect to heat treatment and rolling to have a homogeneous grain structure. This unevenness could also result in increased localised stresses within the grain boundaries, enhancing its susceptibility towards stress corrosion cracking. Thus, this phenomenon could also be an attributing factor to the increased SCC susceptibility of the KK17 and KK18 alloy compared to the 7019 and the 7075 alloy.

In summary, the variation in alloy content, microstructure and the temper state resulted in a varied range of SCC susceptibility which provided a good tool for development of the test method. The MBSC test was used to test all of the above-mentioned materials and was successful in distinguishing between the more susceptible and less susceptible alloys. This fulfilled the condition which was determined in the customer requirement stating that the test method should be valid for all materials independent of the alloy content.

5.5. Critical Review and Practical Applications of the MBSC Test

Stress corrosion cracking is a complex phenomenon with the synergistic effect of three parameters acting simultaneously. It is a material, environment and load specific

phenomenon making it a challenging task to reproduce this phenomenon in a laboratory environment. Most studies on SCC are done iteratively and focuses on understanding the influence of individual parameters under carefully controlled laboratory conditions. This of course has the advantage of understanding SCC behaviour with regard to each parameter, however, an automotive lifecycle is complex and has several environmental and mechanical influences acting simultaneously on the exposed materials. This difference may lead to misinterpretation in behaviour and wrong selection of the 7xxx alloys in the automotive application. This gap has been successfully addressed in this thesis by studying the behaviour of the 7xxx alloys in a holistic perspective rather than individual parameters. For e.g., as shown in the studies of Yu et al. it is seen that the dry:wet ratio has a significant influence on the SCC susceptibility of the 7xxx alloys. However, in this study, the variation in dry:wet ratio was accompanied by other environmental parameters such as salt concentration and temperature variation. This resulted in the dry:wet ratio not being a significant parameter influencing SCC as compared to the other crucial environmental parameters. Thus, a successful accelerated corrosion test identifies the SCC behaviour of the exposed alloy with the whole complex automotive lifecycle in perspective, rather than individual parameters. Through the strategic process of design for six sigma, these conditions were fulfilled and incorporated into successfully designing the MBSC Test. Similarly, this study highlighted the role of additives such as NH_4NO_3 in the salt solution of the accelerated corrosion test. Usual corrosion tests, such as the ASTM G47-98, among many others, use purely NaCl solutions in accelerated corrosion tests. Lastly, observing the various stress conditions in combination with the environmental parameters resulted in a holistic understanding of the SCC susceptibility of the 7xxx alloys and also highlighted its potential risks during an actual application in an automobile.

Observing the results obtained from the final optimised MBSC test it is seen that the test successfully indicates SCC susceptibility level of the materials and is able to identify SCC susceptible alloys and differentiate them from the non-susceptible alloys. Extremely critical materials such as the KK17-T4, KK17-T6 and the KK18-T4 failed within a very short period, and this was also replicated in the early failure of these alloys in the outdoor exposure test. The extremely resistant alloys such as the 7075-T7 and the KK18-T7 alloys did not show failure in any of the conditions tested in the

alloy, thus distinguishing them as resistant alloys. However, the extreme cases are easily detectable in other test environments as well such as the ASTM G44-99[163] and the DIN 11997-1(B)[173] as studied in this thesis. The challenge for a successful test was to detect the SCC susceptibility of the medium and low susceptible alloys. An example of this is the behaviour of the 7075-T6 alloy, which is a popular alloy used in the aerospace industry but is also notoriously known for its SCC susceptibility.[96, 188] On exposing this alloy to the ASTM G47-98 [167] , there was no failure observed. However, a significant reduction in its ductility was observed on testing the residual strength of the alloy. On the contrary, the alloy failed on exposure to the MBSC test, indicating the success of the MBSC test to detect SCC susceptibility. The SEM fractographic analysis of the alloys also showed the embrittlement on its surface and intergranular cracking, confirming the presence of SCC. This was also the case with the 7019-T6 alloy and the KK17-T7 alloy which were also confirmed to be SCC susceptible. Another success of the test was also its ability to qualitatively rank the level of susceptibility of alloys. Based on their results of mean days to failure, the materials were successfully classified into 4 different categories starting from highly susceptible to not susceptible. This ability for qualitative ranking was not observed in other tests such as the incremental step load test or the slow strain rate test. The MBSC test was effective in detecting SCC susceptibility of 7xxx alloys of varying alloying content, thus indicating its effectiveness independent of the alloy content of the material. Therefore, in the future, this test can be used to test a wide range of 7xxx alloys with varied alloy content and temper states.

The reproducibility and repeatability of the test was also an important factor which was encompassed within the designing of this test. With respect to the chosen test specimen, which was the tensile specimen, measurement system analysis was carried out on the stressing of the specimen, to confirm the reproducibility and repeatability of the test. The Gage R&R % of the tested system lay under the target value of 20%, thus fulfilling the criteria of reproducibility and repeatability which was determined in the requirements phase. With respect to the test environment, the MBSC test, the tests were carried out in carefully calibrated test chambers and the test results also showed considerable reproducibility, indicating a considerable confidence in the reproducibility of the test. However, a detailed statistical analysis of the test environment should be

carried out as a future work to statistically determine the Gage R&R % of the test environment and the respective test setup.

Finally, one of the principal advantages of the MBSC test is its inclusion of the possible 'real-world' environments. There are several standardized and non-standardized tests that are already available to test SCC. [15] For e.g., the constant load test under the alternating immersion environment in a neutral salt solution , according to the ASTM G47-98 [167] , is a test method which is currently commonly used in the aerospace industry and partly in the automotive industry. However, its correlation with the real-world environment is uncertain, since the automobile is exposed to varied range of temperatures, humidity, salt solutions etc. in its lifetime, which is not specifically considered in these test environments. Through DFSS every possible critical condition that the automobile would face in its lifetime was analysed and incorporated into the MBSC test, giving it an edge over the other tests which do not have the same validation. The mechanical and environmental parameters were chosen after carefully analysing each of these effects on the SCC susceptibility, with a focus on the automotive lifecycle. Moreover, the laboratory test results were validated by comparison of them to the outdoor exposure results, which showed a good correlation to the laboratory test and validated the test results, thus, giving an advantage to the MBSC test compared to the other test method.

Finally, the ease of preparation and conducting this test is also favours the standardisation of it in the automotive industry. The newly designed constant-load specimen holder, which is used in this thesis is compact, mobile, and economical which are important factors to be considered. These factors make it possible to carry out multiple tests simultaneously without any burden on economic or man-power aspect. Optimisation of the stressing setup could be carried out in future work, to automize the stressing of the specimen and reduce further man-power in doing so. Thus, the MBSC test fulfils all the conditions for a successful test designed to identify the SCC susceptibility of the 7xxx alloys, specifically for the automotive purpose. After statistical validation through reproducibility tests and round-robin tests with different laboratories, this test has the potential to become the standard stress corrosion cracking test for testing the 7xxx alloys for the automotive industry.

Chapter 6 CONCLUSION AND FUTURE OUTLOOK

In this thesis, the complex automotive lifecycle was scientifically analysed by studying the individual and synergistic influence of the key metallurgical, environmental, and mechanical factors in the lifecycle on the SCC susceptibility of the aluminium 7xxx. These key findings were then applied to design a novel accelerated stress corrosion test, called the MBSC test, which was specially designed to classify the susceptibility of the 7xxx alloys for the automotive applications. The designing of the test method was carried out using a strategic design methodology called Design for Six Sigma, in which the design process was carried out in 4 stages: Definition, Conceptualization, Optimization and Validation. The advantages, disadvantages, and the future potential of the DFSS methodology for the development of corrosion tests, especially SCC test was analysed in the thesis. Through the design process, the critical environmental conditions, which an automobile is exposed to in its lifecycle was designed into a novel accelerated corrosion test cycle called the MBSC Corrosion Test Cycle. Methodical analysis of this corrosion test cycle was carried out by means of DoE to understand the influence of key environmental parameters on the SCC behavior of the 7xxx alloys. Parallelly, the influence of mechanical parameters critical to SCC of 7xxx alloys were analysed by testing three mechanical specimens which represented the various mechanical parameters. An optimal mechanical specimen was chosen for the MBSC test based on the analysis. Finally, the results of the MBSC test were compared to outdoor exposure tests for validation of the test method. To carry out the above-mentioned analysis, a material pallet of four different 7xxx alloys with varying contents of Zn, Mg and Cu and each with different temper states of T4, T6 and T7 tempers were chosen. Thus, providing a material pallet with a broad range of SCC susceptibility.

From the results obtained in this thesis and the analysis and discussions of the results obtained, the following conclusions can be derived for the thesis:

The DFSS process provided a structured and methodical approach to design the complex MBSC Test.

The DFSS methodology was used for the first time to develop a stress corrosion cracking test. This methodology provided a structure to break down the complex

process of the SCC test development categorically into various cross-functional requirements. With a novel customer-centric approach, unlike traditional product design methodology, DFSS provided a systematic framework to achieve the objectives and requirements defined in the initial stage of the DFSS. It provided the right tools such as morphological analysis and QFD analysis for prioritization of requirements continually through the designing and allowed for analysis of multifaceted factors parallelly. Finally, the constant focus on quantitative and qualitative analysis of the influencing parameters, resulted in reproducible and reliable test output. Thus, the DFSS process in its modified form as used in this thesis has a potential to be used as a future standard framework for developing of stress corrosion tests.

The key environmental parameters in an automotive lifecycle which influence SCC susceptibility were successfully represented in the novel specially designed accelerated corrosion test cycle called Mercedes Benz Stress Corrosion (MBSC) Test Cycle. The test accurately identified the SCC susceptibility of the tested alloys, indicating the potential of its usage in the automobile design.

The automotive lifecycle was critically evaluated to determine the key environmental conditions that would be affect SCC susceptibility of the 7xxx alloys. These conditions were then incorporated into a novel designed corrosion test cycle, the MBSC corrosion test cycle. The test was designed in three blocks: (i) The storage and transportation block, (ii) the customer lifecycle block, and (iii) the extreme conditions block, with varying environmental conditions in each block that would represent all critical conditions that could occur in the automotive lifecycle in an accelerated form.

The designing of the test cycle was followed by scientific analysis of the various influencing environmental parameters through DoE analysis of the designed test cycle. Studying the influence of anions and cations on the SCC susceptibility revealed that the addition of Na_2SO_4 or NH_4NO_3 increased the general susceptibility of some of the alloys to SCC. This was attributed to higher susceptibility to pitting and intergranular corrosion, which would then act as initiation points for SCC. The salt-solution with concentration of 3.5 wt.% NaCl with an addition of 100mg/l of NH_4NO_3 showed the best differentiation of SCC susceptibility of the materials tested, since it influenced the medium susceptible alloys to SCC failures and showed the best reproducibility of

results. Due to the conclusive evidence of increased SCC risk with the addition of these ions and its clear presence in the field environment of the automobile, the NH_4NO_3 additive within the standard 3.5 wt.% NaCl solution was chosen as the composition of the salt spray solution in the MBSC test.

DoE analysis of the environmental parameters: test temperature, temperature difference between hot and cold phase in the extreme block (ΔT) and the dry: wet ratio was carried out to determine their influence on the SCC susceptibility.

(i) It was observed that as the test temperature increased from 40°C to 60°C, there was an acceleration of SCC failure observed in most tested materials, which is attributed to the increased crack growth rate and rate of diffusion of corrosion products. An inversed effect was observed on the 7075-T4 and 7075-T6, which is hypothesized to be due to metallurgical changes in the material after exposure to higher temperatures for a long duration. At 40°C test temperature, the best differentiability between susceptible and non-susceptible alloys was established, especially indicating the failure of the medium and low susceptible alloys such as 7075-T4, 7075-T6, 7019-T6 and KK17-T7, thus being chosen as the temperature for the second block of the MBSC Test.

(ii) The temperature difference (ΔT) in the extreme block (Block C) of the MBSC test was a 100°C, varying from 80°C dropping to -20°C during the cycle. Higher temperature variation caused higher localized and residual stresses on the tested materials, thus promoting and accelerating SCC in the susceptible alloys. This block was also essential to differentiate between non-susceptible and susceptible materials, especially to identify the low susceptible alloys such as 7019-T6 and 7075-T6 alloys. This was also validated through SEM fracture surface analysis which showed SCC failure in these alloys.

(iii) Contrary to literature, the dry:wet ratio showed very little influence on the SCC susceptibility of the materials tested. This contradiction revalidates, the differences in data observed in controlled laboratory environments compared to universal climatic tests specially designed to represent the automotive lifecycle. The dry:wet ratio 1:1 was observed to be significantly critical for the low susceptible alloy 7019-T6 and was thus chosen for the MBSC test.

Therefore, the MBSC test with its optimal test parameters (test temperature=40°C, ΔT=100°C and dry:wet ratio =1:1) fulfilled the objectives and requirements which were determined in the definition phase of the DFSS. The DoE study also showed that the approach of studying the influencing factors synergistically leads to different and sometimes contradictory results on the SCC susceptibility of alloys compared to controlled laboratory tests. Thus, it is important to consider this for future mechanistic studies of the 7xxx alloys.

The important mechanical factors influencing an automobile were analysed through studying various mechanical specimens. The tensile specimen in a constant load mode stressed to 75% of its yield strength showed the highest accuracy to determine SCC susceptibility of the tested alloys.

Through the use of DFSS tools such as morphological analysis, three mechanical specimens were chosen for testing of SCC susceptibility, namely, tensile specimen, tensile specimen with hole and the KS-8 specimen. These three specimens represented the most important mechanical parameters influencing the SCC susceptibility, which are the load propagation mode, load magnitudes and nature of load.

The KS-8 specimen represented the constant total strain mode, which did not induce SCC even in the critically susceptible alloys due to the stress relaxations that occur on crack propagation. On the contrary, the tensile specimen represented constant load mode, which increases local stresses on crack propagation. The tensile specimen with hole failed to distinguish between SCC failure and residual failure due to the extreme high stresses induced in the hole region which would lead to increased crack propagation rate of residual cracks, rather than SCC cracks. The tensile specimen without hole in constant load mode was the ideal specimen with SCC crack propagation rate higher than residual cracks for the susceptible alloys, which was confirmed by SEM fracture surface analysis and optical microscopy. Evaluation of various load propagation modes on the tensile specimen showed that the slow strain rate test and incremental step load test could not identify the SCC critical alloys through SCC failure in the parameters tested. Thus, the tensile specimen without hole in the constant load mode was considered the optimal one to detect SCC susceptibility.

The study of load magnitude influence on the SCC susceptibility of the alloys revealed that there is a critical threshold of 75%$Rp_{0.2}$ below which certain SCC susceptible alloys do not fail in the SCC test, thus showing insufficient stress magnitude. Beyond this threshold it was observed that the average time-to-failure and the fracture surface does not change for the critical alloys. Moreover, from the stress studies conducted on the automobile, it was seen that the 75%$Rp_{0.2}$ is an optimal representation of the stresses that can occur in the field scenario. Thus, the tensile specimen loaded to 75%$Rp_{0.2}$ in constant load mode was chosen as the optimal mechanical load magnitude in the MBSC test to identify the SCC susceptible alloys.

The MBSC test showed a high correlation to the outdoor exposure test results and succeeded in identifying the SCC susceptible alloys better than the standard ASTM G47-98 and the outdoor exposure test.

To validate the results of the MBSC test, they were compared to the outdoor exposure results as well as the standard ASTM G47-98 results. Outdoor exposure tests were carried out by exposing stressed tensile specimens and U-bend specimens to four sites with varying climatic conditions. A high correlation was observed between the results of the outdoor exposure tests to the MBSC test.

It was seen that the MBSC test was more successful in detecting SCC susceptibility compared to the standard SCC test ASTM G47-98 and the outdoor exposure test, especially for the low susceptible alloys such as 7019-T6, 7075-T6 and KK17-T7. Metallographic examinations and SEM fractographic analysis also confirmed SCC failures in these alloys, thus showing that the higher accuracy of the MBSC test. This can be attributed to the conservative approach of designing of the MBSC test cycle, which was designed by firstly identifying the most critical parameters influencing SCC susceptibility of alloys in the automotive lifecycle and then strategically represented in the MBSC test in an accelerated form, ensuring that all critical parameters were included. Therefore, the MBSC test shows the best potential to successfully identify the use of an SCC alloy in the automobile application.

The alloy content and temper states had a significant influence on the SCC susceptibility of the 7xxx alloys.

The four chosen alloys with different Zn, Mg and Cu content and each in three different temper states T4, T6 and T7 provided a wide range of SCC behavior from SCC resistant to highly susceptible. As expected, it was observed that the alloys with high Zn and Mg content :7075, KK17 and KK18 were more susceptible to SCC compared to the low alloyed 7019 alloy. This has been attributed by many researchers to the higher segregation of precipitates in the grain boundaries, leading to localized anodic dissolution. [116—118] The T4 tempered alloys showed the highest SCC susceptibility in the high alloy content alloys, followed by T6. T7 tempered alloy showed drastic improvement in SCC resistance, especially the 7075 and KK18 alloys which had higher Cu content. These results are also conformed to the several mechanistic studies conducted on the microstructure of the 7xxx alloys, which attribute the improvement in SCC resistance to the migration of Cu towards the grain boundary precipitates and decreasing their anodic nature. [11] Thus, the material pallet studied in this thesis successfully represented a wide range of SCC susceptibility with possible varying mechanisms of propagation and failure.

Future Outlook

This thesis aimed to SCC behaviour of the 7xxx alloys from a top-down approach, with the focus on critical conditions occurring in actual automotive lifecycles. This analysis was then used to develop a test method to test the SCC susceptibility of the 7xxx alloys with respect to the automotive conditions. The development of the MBSC test was the first and an essential step towards determining the potential of the use of 7xxx alloys in the automotive application and understand the risks and mechanisms involved. However, there are several further considerations to be addressed before the full-scale implementation of the MBSC test and the use of 7xxx alloys in the automobile.

Through the four stages of DFSS process, the MBSC test was designed, and the several environmental and mechanical parameters were analysed qualitatively and quantitatively. Through the process of qualitative validation with respect to customer requirements and comparison to outdoor exposure test, it was shown that the MBSC test is capable of successfully identifying the SCC susceptibility of the 7xxx alloys, including the low susceptible alloys. However, for full-scale implementation of the MBSC test, a detailed statistical validation of the testing process needs to be carried

out in order to optimize and eliminate any variabilities which could occur during the testing itself. Through extensive process capability analysis of the test equipment and round robin tests, the MBSC test will be statistically robust to be used on a full industrial scale.

In the lifetime of an automobile, it could encounter an extensive list of varying environmental and mechanical conditions. This thesis covered an extensive list of important environmental and mechanical parameters, however, also excluded several parameters from the study to narrow the scope of the project. For example, the lifetime of the automotive lifecycle which was represented in the MBSC test was from the post-production stage, keeping all production processes specifically out-of-scope. Within the production processes itself, there are several conditions such as environmental conditions during surface treatment, stresses induced due to production processes such as welding, forming and heat treatments which could already have a significant influence on the SCC susceptibility of the alloy in the automobile. To gather further knowledge on the behavior of 7xxx alloys for the automotive application, it is essential to study the influence of these production processes on the SCC behaviour of these alloys.

Similarly, through the vast range of materials tested within this thesis, it was seen that the material and its metallurgical properties have a significant influence on the SCC susceptibility of the material. In order to assess and potentially implement the use of 7xxx alloys in the automobile, it is essential to dive deeper into the mechanistic aspects that influence the 7xxx alloys. An in-depth understanding of the SCC mechanism in the 7xxx alloys is essential to predict the behavior of the 7xxx alloy in the lifecycle of the automobile. The key to assess the application of the 7xxx alloys in the automobile lies in the understanding of several factors. Along with the successful statistical validation of the MBSC test, a deeper understanding of the stress corrosion cracking mechanisms and the influences of production parameters as well as the automotive lifecycle on the SCC susceptibility could finally lead towards successful implementation of using the high strength 7xxx alloys in the automobile.

REFERENCES

1.   Oktav, A., *New Trends and Recent Developments in Automotive Engineering.* no. March, 2018.

2.   Cole, G.S. and A.M. Sherman, *Light weight materials for automotive applications.* Materials Characterization, 1995. 35(1): p. 3-9.

3.   Taub, A.I. and A.A. Luo, *Advanced lightweight materials and manufacturing processes for automotive applications.* MRS Bulletin, 2015. 40(12): p. 1045-1054.

4.   Chebolu, A., *Automotive Lightweighting: A Brief Outline*, in *Advanced Combustion Techniques and Engine Technologies for the Automotive Sector*. 2020, Springer. p. 247-256.

5.   Witik, R.A., et al., *Assessing the lifecycle costs and environmental performance of lightweight materials in automobile applications.* Composites Part A: Applied Science and Manufacturing, 2011. 42(11): p. 1694-1709.

6.   Austin, D., et al., *Changing Drivers. The Impact of Climate Change on Competitiveness and Value Creation in the Automotive Industry.* 2003.

7.   Miller, W.S., et al., *Recent development in aluminium alloys for the automotive industry.* Materials Science and Engineering: A, 2000. 280(1): p. 37-49.

8.   Tisza, M. and I. Czinege, *Comparative study of the application of steels and aluminium in lightweight production of automotive parts.* International Journal of Lightweight Materials and Manufacture, 2018. 1(4): p. 229-238.

9.   Davis, J.R., *Corrosion of Aluminium and Aluminium Alloys*. 1999: A S M International.

10.   Rao, A.C.U., et al., *Stress corrosion cracking behaviour of 7xxx aluminium alloys: A literature review.* Transactions of Nonferrous Metals Society of China, 2016. 26(6): p. 1447-1471.

11.   Rometsch, P.A., Y. Zhang, and S. Knight, *Heat treatment of 7xxx series aluminium alloys—Some recent developments.* Transactions of Nonferrous Metals Society of China, 2014. 24(7): p. 2003-2017.

12.   Dietzel, W., et al., *Stress Corrosion Cracking*, in *Reference Module in Materials Science and Materials Engineering*. 2017, Elsevier.

159

13. Magaji, N., et al., *Comparison of test methods used to analyse stress corrosion cracking of differently tempered 7xxx alloys.* Materials and Corrosion, 2019. 70(7): p. 1192-1204.

14. Parkins, R.N., et al., *Stress Corrosion Test Methods.* British Corrosion Journal, 1972. 7(4): p. 154-167.

15. Dietzel, W., P. Bala Srinivasan, and A. Atrens, *3 - Testing and evaluation methods for stress corrosion cracking (SCC) in metals*, in *Stress Corrosion Cracking*. 2011, Woodhead Publishing. p. 133-166.

16. Jenab, K., C. Wu, and S. Moslehpour, *Design for six sigma: A review.* Management Science Letters, 2018. 8: p. 1-18.

17. Shahin, A., *Design for Six Sigma (DFSS): Lessons learned from world-class companies.* International Journal of Six Sigma and Competitive Advantage, 2008. 4.

18. Kottek, M., et al., *World map of the Köppen-Geiger climate classification updated.* 2006.

19. Vet, R., et al., *A global assessment of precipitation chemistry and deposition of sulfur, nitrogen, sea salt, base cations, organic acids, acidity and pH, and phosphorus.* Atmospheric Environment, 2014. 93: p. 3-100.

20. Furterer, S. and A.K. Elshennawy, *Implementation of TQM and lean Six Sigma tools in local government: a framework and a case study.* Total Quality Management & Business Excellence, 2005. 16(10): p. 1179-1191.

21. Gowen Iii, C.R., G.N. Stock, and K.L. McFadden, *Simultaneous implementation of Six Sigma and knowledge management in hospitals.* International Journal of Production Research, 2008. 46(23): p. 6781-6795.

22. Guarraia, P., et al., *Six Sigma – at your service.* Business Strategy Review, 2009. 20(2): p. 56-61.

23. Zhang, W. and X. Xu, *Six Sigma and information systems project management: A revised theoretical model.* Project Management Journal, 2008. 39(3): p. 59-74.

24. Zu, X., L.D. Fredendall, and T.J. Douglas, *The evolving theory of quality management: The role of Six Sigma.* Journal of Operations Management, 2008. 26(5): p. 630-650.

25. Wang, H.-M.S., S.-P. Wang, and W. Lee, *A Case Study for Reducing Client Waiting Time in a Health Evaluation Center Using Design for Six Sigma.* Engineering Management Journal, 2014. 26(2): p. 62-73.

References

26. Koning, H. and J. Mast, *A rational reconstruction of Six Sigma's Breakthrough Cookbook.* International Journal of Quality & Reliability Management, 2006. 23: p. 766-787.

27. Antony, J., M. Kumar, and M. Tiwari, *An application of Six Sigma methodology to reduce the engine-overheating problem in an automotive company.* Proceedings of The Institution of Mechanical Engineers Part B-journal of Engineering Manufacture - PROC INST MECH ENG B-J ENG MA, 2005. 219: p. 633-646.

28. Canato, A., D. Ravasi, and N. Phillips, *Coerced Practice Implementation in Cases of Low Cultural Fit: Cultural Change and Practice Adaptation During the Implementation of Six Sigma at 3M.* The Academy of Management Journal, 2013.

29. Gremyr, I. and J.B. Fouquet, *Design for Six Sigma and lean product development.* International Journal of Lean Six Sigma, 2012. 3(1): p. 45-58.

30. Yang, K. and X. Cai, *The integration of DFSS, lean product development and lean knowledge management.* International Journal of Six Sigma and Competitive Advantage, 2009. 5.

31. Chung, Y.-C. and Y.-W. Hsu, *Research on the correlation between Design for Six Sigma implementation activity levels, new product development strategies and new product development performance in Taiwan's high-tech manufacturers.* Total Quality Management, 2010. 21: p. 603-616.

32. De Feo, J. and Z. Bar-El, *Creating strategic change more efficiently with a new Design for Six Sigma process.* Journal of Change Management, 2002. 3(1): p. 60-80.

33. Francisco, M., O. Canciglieri Junior, and Â. Sant'Anna, *Design for six sigma integrated product development reference model through systematic review.* International Journal of Lean Six Sigma, 2020. ahead-of-print.

34. Hasenkamp, T., *Engineering Design for Six Sigma—a systematic approach.* Quality and Reliability Engineering International, 2010. 26(4): p. 317-324.

35. Moatari Kazerouni, A., *Design and analysis of gauge R&R studies: Making decisions based on ANOVA method.* 2009. 52.

36. Mathews, P.G., *Design of Experiments with MINITAB.* 2005.

37. Heinz, A., et al., *Recent development in aluminium alloys for aerospace applications.* Materials Science and Engineering: A, 2000. 280(1): p. 102-107.

161

38. Rambabu, P., et al., *Aluminium alloys for aerospace applications.* Aerospace materials and material technologies, 2017: p. 29-52.

39. *DIN EN 573-3:2013-12 :Aluminium and aluminium alloys - Chemical composition and form of wrought products - Part 3: Chemical composition and form of products*.

40. 1706:2020-06, D.E., *Aluminium and aluminium alloys - Castings - Chemical composition and mechanical properties.* 2020.

41. Ostermann, F., *Legierungsaufbau, Wärmebehandlung, Normen. In: Anwendungstechnologie Aluminium. VDI-Buch. Springer Vieweg, Berlin, Heidelberg.* 2014.

42. Gjonnes, J. and C.J. Simensen, *An electron microscope investigation of the microstructure in an aluminium-zinc-magnesium alloy.* Acta Metallurgica, 1970. 18(8): p. 881-890.

43. Mondolfo, L.F., *Structure of the aluminium: magnesium: zinc alloys.* Metallurgical Reviews, 1971. 16(1): p. 95-124.

44. Song, M. and K. Chen, *Effects of the enhanced heat treatment on the mechanical properties and stress corrosion behavior of an Al–Zn–Mg alloy.* Journal of materials science, 2008. 43(15): p. 5265-5273.

45. 515:2017-05, D.E., *Aluminium and aluminium alloys - Wrought products - Temper designations.*

46. Song, R.G., et al., *Stress corrosion cracking and hydrogen embrittlement of an Al–Zn–Mg–Cu alloy.* Acta Materialia, 2004. 52(16): p. 4727-4743.

47. Asano, K. and K.-I. Hirano, *Precipitation Process in an Al–Zn–Mg Alloy.* Transactions of the Japan Institute of Metals, 1968. 9(1): p. 24-34.

48. 8044:2020-08, D.E.I., *Corrosion of metals and alloys - Vocabulary (ISO 8044:2020).* 2020.

49. Kolics, A., et al., *Effect of pH on thickness and ion content of the oxide film on aluminium in NaCl media.* Journal of the Electrochemical Society, 2001. 148(7): p. B251.

50. Yu, S., et al., *Chloride ingress into aluminium prior to pitting corrosion an investigation by XANES and XPS.* Journal of the Electrochemical Society, 2000. 147(8): p. 2952.

References

51. Schnatterer, C. and D. Zander, *Influence of heat treatments on the stress corrosion cracking susceptibility of 7075 aluminium wires in NaCl solutions.* Materials and Corrosion, 2016. 67(11): p. 1164-1172.

52. Szklarska-Smialowska, Z., *Pitting corrosion of aluminium.* Corrosion science, 1999. 41(9): p. 1743-1767.

53. Frankel, G., *Pitting corrosion of metals: a review of the critical factors.* Journal of the Electrochemical society, 1998. 145(6): p. 2186.

54. Ostermann, F., *Korrosion. In: Anwendungstechnologie Aluminium VDI-Buch. Springer Vieweg, Berlin, Heidelberg.* 2014.

55. Fan, L., et al., *Revealing foundations of the intergranular corrosion of 5XXX and 6XXX Al alloys.* Materials Letters, 2020. 271: p. 127767.

56. Davenport, A.J., et al. *Intergranular corrosion and stress corrosion cracking of sensitised AA5182.* in *Materials science forum.* 2006. Trans Tech Publ.

57. Burleigh, T.D., *The Postulated Mechanisms for Stress Corrosion Cracking of Aluminium Alloys: A Review of the Literature 1980-1989.* CORROSION, 1991. 47(2): p. 89-98.

58. Khoshnaw, F.M. and R.H. Gardi, *Effect of aging time and temperature on intergranular corrosion of aluminium alloys.* Anti-Corrosion Methods and Materials, 2006.

59. Popov, B.N., *Stress Corrosion Cracking.* 2015: p. 365-450.

60. Bobby Kannan, M., P. Bala Srinivasan, and V.S. Raja, *Stress corrosion cracking (SCC) of aluminium alloys.* 2011: p. 307-340.

61. Aly, F.O. and M.M. Neto, *Stress Corrosion Cracking.* 2014.

62. Speidel, M.O., *Stress corrosion cracking of aluminium alloys.* Metallurgical Transactions A, 1975. 6(4): p. 631.

63. Wendler-Kalsch, E. and H. Gräfen, *Korrosionsarten mit mechanischer Beanspruchung*, in *Korrosionsschadenkunde*, E. Wendler-Kalsch and H. Gräfen, Editors. 1998, Springer Berlin Heidelberg: Berlin, Heidelberg. p. 257-475.

64. Burnett, T.L., et al., *The role of crack branching in stress corrosion cracking of aluminium alloys.* Corrosion Reviews, 2015. 33(6): p. 443-454.

163

65. Rout, P.K. and K. Ghosh, *Effect of microstructural features on stress corrosion cracking behaviour of 7017 and 7150 aluminium alloy.* Materials Today: Proceedings, 2018. 5(1): p. 2391-2400.

66. Lynch, S.P., *Mechanistic and fractographic aspects of stress-corrosion cracking (SCC).* 2011: p. 3-89.

67. Milella, P.P., *Fracture Mechanics Approach to Stress Corrosion.* 2013: p. 731-765.

68. Mears, R., R. Brown, and E. Dix. *A generalized theory of stress corrosion of alloys.* in *Symposium on Stress-Corrosion Cracking of Metals.* 1945. ASTM International.

69. Choi, Y., H.-C. Kim, and S.-I. Pyun, *Stress corrosion cracking of Al-Zn-Mg alloy AA-7039 by slow strain-rate method (Abstract).* Journal of Materials Science, 1984. 19(5): p. 1517-1521.

70. Uesaki, K., T. Kawakami, and H. Takechi, *Postweld Time Dependence of Aluminium--Zinc--Magnesium Alloy Welds on Stress Corrosion Cracking.* Kenkyu Kiyo-Anan Kogyo Koto Senmon Gakko, 1985. 21: p. 11-19.

71. Speidel, M.O. and M.V. Hyatt, *Stress-Corrosion Cracking of High-Strength Aluminium Alloys,* in *Advances in Corrosion Science and Technology,* M.G. Fontana and R.W. Staehle, Editors. 1972, Springer US: Boston, MA. p. 115-335.

72. Nelson, H.G., *Hydrogen embrittlement.* Treatise on materials science and technology, 1983. 25: p. 275-359.

73. Lynch, S.P., *Environmentally assisted cracking: Overview of evidence for an adsorption-induced localised-slip process.* Acta Metallurgica, 1988. 36(10): p. 2639-2661.

74. Polyanskii, V., *Role of hydrogen embrittlement in the corrosion cracking of aluminium alloys.* Materials Science, 1986. 21(4): p. 301-309.

75. Scamans, G.M., *Discontinuous propagation of stress corrosion cracks in Al-Zn-Mg alloys.* Scripta Metallurgica, 1979. 13(4): p. 245-250.

76. Martin, P., J.I. Dickson, and J.P. Baïlon, *Stress corrosion cracking in aluminium alloy 7075-T651 by discrete crack jumps as indicated by fractography and acoustic emission.* Materials Science and Engineering, 1985. 69(1): p. L9-L13.

77. Braun, R., *Environmentally Assisted Cracking of Alloy 7050-T7451 Exposed to Aqueous Chloride Solutions.* Metallurgical and Materials Transactions A, 2016. 47(3): p. 1367-1377.

References

78.   Holroyd, N.H. and G. Scamans, *Crack propagation during sustained-load cracking of Al-Zn-Mg-Cu aluminium alloys exposed to moist air or distilled water.* Metallurgical and Materials Transactions A, 2011. 42(13): p. 3979-3998.

79.   Albrecht, J., A.W. Thompson, and I.M. Bernstein, *The role of microstructure in hydrogen-assisted fracture of 7075 aluminium.* Metallurgical Transactions A, 1979. 10(11): p. 1759-1766.

80.   Hardie, D., N.J.H. Holroyd, and R.N. Parkins, *Reduced ductility of high-strength aluminium alloy during or after exposure to water.* Metal Science, 1979. 13(11): p. 603-610.

81.   Smiyan, O., *Diffusion of hydrogen into the crack wall metal in corrosion cracking of Al-Zn-Mg-Cu alloy.* Materials Science, 1987. 22(5): p. 457-461.

82.   Papp, K. and E. Kovács-Csetényi, *Diffusion of hydrogen in high purity aluminium.* Scripta Metallurgica, 1981. 15(2): p. 161-164.

83.   Outlaw, R.A., D.T. Peterson, and F.A. Schmidt, *Diffusion of hydrogen in pure large grain aluminium(Abstract).* Scripta Metallurgica, 1982. 16(3): p. 287-292.

84.   Oriani, R.A. and P.H. Josephic, *Equilibrium aspects of hydrogen-induced cracking of steels(Abstract).* Acta Metallurgica, 1974. 22(9): p. 1065-1074.

85.   Christodoulou, L. and H.M. Flower, *Hydrogen embrittlement and trapping in Al6%-Zn-3%-Mg(Abstract).* Acta Metallurgica, 1980. 28(4): p. 481-487.

86.   Oger, L., et al., *Influence of dislocations on hydrogen diffusion and trapping in an Al-Zn-Mg aluminium alloy.* Materials & Design, 2019. 180: p. 107901.

87.   Najjar, D., T. Magnin, and T.J. Warner, *Influence of critical surface defects and localized competition between anodic dissolution and hydrogen effects during stress corrosion cracking of a 7050 aluminium alloy.* Materials Science and Engineering: A, 1997. 238(2): p. 293-302.

88.   Magnin, T. *Recent advances in the environment sensitive fracture mechanisms of aluminium alloys.* in *Materials Science Forum.* 1996. Trans Tech Publ.

89.   Braun, R., *Anion effects on the stress corrosion cracking behaviour of aluminium alloys.* Materials and Corrosion, 2003. 54(3): p. 157-162.

90.   Lifka, B.W. and D.O. Sprowls, *Stress Corrosion Testing of 7079-T6 Aluminium Alloy in Various Environments*, H. Craig, Editor. 1967, ASTM International: West Conshohocken, PA. p. 342-362.

165

91.   Maitra, S. and G. English, *Environmental factors affecting localized corrosion of 7075-T7351 aluminium alloy plate.* Metallurgical Transactions A, 1982. 13(1): p. 161-166.

92.   Nguyen, T.H., B.F. Brown, and R.T. Foley, *On the Nature of the Occluded Cell in the Stress Corrosion Cracking of AA 7075-T651—Effect of Potential, Composition, Morphology.* Corrosion, 1982. 38(6): p. 319-326.

93.   Campbell, J.E., *Effects of Hydrogen Gas on Metals at Ambient Temperature*. 1970, BATTELLE MEMORIAL INST COLUMBUS OH DEFENSE METALS INFORMATION CENTER.

94.   Sevilgen, G. and M. Kılıç, *Three dimensional numerical analysis of temperature distribution in an automobile cabin.* Thermal Science, 2012. 16.

95.   FURUHAMA, S., et al., *Piston temperatures of an automobile engine.* Bulletin of JSME, 1964. 7(28): p. 776-783.

96.   Oñoro, J. and C. Ranninger, *Stress-corrosion-cracking behavior of heat-treated Al−Zn−Mg−Cu alloy with temperature.* Materials Science, 1999. 35(4): p. 509-514.

97.   Young, G.A. and J.R. Scully, *The effects of test temperature, temper, and alloyed copper on the hydrogen-controlled crack growth rate of an Al-Zn-Mg-(Cu) alloy.* Metallurgical and Materials Transactions A, 2002. 33(1): p. 101-115.

98.   Bhaskar, V.V. and P.S.P. Rao, *Annual and decadal variation in chemical composition of rain water at all the ten GAW stations in India.* Journal of Atmospheric Chemistry, 2017. 74(1): p. 23-53.

99.   Xu, Z., et al., *Chemical composition of rainwater and the acid neutralizing effect at Beijing and Chizhou city, China.* Atmospheric Research, 2015. 164: p. 278-285.

100.   Bozau, E., et al., *Chemische Zusammensetzung des atmosphärischen Eintrags – Messstation Clausthal-Zellerfeld (Harz), Oktober 2013 bis November 2014.* Grundwasser, 2015. 20(3): p. 163-168.

101.   Rozenfel'd, I.L. and I.K. Marshakov. *MECHANISM OF CORROSION OF METALS IN NARROW CRACKS AND CREVICES. IV. CORROSION OF ALUMINIUM AND SOME OF ITS ALLOYS*. 1966.

102.   Sedriks, A., J.A. Green, and D. Novak, *Comparison of the corrosion and stress-corrosion behavior of a ternary Al-Zn-Mg alloy.* Metallurgical and Materials Transactions B, 1970. 1(7): p. 1815-1819.

References

103. Rout, P.K., M.M. Ghosh, and K.S. Ghosh, *Effect of solution pH on electrochemical and stress corrosion cracking behaviour of a 7150 Al–Zn–Mg–Cu alloy.* Materials Science and Engineering: A, 2014. 604: p. 156-165.

104. Chu, W.-Y., C.-M. Hsiao, and J.-W. Wang, *Stress corrosion cracking of an aluminium alloy under compressive stress.* Metallurgical Transactions A, 1985. 16(9): p. 1663-1670.

105. John, C.S. and W.W. Gerberich, *The effect of loading mode on hydrogen embrittlement.* Metallurgical Transactions, 1973. 4(2): p. 589-594.

106. Pickens, J.R., J.R. Gordon, and J.A.S. Green, *The effect of loading mode on the stress-corrosion cracking of aluminium alloy 5083.* Metallurgical Transactions A, 1983. 14(4): p. 925-930.

107. Zhang, J., et al., *Effect of Loading History on Stress Corrosion Cracking of 7075-T651 Aluminium Alloy in Saline Aqueous Environment.* Metallurgical and Materials Transactions A, 2011. 42(2): p. 448-460.

108. Endo, K., K. Komai, and I. Yamamoto, *Effects of Specimen Thickness on Stress Corrosion Cracking and Corrosion Fatigue of an Aluminium Alltoy.* Bulletin of JSME, 1981. 24(194): p. 1326-1332.

109. Brown, R.H., D.O. Sprowls, and M.B. Shumaker, *The Resistance of Wrought High Strength Aluminium Alloys to Stress Corrosion Cracking*, H.L. Craig, Editor. 1972, ASTM International: West Conshohocken, PA. p. 87-118.

110. HYATT, M.V., *Effects of Residual Stresses on Stress Corrosion Crack Growth Rates in Aluminium Alloy.* Corrosion, 2013. 26(12): p. 547-551.

111. Brown, J.C., A.J. Robertson, and S.T. Serpento, *2 - Fundamental vehicle loads and their estimation*, in *Motor Vehicle Structures*, J.C. Brown, A.J. Robertson, and S.T. Serpento, Editors. 2001, Butterworth-Heinemann: Oxford. p. 11-25.

112. Wang, Z. *Car front towing hook analysis and structural improvements based on CAE*. in *International Industrial Informatics and Computer Engineering Conference (IIICEC 2015), china*. 2015. Citeseer.

113. Raj, G.P. and B. Ganesha, *OPTIMIZATION STUDY ON TOW HOOK OF A COMMERCIAL VEHICLE TO IMPROVE THE PERFORMANCE AT DIFFERENT LOADING CONDITIONS.*

114. Trotea, M., A. Constantinescu, and L. Simniceanu. *Design Optimization of the Towing Hook Used in Passenger Cars for Light Trailers*. in *The 30th SIAR International Congress of Automotive and Transport Engineering*. 2020. Cham: Springer International Publishing.

167

115. Darwish, S., H. Hussein, and A. Gemeal, *Numerical study of automotive doors.* Int. J. Of Engineering and Technology, 2012. 12(04): p. 82-93.

116. Lin, J.-C., et al., *Effect of heat treatments on the tensile strength and SCC-resistance of AA7050 in an alkaline saline solution.* Corrosion Science, 2006. 48(10): p. 3139-3156.

117. Gruhl, W., *The stress-corrosion behavior of high-strength Al-Zn-Mg alloys.* Aluminium alloys in the aircraft industries, 1978: p. 171-174.

118. Holroyd, N.J.H. and G.M. Scamans, *Stress Corrosion Cracking in Al-Zn-Mg-Cu Aluminium Alloys in Saline Environments.* Metallurgical and Materials Transactions A, 2013. 44(3): p. 1230-1253.

119. Gruhl, W., *Stress corrosion cracking of high strength aluminium alloys.* Chemischer Informationsdienst, 1985. 16(7).

120. Chen, S., et al., *Effect of Zn/Mg ratios on SCC, electrochemical corrosion properties and microstructure of Al-Zn-Mg alloy.* Journal of Alloys and Compounds, 2018. 757: p. 259-264.

121. Viswanadham, R., T. Sun, and J.A. Green, *Grain boundary segregation in Al-Zn-Mg alloys—Implications to stress corrosion cracking.* Metallurgical and Materials Transactions A, 1980. 11(1): p. 85-89.

122. *Scamans, G. M. "Evidence for crack-arrest markings on intergranular stress corrosion fracture surfaces in Al-Zn-Mg alloys." Metallurgical Transactions A 11.5 (1980): 846-850.*

123. Chen, J.M., et al., *Grain boundary segregation of an Al-Zn-Mg ternary alloy.* Metallurgical Transactions A, 1977. 8(12): p. 1935-1940.

124. Wei, R., M. Gao, and P. Pao, *The role of magnesium in CF and SCC of 7000 series aluminium alloys.* Scripta metallurgica, 1984. 18(11): p. 1195-1198.

125. Sarkar, B., M. Marek, and E.A. Starke, *The effect of copper content and heat treatment on the stress corrosion characteristics of Ai-6Zn-2Mg-X Cu alloys.* Metallurgical Transactions A, 1981. 12(11): p. 1939-1943.

126. Lin, F.-S. and E.A. Starke, *The effect of copper content and degree of recrystallization on the fatigue resistance of 7XXX-type aluminium alloys II. Fatigue crack propagation.* Materials Science and Engineering, 1980. 43(1): p. 65-76.

127. Meng, Q. and G.S. Frankel, *Effect of Cu Content on Corrosion Behavior of 7xxx Series Aluminium Alloys.* Journal of The Electrochemical Society, 2004. 151(5): p. B271.

References

128. Hardwick, D.A., A.W. Thompson, and I.M. Bernstein, *The effect of copper content and heat treatment on the hydrogen embrittlement of 7050-type alloys.* Corrosion Science, 1988. 28(12): p. 1127-1137.

129. Birnbaum, H.K., *Mechanisms of hydrogen related fracture of metals*. 1989, DTIC Document.

130. Scamans, G.M., R. Alani, and P.R. Swann, *Pre-exposure embrittlement and stress corrosion failure in Al-Zn-Mg Alloys.* Corrosion Science, 1976. 16(7): p. 443-459.

131. Shi, Y., et al., *Effect of Sc and Zr additions on corrosion behaviour of Al–Zn–Mg–Cu alloys.* Journal of Alloys and Compounds, 2014. 612: p. 42-50.

132. Chen, K.H., et al., *Effect of of Yb, Cr and Zr additions on recrystallization and corrosion resistance of Al–Zn–Mg–Cu alloys.* Materials Science and Engineering: A, 2008. 497(1–2): p. 426-431.

133. Liu, Y.-y., C.-q. Xia, and X.-m. Peng, *Effect of heat treatment on microstructures and mechanical properties of Al-6Zn-2Mg-1.5Cu-0.4Er alloy.* Journal of Central South University of Technology, 2010. 17(1): p. 24-27.

134. Deng, Y., et al., *Effects of Sc and Zr microalloying additions and aging time at 120 °C on the corrosion behaviour of an Al–Zn–Mg alloy.* Corrosion Science, 2012. 65: p. 288-298.

135. Fang, H.C., H. Chao, and K.H. Chen, *Effect of Zr, Er and Cr additions on microstructures and properties of Al–Zn–Mg–Cu alloys.* Materials Science and Engineering: A, 2014. 610: p. 10-16.

136. Li, B., et al., *Microstructures and properties of Al–Zn–Mg–Mn alloy with trace amounts of Sc and Zr.* Materials Science and Engineering: A, 2014. 616: p. 219-228.

137. Holroyd, N., *Environment-induced cracking of high-strength aluminium alloys.* Environment-induced cracking of metals, 1990: p. 311.

138. Buha, J., R. Lumley, and A. Crosky, *Secondary ageing in an aluminium alloy 7050.* Materials Science and Engineering: A, 2008. 492(1-2): p. 1-10.

139. Xu, D., N. Birbilis, and P. Rometsch, *Effect of S-phase dissolution on the corrosion and stress corrosion cracking of an as-rolled Al-Zn-Mg-Cu alloy.* Corrosion, The Journal of Science and Engineering, 2012. 68(3): p. 035001-1-035001-10.

169

140. De Ardo, A. and R. Townsend, *The effect of microstructure on the stress-corrosion susceptibility of a high purity Al− Zn− Mg alloy in a NaCl solution.* Metallurgical Transactions, 1970. 1(9): p. 2573-2581.

141. Sun, X., et al., *Correlations between stress corrosion cracking susceptibility and grain boundary microstructures for an Al–Zn–Mg alloy.* Corrosion science, 2013. 77: p. 103-112.

142. Puiggali, M., et al., *Effect of microstructure on stress corrosion cracking of an Al-Zn-Mg-Cu alloy.* Corrosion Science, 1998. 40(4): p. 805-819.

143. Vasudevan, A.K. and R. Doherty, *Grain boundary ductile fracture in precipitation hardened aluminium alloys.* Acta metallurgica, 1987. 35(6): p. 1193-1219.

144. Taylor, I. and R. Edgar, *A study of stress-corrosion in Al-Zn-Mg alloys.* Metallurgical Transactions, 1971. 2(3): p. 833-839.

145. Thomas, G. and J. Nutting, *Electron microscope studies of alloys based on the aluminium-zinc-magnesium system [J].* J Inst Metals, 1959. 88(81): p. 1960.

146. Tsai, T. and T. Chuang, *Role of grain size on the stress corrosion cracking of 7475 aluminium alloys.* Materials Science and Engineering: A, 1997. 225(1-2): p. 135-144.

147. B., C., *Reducing the susceptibility of alloys, particularly aluminium alloys, to stress corrosion cracking.* 1974, Google Patents.

148. Krishnan, M.A. and V.S. Raja, *Development of high strength AA 7010 aluminium alloy resistant to environmentally assisted cracking.* Corrosion Science, 2016. 109: p. 94-100.

149. Baydogan, M., et al., *Improved resistance to stress-corrosion-cracking failures via optimized retrogression and reaging of 7075-T6 aluminium sheets.* Metallurgical and Materials Transactions A, 2008. 39(10): p. 2470-2476.

150. Ou, B.-L., J.-G. Yang, and M.-Y. Wei, *Effect of homogenization and aging treatment on mechanical properties and stress-corrosion cracking of 7050 alloys.* Metallurgical and Materials Transactions A, 2007. 38(8): p. 1760-1773.

151. Turnbull, A., *Test Methods for Environmentally Assisted Cracking.* British Corrosion Journal, 1992. 27(4).

152. Parkins, R.N., *2.35 - Environmentally Assisted Cracking Test Methods* A2 - Cottis, Bob*, in *Shreir's Corrosion*, M. Graham, et al., Editors. 2010, Elsevier: Oxford. p. 1527-1546.

153. *ASTM G30-97(2016), Standard Practice for Making and Using U-Bend Stress-Corrosion Test Specimens, ASTM International, West Conshohocken, PA, 2016, www.astm.org.* 2016.

154. *ASTM G39-99(2016), Standard Practice for Preparation and Use of Bent-Beam Stress-Corrosion Test Specimens, ASTM International, West Conshohocken, PA, 2016, www.astm.org.* 2016.

155. *ISO 7539-5:1989,* in *Corrosion of metals and alloys -- Stress corrosion testing -- Part 5: Preparation and use of C-ring specimens.* 1989.

156. Brenner, P. and W. Gruhl, *Stress-Corrosion Cracking Tests of Al-Zn-Mg 3 Under Constant Tensile and Bending Strain.* Zeitschrift fuer Metallkunde, 1961. 52(10): p. 599-607.

157. Henthorne, M., *The Slow Strain Rate Stress Corrosion Cracking Test—A 50 Year Retrospective.* Corrosion, 2016. 72(12): p. 1488-1518.

158. *ASTM G129-00(2013), Standard Practice for Slow Strain Rate Testing to Evaluate the Susceptibility of Metallic Materials to Environmentally Assisted Cracking, ASTM International, West Conshohocken, PA, 2013, www.astm.org.*

159. Taheri, M., et al., *Strain-rate effects on hydrogen embrittlement of 7075 aluminium.* Scripta Metallurgica, 1979. 13(9): p. 871-875.

160. Bayoumi, M.R., *The mechanics and mechanisms of fracture in stress corrosion cracking of aluminium alloys.* Engineering Fracture Mechanics, 1996. 54(6): p. 879-889.

161. Tien, J.K., et al., *Dislocation sweeping model for hydrogen assisted subcritical crack growth.* Scripta Metallurgica, 1980. 14(6): p. 591-594.

162. Colvin, E.L. and M.R. Emptage, *The breaking load method - Results and statistical modification from the ASTM interlaboratory test program.* 1992.

163. *ASTM G44-99(Reapproved 2013). Standard Practice for Exposure of Metals and Alloys by Alternate Immersion in Neutral 3.5 % Sodium Chloride Solution.*

164. Oñoro, J., *The stress corrosion cracking behaviour of heat-treated Al–Zn–Mg–Cu alloy in modified salt spray fog testing.* Materials and Corrosion, 2010. 61(2): p. 125-129.

165. Yu, M., et al., *Effects of dry/wet ratio and pre-immersion on stress corrosion cracking of 7050-T7451 aluminium alloy under wet-dry cyclic conditions.* Chinese Journal of Aeronautics, 2018. 31(11): p. 2176-2184.

171

166. *DIN EN ISO 6892-1:2017-02:Metallische Werkstoffe - Zugversuch - Teil 1: Prüfverfahren bei Raumtemperatur (ISO 6892-1:2016); Deutsche Fassung EN ISO 6892-1:2016.* 2017.

167. *ASTM G47-98, Standard Test Method for Determining Susceptibility to Stress-Corrosion Cracking of 2XXX and 7XXX Aluminium Alloy Products, ASTM International, West Conshohocken, PA, 1998, www.astm.org.*

168. Antony, J., *2 - Fundamentals of Design of Experiments*, in *Design of Experiments for Engineers and Scientists (Second Edition)*, J. Antony, Editor. 2014, Elsevier: Oxford. p. 7-17.

169. Montgomery, D.C., *Design and analysis of experiments*. 2017: John wiley & sons.

170. Antony, J., *4 - A Systematic Methodology for Design of Experiments*, in *Design of Experiments for Engineers and Scientists (Second Edition)*, J. Antony, Editor. 2014, Elsevier: Oxford. p. 33-50.

171. Zwicky, F., *The morphological approach to discovery, invention, research and construction*, in *New methods of thought and procedure*. 1967, Springer. p. 273-297.

172. Klokkers, F., G. Meschut, and O. Hahn, *Fügen pressharter Stähle in Mischbauweise. 2.* Wissenschaftliche Tagung" Jugend forscht und schweißt", Vortrag, Duisburg, 2011. 1.

173. *DIN EN ISO 11997-1:2016-05 Beschichtungsstoffe - Bestimmung der Beständigkeit bei zyklischen Korrosionsbedingungen - Teil 1: Nass (Salzsprühnebel)/trocken/Feuchte.* 2016.

174. *DIN 50125:2009-07*, in *Testing of metallic materials - Tensile test pieces*. 2009-07.

175. Edgar Dietrich, S.C., *Eignungsnachweis von Messsystemen.* Hanser Fachbuch, 2014.

176. Rejeb, H.B., V. Boly, and L. Morel-Guimaraes, *Attractive quality for requirement assessment during the front-end of innovation.* The TQM journal, 2011.

177. Füller, J. and K. Matzler, *Virtual product experience and customer participation—A chance for customer-centred, really new products.* Technovation, 2007. 27(6-7): p. 378-387.

178. Kano, N., *Attractive quality and must-be quality.* Hinshitsu (Quality, The Journal of Japanese Society for Quality Control), 1984. 14: p. 39-48.

179. Lutze, F.W., et al., *Update on the Developments of the SAE J2334 Laboratory Cyclic Corrosion Test.* SAE transactions, 2003: p. 1209-1214.

180. Townsend, H. and A. Borzillo, *Thirty year atmospheric corrosion performance of 55% aluminium-zinc alloy-coated sheet steel.* Materials performance, 1996. 35(4).

181. LeBozec, N. and D. Thierry, *Influence of climatic factors in cyclic accelerated corrosion test towards the development of a reliable and repeatable accelerated corrosion test for the automotive industry.* Materials and Corrosion, 2010. 61(10): p. 845-851.

182. Santos, P.S., et al., *Chemical composition of rainwater at a coastal town on the southwest of Europe: what changes in 20 years?* Sci Total Environ, 2011. 409(18): p. 3548-53.

183. Fay, J.A., D. Golomb, and S. Kumar, *Modeling of the 1900–1980 trend of precipitation acidity at Hubbard Brook, New Hampshire.* Atmospheric Environment (1967), 1986. 20(9): p. 1825-1828.

184. Tsai, T.C. and T.H. Chuang, *Role of grain size on the stress corrosion cracking of 7475 aluminium alloys.* Materials Science and Engineering: A, 1997. 225(1): p. 135-144.

185. Kröger, B., R. Holbein, and S.G. Klose, *Hydrogen assisted cracking in a high strength dual phase steel DP1180HY.* Materials Testing, 2017. 59(5): p. 430-437.

186. Krishna, M.M., V. Moskal, and P. Randle, *Non-Linear Finite Element Recovery Analysis of an Automotive Chassis Frames*. 2005, SAE Technical Paper.

187. Runje, B., A.H. Novak, and A. Razumić. *Measurement system analysis in production process*. in *XVII International Scientific Conference on Industrial Systems*. 2017.

188. Ricker, R.E., et al., *Chloride ion activity and susceptibility of Al alloys 7075-T6 and 5083-H131 to stress corrosion cracking.* Metallurgical and Materials Transactions A, 2013. 44(3): p. 1353-1364.

189. Cohen, Jacob. "Statistical power analysis." *Current directions in psychological science* 1.3 (1992): 98-101.

190. VDI 2221 Blatt 1: 2019-11 , Entwicklung technischer Produkte und Systeme-Modell der Produktentwicklung

173

LIST OF FIGURES

LIST OF TABLES

APPENDIX

| Anforderung (VoC oder CTQ) 0 = ist weniger wichtig als 1 = gleich wichtig 2 = wichtiger als	Test_Einfach zu bedienendes Equipment	Test_Möglich Schnell	Test_Keine besondere Qualifizierung der MA	Test_Weltweit durchführbar	Test_Kostengünstig	Test_So wenig manuelle Interventionen des Operators wie möglich	Test_Kein Cr-VI, Hexan, HF oder andere	Test_Die Korrosionslösung nicht zu oft wechseln müssen	Test_Probenhalter müssen korrosionsbeständig sein	Test_Klare Definition der Testparameter, keine Grauzonen (z.B Temperatur >20°C à das ist zu ungenau)	Test_Mehrere Proben auf einmal Testen	Test_Von Externe Dienstleister durchführbar sein	Ergebnisse_Reproduzierbar und Wiederholbar	Ergebnisse_Einzelne Legierungen gut differenzierbar --> Großer Bereich von Werkstoff (Ranking)	Ergebnisse_Ermittlung zeit dauer bis zum Auftreten von Rissen in Abhängigkeit der Spannung	Ergebnisse_Ermittlung v. Grenzspannung (Laststufen) bei einer definierten Zeit
Feld_Korrelation zum Verhalten im Fahrbetrieb ist sichergestellt	0	0	0	0	0	0	0	2	0	0	2	0	0	2	0	0
Feld_Kritische Zustände und Klima müssen in Prüfmethode abgebildet werden	0	0	0	0	0	0	0	2	0	0	2	0	0	2	2	0
Probe_Test auch gültig für 7xxx Material mit Yield > 600Mpa (Eventuell in Zukunft von 3-5 Jahren > 800 MPa)	0	0	0	0	0	0	0	2	0	2	2	0	0	2	2	2
Probe_Probenvorbereitung klar definiert (MEK, ISOPROP, WYPALL, all)	0	0	0	0	0	0	0	2	0	0	1	0	0	2	2	2
Test_Von Externe Dienstleister durchführbar sein	0	0	0	0	2	0	0	2	0	2	2	0	1	2	2	2
Test_Mehrere Proben auf einmal Testen	2	0	0	0	2	0	2	2	0	2	2	1	0	2	2	2
Test_Klare Definition der Testparameter, keine Grauzonen (z.B Temperatur >20°C à das ist zu ungenau)	0	0	0	0	0	0	2	0	0	1	2	0	0	2	2	2
Test_Probenhalter müssen korrosionsbeständig sein	0	0	0	0	0	0	2	1	2	1	2	0	0	2	2	2
Test_Die Korrosionslösung nicht zu oft wechseln müssen	0	2	0	2	0	2	2	1	2	2	2	0	2	2	2	2
Test_Kein Cr-VI, Hexan, HF oder andere	0	0	0	0	0	0	1	0	0	0	0	0	0	0	0	0
Test_So wenig manuelle Interventionen des Operators wie möglich	0	0	0	0	0	1	2	0	2	2	2	0	2	2	2	2
Test_Kostengünstig	2	2	2	2	1	2	2	2	2	2	2	2	2	2	2	2
Test_Weltweit durchführbar	2	0	0	1	0	2	2	0	2	2	2	0	2	2	2	2
Test_Keine besondere Qualifizierung der MA	2	0	1	2	2	2	2	2	2	2	2	2	2	2	2	2
Test_Möglich Schnell	2	1	2	2	0	2	2	0	2	2	2	2	2	2	2	2
Test_Einfach zu bedienendes Equipment	1	0	0	0	0	2	2	2	2	2	2	0	2	2	2	2

APPENDIX 1 EXAMPLE OF PAIRWISE COMPARISON TO DETERMINE THE WEIGHTAGE OF CUSTOMER REQUIREMENTS

Appendix

Block	Phase	Time (Hours)	Time(Hours) Programmed	Temperature(C)	Relative Humidity (%)	Salt Spray	Time	Day
A	**Preparation Phase**	3	2:50	23-25	50			Friday
	Before Salt-Spray		0:10					
	Salt-Spray	2	2	35	95	Yes		
	Humid Phase	6	5:56	35	50		11:00	Sunday
	Humid Phase	16	15:50	35	80		17:00	Sunday
	Before Salt-Spray		0:10	35	98		8:50	Monday
	Duration Block A: 27 hours							
B	Salt Spray	2	2	35	98/KK	Yes	9:00	Monday
	Cleaning Phase		0:04				11:00	Monday
	Dry Phase	3	2:56	40	50		14:00	Monday
	Humid Phase	3	3	40	98/KK		17:00	Monday
	Dry Phase	3	3	40	50		20:00	Monday
	Humid Phase	3	3	40	98/KK		23:00	Monday
	Dry Phase	3	3	40	50		2:00	Tuesday
	Humid Phase	3	3	40	98/KK		5:00	Tuesday
	Dry Phase	3	3	40	50		8:00	Tuesday
	Humid Phase	3	3	40	98/KK		11:00	Tuesday
	Dry Phase	3	3:00	40	50		14:00	Tuesday
	Humid Phase	3	3	40	98/KK		17:00	Tuesday
	Dry Phase	3	3	40	50		20:00	Tuesday
	Humid Phase	3	3	40	98/KK		23:00	Tuesday
	Dry Phase	3	3	40	50		2:00	Wednesday
	Humid Phase	3	3	40	98/KK		5:00	Wednesday
	Dry Phase	3	3	40	50		8:00	Wednesday
	Salt Spray	2	2	35	95	Yes	11:00	Wednesday
	Dry Phase	3	3	40	50		13:00	Wednesday
	Humid Phase	3	3	40	98/KK		16:00	Wednesday
	Dry Phase	3	3	40	50		19:00	Wednesday
	Humid Phase	3	3	40	98/KK		22:00	Wednesday
	Dry Phase	3	3	40	50		1:00	Thursday
	Humid Phase	3	3	40	98/KK		4:00	Thursday
	Dry Phase	3	3	40	50		7:00	Thursday
	Humid Phase	3	3	40	98/KK		10:00	Thursday
	Dry Phase	3	3	40	50		13:00	Thursday
	Humid Phase	3	3	40	98/KK		16:00	Thursday
	Dry Phase	3	3	40	50		19:00	Thursday
	Humid Phase	3	3	40	98/KK		22:00	Thursday
	Dry Phase	3	3	40	50		1:00	Friday
	Humid Phase	3	3	40	98/KK		4:00	Friday
	Dry Phase	3	3	40	50		7:00	Friday
	Humid Phase	3	3	50	98/KK		10:00	Friday
	Salt Spray	2	2	35	95	Yes	13:00	Friday
	Dry Phase	3	3	40	50		15:00	Friday
	Humid Phase	3	3	40	98/KK		18:00	Friday
	Dry Phase	3	3	40	50		21:00	Friday
	Humid Phase	3	3	40	98/KK		0:00	Saturday
	Dry Phase	3	3	40	50		3:00	Saturday
	Humid Phase	3	3	40	98/KK		6:00	Saturday
	Dry Phase	3	3	40	50		9:00	Saturday
	Humid Phase	3	3	40	98/KK		12:00	Saturday
	Dry Phase	3	3	40	50		15:00	Saturday
	Humid Phase	3	3	40	98/KK		18:00	Saturday
	Dry Phase	3	3	40	50		21:00	Saturday
	Humid Phase	3	3	40	98/KK		0:00	Sunday
	Dry Phase	3	3	40	50		3:00	Sunday
	Humid Phase	3	3	40	98/KK		6:00	Sunday
	Total Time(Block B) = 141 hours (6 days)							
C	Hot Phase	15	14	80	50		20:00	Sunday
	Pause	3	3	25	50		23:00	Sunday
	Cold Phase	6	6	-20	undefined		2:00	Monday
	Before Salt-Spray	1	1	35	98		8:00	Monday
	Total Time(Block C) = 24hours (1 day)							

APPENDIX 1 PROGRAMMING OF THE FINAL MBSC TEST CYCLE IN THE CLIMATE CHAMBER

183
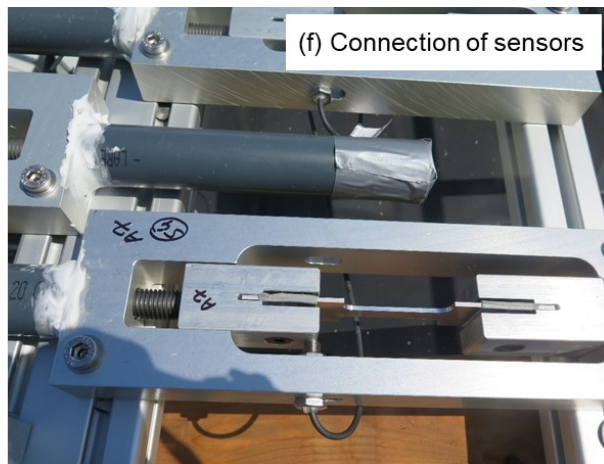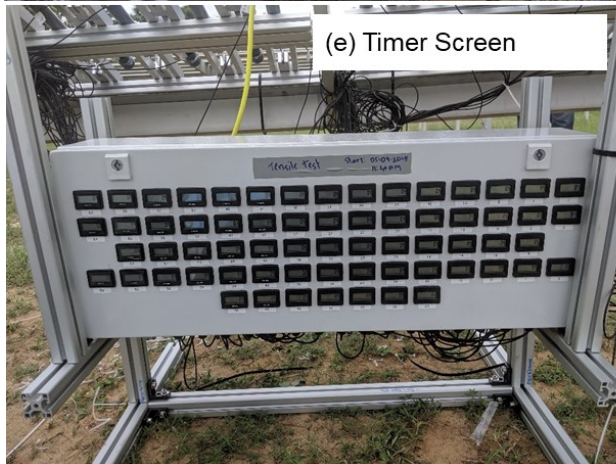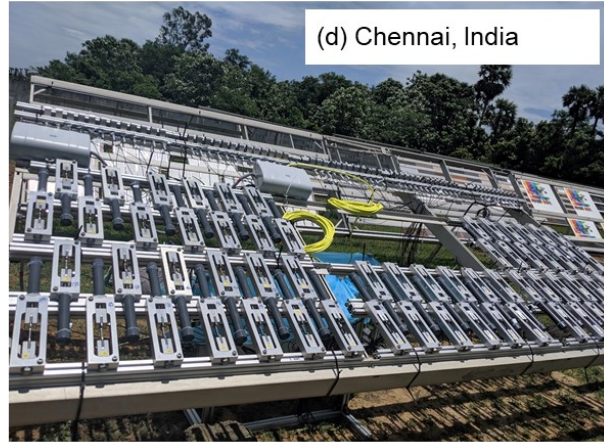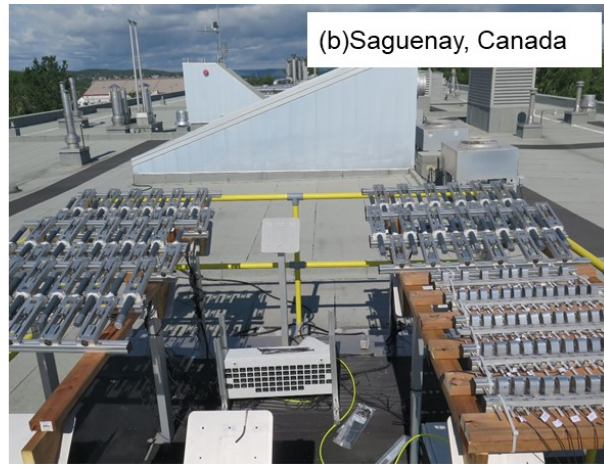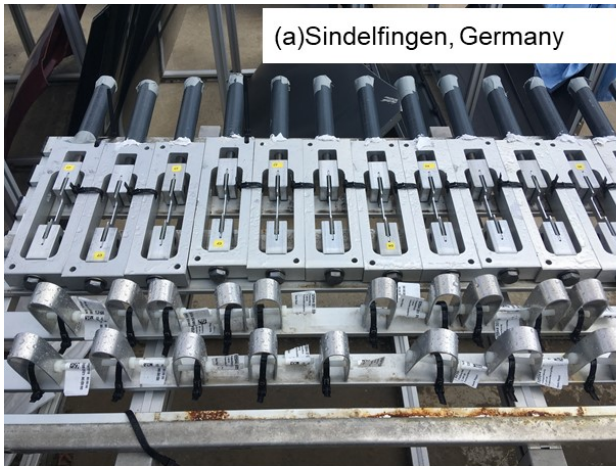
APPENDIX 2 OVERVIEW OF COMPLETE OUTDOOR EXPOSURE SETUP IN THE DIFFERENT LOCATIONS (A) SINDELFINGEN, GERMANY (B) SAGUENAY, CANADA (C) LONG KEY, USA (D) CHENNAI, INDIA AND THE (E) TIMER SCREEN TO DETERMINE TIME OF FAILURE (F) SENSOR CONNECTION TO CONSTANT LOAD SPECIMEN